Phase 1A
Final Report
for the AREVA Team
Enhanced Accident Tolerant Fuels Concepts

Contract No. DE-NE-0000567
RPT-3011235-001
DOE Identifier: DOE-AFS-0000567

Prepared by:
AREVA Federal Services, LLC

Acknowledgements

This report is the result of a joint effort performed for the Department of Energy (DOE) by a team comprising AREVA, Duke Energy and Tennessee Valley Authority (TVA), University of Florida (UF), University of Wisconsin (UW), and Savannah River National Laboratory (SRNL).

It is the result of technical contributions from many subject matter experts, including:

Kevin McCoy, *AREVA NP*
James Tulenko, *UF*
Ghatu Subhash, *UF*
Kumar Sridharan, *UW*
Ben Hauch, *UW*
Rose Montgomery, *TVA*
Ben Howell, *Duke Energy*
Heather Burns, *SRNL*
Brenda Garcia-Diaz, *SRNL*
Luke Olson, *SRNL*
Elizabeth Hoffman, *SRNL*
Robert Sindelar, *SRNL*
Ron Kesterson, *SRNL*
M. Barsoum, *DREXEL*

Executive Summary

In response to the Department of Energy (DOE)[1] funded initiative to develop and deploy lead fuel assemblies (LFAs) of Enhanced Accident Tolerant Fuel (EATF) into a US reactor within 10 years, AREVA put together a team to develop promising technologies for improved fuel performance during off normal operations. This team consisted of the University of Florida (UF) and the University of Wisconsin (UW), Savannah River National Laboratory (SRNL), Duke Energy and Tennessee Valley Authority (TVA). This team brought broad experience and expertise to bear on EATF development. AREVA has been designing; manufacturing and testing nuclear fuel for over 50 years and is one of the 3 large international companies supplying fuel to the nuclear industry. The university and National Laboratory team members brought expertise in nuclear fuel concepts and materials development. Duke and TVA brought practical utility operating experience. This report documents the results from the initial "discovery phase" where the team explored options for EATF concepts that provide enhanced accident tolerance for both Design Basis (DB) and Beyond Design Basis Events (BDB). The main driver for the concepts under development were that they could be implemented in a 10 year time frame and be economically viable and acceptable to the nuclear fuel marketplace.

The economics of fuel design make this DOE funded project very important to the nuclear industry. Even incremental changes to an existing fuel design can cost in the range of $100M to implement through to LFAs. If this money is invested evenly over 10 years then it can take the fuel vendor several decades after the start of the project to recover their initial investment and reach a breakeven point on the initial investment. Step or radical changes to a fuel assembly design can cost upwards of $500M and will take even longer for the fuel vendor to recover their investment. With the projected lifetimes of the current generation of nuclear power plants large scale investment by the fuel vendors is difficult to justify.

Specific EATF enhancements considered by the AREVA team were:

- Improved performance in DB and BDB conditions.
- Reduced release to the environment in a catastrophic accident.
- Improved performance during normal operating conditions.
- Improved performance if US reactors start to load follow.
- Equal or improved economics of the fuel.
- Improvements to the fuel behavior to support future transportation and storage of the used nuclear fuel (UNF).

AREVA's advanced PWR fuel assembly design GAIA.

- Evolutionary spring hull grid design with 8-line contact for fretting resistance
- Improved Critical Heat Flux performance and thermal margins
- In operation since 2012

[1] See Section 7.0 for a list of all acronyms.

In pursuit of the above enhancements, EATF technology concepts that our team considered were:

1) Additives to the fuel pellets which included:

- Chromia doping to increase fission gas retention. Chromia doping has the potential to improve load following characteristics, improve performance of the fuel pellet during clad failure, and potentially lock up cesium into the fuel matrix.
- Silicon Carbide (SiC) Fibers to improve thermal heat transfer in normal operating conditions which also improves margin in accident conditions and the potential to lock up iodine into the fuel matrix.
- Nano-diamond particles to enhance thermal conductivity.

2) Coatings on the fuel cladding:

- Nine coatings on the existing Zircaloy cladding to increase coping time and reduce clad oxidation and hydrogen generation during accident conditions, as well as reduce hydrogen pickup and mitigate hydride reorientation in the cladding.

To facilitate the development process AREVA adopted a formal "Gate Review Process" (GR) that was used to review results and focus resources onto promising technologies to reduce costs and identify the technologies that would potentially be carried forward to LFAs within a 10 year period. Our approach is shown in Figure 1.

Figure 1: AREVA Gate Review Process for EATF

During the initial discovery phase of the project AREVA took the decision to be relatively hands off and allow our university and National Laboratory partners to be free thinking and consider options that would not be constrained by preconceived ideas from the fuel vendor. To counter this and to keep the partners focused, the GR process was utilized. During this GR process each of the team members presented their findings to a board made up of technical experts from utilities, fuel manufacturing experts, fuel technical experts, and fuel research and development (R&D) experts. The results of these GR's are depicted in Figure 2, showing the technology concepts that were not carried forward and those concepts that were carried forward for further development.

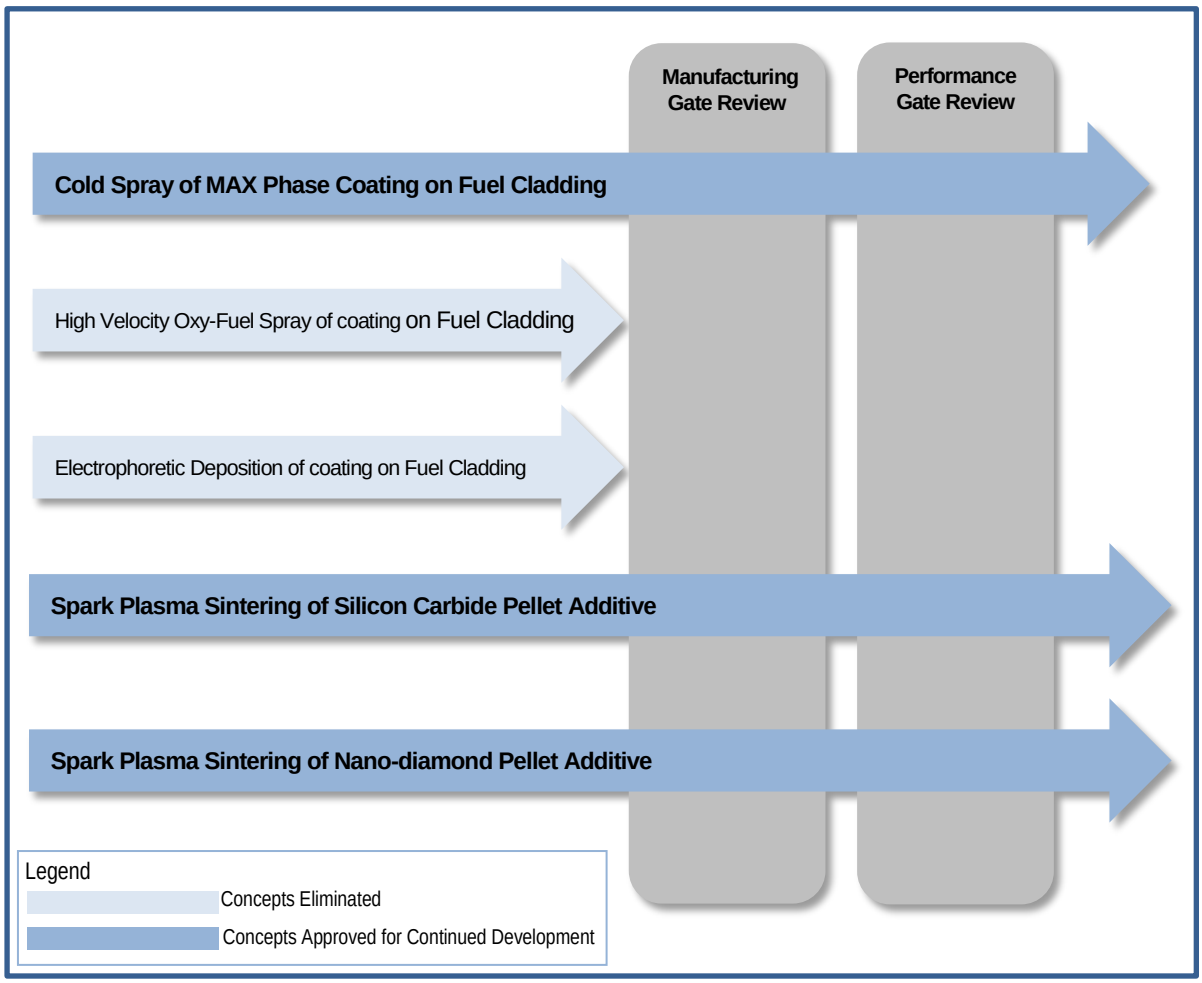

Figure 2: Effects of Gate Review Process on Technology

During the initial 2 years of the project there were several major accomplishments. These accomplishments, along with the implications for successfully implementing EATF, are:

1) The experimental spark plasma sintering process (SPS) process was successfully used to produce fuel pellets containing either 10% SiC whiskers or nano-diamond particles. The ability to use this process enables the thermal margin enhancements of the fuel additives to be realized. Without the SPS process, the conventional process cannot support adding pellet additives in the required quantities.

2) Coatings of Ti_2AlC were successfully applied to Zircaloy-4 cladding. Testing of Ti_2AlC coatings at Loss of Cooling Accident (LOCA) conditions showed reduced cladding oxidation compared to present un-coated Zircaloy-4 cladding. This achievement allows the presently used cladding system to be retained so that the 10 year schedule can be met. Having to implement a new cladding material will extend the development schedule beyond 10 years.

3) Several documents were produced to support future development, testing, and licensing of EATF, including a design requirements traceability matrix, a draft business plan, a draft test plan, a draft regulatory plan, and the acceptance criteria for lead fuel assembly insertion into a commercial reactor. This preparatory work lays the foundation for ensuring the future development plans address all the areas required to test, license, and manufacture the new EATF.

4) In addition, the high velocity oxy-fuel and electrophoretic deposition (EPD) coating application processes were dropped from further consideration due to their inability to meet manufacturing criteria. This allows the resources to be focused on the most promising EATF concepts identified. These accomplishments are depicted in Figure 3.

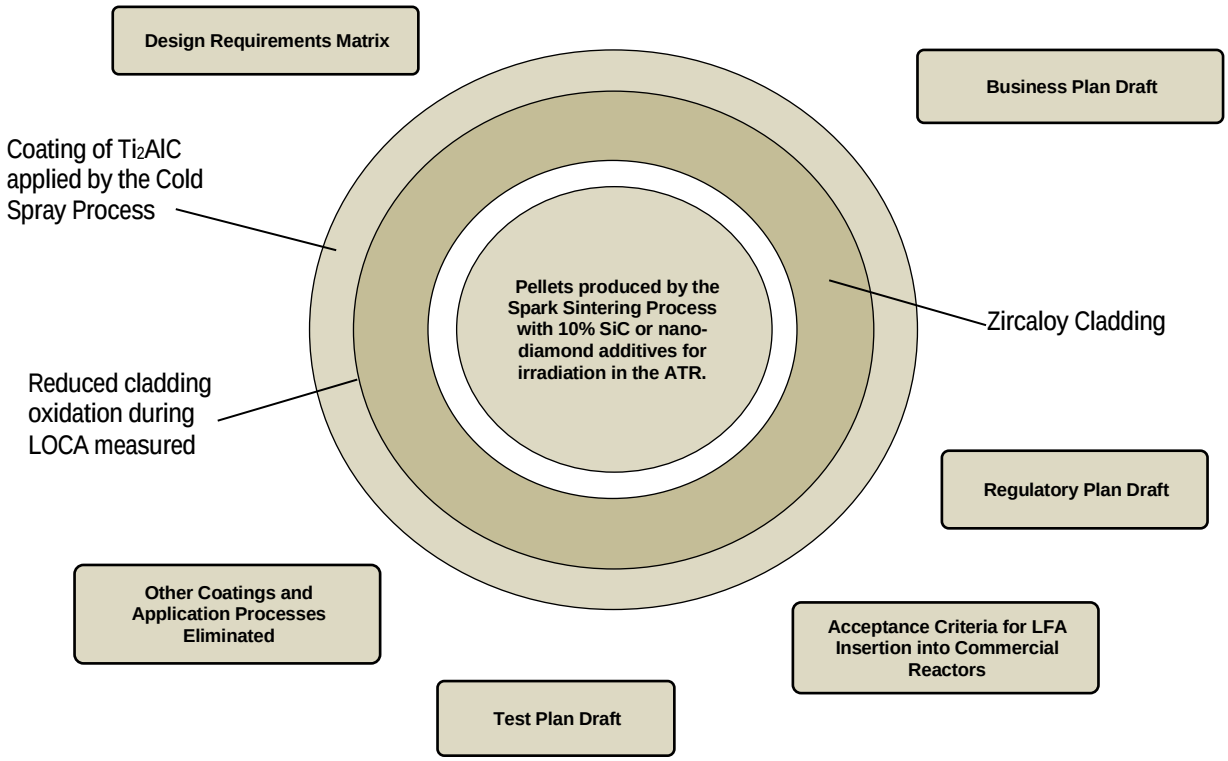

Figure 3: AREVA Team Accomplishments

Future development opportunities that were identified during this work include:

1) The use of SiC or diamond requires that a new pellet production technique (Spark Plasma Sintering), be developed. This entails investment in developing, proving and implementing a new commercial pellet production process. Development of the process to apply thinner coatings is required.

2) Coatings cannot be too "thick" or they will displace a significant volume of water in the core resulting in reduced thermal hydraulic characteristics.

3) Application of the coating at high temperature can affect the Zircaloy substrate. This will require the development and implementation of a new cladding coating manufacturing process.

4) Replace the Cold Spray (CS) cladding coating application with the Physical Vapor Deposition (PVD) process to eliminate duplication of work and provide greater control over coating thicknesses. This can result in a reduction in the final cycle economic penalty of coatings.

TABLE OF CONTENTS

EXECUTIVE SUMMARY ii

1.0 INTRODUCTION 1
2.0 PROJECT SCHEDULE FOR EATF TO DEPLOY LFA'S WITHIN 10 YEARS. 5
2.1. US NUCLEAR MARKET FOR FUELS. 6
3.0 DEVELOPMENT PROCESS FOR THE DISCOVERY PHASE 7
3.1. REQUIREMENTS TRACEABILITY MATRIX 8
3.2. GATE REVIEW PROCESS 8
3.3. PRELIMINARY BUSINESS PLAN 9
3.4. TEST PLAN AND DOE SUPPORT TO FUTURE TESTING 10
3.5. REGULATORY PLAN 11
4.0 DISCOVERY PHASE RESULTS 13
4.1. FUEL PELLETS 13
4.2. CLADDING COATINGS 19
4.3. CLADDING 26
4.4. NANO-PARTICLES IN THE COOLANT 26
5.0 POST IRRADIATION EXAMINATIONS 27
6.0 SUMMARY OF ACCOMPLISHMENTS 28
7.0 ACRONYMS 29
8.0 REFERENCES 31

APPENDICIES A – Q 32

APPENDIX A - Requirements Traceability Matrix for the Draft Final Report for Enhanced Accident Tolerant Fuels
APPENDIX B - Preliminary Business Plan for the Draft Final Report for Enhanced Accident Tolerant Fuels
APPENDIX C - Results of Gate Review #1 for the Draft Final Report for Enhanced Accident Tolerant Fuels
APPENDIX D - Results of Gate Review #2 for the Draft Final Report for Enhanced Accident Tolerant Fuels
APPENDIX E - UO_2-Composite LWR Fuel Pellets with Increased Thermal Conductivity Fabricated by Spark Plasma Sintering for the Draft Final Report for Enhanced Accident Tolerant Fuels
APPENDIX F - Electrophoretic Deposition (EPD) Coatings for the Draft Final Report for Enhanced Accident Tolerant Fuels
APPENDIX G - MAX Phase Coatings for the Draft Final Report for or Enhanced Accident Tolerant Fuels
APPENDIX H - Nano-Particles in Coolant during Accident Conditions for the Draft Final Report for Enhanced Accident Tolerant Fuels
APPENDIX I - Fuel Cycle Impacts for the Draft Final Report for Enhanced Accident Tolerant Fuels
APPENDIX J - ATR Irradiation Test for the Draft Final Report for Enhanced Accident Tolerant Fuels
APPENDIX K - Enhanced Accident Tolerant Fuel Test Plan for the Draft Final Report for EATF
APPENDIX L - Publication's for the Draft Final Report for Enhanced Accident Tolerant Fuels
APPENDIX M - Typical LFA Acceptance Review for the Draft Final Report for Enhanced Accident Tolerant Fuels
APPENDIX N - Regulatory Plan for the Draft Final Report for Enhanced Accident Tolerant Fuels
APPENDIX O - Materials Effects of EATF Pellet Additives and Coatings for the Draft Final Report for Enhanced Accident Tolerant Fuels
APPENDIX P - Performance Test Plan for the Draft Final Report for Enhanced Accident Tolerant Fuels
APPENDIX Q - ATF Fuel Design Impacts for the Draft Final Report for Enhanced Accident Tolerant Fuels

LIST OF FIGURES

Figure 1: AREVA Gate Review Process for EATF....iii
Figure 2: Effects of Gate Review Process on Technology....iv
Figure 3: AREVA Team Accomplishments v
Figure 4: Enhanced Accident Tolerant Fuel Development Schedule 1
Figure 5: AREVA Team Composition 3
Figure 6: Operational Reactors in the US. 6
Figure 7: Projected Operational Reactors in the US Assuming Life Extensions to 80 years. 7
Figure 8: AREVA Gate Review Process for EATF. 9
Figure 9: Enhanced Accident Tolerant Fuel Regulatory Plan 12
Figure 10: Comparison of Conventional Sintering and Spark Plasma Sintering 14
Figure 11: Thermal conductivity of various sintered UO_2 – 10vol%SiC pellets 14
Figure 12: Fuel Pellet Additives 15
Figure 13: Sintered pellet density as a function of Chromia concentration 15
Figure 14: Graph of axial variance of grain size in dope UO_2 pellets sintered at 1600°C for 30 seconds 16
Figure 15: 17 x 17 sized Pellets for Irradiation in the ATR 17
Figure 16: Rodlet with EATF Fuel Pellets Fabricated for Testing in the ATR. 17
Figure 17: "Lipped punch" used to try to reduce the current density through the punches 19
Figure 18: The detail design of the tube-geometry coating apparatus and the fabricated apparatus. The titanium tube and the Zircaloy tube sample serve as electrodes, electrically isolated via HDPE .... High Density Polyethylene (HDPE) mounting blocks and connected via external wires (not shown) to a direct current power supply 21
Figure 19: Zircaloy Fuel Cladding Coated with MAX Phase material by the cold spray process. 23
Figure 20: Coated Zircaloy-4 coupon after steam oxidation 25

LIST OF TABLES

Table 1: Appendices Subject List 4
Table 2: AREVA's Accomplishments 5
Table 3: Difference in average density of sintered pellets for a die OD of 0.944" 18
Table 4: Cladding Coatings and Coating Processes Previously Investigated 20
Table 5: Initial EPD Coatings Investigated in this Study 20
Table 6: EPD Pin-on-Disk Results 21
Table 7: Benefits of Each Spray Process 22
Table 8: Rotating Pin-on-Disc test results for spray-coated samples prepared for the Manufacturing Gate Review. No results could be measured for the sample produced by HVOF spraying. All samples tested with a 10 g load for 120 minutes. 24
Table 9: Measured oxide thicknesses of various surfaces after 3 days of 400°C, 1500 psi steam exposure. As in the supercritical water exposure, the sprayed surfaces exhibit a higher oxidation rate as measured via cross-sectional SEM. 24
Table 10: AREVA's Accomplishments 28

1.0 INTRODUCTION

This report provides the results of a 2 year effort by a team led by AREVA and funded by the DOE to develop nuclear fuel technologies that will enhance accident tolerance of present Light Water Reactor (LWR) fuel. This work includes the results of a Discovery Phase where a number of technology concepts were investigated. The Discovery Phase is the first part of a multi-phased research and development (R&D) program to identify, test, and select the best EATF pellet and cladding technology options for enhancing the performance of the present UO_2- Zircaloy standard fuel pellet cladding system under normal operating conditions, DB (small-break and large-break loss-of-coolant accidents, and BDB (severe) accidents, such as TMI-2 and Fukushima. Requirements were established for the development which included both regulatory, plant operator, and vendor requirements, and accident tolerance enhancement goals. The focus of this Discovery Phase was particularly manufacturability and performance. The Discovery Phase is the first of a three phase program to develop, test, license, and manufacture EATF Lead Fuel Assemblies (LFA). The second phase will complete development of the selected technologies, including the manufacturing processes and performance testing. It will also include establishing a plan to license the fuel and a plan to address the market aspects of selling and implementing EATF. The final phase will include the work to develop and license analytical model, generate licensing documents and obtain Nuclear Regulatory Commission (NRC) approval, and manufacture the LFAs. The general activities in each of these phases are shown in Figure 4.

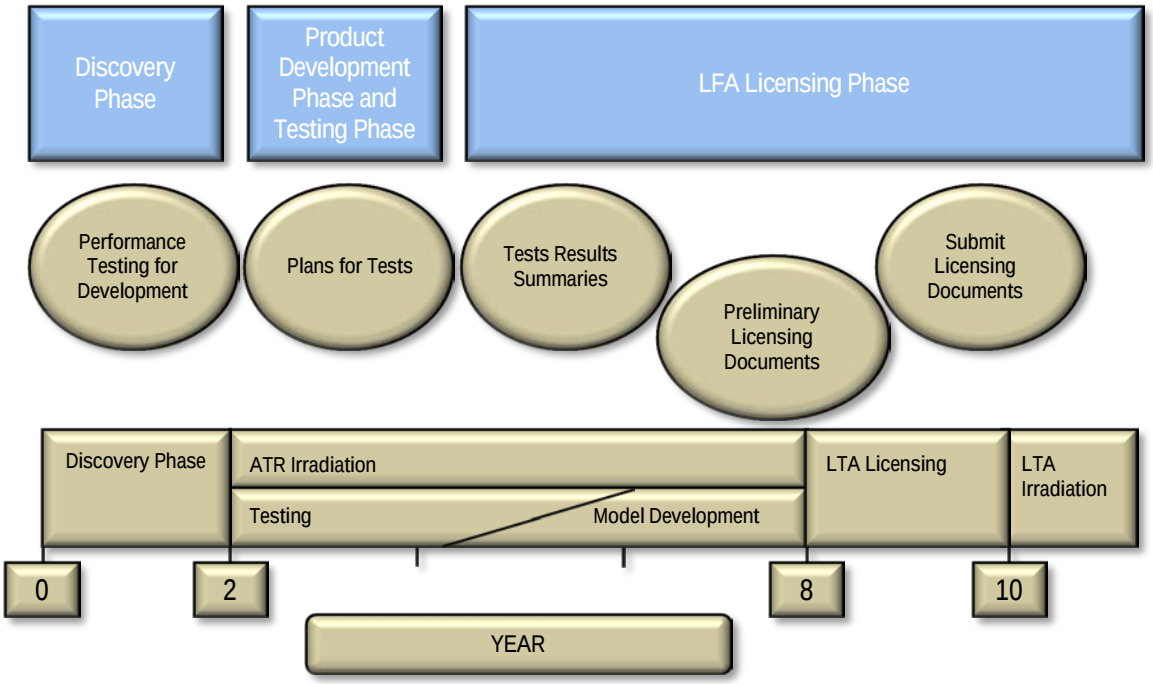

Figure 4: Enhanced Accident Tolerant Fuel Development Schedule

A process called the Gate Review (GR) was used to eliminate those concepts and technologies that did not prove to be able to meet the manufacturability and performance requirements and goals. This process is presented in Section 3.2 of this report.

Specific EATF enhancements considered by the AREVA team were:

- Improved performance in DB and BDB conditions.
- Reduced release to the environment in a catastrophic accident.
- Improved performance during normal operating conditions.
- Improved performance of the fuel if reactors operate under load following conditions.
- Equal or improved economics of the fuel.
- Improvements to the fuel behavior to support future transportation and storage of the UNF.

In pursuit of the above enhancements, EATF technology concepts that our team considered were:

1) Additives to the fuel pellets which included:

- Chromia doping to increase fission gas retention. Chromia doping has the potential to improve load following characteristics, improve performance of the fuel pellet during clad failure, and potentially lock up cesium into the fuel matrix.

- Silicon Carbide (SiC) Fibers to improve thermal heat transfer in normal operating conditions which also improves margin in accident conditions and the potential to lock up iodine into the fuel matrix.

- Nano-diamond particles to enhance thermal conductivity.

2) Coatings on the fuel cladding:

- Nine coatings on the existing Zircaloy cladding to increase coping time and reduce clad oxidation and hydrogen generation during accident conditions, as well as reduce hydrogen pickup and mitigate hydride reorientation in the cladding.

This document provides a report of the Discovery Phase of the AREVA Team's concepts for manufacturing, testing, licensing, and producing operationally and economically acceptable EATF. It also provides a preliminary business plan for manufacturing EATF as a viable commercial product and an assessment of the regulatory path to an EATF/LFA.

AREVA has been designing; manufacturing and testing nuclear fuel for over 50 years and is one of the 3 large international companies supplying fuel to the nuclear industry. In response to the DOE funded initiative to develop and deploy LFAs of EATF into a US reactor within 10 years, a team was put together to develop promising technologies for improved fuel performance. The team consisted of the University of Florida (UF) and the University of Wisconsin (UW), Savannah River National Laboratory (SRNL), Duke Energy and Tennessee Valley Authority (TVA), as depicted in Figure 5.

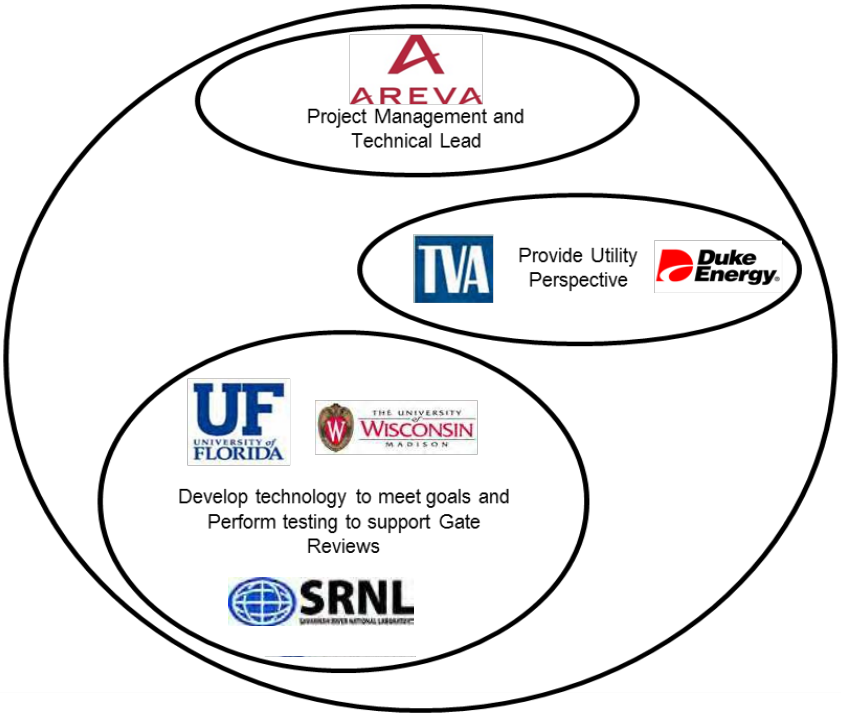

Figure 5: AREVA Team Composition

The following report documents the development in the Discovery Phase of the AREVA Team's concepts for manufacturing, testing, licensing, and producing operationally and economically acceptable EATF. The rationale for pursuing the particular technology concepts described herein to meet a 10 year schedule is presented in Section 2. Section 3 presents the development process and Section 4 presents the development results. A summary of the accomplishment in this phase of the development is provided in Section 5.

The details of the subjects presented in this report are contained in appendices. The following is a list of these and their contents.

APPENDIX	CONTENT
A	The matrix of requirements and goals for EATF covering the discovery phase through commercialization.
B	A draft business plan which evaluates the commercial viability of the proposed EATF. This is a living document and is improved and additional knowledge is gains on the technologies and processes necessary to produce EATF.
C	The record of the first Gate Review meeting held in September 2013.
D	The record of the second Gate Review held in April 2014.
E	Pellet development work by UF, testing, and results.
F	EPD work by UW, testing and results.
G	Spray Coating work by SRNL, testing, and results.
H	A report on using nano-particles injected into the emergency cooling water to enhance LOCA performance.
I	Impacts of changes to the fuel pellet and cladding coatings on the fuel energy extraction.

APPENDIX	CONTENT
J	Activities performed by UF and AREVA to prepare EATF pellets for irradiation experiments in the Advanced Test Reactor (ATR).
K	A draft of the EATF Test Plan which lists all the types of testing that will need to be performed to carry EATF through licensing and implementation.
L	List of publications, web sites and other information requested by DOE which resulted from this work.
M	Typical utility LFA acceptance criteria to be met when inserting EATF test assemblies into a commercial reactor.
N	A draft Regulatory Plan describing the licensing process and the steps required to license EATF.
O	A survey of possible effects of the additional materials on the fuel and its performance.
P	The Test Plan for the discovery phase of the work to use in assessing the performance benefits of EATF.
Q	An estimation by the AREVA fuel experts of the possible impacts of EATF changes on in-reactor fuel performance.

Table 1: Appendices Subject List

In summary, the AREVA Team was successful in identifying several technology candidates to enhance the accident tolerance of nuclear fuel. These candidates include the addition of SiC or nano-diamond to the fuel pellet by means of the SPS process and the application of a MAX Phase coating to the fuel cladding by the CS process. During the course of this work, a number of other significant things were accomplished that contribute to the effort of developing this fuel. These accomplishments are summarized in Table 2.

DESCRIPTION	ACCOMPLISHMENTS
FUEL PELLET	1. Pellets were successfully made using the SPS process. These included 10% by volume SiC particles, whiskers, or diamond. Process eliminates grinding to final size. 2. Optimum chromia content for large pellet identified. 3. Significant thermal conductivity improvement confirmed by measurements at Los Alamos National Laboratory (LANL). 4. Preliminary thermal conductivity as a function of displacements per atom established. This is to be confirmed by irradiation in the ATR. 5. Significant reduction in fission gas release estimated. This is to be confirmed by irradiation in the ATR. 6. Provisional costs for producing pellets with the SPS process were estimated. 7. The Master Sintering Curve for producing pellets of one size was defined.
CLADDING COATING	1. The EPD method of depositing Ti, TiO_2, Y_2O_3, YSZ, and Al_2O_3 was proven. 2. The CS method of depositing MAX phase coatings of Ti_2AlC was proven. 3. The High Velocity Oxy-Fuel (HVOF) method of applying coatings was eliminated. 4. TiO_2, YSZ, and Ti_2AlC coatings were selected for further development. 5. The EPD method of applying coatings was eliminated. 6. The wear resistance of the coatings was demonstrated. TiO_2 was 50% better than bare Zircaloy-4. Ti_2AlC was 10 times better. 7. The testing criteria were refined to cover 1) normal operation, 2) DBE, and 3) B-DBE. 8. It was shown that coatings are able to provide significant reduction in ZY oxidation for LOCA conditions. 9. It was shown that edge effects are a factor in the ability of the coatings to provide protection from oxidation. 10. Application of MAX Phase coatings by the CS method was demonstrated.

DESCRIPTION	ACCOMPLISHMENTS
PRODUCT DEVELOPMENT	1. A Requirements Matrix was completed to provide a complete overview of the development requirements for EATF nuclear fuel. This is organized by Manufacturing, Performance Testing, and Further Development. 2. A draft Regulatory Plan was generated defining the path to Lead Test Assembly (LTA) licensing and eventually batch implementation. 3. A draft Business Plan was generated defining the path to commercialization. 4. A draft Test Plan was generated to define the scope of testing required to develop, license and sell a new nuclear fuel. 5. The acceptance criteria for inserting a Lead Fuel Assembly into a commercial reactor were identified. 6. A general engineering review of the impacts of the EATF technology concepts on the fuel performance and licensing was performed. This included the effects of the new EATF materials used in the pellet and cladding coating. 7. Fuel pellets were manufactured for irradiation testing in the ATR. This will address irradiation effects. 8. Gate Reviews were held to focus the discovery phase of the development process.

Table 2: AREVA's Accomplishments

2.0 PROJECT SCHEDULE FOR EATF TO DEPLOY LFA'S WITHIN 10 YEARS.

The AREVA Team has a multi-phased approach to meet the R&D challenges of developing EATF that will improve the performance when compared to the standard UO_2 – Zircaloy system currently used by the nuclear industry. Under this approach, the R&D progresses from the conceptual stage through beginning of irradiation of an LFA in a commercial nuclear reactor within 10 years.

The initial discovery phase of the project considered all options that were viable to be matured and industrialized in a 10 year period. This Discovery Phase addressed the manufacturability of the EATF technology options that were under consideration. It also addressed major performance attributes such as improved reaction kinetics with steam, improved fuel properties, slower hydrogen generation rate, and improved cladding properties, including coatings.

Following the discovery phase a 2 year detailed development phase will mature the viable technologies allowing a final selection of the AREVA team concept that could be considered for deployment as a LFA into a commercial reactor.

Following the final selection of the AREVA Team EATF concept, the next 6 years matures the design and conducts performance testing that includes Advanced Test Reactor (ATR) irradiation, synthesis of ATR results, development and execution of the licensing strategy, and finalizing of the EATF design for Lead Fuel Assembly/Lead Test Rod (LFA/LTR) manufacturing. The final phase involves manufacturing the LFA/LFR.

The AREVA Team developed a Requirements Traceability Matrix (RTM), Appendix A, which was used in a Gate Review process to address the manufacturing and performance attributes of the EATF. The Performance Test Plan contains metrics for quantifying EATF enhancements that must be developed in conjunction with the safety features of LWR design for specific accident scenarios. Section 3.2 of this document provides further details on the GR process.

2.1. US NUCLEAR MARKET FOR FUELS.

The economics of fuel design make this DOE funded project very important to the nuclear industry. Even incremental changes to an existing fuel design can cost in the range of $100M to implement through to LFAs. If this money is invested evenly over 10 years and the cost of money is 7% then it can take the fuel vendor several decades after the start of the project to reach a breakeven point on the initial investment. Step or radical changes to a fuel assembly design can cost upwards of $500M and take even longer to reach the breakeven point for a fuel vendor.

Currently there are 100 operating reactors in the US operating in 32 states (Figure 6). These reactors are supported by an established nuclear supply infrastructure that supplies fuel, services and new equipment to the utility operators.

Figure 6: Operational Reactors in the US

Based upon current market trends in the nuclear industry it can be expected that the current fleet of reactors (assuming all reactors apply for life extension to 80 years) will start to shut down starting 2050 and all will be shut down by 2070 (Figure 7).

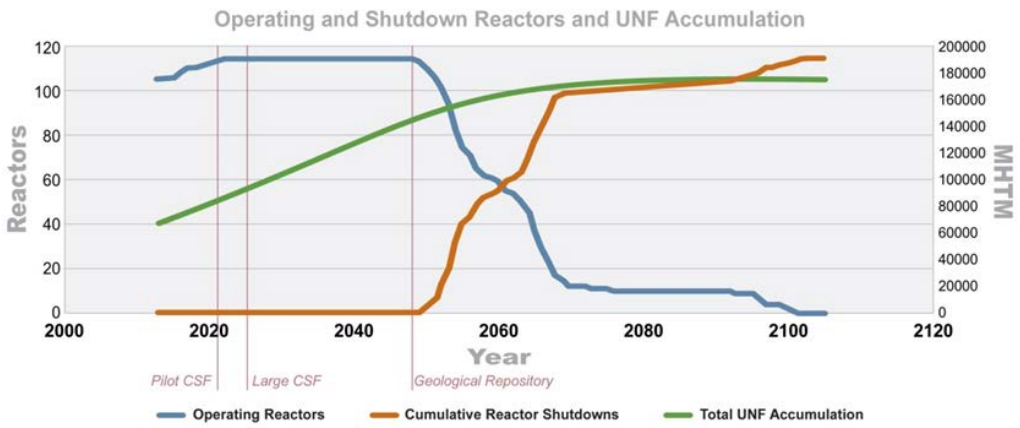

Figure 7: Projected Operational Reactors in the US Assuming Life Extensions to 80 years

For a fuel developer, this is a dilemma. The operational reactors in the US are projected to be operational for the next 25 years before there is a decline in the size of the market for nuclear fuel. On the other hand based on a lead time of at least 16 to 20 years to bring a new fuel design to market and the additional time required to recover the large investment in a declining market, there is a disincentive to invest heavily in radical design changes. Realizing that the current fuel designs are considered safe, it is clearly necessary for DOE to take a leadership role for the US reactor fleet and invest in new fuel designs to ensure that the current operational fleet of reactor can benefit from improved and enhanced fuel performance over their remaining years of operation. The preliminary business case for the EATF program is provided in Appendix B of this report.

3.0 DEVELOPMENT PROCESS FOR THE DISCOVERY PHASE

EATF needs to tolerate the loss of active cooling in the reactor core for a longer time compared to the UO_2 – Zircaloy fuel system while maintaining or improving fuel performance during normal operations, operational transients, Design Basis Event (DBE), and Beyond Design Basis Event (BDBE). The fuel should also consider future trends in the nuclear industry such as the move from base load to load following and the EATF should, if possible, exhibit improved performance for long term storage, transportation, and geological disposal.

To ensure all of the many nuclear fuel design requirements and EATF goals are met while minimizing development time and expense, a number of reference documents for the development process were established. These include:

1. A Requirements Matrix to summarize and organize all of the regulatory, plant operator, manufacturing, and performance requirements.
2. A GR process to guide the technology concepts development relative to the requirements.
3. An initial business plan to ensure the new EATF is commercially viable.
4. A testing plan to identify the testing needed to support model development, licensing, and prove performance.
5. A Regulatory Plan to identify the path to license a LFA.

Each of the key development process components is described in more detail in the following sections.

3.1. REQUIREMENTS TRACEABILITY MATRIX

A team comprising AREVA, Duke Energy, and TVA developed a RTM containing design requirements and goals for EATF based on sources that includes regulatory requirements, plant operator requirements, and fuel vendor requirements. Beyond this, there are also additional EATF design goals that were established to optimize fuel performance and reduce risk.

The RTM divides requirements into groups based on the EATF development phases, which include:

- Manufacturability
- Mechanical Performance
- Lead Fuel Assembly
- Batch Implementation

The RTM is provided in Appendix A. The following are provided by this matrix for each requirement or goal.

- Source of each requirement or goal
- Applicability to the
  - Fuel Pellet
  - Cladding
  - Cladding coating
  - Fuel pellet dispersoid or additive
- Applicability to the initial phases of manufacturing and performance testing

3.2. GATE REVIEW PROCESS

During the initial discovery phase of the project AREVA took the decision to be relatively hands off and allow our university and National Laboratory Partners to be free thinking and consider options that would not be constrained by preconceived ideas from the fuel vendor. To counter this and to keep the partners focused, the GR process was utilized.

AREVA uses a GR development process for all new technologies considered by the company for development and future deployment. The GR process is employed to focus R&D work on the most promising technology candidates. During the Discovery Phase, the initial GR process was rigorous enough to accommodate the options considered by the universities and National Laboratory and focus resources onto promising technologies to reduce costs and identify the technologies that would potentially be carried forward to LFA. This approach is shown in Figure 8.

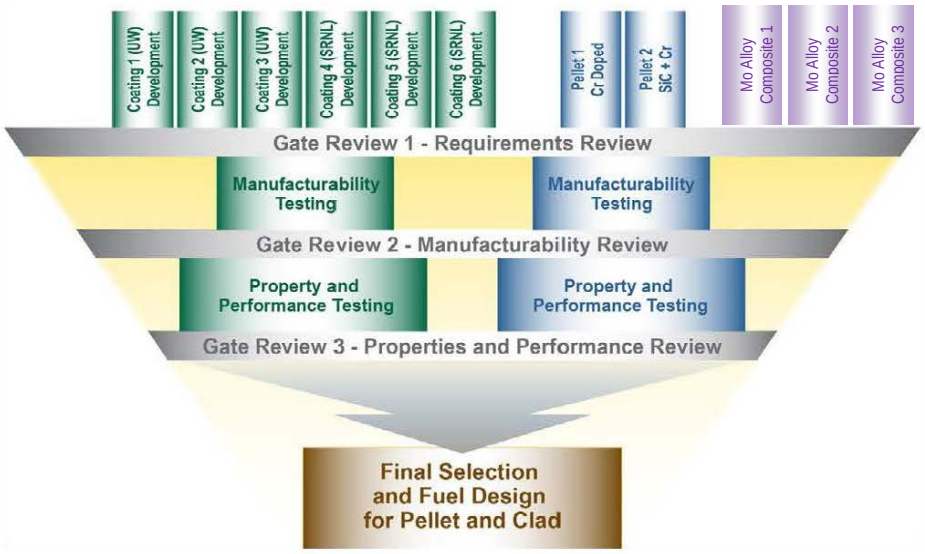

Figure 8: AREVA Gate Review Process for EATF

The appropriate requirements from the Requirements Traceability Matrix were used for guidance by the GR Board. In addition, performance test requirements, presented were used to evaluate technical concepts performance.

During the Discovery Phase of the project, the GR process addressed the following:

- Manufacturability (Manufacturing Discovery Phase)
- Mechanical Performance (Mechanical Performance Evaluation Discovery Phase)
- Test rods for Irradiation in a test reactor

The results of the two GR Board Meetings are provided in Appendices C and D.

3.3. PRELIMINARY BUSINESS PLAN

The success of EATF will depend on a business plan that can yield a high probability of commercial success. This requires a schedule, development and licensing plans, an experienced vendor, and potential customers that all contribute to the document. Since the AREVA team is still in the selection phase of the final EATF design, the business plan will be a living document. The document, as it stands at the end of Year 2, is presented in Appendix B and described briefly below.

One of the key elements in this plan is to introduce innovative features into commercial use that are incremental changes to the present fuel. AREVA has successfully done this with several innovations, namely the Mixed Oxide (MOX) fuel LTAs, the M5® Zirconium alloy fuel rod cladding, the Advanced Mark BW 17x17 fuel assembly, the ATRIUM™ 10XM Boiling Water Reactor (BWR) fuel assembly, and Chromia-doped pellets. This provides confidence that AREVA will be able to address all of the design and licensing issues that will be seen in EATF development program.

AREVA is also familiar with factors that affect fuel costs, including the costs of enriched uranium and fuel assembly manufacture. There are also issues that will affect the success of EATF, such as changing the operation of the current reactor fleet from base load to load following. This in turn will affect the safety margins and make-up of the fuel to accommodate this changed mission.

Finally, the AREVA financial plan will determine the value of each of the EATF enhancements to nuclear utilities customers in the areas of fuel limits that affect both the Limiting Safety System Settings (LSSS) and Limiting Conditions for Operation (LCO) Technical Specification Limits. The benefits of improving these limits will be identified in terms of fuel cycle cost improvements and power uprate capability.

More importantly, during the next phase of the project the cost to implement the proposed technology enhancements will begin to be quantified. This will include the cost of production of the pellets and the clad, effects of the rate of production of the pellets and the clad, and throughput of fabricating the fuel assembly. Utilities will be engaged to determine what would be an acceptable variance in the cost of the new EATF concept compared to the current Zircaloy-UO_2 fuel.

3.4. TEST PLAN AND DOE SUPPORT TO FUTURE TESTING

A range of testing will be required in the development of EATF. Performance testing has been developed in conjunction with Idaho National Laboratory to quantify the EATF accident performance improvement. This provides a common set of tests to follow when evaluating EATF performance improvements of different technologies. A summary of the present status is provided in Appendix P.

All the industry teams, universities and national laboratories developing EATF concepts are conducting the same test using different test equipment and test conditions. This makes it very difficult to compare and contrast results of testing. AREVA strongly commends the DOE effort to have Idaho National Laboratory to identify test conditions for Beyond Design Basis Events and to provide the Oak Ridge National Laboratory test facility for conducting those tests. AREVA also recommends the restart of the TREAT facility to measure the effectiveness of the EATF concepts.

Beyond this, data will be needed for model development and licensing. This testing is much more extensive and has a different objective than the performance testing in Appendix P. The EATF Test Plan is provided in Appendix K. This provides the scope of testing and will be refined to specify specific testing quality assurance (QA) requirements, and results required as the development moves into the licensing phase.

TESTING IN REACTORS

The AREVA team supports testing of EATF concepts in the ATR and subsequent Post Irradiation Examination (PIE) inspections. At the same time, DOE is encouraged to examine the use of the Halden Reactor to test at least one new clad type and one new pellet design, SiC/Chromia-doped pellets.

DOE R&D FACILITIES REQUIRED FOR PHASE

AREVA strongly encourages DOE to continue with the preparation for the restart of TREAT and to enter into discussions with the industry teams to determine a common set of critical test facilities required to start collecting data to support advanced modeling for licensing and design of the EATF. This should leverage existing industry R&D facilities.

3.5. REGULATORY PLAN

The purpose of the regulatory plan (Appendix N) was to provide the approach to introducing the NRC to the AREVA Team's EATF changes and the resulting licensing issues to ensure that the licensing of EATF goes as smoothly as possible. It also helps identify the testing and analytical models that will be required to support licensing.

AREVA has extensive licensing and regulatory experience as evidenced by successfully licensing LFAs for numerous commercial nuclear fuel assemblies, such as the recently developed MOX and High Thermal Performance (HTP) fuel assemblies. AREVA is confident it can achieve the 10 year development, licensing, and regulatory schedule envisioned for the EATF LFA/LFR.

The EATF goals presented to the NRC will include accident performance goals discussed in the Requirements Traceability Matrix (Appendix A). Other goals include minimal impact on operation, minimal cost impact, and acceptability to both the utility and vendor.

The plan will also present the technology being pursued, the EATF Program schedule, the accidents impacted, the anticipated benefits, experimental data, analytical codes and methods, and progress to date.

The plans for testing will be made available as they are developed. As the test results become available, they will be incorporated into preliminary licensing documents and provided to the NRC.

The process used by a utility to implement fuel changes is provided in Appendix M, "Typical LFA/LFR Acceptance Review Requirements".

Finally, a formal licensing submission for an LFA will be sent to the NRC. Informal or formal feedback will also be sought from the NRC to aid in future program planning.

As depicted in Figure 9, the regulatory plan involves a multi-phased development process that will introduce the EATF concept to the NRC and progress to a LFA within 10 years. The regulatory plan activity features three phases starting with the Discovery Phase in years 1-2, the Product Development and Testing Phase in years 2-3, and the LFA Licensing Phase in years 4-10. The process includes:

- Presenting requirements and accident performance goals in the EATF Requirements Traceability Matrix (Appendix A)
- Developing and testing technology options for fuel pellets, cladding, and cladding coatings
- EATF program schedule
- Evaluating accidents impacted and the anticipated benefits of the EATF

- Experimental data from development and testing
- Analytical codes and methods
- Progress to date
- Test plans as they are developed

Part of the licensing process will involve establishing the applicability of the computer codes and models to reliably predict the behavior of the reactor and the fuel under all conditions, including normal operation, anticipated transients and DB accidents. Developing these models requires a mathematical model of the processes occurring in and around the reactor, and the evaluation of the data necessary to adjust and benchmark these models. Four main technical areas related to fuel licensing will be discussed. These include nuclear, thermal, accident, and fuel mechanical performance.

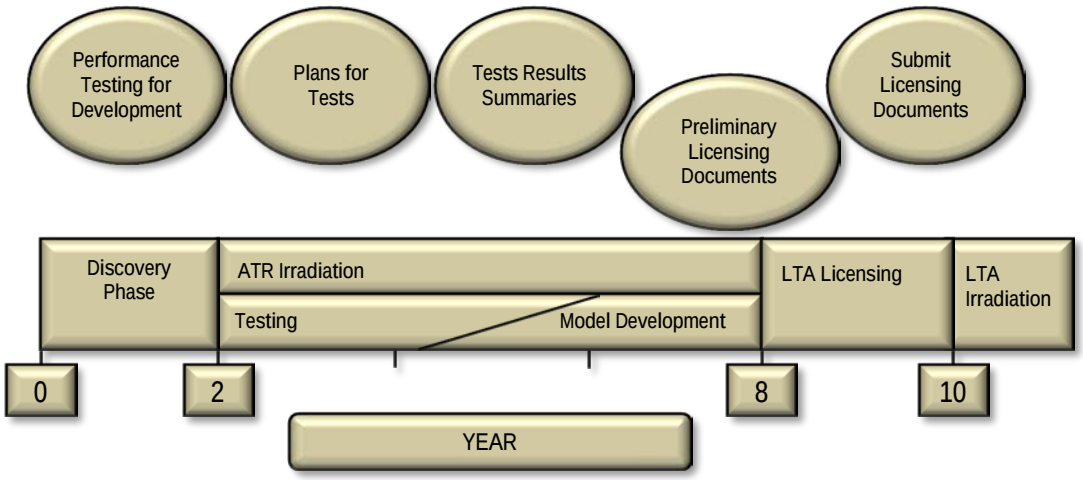

Figure 9: Enhanced Accident Tolerant Fuel Regulatory Plan

The plan includes the generation of a number of topical reports and supporting analyses to address all of the following:

- Fuel Design
- Neutronics Reload Analysis
- Power Distribution Control
- Fuel Rod/Fuel Assembly Bow
- Setpoints
- Reactivity Initiated Accident (RIA)
- Large Break Loss of Coolant Accident (LOCA)
- Small Break LOCA
- Non-LOCA
- Chapter 15 Events (Transient and Accident Analysis)
- Anticipated Operational Occurrence (AOO)
- Stability Analysis Methodology (STAIF)
- Delta over Initial Versus Oscillation Magnitude (DIVOM)
- Analysis of Anticipated Transient Without Scram (ATWS)
- Instability

4.0 DISCOVERY PHASE RESULTS

This section details fuel pellet and cladding manufacturing activities (process description and materials used) and the rationale behind particular process parameterizations. It also describes performance testing of the pellets and cladding materials and summarizes the test results. The reasons certain technologies were chosen for further development and the reasons others were dropped from further development are also presented.

4.1. FUEL PELLETS

The EATF designed by the UF introduced a high thermal conductivity additive to UO_2. The additive materials employed were silicon carbide whiskers (SiC(w)) and powder. UO_2 – SiC composite fuel was shown to have the ability to increase the thermal conductivity of the pellets by up to 40%. Increasing the thermal conductivity of the fuel allowed for a decrease in fuel temperature as well as a more uniform radial temperature gradient through the pellet. Moreover, the decreased temperature gradient reduced thermal stresses and cracking in pellets [2]. In addition, during accident scenarios, an increase in thermal conductivity decreased the amount of stored thermal energy resulting in a reduction in the peak cladding temperature. Simulations using the FRAPCON computer code for fuel with increased thermal conductivity revealed a ~ 250°C decrease in fuel centerline temperature. Additionally, the increase in thermal conductivity allowed for approximately 100°C decrease in average fuel temperature. These decreases allowed for improved LOCA response with minimal fission gas release.

The Spark Plasma Sintering (SPS) process was used to add Silicon Carbide particles (SiC(p)), whiskers, nano-diamond particles, or chromia to the UO_2 pellet. This process required a recipe called a Master Sintering Curve (MSC). The materials were mixed with a specific process and placed in a die. The size of the die showed specific effects on the pellet produced. This process was developed and used to produce pellets for the ATR irradiation experiments. This section describes the SPS process, the additive materials, the Master Sintering Curve, the mixing process, the SPS die size, and the ATR pellet results.

4.1.1. SPARK PLASMA SINTERING

SPS or Field Assisted Sintering Technique (FAST) is an advanced manufacturing process that allows the rapid sintering of a variety of materials, particularly, difficult-to-sinter ceramics and metallics. This process provides the potential to manufacture pellets at lower cost than the standard process due to the decreased time and energy requirements. Due to the fact that conventional sintering methods were not able to achieve industry standards for the advanced composite UO_2 fuels, SPS was utilized. This process is compared with conventional sintering in Figure 10. While conventional sintering can only produce composite pellets with <90% density, the SPS process can produce composite pellets with at least 95% density. The SPS process is presented in detail in Appendix E.

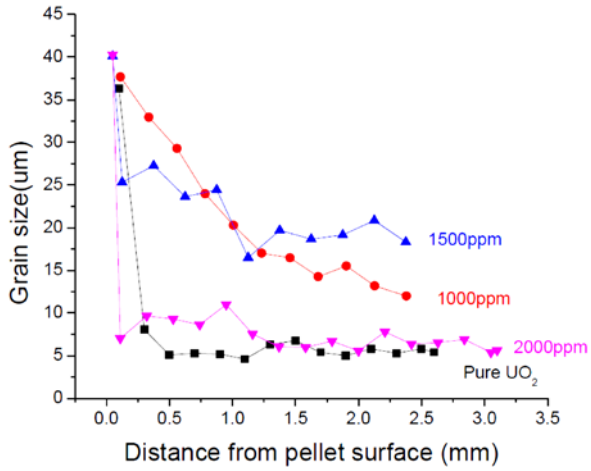

Figure 10: Comparison of Conventional Sintering and Spark Plasma Sintering

4.1.2. MATERIALS ADDED TO PELLETS

Several additives were considered, along with a dopant. Silicon carbide (SiC) was the initial additive chosen for the EATF fuels. Silicon carbide has long been considered a prime candidate for use as a fuel matrix material, cladding, and as a fuel-particle diffusion barrier. This is due to a low neutron cross section, high thermal conductivity, chemical stability (strong resistance to oxidation in air and air-moisture environments), and high melting temperature. SiC also has the advantage of being non-toxic over alternatives such as beryllium oxide [2]. Both SiC(p) and SiC(w) were considered for the fuel. The effect of SiC additives on thermal conductivity is shown in Figure 11.

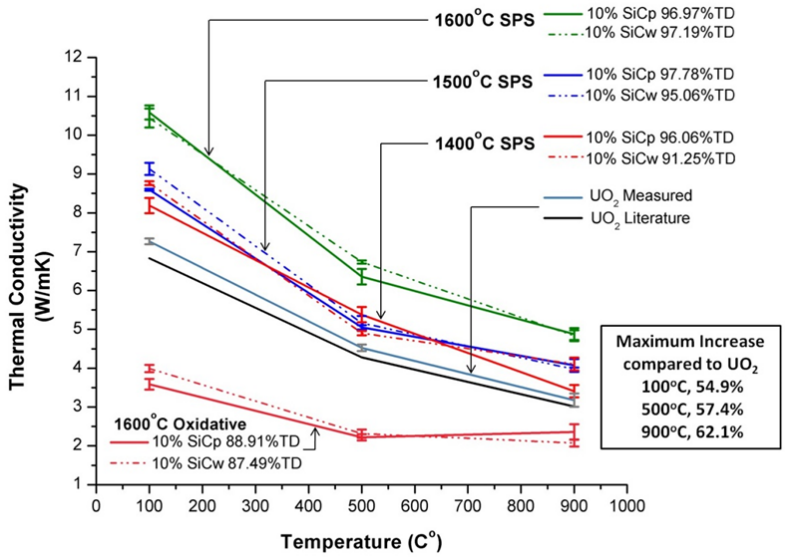

Figure 11: Thermal conductivity of various sintered UO_2 – 10vol%SiC pellets

Nano-diamond was also considered due to its chemical inertness, very small neutron cross section, and superior thermal conductivity. Figure 12 shows each of these additives.

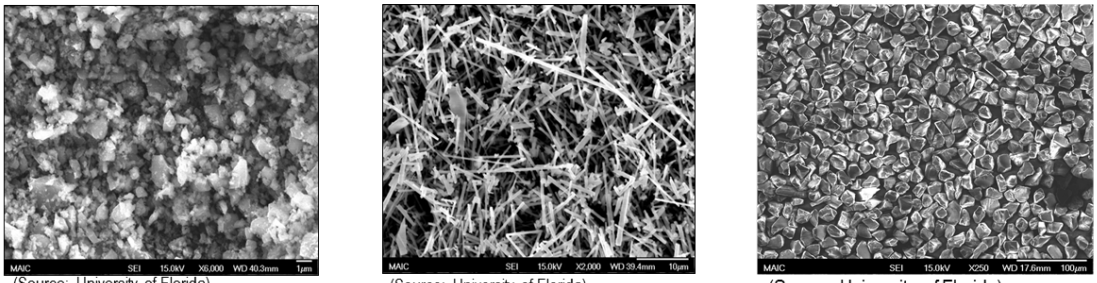

(Source: University of Florida)
SiC powder with a mean diameter of 1 µm

(Source: University of Florida)
SiC Fibers with a mean diameter of 0.65 µm and a mean length of 10 µm

(Source: University of Florida)
Diamond with a mean diameter of 12 µm

Figure 12: Fuel Pellet Additives

It has been shown that an increase in a fuel's grain size can decrease the rate of fission gas release within the fuel. To promote grain growth within UO_2 fuel, a dopant of chromia (Cr_2O_3) was used. The influence of the Cr_2O_3 concentration on the density of the sintered pellets was studied. The results of this study are shown in Figure 13. As shown in the graph, the density of the sintered UO_2 chromia pellet is generally decreased as doping amount is increased.

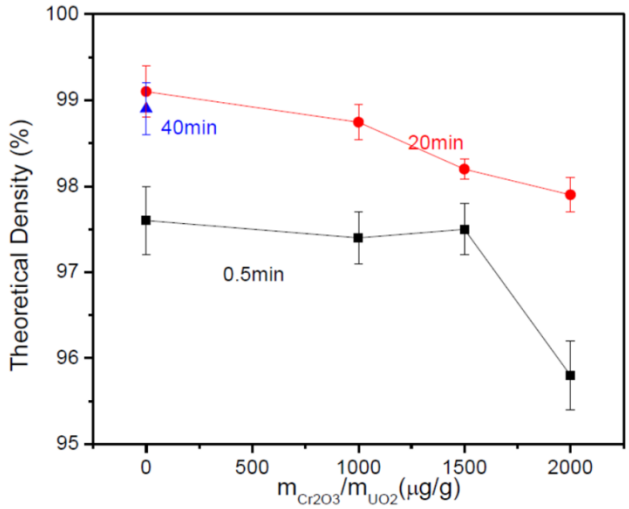

Figure 13: Sintered pellet density as a function of Chromia concentration

It was found that the high grain size was found at the outer surface of the pellet and that there was a large gradient in grain size through the length of the pellet. This fact is evident in the graph of grain size versus distance from pellet surface seen in Figure 14. Although there is a significant drop in grain size in the interior of the pellet, the doped pellets still were able to achieve grain sizes much higher than pure UO_2. It was determined that 1200 to 1600 ppm by mass was the optimal level of chromia dopant for UO_2 pellets sintered by SPS to promote grain growth.

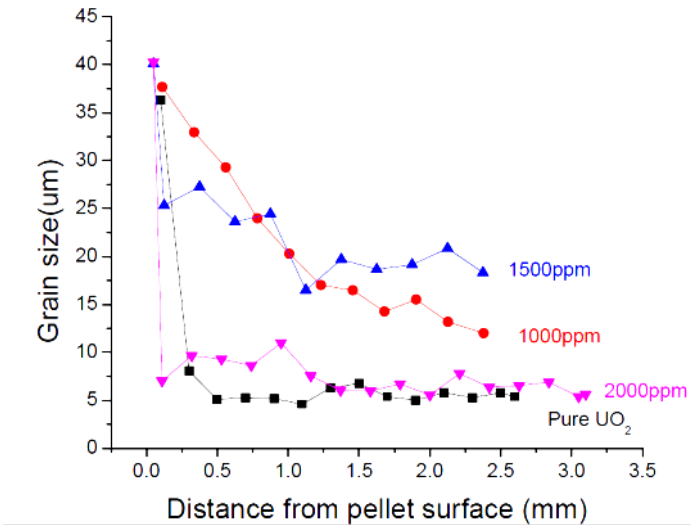

Figure 14: Graph of axial variance of grain size in dope UO_2 pellets sintered at 1600°C for 30 seconds

4.1.3. MASTER SINTERING CURVE

The MSC is a sintering model which describes the empirical relationship between the evolution of densification and the microstructure. This curve is the "recipe" used by the SPS to process acceptable pellets.

MSC theory has been applied successfully to UO_2 and UO_2-SiC composite ceramics sintered by SPS. Utilizing just one temperature and time dependent parameter, the work of sintering, the densification process was quantified. The activation energy for SPS has been determined to be 140 KJ/mol for UO_2 and 420 KJ/mol for UO_2-SiC composite. The master sintering curve is proven to be an effective tool to describe the densification behavior of UO_2 and UO_2-SiC powder compact during SPS. The ability of MSC to control and predict density has been demonstrated by experimental runs using the isothermal method. It should be noted that the MSC work done in the Discovery Phase 1A was for 15x15 dimension fuel. MSCs will be constructed for 17x17 dimension fuel to quantify the densification behavior of the smaller diameter Mark C fuel pellet.

4.1.4. ATR IRRADIATION EXPERIMENT PELLETS

In accordance with the EATF project, the pellets were fabricated with enriched UO_2 intended for irradiation in the ATR. Work was done to fabricate, characterize, and maintain quality control of ATR sized fuel pellets. The ATR rodlets required pellets to be placed in 17x17 nuclear fuel assembly cladding. This size required pellets to have a diameter of ~7.8mm, much smaller than the 12.5mm pellets that had been fabricated previously. Additionally, following work done on a Nuclear Energy University Program (NEUP) for the development of a UO_2 – Diamond composite fuel, the UF felt that UO_2 – Diamond pellets also had favorable thermal properties and should be included in AREVA irradiation tests in the ATR. Pictures of these pellets are shown in . One of the rodlets successfully fabricated at INL is shown in Figure 16.

Figure 15: 17 x 17 sized Pellets for Irradiation in the ATR

Figure 16: Rodlet with EATF Fuel Pellets Fabricated for Testing in the ATR.

During the production of the ATR pellets many challenges were encountered. In particular, the transitioning from 15x15 fuel dimensioned pellets to 17x17 ATR size pellets proved difficult. The sintering profiles defined for the 15x15 fuel pellets were not applicable for the 17x17 fuel pellets and sintering parameters had to be actively determined during production. In addition, many pellets at the 17x17 size were seen to delaminate, break, and chip. Many factors were thought to have caused these issues including pre-sintering powder preparation (mixing, drying, particle size), and the 17x17 die tooling.

4.1.5. MIXING PROCESS

The effect of mixing additives into UO_2 powder was studied to better understand the failure modes experienced during the production of pellets for the ATR. The possibility that the mixing procedure may contribute to negative effects was first proposed during some of the early testing where the failure to sinter pellets with the SiC powder additive was observed. The parameters of the mixing process studied were the effects of mixing time, steel balls and mixing aid on pellet sintering behavior. The detailed investigation is presented in Appendix E. In summary, the exact nature of the failure mode introduced by mixing aid should be investigated specifically the dark spots on scanning electron microscope (SEM)

images and the bright spots in the powders that used steel balls. Furthermore, the effect of mixing time on other powder properties such as surface area and porosity may provide a greater understanding of sintering behavior and failure mechanisms. Also a comparison of the mixing time on the thermal conductivity (TC) of additive powders would be informative. Given particle size and matrix material, interfacial bonding is the largest variable that may be altered. Further investigation on ensuring the effect of mixing time on TC will be helpful. Further investigation on ensuring removal of mixing aid after mixing is also planned.

4.1.6. SPS DIE SIZE

It was found during the manufacturing of the 17x17 ATR pellets that the graphite die and punch used in SPS was not able to reach high temperatures without failure. A large current was necessary to achieve high temperatures required for sintering. Because of the small diameter of the 17x17 fuel pellet, there was a large localized current density found in the punches. This large current density created very high temperature zones and caused the punches to deform and bow. This phenomenon was observed at approximately 1400°C. To try to overcome this problem in future 17x17 SPS processing, a study was conducted on the die size and on the punch shape to reduce the current density in the punches.

Chips and cracks resulted from high thermal radial gradients during sintering. Because of this, the smallest die outside diameter (OD) was the most favorable. However, to maintain a safe loading of the sample in the SPS furnace the die OD was increased to 0.944” to withstand pressures of the sample on the die wall. 0.944” was three times the 17x17 pellet diameter, meaning that the die walls were the same thickness as the sample itself. Using these smaller thickness dies, resulted in successful sintering of high density full size UO_2 – SiC(w) and UO_2 – Diamond 17x17 pellets, as shown in Table 3.

Pellet Type	Average Density (%TD) (die OD = ~1.5”, ATR production)	Average Density (%TD) (die OD = 0.944”)
UO_2 – SiC Whiskers (1400°C)	94.4%	95.6%
UO_2 – Diamond (1350°C)	95.3%	96.1%
UO_2 (1150°C)	96.5%	97.1%

Table 3: Difference in average density of sintered pellets for a die OD of 0.944”

Once the optimal die size was set at 0.944”, a novel punch shape was tooled to mitigate the problem of high current density. A “lipped” punch was designed as shown in Figure 17 to direct more of the current through the die wall as opposed to directly through the sample.

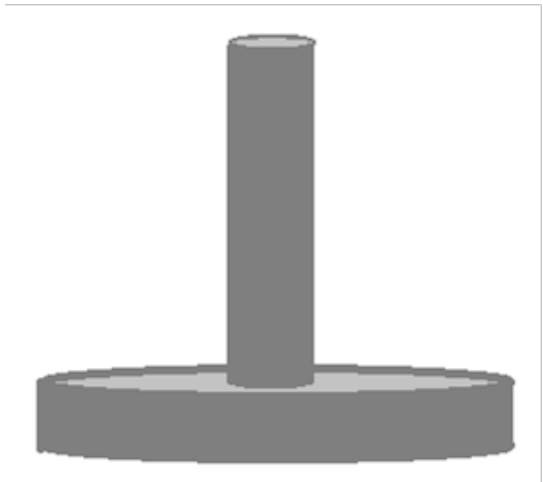

Figure 17: "Lipped punch" used to try to reduce the current density through the punches

All pellets sintered with the lipped punches were shown to have an increased density relative to those sintered with regular cylindrical punches. Material characterization needs to be performed to ensure that the pellets produced will have uniform microstructure throughout the pellet regardless of the asymmetrical set up.

4.1.7. CONCLUSIONS

The University of Florida has successfully proven that the SPS process is physically viable for the sintering of composite fuels. UF was able to fabricate and characterize UO_2 – composite pellets at the 15x15 size and conclude that high density, high thermal conductivity pellets were achievable. A MSC was constructed for 15x15 size fuel for both UO_2 and UO_2 – SiC. Work is underway and will be completed to create an MSC for 17x17 size fuels for both pure UO_2 and UO_2 – composites. The production of 17x17 fuel pellets for irradiation in the ATR exposed challenges with transitioning from 15x15 to 17x17 dimensioned fuel pellets fabricated by SPS. Because of this, work was done to determine the cause of defects in many of the 17x17 dimensioned fuel pellets. Mixing time, mixing agent, particle size, and powder drying were investigated to determine their effect on sintering behavior of 17x17 fuel. In addition, novel concepts of punch shapes and die sizes were studied to determine their influence on sintering and pellet quality. Further work is to be completed in the area of 17x17 production fuel pellets, and the determination of the economic viability of the SPS process.

4.2. CLADDING COATINGS

The main goal of coating Zircaloy fuel cladding is to reduce cladding oxidation and hydrogen generation during accident conditions. Table 4 shows a number of efforts, including both the coating material and the process for applying the coating. Of the many possible materials and coating processes, EPD was selected for use with 5 coating materials and CS and High Velocity Oxy-Fuel for use with two other coating materials. Each process had certain positive attributes. EPD has been used to apply thin, uniform coatings, which is a key requirement for nuclear fuel cladding coatings. High Velocity

Oxy-Fuel (HVOF) can produce dense coatings to reduce the potential for oxidation of the cladding. Unlike HVOF, CS does not induce substantial phase transformation in the substrate. The coating materials were chosen to be compatible with the specific deposition process, to provide robustness in the nuclear environment, and have a relatively small neutron cross section.

Coating	Application Process
TiN	Pulsed Laser Deposition
Multi-layer TiN	Hollow Cathode Discharge
SiC	Chemical Vapor Deposition (CVD)
$MoSi_2$	High Velocity Oxy-Fuel
Cr_2O_3	Reactive Radio Frequency Magnetron Sputtering
Cr_2O_3	Plasma Assisted Chemical Vapor Deposition (PACVD)
Ti	Electrophoretic Deposition
TiO_2	Electrophoretic Deposition
YSZ	Electrophoretic Deposition
Ti_2AlC	Cold Spray
Ti_3AlC_2	Cold Spray
Cr_2AlC	Cold Spray

Table 4: Cladding Coatings and Coating Processes Previously Investigated

The EPD process and the coating materials investigated are described, along with the results of the investigations and the GR Board recommendations in Section 4.2.1. The spray processes used for the MAX Phase coatings will be presented in Section 4.2.2.

4.2.1. ELECTROPHORETIC DEPOSITION PROCESS

Initially five different nanoparticles were used to make EPD coatings; Ti, TiO_2, YSZ, Y_2O_3, and Al_2O_3.

Table 5 shows the sizes of the nano-particle materials initially investigated.

Nanoparticle Thickness
Ti (60-80 nm)
TiO_2 (50 nm)
YSZ (200-300 nm)
Y_2O_3 (32-36 nm)
Al_2O_3 (40-80 nm)

Table 5: Initial Electrophoretic Deposition (EPD) Coatings Investigated in this Study

The EPD process is easily capable of coating Zircaloy tubes using the apparatus shown in Figure 18. Details of this process are provided in Appendix F.

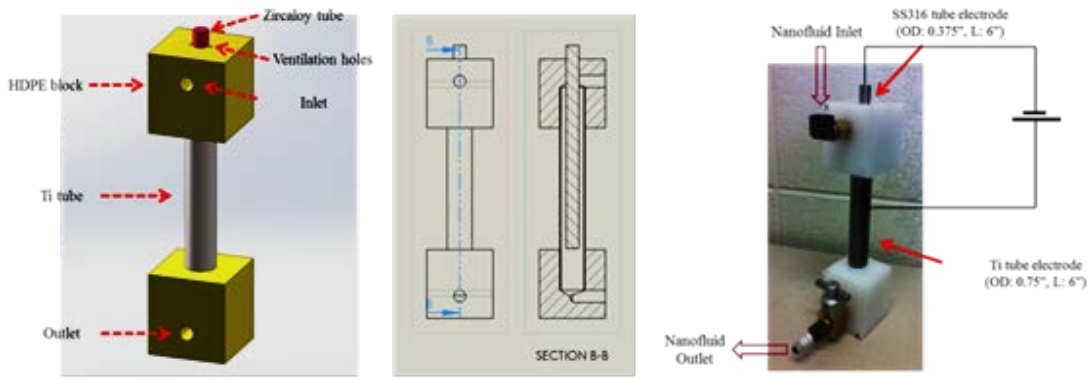

Figure 18: The detail design of the tube-geometry coating apparatus and the fabricated apparatus. The titanium tube and the Zircaloy tube sample serve as electrodes, electrically isolated via HDPE High Density Polyethylene (HDPE) mounting blocks and connected via external wires (not shown) to a direct current power supply.

HEAT TREATMENT

Heat treatments were used to achieve better adhesion between the coating material and the substrate. First, air furnaces were used unsuccessfully. This resulted in either oxidation of the cladding or cracking of the cladding, depending whether air or argon was used as the fill gas. Laser surface treatments were tried since it offered the possibility of a localized thermal exposure. An extremely sensitive threshold between essentially "no effect" and "complete ablation" was discerned for most laser settings, with only one parameter set producing visible modifications of the EPD coating without any ablation. SEM characterization of this parameter set indicates that, even then, laser sintering of current EPD coatings occurs only in extremely local regions of the treated area. In the end, no viable method was found to heat treat the coatings.

MECHANICAL PERFORMANCE

Without heat treatment, pin-on-disk wear tests showed that the average volume lost was greater than 0.032 mm^3 as compared to bare Zircaloy which showed less than 0.017 mm^3 lost, as shown in Table 6.

Treatment	Coating Material	Avg. Width (±µm)	Avg. Depth (±µm)	Avg. Volume Lost (mm^3)
HT	TiO_2	673.21 ± 44.43	13.65 ± 1.30	0.0937
HT	TiO_2	695.65 ± 64.92	11.31 ± 1.61	0.0822
HT	YSZ	640.40 ± 88.89	11.32 ± 4.73	0.0743
HT	YSZ	621.90 ± 40.96	11.89 ± 2.52	0.0794
LS	TiO_2	590.79 ± 49.29	4.926 ± 3.13	0.0352
LS	TiO_2	646.54 ± 80.47	4.564 ± 3.67	0.0346
LS	YSZ	653.14 ± 72.17	6.021 ± 3.03	0.0455
LS	YSZ	603.85 ± 70.91	4.452 ± 6.84	0.0321

Table 6: EPD Pin-on-Disk Results

GATE REVIEW RESULTS

Due to the poor mechanical performance, the EPD process was dropped from further development per the recommendation of the GR Board in April 2014.

4.2.2. SPRAY PROCESSES

Savannah River National Laboratory (SRNL) selected the carbide powder compounds, Ti_2AlC and Ti_3AlC_2/Ti_3SiC_2 as MAX Phase coating candidates based on their good thermal conductivity, elevated temperature ductility, fracture toughness, weldability, high temperature mechanical stability, chemical stability, and high resistance to chemical attack.

SRNL and UW were using spray methods to produce coatings of a MAX phase, specifically Ti_2AlC. ("MAX" is a contrived acronym for a set of compounds with the chemical formula Mn+1AXn, where n = 1, 2, or 3, and where M = early transition metal, A = group A element, and X = carbon or nitrogen.) Advantages of the MAX phase included a high thermal conductivity and a coefficient of thermal expansion that was close to that of Zircaloy.

Spray coating methods used by SRNL/UW included the HVOF and the CS Processes. The benefits of each of these spray methods is summarized in Table 9.

Spray Process	Description
HVOF	Previous successful applications of the High Velocity Oxy-Fuel (HVOF) process provided confidence that it would be a viable candidate for the EATF cladding coating application. In this process, the coating material in powder form was injected into the gas stream from a controlled feeder, where it is heated and accelerated as it is exiting the nozzle. The material stream impacted the work surface to form a solid homogenous coating. The HVOF velocity was much higher than other application methods and resulted in higher quality coatings in terms of bond, wear, and corrosion.
Cold-Spray	CS is a relatively new process that does not heat up the powders and, therefore, maintains the chemistry of the MAX powders and their superior properties after deposition onto a substrate. CS is a high kinetic thermal energy coating process. It follows the trend of increasing particle spray velocity and reducing particle temperature as with the HVOF process but to a more extreme level. The CS process uses the energy stored in high pressure compressed gas to propel fine powder particles at very high velocities (500 - 1500 m/s). Compressed gas (usually nitrogen or helium) is fed via a heating unit to the gun where the gas exits through a specially designed nozzle (Laval type convergent-divergent nozzle mostly) at a high velocity. Compressed gas is also fed via a high pressure powder feeder to introduce powder material into the high velocity gas jet. The powder particles are accelerated and moderately heated to a certain velocity and temperature where on impact with a substrate they deform and bond to form a coating. As with the other processes a fine balance of particle size, density, temperature and velocity is important for producing the desired coating properties.
Particle Vapor Deposition	Provides good control over coating thickness, which reduces the fuel cycle economic penalty. Presently used by the CEA and EPRI to coat cladding.

Table 7: Benefits of Each Spray Process

Difficulties were encountered with the high velocity oxy-fuel process both within the coating/substrate and in the spray application method. First, there was discoloration on the back surfaces of the samples, indicating that the Zircaloy-4 substrate had been heated to high temperatures and the composition of the deposited coating was substantially different from that of the original powder. Second, the process sometimes caused combustion of the coating material in that the powder caused an energetic excursion. In addition, micro-cracks were observed in HVOF coatings, even though the samples were handled gently. However, it was still possible that they could have been formed during sample handling. Therefore, the HVOF process was dropped and later work focused on cold sprayed coatings.

POWDER

MAX phase powder is commercially available and identified as Maxthal 211 Aluminum Titanium Carbide (Ti_2AlC Powder). It is available at a size of d90 = 25 μm / d50 = 10 μm (i.e., 90% of the particles are below 25 μm in size and 50% of the particles are below 10 μm).

SPRAY APPLICATION

MAX Phase coatings were successfully applied to fuel rod cladding, as shown in Figure 19.

Figure 19: Zircaloy Fuel Cladding Coated with MAX Phase material by the cold spray process.

MECHANICAL PERFORMANCE

Scratch adhesion testing assessed mechanical integrity, failure modes, and practical adhesion strength of a specific hard ceramic coating on a given metal or ceramic substrate.

For EATF MAX coatings, the scratch adhesion test measurements were conducted by a technique based upon ASTM C1624. The process of scratching was simulated in a controlled and monitored manner to observe adhesive or cohesive failures. In this application, the Nanovea Mechanical Tester in its micro scratch testing mode was used to measure the load required to cause failure to a MAX coating on a flat Zircaloy substrate. A 20 μm spherical diamond stylus was used at progressive loads ranging from 0.1 N to 200 N to scratch the coating. Initial testing was based upon a progressive increasing load up to this maximum applied pressure.

AREVA worked with SRNL/UW to define the maximum pressure that should be anticipated during reactor manufacturing, normal reactor operation, and off-normal events. Current planning calls for future testing based on a design-basis scratch of

50 N applied load. The initial testing has shown that the Ti_2AlC MAX coatings applied by both HVOF and CS hold up beyond the 50 N design-base scratch load. This test is much more severe than the rubbing that will occur during fuel assembly fabrication.

Table 8 summarizes the test results for "As-Received" AREVA Zircaloy and the polished cold sprayed Ti_2AlC-coated sample. No measurement could be made on the HVOF-sprayed sample due to the minimal effect of the 2-hour test. The cold sprayed sample exhibits an improvement in sliding wear properties of an order of magnitude over the 400-grit Zircaloy-4 sample.

Sample	Avg. Width (µm)	Avg. Depth (µm)
AR Zircaloy 4	475.75	4.55
CS Ti_2AlC	47.66	0.41
HV Ti_2AlC	*0	*0

Table 8: Rotating Pin-on-Disc test results for spray-coated samples prepared for the Manufacturing Gate Review. No results could be measured for the sample produced by HVOF spraying. All samples tested with a 10 g load for 120 minutes.

As can be seen in the table, an order of magnitude improvement over bare Zircaloy was obtained for the CS MAX Phase coatings.

PERFORMANCE TESTING

Testing for Normal Operating conditions was performed using the ASTM G2 test, as listed in Appendix P. Table 9 shows the weight gain of bare Zircaloy, HVOF and CS MAX Phase samples. This data indicated poorer performance for the coated surfaces than for the uncoated surfaces.

Sample	Coated Side (if applicable) (µm)	Not Coated Side (if applicable) (µm)
Zr4 ZrO_2 layers	--	1.4 ± 0.5
HVOF-sprayed Zircaloy-4 Oxide layer	4.2 ± 1.3	2.3 ± 0.4
Cold-Spray Zircaloy-4 Oxide layer	3.1 ± 0.9	1.4 ± 0.3

Table 9: Measured oxide thicknesses of various surfaces after 3 days of 400°C, 1500 psi steam exposure. As in the supercritical water exposure, the sprayed surfaces exhibit a higher oxidation rate as measured via cross-sectional SEM.

Heat treatment to sinter the coating was attempted but showed no improvement in results.

Since this testing was performed on small coupons where the effects of the large amount of coating edge can significantly affect results, this test is considered inconclusive. ASTM G2 testing will be performed on coated tubing to obtain results that will be indicative of what will be seen in Normal Operation.

Under LOCA conditions, cladding temperatures may exceed 1000°C for seconds to minutes, depending on the specific accident cause. The AREVA team set the test LOCA conditions for 1100°C for 4 minutes to mimic the reactor conditions of a temporary loss of coolant from a large-pipe break.

Figure 20 shows a cross section of a coupon that was coated on one surface and then oxidized in steam at 1100°C. The coating is visible at the top as dark gray; the unoxidized metal is white, and the Zirconium Oxide (ZrO_2) scale is medium gray. There is no preferential penetration of oxidation under the coating. Equally significant, there is no visible oxidation on the outer surface of the coating. The results indicate that the coating continues to protect the coated portions of the substrate even if discontinuities are present.

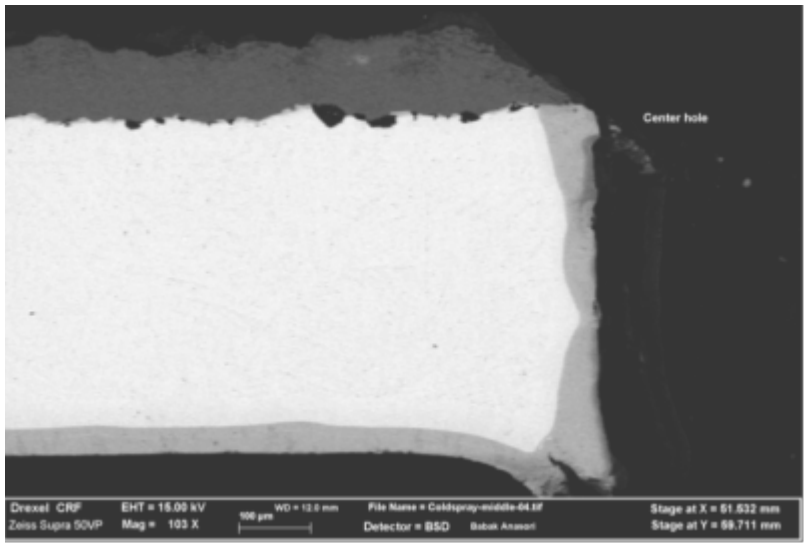

Figure 20: Coated Zircaloy-4 coupon after steam oxidation

Since the ASTM G2 testing, representing normal operation, was inconclusive, the decision regarding continuing further development of the CS MAX Phase coating was made on the basis of the LOCA testing results, which were positive.

GATE REVIEW RESULTS

The HVOF process was dropped from further development per the recommendation of the GR Board.

Work on the CS Ti_2AlC coating was continued.

Towards the end of Phase 1A, plans and preparations for seamless movement into Phase 1B were considered. This involved detailed discussions with UW and SRNL regarding the results achieved to date for the CS MAX Phase coating. A team of

AREVA technical experts participated in several discussions, including face-to-face meetings with UW and SRNL. It was realized that another FOA team is pursuing the CS MAX Phase technology. SRNL had previously completed extensive work on PVD through and Laboratory Directed Research and Development (LDRD) project. As the AREVA team reviewed the results of this work, it became evident that the PVD technology had significant potential. The PVD process is capable of controlling the coating thickness to less than ±0.0008 inches. This control supports producing coating thicknesses of 20 to 30 µm, as compared to the 50 µm, practically achievable with the CS process. This thinner coating directly reduces parasitic neutron absorption, which reduces the economic penalty incurred by using coatings. As further discussions ensued, it was learned that the PVD technology is used by both the Atomic Energy and Alternative Energies Commission (CEA) and Electric Power Research Institute (EPRI) to coat cladding. This, combined with the overall technical merit of the process (thinner coatings, etc) drove the decision to drop the CS MAX phase and carry PVD forward into Phase 1B. This not only brings technical merit and greater chances of success to the project, it creates synergies with multiple organizations, focuses technical evaluation criteria, and diversifies the overall project technologies for the client.

4.3. CLADDING

In consideration of EPRI joining the AREVA EATF team in the next phase of the program the gate review board reviewed the progress of EPRI self-funded work at each meeting.

The performance of Zircaloy alloys in severe accidents is limited by their loss of strength at high temperature and by hydrogen generation in high-temperature, oxidizing environments. Molybdenum alloys are being investigated for fuel cladding since they provide superior strength at high temperatures. A common concern about molybdenum is that it oxidizes to volatile MoO_3 at high temperatures. Initial tests showed surprising resistance to this effect. Oxidation could be addressed by applying an outer coating of Zircaloy or a FeCrAl alloy. The outer layer could be applied by coating techniques (physical vapor deposition, vacuum plasma spray, etc.) or by coextrusion. Molybdenum has a thermal neutron capture cross section comparable to that of FeCrAl, so there is a neutronic penalty unless the molybdenum is depleted in Mo-95.

The requirements and goals in the requirements traceability matrix were not explicitly addressed.

This work was funded by EPRI and the board passed on the comments directly on this work.

4.4. NANO-PARTICLES IN THE COOLANT

The information in this section is summarized, which is provided in its entirety in Appendix H.

Results demonstrate that the injection of nanoparticles into the reactor coolant effectively creates a colloidal dispersion known as a “nanofluid”. The deposition of nanoparticles from the nanofluid to the fuel cladding surface can considerably increase the critical heat flux (CHF), which is the heat flux corresponding to a departure from nucleate boiling (DNB) in the reactor core. The AREVA study showed that a corresponding benefit from these CHF improvements is on the order of 150°C in cladding temperature margin.

Improved thermo-physical properties were attributed to the creation of "nanoporosity" and the related change of the contact angle between steam bubbles and the heated surfaces, the combined effect of which is to considerably increase the wettability of the cladding surface. Nanoporosity also allowed a substantial increase in the number of steam chimneys and capillaries present per unit of surface, which increased the capability to evacuate heat from a nanodeposited surface.

To date, research has investigated the use of alumina, zirconia, silica, carbon, gold, platinum, and iridium as nanoparticles. Of these, zirconia has shown particular promise.

These materials have clearly demonstrated their ability to increase CHF and mitigate the consequences of DB accidents including cladding failure, fission product releases, and mechanical failure of the coolable fuel rod geometry.

The introduction of various nanoparticles into the emergency coolant has been considered for increasing the heat transfer, CHF, and quenching capabilities needed to prevent overheating and damage to fuel assemblies during a DBE. It has been concluded that such an enhancement to the Emergency Core Cooling System (ECCS) is feasible. However, this approach presents challenges to achieving the colloidal stability and other colloidal physical properties needed for the fluid mixture to be effective.

5.0 POST IRRADIATION EXAMINATIONS

Two PIE exams were provided as in-kind contributions to the project.

The first report was a cause of failure exam on BWR fuel. This is contained in Appendix R for a plant identified as A23. The fuel failure appears to be the result of an internal contamination issue in BWR fuel but has equal relevance to PWR fuel failures. This failure mode could be relevant to EATF concepts such as clad coatings since they involve the application of additional materials to the exterior of the cladding. Such application involves an additional manufacturing step and potentially new materials introduced into the reactor with which there is little or no radiation experience. Additionally with another manufacturing step there is another point in the process for which contamination may enter into the cladding. When evaluating EATF LTAs in the future care will need to be taken due to this contamination mechanism, if any fuel failure with a signature similar to the failure examined in the A23 PIE report are observed. The results in the PIE report provide a baseline of failure signatures that will be used to identify any failures from this cause. Also, during industrialization of this process there needs to be great care to design a process to help preclude this possibility.

Appendix S contains the PIE report on the plant identified as A33. This PIE campaign obtained BWR Fuel Channel dimensional data with burnup. The significance of this data is to provide baseline fuel channel distortion data at medium to higher burnups which can serve as a reference for comparison of later EATF concepts. In particular, maximum bulge, bow, twist, and total deformation are provided for two Zircaloy based fuel channels used in current commercial BWR operation. Additionally, four fuel channels were examined to measure channel oxide thickness and growth providing an even more detailed picture of current BWR fuel channel behavior in commercial reactor operations. This data provides a starting point for development of a reference database against which to compare future EATF fuel channel concepts to determine relative performance.

6.0 SUMMARY OF ACCOMPLISHMENTS

In summary, the AREVA Team was successful in identifying several technology candidates to enhance the accident tolerance of nuclear fuel. These candidates include the addition of SiC or nano-diamond to the fuel pellet by means of the SPS process and the application of a MAX Phase coating to the fuel cladding by the CS process. During the course of this work, a number of other significant things were accomplished that contribute to the effort of developing this fuel. These accomplishments are summarized in Table 10.

DESCRIPTION	ACCOMPLISHMENTS
FUEL PELLET	1. Pellets were successfully made using the SPS process. These included 10% by volume SiC particles, whiskers, or diamond. Process eliminates grinding to final size. 2. Optimum chromia content for large pellet identified. 3. Significant thermal conductivity improvement confirmed by measurements at LANL. 4. Preliminary thermal conductivity as a function of dpa established. This is to be confirmed by irradiation in the ATR. 5. Significant reduction in fission gas release estimated. This is to be confirmed by irradiation in the ATR. 6. Provisional cost's for producing pellets with the SPS process was estimated. 7. The master Sintering Curve for producing pellets of one size was defined.
CLADDING COATING	1. The EPD method of depositing Ti, TiO_2, Y_2O_3, YSZ, and Al_2O_3 was proven. 2. The CS method of depositing MAX phase coatings of Ti_2AlC was proven. 3. The HVOF method of applying coatings was eliminated. 4. TiO_2, YSZ, and Ti_2AlC coatings were selected for further development. 5. The EPD method of applying coatings was eliminated. 6. The wear resistance of the coatings was demonstrated. TiO_2 was 50% better than bare Zircaloy-4. Ti_2AlC was 10 times better. 7. The testing criteria were refined to cover a) normal operation, 2) DBE, and 3) B-DBE. 8. It was shown that coatings are able to provide significant reduction in ZY oxidation for LOCA conditions. 9. It was shown that edge effects are a factor in the ability of the coatings to provide protection from oxidation. 10. Application of MAX Phase coatings by the CS method was demonstrated on rods. 11. The decision was taken to pursue the PVD coating process instead of the CS process to improve control over coating thickness and reduce fuel cycle economic penalty.
PRODUCT DEVELOPMENT	1. A Requirements Matrix was completed to provide a complete overview of the development requirements for EATF nuclear fuel. This is organized by Manufacturing, Performance Testing, and Further Development. 2. A draft Regulatory Plan was generated defining the path to LTA licensing and eventually batch implementation. 3. A draft Business Plan was generated defining the path to commercialization. 4. A draft Test Plan was generated to define the scope of testing required to develop, license and sell a new nuclear fuel. 5. The acceptance criteria for inserting a Lead Fuel Assembly into a commercial reactor were identified. 6. A general engineering review of the impacts of the EATF technology concepts on the fuel performance and licensing was performed. This included the effects of the new EATF materials used in the pellet and cladding coating. 7. Fuel pellets were manufactured for irradiation testing in the ATR. This will address irradiation effects. 8. Gate Reviews were held to focus the discovery phase of the development process.

Table 10: The AREVA's Team's Accomplishments

7.0 ACRONYMS

AC	Alternating Current
ACAC	Acetylacetone
AFS	AREVA Federal Services, LLC
ANSI/ANS	American National Standards Institute/American National Standard
AOO	Anticipated Operational Occurrence
AOR	Analysis of Record
APS	Air Plasma Spraying
AR	As-Received
ASME	American Society of Mechanical Engineers
ASTM	American Society for Testing and Materials
ATF	Accident Tolerant Fuel
ATR	Advanced Test Reactor
ATWS	Analysis of Anticipated Transient without Scram
AVG	Average
BAW	Babcock & Wilcox
BDB	Beyond Design Basis
BDBE	Beyond Design Basis Event
BTU	British Thermal Unit
BWR	Boiling Water Reactor
CE	Combustion Engineering
CFR	Critical Heat Flux Ratio
CHF	Critical Heat Flux
CPU	Central Processing Unit
CRUD	Crudding of fuel surfaces during normal operation
CS	Cold Spray
CVD	Chemical Vapor Deposition
CW	Continuous Wave
CY	Calendar Year
DB	Design Basis
DBE	Design Basis Events
DC	Direct Current
Deca	Decafluoropentane
DI	De-Ionized
DIVOM	Delta over Initial versus Oscillation Magnitude
DL	Double Layer
DNB	Departure from Nucleate Boiling
DNBR	Departure from Nucleate Boiling Ratio
DOE	Department of Energy
DP	Diamond Powder (nanoparticles, 12 microns average size)
DWG	Drawing
EATF	Enhanced Accident Tolerant Fuel
ECCS	Emergency Core Cooling System
EDM	Electrical Discharge Machining
EDS	Energy-Dispersive Spectroscopy
EOC	End Of Cycle
EP	Edge-Protected
EPD	Electrophoretic Deposition
EPRI	Electric Power Research Institute
FA	Fuel Assembly
FAST	Field Assisted Sintering Technique

FCM	Fuel Centerline Melt
FGR	Fission Gas Release
FIB	Focused Ion Beam
FMEA	Failure Modes And Effects Analysis
FSAR	Final Safety Analysis Report
GAIA	Generation of Advanced Innovative Assembly
GDC	General Design Criteria
GR	Gate Review
GWD	Giga-Watt Day
HDPE	High Density Polyethylene
HT	Heat Treatment
HTP	High Thermal Performance
HVOF/HV	High Velocity Oxy-Fuel
ID	Inside Diameter
INL	Idaho National Laboratory
INPO	Institute of Nuclear Power Operations
IVR	In Vessel Retention
LANL	Los Alamos National Laboratory
LAR	License Amendment Request
LB	Large Break
LB-LOCA	Large Break Loss of Coolant Accident
LCO	Limiting Conditions for Operation Technical Specification Limits
LFA	Lead Fuel Assembly
LFP	Leidenfrost point
LFR	Lead Fuel Rods
LHGR	Linear Heat Generation Rate
LOCA	Large Break Loss of Coolant
LS	Laser Light Scattering/Laser Surface Treatments
LSSS	Limiting Safety System Settings Technical Specification Limits
LTA	Lead Test Assembly
LTR	Lead Test Rod
LWR	Light Water Reactor
MAX Phase	"MAX" is a contrived acronym for a set of compounds with the chemical formula Mn+1AXn, where n = 1, 2, or 3, and where M = early transition metal, A = group A element, and X = carbon or nitrogen.
MHF	Minimum Heat Flux
MIT	Massachusetts Institute of Technology
MOX	Mixed Oxide
MSC	Master Sintering Curve
MTC	Moderator Temperature Coefficient
MTU	Metric Tonnes of Uranium
NEUP	Nuclear Energy University Program
NG	Next Generation
NPP	Nuclear Power Plant
NRC	Nuclear Regulatory Commission
OD	Outer Diameter
OSHA	Occupational Safety and Health Administration
PACVD	Plasma Assisted Chemical Vapor Deposition
PCI	Power Thresholds for Pellet-Clad Interaction
PCMI	Pellet-Clad Mechanical Interaction
PCT	Peak Cladding Temperature
PIE	Post Irradiation Examination

PLD	Pulsed Laser Deposition
PORC	Plant Oversight Review Committee
PQAP	Project Quality Assurance Plan
PRA	Probabilistic Risk Assessment
PSD	Particle Size Distribution
PWR	Pressurized Water Reactor
QA/QC	Quality Assurance/Quality Control
QCW	Quasi-Continuous Wave
R&D	Research and Development
RG	Regulatory Guide
RIA	Reactivity Initiated Accident
RTM	Requirement Traceability Matrix
RX	Reactor
SB	Small Break
SEM	Scanning Electron Microscope
SER	NRC Safety Evaluation Report
SiC	Silicon Carbide
SiC(p)	Silicon Carbide (particle form)
SiC(w)	Silicon Carbide (whiskers)
SPS	Spark Plasma Sintering
SRNL	Savannah River National Laboratory
SS	Stainless Steel
SSC	Structure, System, or Component
SSC	Structure, System, or Component
STAIF	Stability Analysis Methodology
TC	Thermal Conductivity
TD	Theoretical Density
TEA	Triethanolamine
Ti2AlC Powder	MAX phase powder is commercially available and identified as Maxthal 211 Titanium Aluminum Carbide
Ti2AlC	Aluminum Titanium Carbide
TMI	Three Mile Island Nuclear Plant
TVA	Tennessee Valley Authority
UF	University of Florida
UHP	Ultrahigh Purity
UNF	Used Nuclear Fuel
US/USA	United States of America
UTS	Ultimate Tensile Strength
UW	University of Wisconsin
W	Westinghouse
XRD	X-Ray Diffraction
YSZ	Yttria-Stabilized Zirconia
ZY	Zircaloy

8.0 REFERENCES

1. AREVA Federal Services LLC, Regulatory Plan for Enhanced Accident Tolerant Fuel, RPT-3008873-000, Enhanced Accident Tolerant Fuel, Contract Number: DE-NE-00567.

2. AREVA Federal Services LLC, Requirements Traceability Matrix, RPT-3008640-000, Enhanced Accident Tolerant Fuel, Contract Number: DE-NE-00567.

APPENDIX A

Requirements Traceability Matrix for the Phase 1A Final Report for Enhanced Accident Tolerant Fuels

Prepared by:
AREVA Federal Services, LLC

TABLE OF CONTENTS

1.0 INTRODUCTION 1
2.0 THE DEVELOPMENT OF GOALS AND REQUIREMENTS 1
3.0 SOURCES OF REQUIREMENTS AND GOALS 2
3.1. ANS-57.5 2
3.2. NUREG-0800, SECTION 4.2 2
3.3. 10 CFR PART 50, APPENDIX A 2
3.4. NRC REGULATORY GUIDE 1.25 2
3.5. LWR EATF METRICS 2
3.6. INDUSTRY PRACTICE 2
3.7. MANUFACTURABILITY 3
3.8. UTILITY REQUIREMENTS 3
4.0 TABLE OF REQUIREMENTS 3
5.0 REFERENCES 3

LIST OF TABLES

TABLE 1: DESIGN REQUIREMENTS AND GOALS TRACEABILITY MATRIX 4

1.0 INTRODUCTION

The purpose of this Appendix is to summarize the design requirements from the fuel vendors and utility perspective for new nuclear fuel, including the additional goal related to Enhanced Accident Tolerant Fuel (EATF). The design requirements for nuclear fuel come from a number of sources. These sources include regulatory requirements, plant operator requirements (utilities), and fuel vendor requirements. Beyond this, there are also design goals which are established to optimize fuel performance and reduce risk. The development of these requirements, their division among the phases of fuel development, and the sources of requirements are discussed. The requirements are provided in Table 1.

To develop any new technology, AREVA uses a Gate Review process in research and development projects to narrow potential technology candidates as the development progresses. This approach helps insure that the resources are focused on the candidates with the most potential to succeed. In this process, the potential for the candidates to achieve the design requirements and goals is assessed at multiple points within the development program (stages of development). For the EATF project, the first development stage and the initial Gate Review focus is a manufacturing stage and those requirements and goals which apply to manufacturing (prototype, reliable, full scale product) are specified for assessment in the first Gate Review. The second stage is mechanical fuel performance testing and therefore those requirements and goals appropriate to performance are specified for assessment in the second Gate Review. As the development progresses to irradiation testing, and then to Lead Test Assembly and finally to batch implementation (this scope is beyond the initial EATF project funding), eventually all of the design requirements and goals will have been assessed.

2.0 THE DEVELOPMENT OF GOALS AND REQUIREMENTS

Requirements can come from a number of sources such as the Nuclear Regulatory Commission (NRC), Occupational Safety and Health Administration (OSHA), local and state governments, utility customers for the fuel, and fuel vendors. In most cases fuel vendors set requirements upon themselves embodied in Quality Assurance/Quality Control (QA/QC) plans. In turn, requirements are placed on subcontractors and suppliers. Typically there is an arrangement by contract in which the fuel vendors set requirements on the utility to operate the reactor within certain limits on items such as water chemistry.

Goals are desired features. They are not requirements that must be met. Some of these are taken from the EATF goals.

This document includes both fuel development goals and requirements, and differentiates between them.

This document provides a list of requirements and goals along with the sources for each of them. These requirements are divided into groups based on the development phase. These phases include:

- Gate Review 1 — Manufacturability
- Gate Review 2 — Mechanical Performance
- Test Rod for Irradiation in the a Test Reactor
- Lead Test Assembly (LTA)
- Batch Implementation

For this phase of development, the requirements pertaining to the Gate Reviews are indicated in the table, but the requirements for the test rod, LTA, and for batch implementation are combined together for future consideration.

3.0 SOURCES OF REQUIREMENTS AND GOALS

There are a number of sources of fuel design requirements for commercial nuclear fuel and EATF. These are discussed briefly in this section.

These sources are specifically for a fuel system incorporating a uranium oxide pellet and a Zircaloy cladding. It is recognized that these requirements may have to be modified, in some instances, to be applicable to the new EATF Fuel system being developed since the EATF system will incorporate additional or different materials.

3.1. ANS-57.5

American National Standards Institute/American National Standard (ANSI/ANS) ANSI/ANS-57.5-1996, renewed in 2006, provides fuel assembly mechanical design and evaluation requirements for light water reactor fuel [1].

3.2. NUREG-0800, SECTION 4.2

The NRC NUREG-0800 provides the Standard Review Plan for the review of Safety Analysis Reports for light water reactors [2].

3.3. 10 CFR PART 50, APPENDIX A

10 CFR Part 50, Appendix A provides the U.S. NRC's General Design Criteria (GDC) for nuclear power plants [3].

3.4. NRC REGULATORY GUIDE 1.25

The NRC, Office of Nuclear Regulatory Research, has produced Regulatory Guide 1.25.This document provides assumptions used for evaluating the potential radiological consequences of a fuel handling accident in the fuel handling and storage facility for boiling and pressurized water reactors [4].

3.5. LIGHT WATER REACTOR (LWR) EATF METRICS

A National Metrics Workshop was held October 11-12, 2012 in Germantown, MD to define the attributes of EATF. This work was compiled into a report entitled National Metrics Work- shop Report and issued by Lori Braase in January 2013 as DOE document INL/EXT-13-28090 [5].

3.6. INDUSTRY PRACTICE

The generally accepted practice of the industry represents the experience of industry in developing, licensing, manufacturing, and using Light Water Reactor (LWR) nuclear fuels. The results of this experience are also applied to the development of EATF.

3.7. MANUFACTURABILITY

Manufacturability is the ease and cost of manufacture. Vendor experience has shown that certain practices and approaches are required to manufacture nuclear fuel that is reliable and cost-effective.

3.8. UTILITY REQUIREMENTS

Duke Energy and TVA developed a list of utility requirements [6]. These emphasize safe and reliable operation of the fuel and compatibility with the remainder of the power plant.

4.0 TABLE OF REQUIREMENTS

TABLE 1 provides a list of all of the fuel design requirements and goals for this project. The source of each requirement is provided. The applicability of each requirement or goal to the fuel pellet, the cladding, the cladding coating, and to the fuel pellet dispersoid is indicated. Finally, the applicability of each requirement or goal to the initial design phases of manufacturing and performance testing is indicated.

5.0 REFERENCES

[1] American Nuclear Society. Light Water Reactors Fuel Assembly Mechanical Design and Evaluation. ANSI/ANS-57.5-1996; R2006, 2006.

[2] U.S. Nuclear Regulatory Commission. Standard Review Plan for the Review of Safety Analysis Reports for Nuclear Power Plants: LWR Edition. NUREG-0800, Section 4.2, "Fuel System Design", Rev. 3, March 2007.

[3] U.S. Nuclear Regulatory Commission. General Design Criteria for Nuclear Power Plants. 10 CFR Part 50, Appendix A, February 19, 2013.

http://www.nrc.gov/-reading-rm/doc-collections/cfr/part050/part050-appa.html

[4] U.S. Nuclear Regulatory Commission, Office of Nuclear Regulatory Research. REGULATORY GUIDE 1.25 — ASSUMPTIONS USED FOR EVALUATING THE POTENTIAL RADIOLOGICAL CONSEQUENCES OF A FUEL HANDLING ACCIDENT IN THE FUEL HANDLING AND STORAGE FACILITY FOR BOILING AND PRESSURIZED WATER REACTORS. REGULATORY GUIDE 1.25, Revision 0, March 1972.

[5] Lori Braase. Enhanced Accident Tolerant LWR Fuels National Metrics Workshop Report. INL/EXT-13-28090, January 2013.

[6] Rose Montgomery and Ben Howell, Utility Recommended Criteria for the Gate Review Process, January 2013.

TABLE 1: DESIGN REQUIREMENTS AND GOALS TRACEABILITY MATRIX

		Source		Applies to				Gate Review				Pellet Qualification									Cladding/Coating Qualification								
No.	Requirement/Goal	Document	Section	Pellet	Cladding	Coating	Dispersoid	Manufacturing	Performance	Later Review	Reqt./Goal	Analysis	As-mfd.	Autoclave	Capsule	Flow Loop	Power RX	Ramp	RIA	LOCA	Analysis	As-mfd.	Autoclave	Capsule	Flow Loop	Power RX	Ramp	RIA	LOCA
1	The material must give satisfactory performance at LWR coolant temperatures (30 to 325 °C).	ANS-57.5	5.3.1		X	X	X		X	X	R											X	X	X	X	X			
2	The material must give satisfactory performance at LWR fuel temperatures (from 30 °C to fuel centerline temperature).	ANS-57.5	5.3.1*	X						X	R		X		X	X	X												
3	The material must give satisfactory performance at LWR coolant pressures (0.1 to 15.5 MPa).	ANS-57.5	5.3.1		X	X	X		X	X	R											X	X	X	X	X			
4	The material must give satisfactory performance at LWR coolant flow rates.	ANS-57.5	5.3.1		X	X	X			X	R														X	X			
5	The material must give satisfactory performance in LWR coolant chemistry.	ANS-57.5	5.3.1		X	X	X		X	X	R														X	X			
6	The material must give satisfactory performance at LWR neutron flux and fluence.	ANS-57.5	5.3.1	X	X	X	X			X	R				X	X	X							X	X	X			
7	The material must give satisfactory performance under wet spent fuel storage conditions (water, boric acid, 30 to 60 °C, 0.3 MPa).	ANS-57.5	5.3.1*	X	X	X				X	R				X	X	X					X		X	X	X			
8	The material must give satisfactory performance under dry spent fuel storage conditions (helium, water vapor, 0.1 to 0.2 MPa, 30 to 400 °C).	ANS-57.5	5.3.1*	X	X	X				X	R						X					X			X	X			
9	The design must give satisfactory performance under "normal conditions of transport" and "hypothetical accident conditions" (10 CFR 71.71 and 10 CFR 71.73).	ANS-57.5	5.3.1	X	X	X				X	R		X		X	X	X					X		X	X	X			

		Source		Applies to				Gate Review				Pellet Qualification									Cladding/Coating Qualification								
No.	Requirement/Goal	Document	Section	Pellet	Cladding	Coating	Dispersoid	Manufacturing	Performance	Later Review	Reqt./Goal	Analysis	As-mfd.	Autoclave	Capsule	Flow Loop	Power RX	Ramp	RIA	LOCA	Analysis	As-mfd.	Autoclave	Capsule	Flow Loop	Power RX	Ramp	RIA	LOCA
10	The design must give satisfactory performance under seismic, transient, and accident conditions.	ANS-57.5	5.3.1	X	X	X				X	R	X									X								
11	The material must be stable under ambient conditions (dry air, 0.1 MPa, room temperature, various humidities).	ANS-57.5	5.3.1*	X	X	X		X			R		X									X							
12	The process must be capable of fabricating fuel pellets of appropriate size.	ANS-57.5	5.3.2.1	X				X			R		X																
13	The process must be capable of achieving high density.	ANS-57.5	5.3.2.1	X				X			R		X																
14	The process must provide acceptable control of dimensions and geometry (e.g., diameter, surface finish, straightness, ovality, uniformity of thickness, pellet end geometry, etc. as applicable).	ANS-57.5	5.3.2.1, 5.3.3.1	X	X	X		X			R		X									X							
15	The process must yield pellets with acceptable integrity and must control chipping.	ANS-57.5	5.3.2.1	X				X			R		X																
16	The material should not lead to formation of mixed wastes.	manufactur ability	5.3.2.2	X	X	X	X		X		G		X									X							
17	The process should not lead to formation of mixed wastes.	manufactur ability	5.3.2.2	X	X	X	X	X			G		X									X							
18	Performance of a fuel rod must be predictable (e.g., for processes listed in ANS-57.5, section 5.3.3.4).	ANS-57.5	5.3.3.4	X	X	X	X			X	R	X									X								
19	The material must have acceptable densification and swelling behavior.	ANS-57.5	5.5.1	X						X	R				X	X	X												

		Source		Applies to				Gate Review				Pellet Qualification									Cladding/Coating Qualification								
No.	Requirement/Goal	Document	Section	Pellet	Cladding	Coating	Dispersoid	Manufacturing	Performance	Later Review	Reqt./Goal	Analysis	As-mfd.	Autoclave	Capsule	Flow Loop	Power RX	Ramp	RIA	LOCA	Analysis	As-mfd.	Autoclave	Capsule	Flow Loop	Power RX	Ramp	RIA	LOCA
20	Pellet-cladding interactions and fuel-side stress corrosion cracking of the cladding must be controlled.	ANS-57.5	5.5.13	X	X					X	R				X	X	X							X	X	X			
21	The material must tolerate expected crud deposits.	ANS-57.5	5.5.16		X	X				X	R														X	X			
22	The design should have a design life of three cycles of irradiation with a total core residence time of six calendar years.	industry practice		X	X	X				X	G	X									X								
23	The design must be able to accommodate an appropriate number of Condition I and Condition II transients.	ANS-57.5	5.1*	X	X	X				X	R	X									X								
24	The design must have adequate resistance to fuel rod bow.	ANS-57.5	5.3.3.4	X	X	X				X	R						X									X			
25	The design must maintain structural integrity under shipping and handling loads (fresh fuel).	industry practice		X	X	X				X	R	X									X								
26	The design must not undergo departure from nucleate boiling under Condition I transients allowed by the technical specifications.	NUREG-800, §4.4.II			X	X	X			X	R											X					X		
27	The design must not undergo departure from nucleate boiling under Condition II transients.	NUREG-800, §4.4.II			X	X	X			X	R											X					X		
28	The design must not be subject to flow induced vibration that would decrease the design life.	10 CFR 50, App. A	GDC 10		X	X				X	R											X							
29	The material must provide adequate water-side corrosion and erosion resistance.	NUREG-800, §4.2	p. 6		X	X	X		X	X	R											X	X		X	X			
30	Coatings must be deposited uniformly over substantially the entire exterior cladding surface.	manufacturability				X		X			R											X							

		Source		Applies to				Gate Review				Pellet Qualification									Cladding/Coating Qualification								
No.	Requirement/Goal	Document	Section	Pellet	Cladding	Coating	Dispersoid	Manufacturing	Performance	Later Review	Reqt./Goal	Analysis	As-mfd.	Autoclave	Capsule	Flow Loop	Power RX	Ramp	RIA	LOCA	Analysis	As-mfd.	Autoclave	Capsule	Flow Loop	Power RX	Ramp	RIA	LOCA
31	The material must not promote excessive crud deposition.	NUREG-800, §4.2	p. 6		X	X	X			X	R														X	X			
32	The material must provide acceptable fuel-side corrosion performance.	NUREG-800, §4.2	p. 9	X	X					X	R				X	X	X							X	X	X			
33	The design should provide an acceptable heavy metal loading.	industry practice		X	X	X			X		G	X									X								
34	The design should provide an acceptable water-to-fuel ratio.	industry practice		X	X	X			X		G	X									X								
35	Fuel rod handling and insertion into grids must not degrade cladding or coating performance.	manufacturability			X	X		X			R											X							
36	Fuel pellet insertion must not degrade cladding performance.	manufacturability		X	X			X			R		X									X							
37	Fuel pellet insertion must not damage pellets.	manufacturability		X	X			X			R		X									X							
38	Fuel rod insertion and reconstitution must not damage grids.	industry practice			X	X	X		X		R											X							
39	Axial clearance for the plenum spring must be maintained.	NUREG-800, §4.2	p. 6	X	X	X				X	R				X	X	X							X	X	X			
40	Growth of the fuel rod must be appropriately controlled.	NUREG-800, §4.2	p. 6	X	X	X				X	R				X	X	X							X	X	X			
41	The design must have acceptable cladding stress, resistance to creep collapse, and fatigue life usage.	NUREG-800, §4.2	p. 6	X	X	X	X			X	R	X									X								
42	The fuel rod internal pressure during operation shall not exceed the maximum allowed value at any time in life. Calculations must include applicable transients.	NUREG-800, §4.2	p. 7	X	X	X				X	R	X			X	X	X				X				X	X			

		Source		Applies to				Gate Review				Pellet Qualification									Cladding/Coating Qualification								
No.	Requirement/Goal	Document	Section	Pellet	Cladding	Coating	Dispersoid	Manufacturing	Performance	Later Review	Reqt./Goal	Analysis	As-mfd.	Autoclave	Capsule	Flow Loop	Power RX	Ramp	RIA	LOCA	Analysis	As-mfd.	Autoclave	Capsule	Flow Loop	Power RX	Ramp	RIA	LOCA
43	Mechanical stresses under normal operating conditions must not cause fuel failure.	NUREG-800, §4.2	p. 10	X	X	X				X	R	X									X								
44	The design shall provide acceptable LHGR at 1.0% (or other applicable) transient cladding strain.	NUREG-800, §4.2	p. 9	X	X	X				X	R	X									X								
45	Centerline fuel melting must not occur during Condition I or Condition II transients.	NUREG-800, §4.2	p. 9	X	X	X	X			X	R	X						X			X						X		
46	The process must, in principle, be capable of producing full-length cladding tubes.	manufacturability			X	X		X			R											X							
47	The composition should not challenge available supplies of an isotope, element, or material.	manufacturability		X	X	X	X	X			G	X									X								
48	Each fuel rod must be capable of being marked with a unique, legible identifier.	industry practice			X	X		X			G											X							
49	The material must allow reliable, hermetic joining of cladding and end caps.	manufacturability			X			X			R											X							
50	Welds should accommodate inspection.	manufacturability			X			X			G											X							
51	The fuel rod internal pressure for spent fuel pool conditions shall not exceed the maximum allowed value.	RG-1.25	p. 3	X	X	X				X	R	X			X	X	X				X			X	X	X			
52	The design should be capable of achieving a rod-average burn-up of 60 GWd/MTU.	industry practice		X	X	X	X		X		G		X									X			X	X			
53	Probability of fuel rod failure should be comparable to that for current designs.	INL/EXT-13-28090	p. 24	X	X	X	X			X	G	X									X								
54	Material should be compatible (with regard to general and galvanic corrosion and stress corrosion cracking) with other engineered components of the primary coolant system during normal operation and AOOs.	INL/EXT-13-28090	p. 24		X	X	X		X		G										X	X				X			

		Source		Applies to				Gate Review				Pellet Qualification									Cladding/Coating Qualification								
No.	Requirement/Goal	Document	Section	Pellet	Cladding	Coating	Dispersoid	Manufacturing	Performance	Later Review	Reqt./Goal	Analysis	As-mfd.	Autoclave	Capsule	Flow Loop	Power RX	Ramp	RIA	LOCA	Analysis	As-mfd.	Autoclave	Capsule	Flow Loop	Power RX	Ramp	RIA	LOCA
55	Material should not generate debris that could harm engineered components of the primary coolant system.	INL/EXT-13-28090	p. 24		X	X	X		X		G												X		X	X			
56	Release of tritium into the coolant should be controlled.	INL/EXT-13-28090	p. 24		X				X		G														X	X			
57	Hydrogen pickup during normal operation should be controlled.	INL/EXT-13-28090	p. 24		X	X			X		G														X	X			
58	Material should provide low rates of hydrogen generation under LOCA conditions.	INL/EXT-13-28090	p. 27		X	X				X	G																		X
59	Material should provide low rates of enthalpy release under LOCA conditions.	INL/EXT-13-28090	p. 27		X	X				X	G																		X
60	Material must provide acceptable postquench ductility under LOCA conditions.	INL/EXT-13-28090	p. 27		X					X	R																		X
61	Any eutectics formed with other engineered components of the primary coolant system should have acceptable melting temperatures.	INL/EXT-13-28090	p. 26		X	X	X		X		G										X	X							
62	Enthalpy deposition at failure should be comparable to that of current fuels under conditions of reactivity insertion.	INL/EXT-13-28090	p. 25*	X	X	X	X			X	G								X									X	
63	Severing of fuel rods under LOCA conditions should be controlled.	INL/EXT-13-28090	p. 28		X	X	X			X	G																		X
64	Breakaway oxidation under LOCA conditions should be controlled.	INL/EXT-13-28090	p. 27*		X	X	X			X	G																		X
65	Cost should be comparable to that of present fuels.	INL/EXT-13-28090	p. 29*	X	X	X	X	X			G	X									X								
66	Fuel should be operable at 5% enrichment.	INL/EXT-13-28090	p. 29	X	X	X	X		X		G	X									X								

		Source		Applies to				Gate Review				Pellet Qualification									Cladding/Coating Qualification								
No.	Requirement/Goal	Document	Section	Pellet	Cladding	Coating	Dispersoid	Manufacturing	Performance	Later Review	Reqt./Goal	Analysis	As-mfd.	Autoclave	Capsule	Flow Loop	Power RX	Ramp	RIA	LOCA	Analysis	As-mfd.	Autoclave	Capsule	Flow Loop	Power RX	Ramp	RIA	LOCA
67	Fretting wear at contact points on the structural members must be limited.	NUREG-800, §4.2	p. 6		X	X			X		R											X							
68	The process should have an acceptable scrap rate.	manufacturability		X	X	X	X	X			G		X									X							
69	Subsequent processing steps should not cause unacceptable degradation of materials prepared previously.	manufacturability		X	X	X	X	X			G		X									X							
70	Surface finish should not produce unacceptable levels of drag.	utility req'ts			X	X			X		G											X							
71	Thermal resistance should be low.	utility req'ts			X	X			X		G											X							
72	Material should accommodate acceptable power ramp rates.	utility req'ts		X	X	X			X		G							X									X		
73	Coating must be stable and adherent under LWR operating conditions.	utility req'ts				X			X		R														X	X			
74	Activation products from new materials should not result in significant dose increases to personnel.	utility req'ts		X	X	X			X		G						X								X	X			
75	Washout from failed fuel rods should not be significantly greater than that for conventional fuel.	utility req'ts		X					X		G				X	X	X												
76	Secondary failures should be limited in severity.	utility req'ts			X					X	G														X	X			

*** The source document implies this requirement or goal.**

APPENDIX B

Preliminary Business Plan
for the
Phase 1A Final Report
for Enhanced Accident Tolerant Fuels

Prepared by:
AREVA Federal Services, LLC

TABLE OF CONTENTS

1.0 INTRODUCTION 1
2.0 INTRODUCING INNOVATIVE FEATURES INTO COMMERCIAL NUCLEAR POWER PLANTS 2
2.1. MIXED OXIDE (MOX) LEAD TEST ASSEMBLIES (LTA) 3
2.2. ZIRCONIUM ALLOY M5® FUEL ROD CLADDING 3
2.3. ADVANCED MARK BW 17X17 FUEL ASSEMBLY INTRODUCTION 3
2.4. ATRIUM™ 10XM BOILING WATER REACTOR FUEL ASSEMBLY 4
2.5. CHROMIA DOPED (CR_2O_3) FUEL PELLETS 4
3.0 CURRENT FUEL ASSEMBLY PRICES 4
4.0 MARKET DRIVERS 5
4.1. COST OF NUCLEAR FUEL 5
4.1.1. COST OF THE URANIUM IN THE FUEL PELLETS 5
4.1.2. COST OF THE FUEL ASSEMBLY DESIGN 5
4.2. IMPACT OF RENEWABLE ENERGY ON NUCLEAR POWER PLANT OPERATIONS 6
5.0 INCREMENTAL DESIGN CHANGES FOR EATF 6
6.0 COST OF INCREMENTAL CHANGE TO FUEL DESIGN AND ESTIMATED SCHEDULE 7
6.1. DEVELOPMENT COSTS 7
6.1.1. Testing 7
6.1.2. ITA 7
6.1.3. licensing 7
6.1.4. schedule of expenditures 8
6.1.5. SUMMARY OF DEVELOPMENT COSTS 8
6.2. MANUFACTURING COSTS 8
6.2.1. capital 8
6.2.2. operating 8
6.3. PROJECTED SALES 9
6.3.1. Market 9
6.3.2. schedule 9
6.3.3. Return of development and costs 9
7.0 COST BENEFITS TO UTILITY AND FUEL VENDOR 9
7.1. AREVA CONCEPTS FOR BENEFITS TO UTILITY 9
7.1.1. IMPROVED THERMAL CONDUCTIVITY 9
7.1.2. CHROMIA DOPED FUEL PELLETS 10
7.1.3. SILICON CARBIDE WHISKERS 10
7.1.4. COATINGS 10
7.2. COST TO DEVELOP VS. PAYBACK TO VENDOR 10

LIST OF FIGURES

FIGURE 1: PROJECT SCHEDULE 2
FIGURE 2: HYPOTHETICAL OPERATING LIFE OF U.S. REACTOR FLEET 11

1.0 INTRODUCTION

This Appendix has been prepared as an initial input to the Department of Energy (DOE) on the business plan for the development of new fuels. This is seen as a living document and will be updated when the AREVA team makes a formal down selection of the concepts that it will take forward as the proposed fuel that exhibits improved performance in an accident condition.

Nuclear fuel vendors produce and sell fuel under commercial terms to the nuclear utilities, who will buy fuel from the market as long as the fuel meets their requirements for the safe and economical operation of the nuclear power plant (NPP). The current nuclear fuel market has an established infrastructure that includes manufacturing, regulation, transportation, operation, and used fuel storage. Therefore, changes to the fuel design tend to evolve incrementally and use the existing industrial infrastructure. Even minor modifications to the fuel design can take 10 or more years to achieve based on the regulatory environment, verification testing, codes and methods modeling, and modifications to the fabrication process. It is important to note that the Institute of Nuclear Power Operations (INPO) reviews the number of failed fuel rods that a utility has in the core when setting the insurance rate for a reactor. Therefore, step changes to fuel designs have a high utility resistance due to increased risks and, as such, new fuel designs are carefully assessed and reviewed.

To meet the DOE requirement for deploying lead test assemblies (LTA's) within 10 years, it is important to recognize that initial improvements in new Enhanced Accident Tolerant Fuel (EATF) designs will have to come from incremental improvements to the current nuclear fuel concepts. Wholesale design changes to the fuel at this time would not meet the 10 year requirement and would not be economical to implement under the present regulatory and financial environment.

This plan outlines the AREVA team's business case for improving nuclear fuel to better tolerate accident conditions while taking into account the economics of fuel supply in the U.S. market. Preparations to introduce LTAs into an operating commercial reactor can take several years or more depending on the nature of the new design features. LTAs may need up to 6 years of in-reactor irradiation to reach the extended burnups desired before the fuel rods can be extracted from the reactor and sent to a hot cell facility to perform post-irradiation examinations to collect data and analyze the results and potentially modify the design.

Enhanced Accident Tolerant Fuel (EATF) development costs by the nuclear fuel vendor must be repaid along with a reasonable profit and within a reasonable time. Development costs for new fuel taken through to LTAs can be prohibitively expensive and the associated investment costs, cost of money, and the long time period to bring a new design to market can act as a barrier to major technological changes. Support by the federal government can encourage innovation and free thinking by challenging the fuel vendors to think outside the box. These new fuel concepts could allow for beneficial improvements to be made at a lower cost to the utility customer for fuel design improvements that are not market driven.

Recognizing that the current design of nuclear fuel is considered safe, improvements in EATF may or may not be accompanied by improvements in a utility's operating costs. At best, the cost of EATF should be neutral compared to the current fuel design, or, even better, reduce the cost of the fuel and reload requirements. Any improvement in operating costs would add to the attractiveness of EATF to the utility. The addition of silicon carbide whiskers (SiC(w)) is an example of an improvement that may increase heat transfer and reduce the release fission gases

into the fuel rod. Better heat transfer decreases operating costs by increasing the reactor's thermal output, i.e., more BTUs per kilogram of uranium. Lower fission gas pressure allows higher burnups to be considered.

The objective of the AREVA team EATF project is to build on existing work that AREVA is conducting in fuel development while examining technology improvements that offer incremental benefits to the current fuel design. Therefore, the team is investigating a coating on the nuclear fuel cladding material and improvements to the fuel pellets to increase the coping time of the nuclear fuel in currently postulated accident conditions. Multiple technical concepts will be evaluated, analyzed, and tested to assess their viability, suitability, and manufacturability. The concepts will be evaluated with a "gate" review process to determine the best approach to pursue at each phase of development process.

The significance of this EATF development project, the schedule for which is shown in Figure 1, will be to introduce into commercial nuclear power reactors an improved and more robust nuclear fuel design that will reduce or mitigate the consequences of reactor accidents and improve the economics of the reactor's thermal output and reliability.

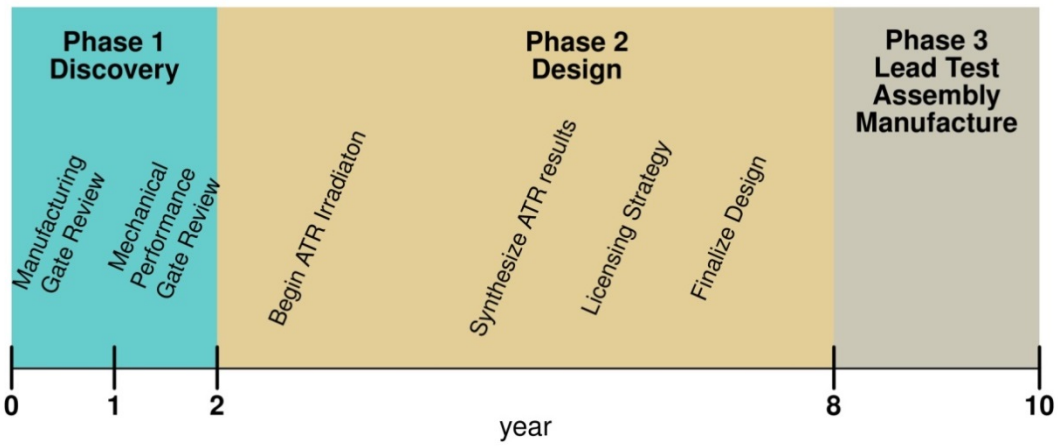

Figure 1: Project Schedule

2.0 INTRODUCING INNOVATIVE FEATURES INTO COMMERCIAL NUCLEAR POWER PLANTS

AREVA has been designing, manufacturing and supplying nuclear fuel for over 50 years. During this time AREVA has introduced many fuel assembly (FA) innovations and improvements, including the introduction of completely new Pressurized Water Reactor (PWR) FA designs such as the Generation of Advanced Innovative Assembly (GAIA) and the Mark-BW 17X17.

2.1. MIXED OXIDE (MOX) LEAD TEST ASSEMBLIES (LTA)

As part of a team to reduce the U.S. inventory of weapons grade plutonium, AREVA designed, fabricated and tested 4 LTAs that were irradiated in a Duke Power Co. commercial light water reactor (LWR).

2.2. ZIRCONIUM ALLOY M5® FUEL ROD CLADDING

To address fuel rod cladding failures (leakers) experienced by NPP utilities, AREVA introduced into the U.S. nuclear fuel market for PWRs nearly 20 years ago a new cladding having more enhanced properties than the previously used zirconium alloys and stainless steel cladding. The new M5® cladding provided a more robust, corrosion-resistant fuel rod that can survive increasingly more demanding operating conditions in LWRs and increased burnup to 75 GWD/MTU.

For the introduction of M5®, there were no significant perturbations in the FA manufacturing processes to be overcome. The change of cladding material did require a significant technical effort to be completed for the acceptance of the new material by the U.S. Nuclear Regulatory Commission (NRC). NPP's in the U.S. for which AREVA supplies PWR fuel have now been successfully converted to the M5® cladding.

The introduction of improved zirconium alloy claddings into the U.S. market has significantly reduced fuel cladding failures. This improvement helps give commercial nuclear utilities a high operating capacity factor (~90%), which leads to high production of electricity output and lower operating costs.

AREVA is now testing pre-operation oxide film on improved zirconium alloy cladding. The cladding is processed during manufacturing to produce a thin zirconium oxide film on the cladding. The oxide film acts like anodizing aluminum, forming a protective oxide layer that prevents further oxidation by providing a barrier and also prevents the formation of hydrides in the cladding.

The oxidized cladding has been inserted into fuel assemblies (FAs) in a European reactor to subject the test rods to actual operating conditions. The results are expected to show that the protective zirconium oxide layer prevents further oxidation of the cladding surface, therefore reducing cladding corrosion and spalling. It also prevents the uptake of hydrogen, which can cause cladding hydriding under certain reactor operations or events.

2.3. ADVANCED MARK BW 17X17 FUEL ASSEMBLY INTRODUCTION

Better fuel performance can be obtained by improving a number of features in a FA. For example, increasing the number of fuel rods within the existing dimensional envelope can create the ability to increase the thermal output of the FA.

Examples of other FA improvements that have enhanced fuel performance include a lower pressure drop upper end fitting/top nozzle design, the addition of a debris filter in the lower end fitting/bottom nozzle, and the use of M5® material for the cladding grids and other components such as mid span mixing grids.

2.4. ATRIUM™ 10XM BOILING WATER REACTOR FUEL ASSEMBLY

The ATRIUM™ Boiling Water Reactor (BWR) FA was introduced into the U.S. market to help BWR utilities increase the electricity output and capacity factor of their plants.

This advanced fuel provides the utilities reliable and dependable fuel performance by incorporating innovative and proven features such as the corrosion resistant cladding, debris filtering lower nozzle, and defect-free pellets with increased fuel mass and superior critical power performance to deliver fuel cost savings for 18 to 24 month operating cycles.

2.5. CHROMIA DOPED (CR_2O_3) FUEL PELLETS

Chromia doped pellet development began in Europe over 20 years ago. A significant amount of proprietary in-reactor pellet data has been accumulated on the pellet characteristics. Chromium oxide is added to the uranium oxide powder in pellets to provide for a more robust, chip-resistant, reliable pellet during manufacturing and rod loading. Chromia doped pellets were placed in fuel rods in the ATRIUM™ 10 BWR fuel type and have been inserted into the U.S. LaSalle reactor.

During verification testing, AREVA's large-grained chromia doped pellets were found to reduce the "washout" rate (release of fuel particles from breached cladding) by up to a factor of 5 in comparison with non-doped fuel. The lower washout rate helps to mitigate contamination of the reactor's primary coolant system.

The optimized grain structure of the chromia doped uranium oxide pellet provides a thermo-mechanically improved product that reduces fission gas release (FGR) and increases the power thresholds for pellet-clad interaction (PCI). This translates into a more economical and competitive product for upgrading NPP's operating with high burnup and extended fuel cycles.

3.0 CURRENT FUEL ASSEMBLY PRICES

A single PWR or BWR FA can cost approximately $800,000 to $1,200,000. The FA cost can vary significantly depending on the features incorporated into its design. The bulk of the cost is the amount of enriched uranium in the pellet. Therefore, more enriched pellets (up to 5 wt%) will make the FA cost more.

Most U.S. utilities operate their NPP's for base loading, which means that a particular plant is continuously operated at full power until the reactor's core begins to drop in heat production. The reactors are reloaded at 18 or 24 month intervals. The combination of improved FA designs and higher enriched pellets (less than 5wt%) has allowed the utilities to extend their plant run times from one year to up to 24 months with the higher burn up fuel. Typically, utilities perform their reactor core reloads and plant maintenance in the spring and fall months when the demand for electricity is at its lowest.

During a reload approximately one third of the reactor's core is replaced with new FAs. These assemblies are shuffled to arrange the older once or twice burned fuel and the new batch of fuel into an optimized arrangement that will generate the most heat and electricity. The thrice burned FAs are offloaded from the core and transferred underwater to the spent fuel pools for cooling

until they can be moved to a site's dry storage facility. A typical batch of PWR reactor fuel replacing approximately one-third of the core can cost $50 million or more.

4.0 MARKET DRIVERS

4.1. COST OF NUCLEAR FUEL

There are mainly two drivers for the cost of nuclear fuel – (1) the cost of the FA design (R&D, testing, and licensing) and (2) the cost of the enriched uranium in the fuel pellets

4.1.1. COST OF THE URANIUM IN THE FUEL PELLETS

The cost of uranium oxide has remained fairly stable for the past 5 years. Owners and operators of U.S. civilian NPP's purchased a total of 57 million pounds U_3O_8e (equivalent: Uranium quantities are expressed in the unit of measure U_3O_8e (equivalent)). Delivery of uranium oxide (or uranium concentrate) and the equivalent uranium-component of hexafluoride (UF_6) and enriched uranium from U.S. suppliers and foreign suppliers during 2013 had a weighted-average price of $51.99 per pound U_3O_8e. The 2013 total of 57 million pounds U_3O_8e decreased 5 percent compared with the 2012 total of 58 million pounds U_3O_8e.

The 2013 weighted-average price of $51.99 per pound U_3O_8e increased 412 percent compared with the 2001 weighted-average price of $10.15 per pound U_3O_8e, the lowest weighted-average price from 1994-2012, [Source: U.S. Energy Information Administration, 2013 Uranium Marketing Annual Report, dated May 2014].

There is approximately 1000 pounds of heavy metal content in the average PWR FA. Considerable expense is incurred to enrich the uranium to the nearly 5 wt% used today.

4.1.2. COST OF THE FUEL ASSEMBLY DESIGN

The cost drivers for the FA, excluding the cost of the heavy metal, are the design, materials, fabrication, testing, and licensing. The significant cost of these elements must be factored into the pricing and recovered in a reasonable time for reactor core reloads. If these development costs are not recovered during early batch reloads, their costs can be lost due to emerging designs by competitors.

The above cost elements have remained fairly constant. New regulations are being mandated by the NRC as a result of the March 2011 nuclear accident at Fukushima-Daiichi in Japan and the August 2011 U.S. Virginia earthquake, which will increase costs associated with new seismic criteria for designing and analyzing new fuel designs. Most NPP's located in the eastern U.S. previously had lower seismic criteria than plants on the west coast and the more earthquake prone areas.

4.2. IMPACT OF RENEWABLE ENERGY ON NUCLEAR POWER PLANT OPERATIONS

For the past decade or more, the U.S. NPP's have been operating as supplying the base load electricity for the utility. Base load power plants operate at full power and do not add supplemental electricity at peak usage periods during the day or during seasons of high demand, such as extremely hot temperatures in the summer and extremely cold periods in the winter. These peak periods where the demand for electricity is needed in a short period of time are provided by the utilities with natural gas (NG) turbine generating units and starting up idled power plants. The NG plants can be turned on and shut off quickly and can handle the daily peak periods. Fossil power plants are generally used to handle load demands for the extended peak periods for hot and cold spells.

As renewable intermittent energy sources of electricity, such as solar and wind power, have come into wider use to reduce carbon dioxide emissions, utilities are now being compelled by governmental mandates to include these energy sources as a part of their energy mix. As a result, some utilities will be forced to begin load following operations on their NPP's. Most NPP's in Europe already operate as load following units because nuclear generated electricity is a high percentage of the electricity generating capacity.

The nuclear fuel designs and core loading patterns are different for base load and load following units. Base load nuclear fuel is designed to produce heat generation at a steady rate and does not undergo the daily up and down power ramping (maneuvering) as the load following fuel. Thus, the fuel design parameters are generally less stringent than fuel designed for load following. The fuel service/operating conditions for the load following fuel are more stringent. Therefore, the design of the future EATF must anticipate this future operating requirement.

5.0 INCREMENTAL DESIGN CHANGES FOR EATF

Incremental design changes are accomplished through small changes and testing that causes the fewest perturbations to the R&D cycle. Conceptual designs are subjected to rigorous reviews before being approved for further development. Once the design is verified, usually by computer modeling and unirradiation testing, a limited number of test samples are inserted either into a test reactor or into a commercial reactor.

AREVA presently has several sets of LTAs in commercial reactors. In additional to these, several fuel rods in the LaSalle reactor contain chromia doped fuel pellets. Also, in a reactor in Europe several M5® fuel rods that received a pre-service application of zirconium oxide film during cladding fabrication have been inserted into LTAs.

It is expected that the results of the chromia doped pellets experiment should prove the benefit of providing to the market a pellet that can increase the heavy metal density, substantially limit pellet chipping, be more amenable to load following maneuvers, reduce FGR, and mitigate the washout of fuel particles under an accident condition. Less FGR is highly beneficial as less gas in the fuel rod plenum at high burnup means a safer core and fuel that can burn longer. There is also the distinct potential for the chromia doped pellets to capture and secure cesium. These incremental changes to the fuel pellet and cladding will achieve greater economic benefits.

6.0 COST OF INCREMENTAL CHANGE TO FUEL DESIGN AND ESTIMATED SCHEDULE

Design changes for nuclear fuel can have very long R&D time spans measured in decades. One method of reducing implementation time and managing risk is to incorporate changes incrementally. These changes are generally small and cause the least intrusiveness to the fuel manufacturer, the utility operator, and the nuclear regulator. The new product can be introduced sooner to market and capture the economic benefits in the development life cycle. For example, several experimental pellets may be inserted into a fuel rod pellet stack rather than testing a full stack of experimental pellets. The pellets are retrieved from the rods and their radiochemistry is examined in a hot cell to confirm the critical factors of performance. This approach shortens the design cycle and makes the fuel rods available sooner for use in the reactor core reloads.

Thus, incremental changes shorten the development schedule by reducing the time needed for design and analyses. In the case of the chromia doped pellet, it has been designed and inserted into a current generation FA and rod design. AREVA's experience with LTAs has shown that incremental changes may achieve a reduction of 1-2 years in the development cycle and provide a substantial reduction in the associated development costs.

Implementation of these improvements can be accomplished by:

- Selecting a utility customer that is friendly to change, and then selecting one of that customer's fuel supply units that need to improve its fuel costs.
- Proposing an implementation cost share or proposing to provide the improved fuel in return for a percentage of the utility's revenue tied to the increased fuel performance.

The next section identifies the types of development expenses that must be recovered. These will be established during the next phases of EATF development.

6.1. DEVELOPMENT COSTS

6.1.1. TESTING

The range of tests is described in Appendix K. As the tests are defined in greater detail, the costs can be established.

6.1.2. LTA

The costs for manufacture, licensing, irradiation, and post-irradiation examination of a Lead Test Rod (LTR) or LTA can be established once the final EATF technologies are selected.

6.1.3. LICENSING

Based on the initial testing and the results of the LTA PIE, modifications may be made to analytical models. Modifications may need to be made to analytical models, analyses for both implementations performed and licensing documents will be submitted, defended, and the approval methodologies implemented.

6.1.4. SCHEDULE OF EXPENDITURES

A cash flow analysis will require establishing both a range for the cost of money, which is normally proprietary, and a schedule for the expenditures.

6.1.5. SUMMARY OF DEVELOPMENT COSTS

Since the costs described above have not yet been established, AREVA's experience in developing, licensing, and implementing new fuel types will be used as the basis for a general, lumped estimate of $100M. This experience has been summarized in section 2.0 of this Appendix.

6.2. MANUFACTURING COSTS

6.2.1. CAPITAL

Capital is required to implement and qualify manufacturing processes and train personnel. The AREVA Team EATF will require implementing the following new processes.

- Acquire and Industrialize SPS

  The present SPS process produces a single pellet at a time. Even though less time is required per pellet than the present manufacturing process, it is not enough to compensate for the volume of pellets required commercially. This will require effort to industrialize the SPS process for commercial nuclear use.

- Acquire & Industrialize Coating Process

  The Cold Spray (CS) process is presently used for coating a range of commercial objects. The configuration to meet the volume and requirements for commercial nuclear fuel coating will have to be established. The capital cost of that configuration can then be established.

- Acquire & Industrialize Cladding Process

  Nuclear fuel cladding has been made from both stainless steel and zircalloy. A molybdenum cladding will require its own specific process for manufacture. These are not well developed at this point. Once they are developed, a configuration to supply the volume meeting commercial nuclear requirements will be established. The capital cost of that configuration can then be estimated.

6.2.2. OPERATING

<u>Manufacturing impacts on labor</u>

Each process configurations will require a certain amount of labor to produce a given volume of product. These need to be estimated once the production configurations are established.

Manufacturing impacts on materials

Similar to the labor content, the material content and cost can be established once the manufacturing and the waste amounts and rejection rates are established.

6.3. PROJECTED SALES

6.3.1. MARKET

The market size is perhaps the most difficult part of the financial analysis to estimate. For the present analysis, it is assumed that the present fuel market share remains constant into the future. It is also conservatively assumed that the market for an incremental LWR EATF will only include presently operating Gen III and planned Gen III reactors operating for 60 year-extended lifetimes.

6.3.2. SCHEDULE

- Delay from sales to delivery

  The schedule for payments will include the normal, customary fuel cycle delays for payments.

- Schedule of income

  An annualized schedule of fuel delivery will be used to estimate income form sales.

6.3.3. RETURN OF DEVELOPMENT AND COSTS

The income from sales, as a function of time will be used to establish the date at which all development costs will be recovered. An estimate based on the present development costs, and not the detailed costs, is provided in Section 7.2.

7.0 COST BENEFITS TO UTILITY AND FUEL VENDOR

As noted previously, implementing the product improvement that has the least impacts (cost, modifications & schedule) but produces a significant performance improvement will be more readily accepted by the fuel vendor and the customer.

7.1. AREVA CONCEPTS FOR BENEFITS TO UTILITY

The concepts being developed by the AREVA team will have the following benefits to the market:

7.1.1. IMPROVED THERMAL CONDUCTIVITY

Increasing the thermal output of the fuel pellet and cladding will potentially give a high return versus other improvements. This improvement will be providing more heat energy over an extended period of time.

7.1.2. CHROMIA DOPED FUEL PELLETS

Chromia doped fuel pellets will provide an improvement to fuel performance for load following maneuvers. Currently, most U.S. NPP's generate electricity for their utility as a base load. As base loaded power plants undergo modifications to load following, the chromia doped pellets will enable the conversion to offset the cost of these changes by providing more margins of safety during daily maneuvering

Chromia doped pellets increase uranium density in the pellet and reduce the amount of FGR. This will allow the utility to consider going to higher burnups.

7.1.3. SILICON CARBIDE WHISKERS

The introduction of SiC whiskers into the fuel pellet has the potential to enhance the pellet's thermal conductivity (TC) and reduce the amount of FGR. This has the potential to increase the thermal margin available to the utility while potentially allowing the utility to go to higher burn-ups in the reactor without the risk of fuel failure from fission gas build-up. A trade study needs to be conducted in the next stage of the project that considers the loss of uranium in the fuel pellet compared to the increased thermal margin, reduced fission gas, and small positive improvement available for uranium density in the pellet.

7.1.4. COATINGS

Coatings on the outside of the cladding have the potential to improve the performance of the fuel in the following ways:

1. Oxide films are pre-inducted on the cladding during manufacturing. These films protect the cladding by inhibiting further oxidation. These films also reduce the absorption of hydrogen and the subsequent formation of hydrides. The hydrides are detrimental to the integrity of the cladding and can cause spalling defects, which weaken the cladding and reduce margins of safety during reactor upsets or accident conditions.

2. Coatings are used to protect the fuel cladding base metal from corrosion and erosion and to enhance TC.

7.2. COST TO DEVELOP VS. PAYBACK TO VENDOR

The cost to develop a new FA versus payback to the vendor depends on the development cost of the LTA and sales of the new fuel to the utilities. With incremental improvements, new fuel presently costs about $100 million to develop. If AREVA will continue to supply fuel to 39 reactors in the U.S., it can expect to receive orders for about 530 fuel assemblies for reloads each year.

If the newly developed FA goes into one 177 FA plant refueled once every two years at a cost of $1 million per assembly and if each reload requires 59 new assemblies (one-third of the core), then AREVA could expect to recover its development costs within about 25 years from the start of the Discovery Phase of development. This schedule assumes 10 years to develop an LTA, 6 years for in-plant testing of the LTA, a one-third core reload of the new FA at the 12-year point, and 2 years for the Post Irradiation Examination

(PIE). Therefore, for an incremental improvement to FA design starting in 2012 the fuel vendor will not receive pay back of its investment until 2037.

The market for new fuel designs is further complicated by the current energy mix in the U.S. as of 2013. Based on current market conditions it can be expected that the reactor fleet will cease operations between 2050 and 2070, if it is assumed that all reactors go for a life extension to 80 years. If reactors close at 60 years then this time horizon can be moved back 20 years, Figure 2.

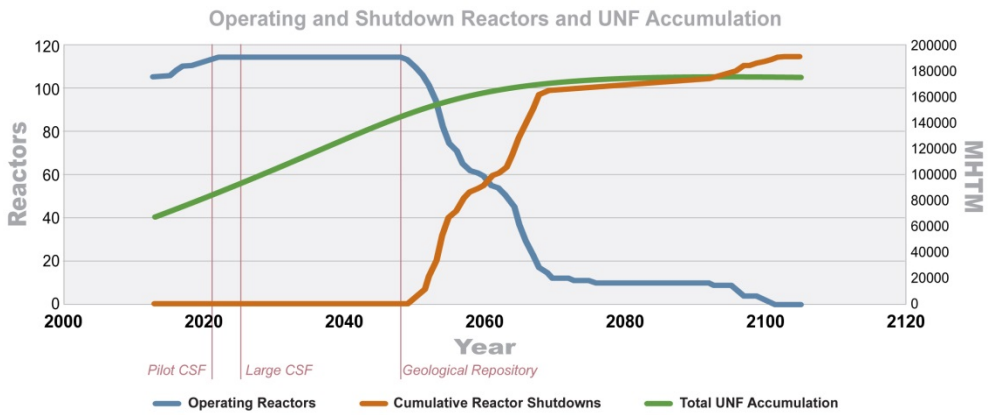

FIGURE 2: Hypothetical Operating Life of U.S. Reactor Fleet

At current market conditions it is not feasible or reasonable to expect to go to higher development costs resulting in longer payback times to the fuel vendor unless supported by a government sponsored program for EATF development. In the future, as the technologies evolve and the costs are better defined, the Business Plan will be updated.

APPENDIX C

Results of Gate Review #1
for the
Phase 1A Final Report
for Enhanced Accident Tolerant Fuels

Prepared by:
AREVA Federal Services, LLC

TABLE OF CONTENTS

1.0 INTRODUCTION 1
2.0 RECOMMENDATIONS BASED ON MANUFACTURING GATE REVIEW 7

LIST OF TABLES

Table 1: Pellet Spark Plasma Sintering Process with SiC Particles 1
Table 2: Pellet Spark Plasma Sintering Process with SiC Whiskers 2
Table 3: Cladding and Coating Cri Process (YSZ) 3
Table 4: Cladding and Coating Electrophoretic Deposition Process (TiO_2) 4
Table 5: Cladding and Coating Cold-Spray Process (Ti_2AlC) 5
Table 6: Molybdenum Cladding 6

1.0 INTRODUCTION

The following tables contain the evaluation of the technical options for Enhanced Accident Tolerant Fuel (EATF) based on the criteria from the Requirements Matrix (Appendix A) that are relevant to manufacturing.

Table 1: Pellet Spark Plasma Sintering (SPS) Process with Silicon Carbide (SiC) Particles

Technical Element 1: Pellet Spark Plasma Sintering Process with SiC Particles Manufacturing Gate Review Evaluation for EATF Discovery Phase			
RTM No.	Manufacturing Requirements / Goals	Y/N	Basis, Supporting Documentation, and Mitigation Strategy for Allowing Development to Continue
11	The fuel pellet material is stable under ambient conditions (dry air, 0.1 MPa, room temperature, various humidities).	Y	Long term observation
12	The fuel pellet process is capable of fabricating pellets of the appropriate size.	Y	Fabricated
13	The fuel pellet process is capable of achieving high density (≥95% TD).	Y	Shown
14	The fuel pellet process provides acceptable control of dimensions and geometry (e.g., diameter, surface finish, straightness, ovality, uniformity of thickness, pellet end geometry, etc., as applicable).	Y	Shown
15	The fuel pellet process yields pellets with acceptable integrity and controls chipping.	Y	Shown
17	The fuel pellet process will not lead to the formation of mixed wastes. (Goal)	Y	Net-shape fabrication
36	Fuel pellet insertion will not degrade cladding performance.	Y	Hard and high strength
37	Fuel pellet insertion will not damage fuel pellets.	Y	Hard and high strength
47	The fuel pellet composition will not challenge the available supplies of an isotope, element, or material. (Goal)	Y	No rare materials
65	The cost of the fuel pellet process is comparable to that of present fuels. (Goal)	Y	Our calculations yield lower cost
68	The fuel pellet process has an acceptable scrap rate. (Goal)	Y	Trace amounts of carbon layer
69	Subsequent fuel pellet processing steps will not cause unacceptable degradation of materials prepared previously. (Goal)	Y	Net-shape single processing step

Table 2: Pellet Spark Plasma Sintering Process with SiC Whiskers (SiC(w))

Technical Element 2: Pellet Spark Plasma Sintering Process with SiC Whiskers Manufacturing Gate Review Evaluation for EATF Discovery Phase			
RTM No.	Manufacturing Requirements / Goals	Y/N	Basis, Supporting Documentation, and Mitigation Strategy for Allowing Development to Continue
11	The fuel pellet material is stable under ambient conditions (dry air, 0.1 MPa, room temperature, various humidities).	Y	Long term observation
12	The fuel pellet process is capable of fabricating pellets of the appropriate size.	Y	Fabricated
13	The fuel pellet process is capable of achieving high density (≥95% TD).	Y	Shown
14	The fuel pellet process provides acceptable control of dimensions and geometry (e.g., diameter, surface finish, straightness, ovality, uniformity of thickness, pellet end geometry, etc., as applicable).	Y	Shown
15	The fuel pellet process yields pellets with acceptable integrity and controls chipping.	Y	Shown
17	The fuel pellet process will not lead to the formation of mixed wastes. (Goal)	Y	Net-shape fabrication
36	Fuel pellet insertion will not degrade cladding performance.	Y	Hard and high strength
37	Fuel pellet insertion will not damage fuel pellets.	Y	Hard and high strength
47	The fuel pellet composition will not challenge the available supplies of an isotope, element, or material. (Goal)	Y	No rare materials
65	The cost of the fuel pellet process is comparable to that of present fuels. (Goal)	Y	Our calculations yield lower cost
68	The fuel pellet process has an acceptable scrap rate. (Goal)	Y	Trace amounts of carbon layer
69	Subsequent fuel pellet processing steps will not cause unacceptable degradation of materials prepared previously. (Goal)	Y	Net-shape single processing step

Table 3: Cladding and Coating Electrophoretic Deposition (EPD) Process Yttria-Stabilized Zirconia (YSZ)

Technical Element 3: Cladding and Coating Electrophoretic Deposition Process (YSZ) Manufacturing Gate Review Evaluation for EATF Discovery Phase			
RTM No.	Manufacturing Requirements / Goals	Y/N	Basis, Supporting Documentation, and Mitigation Strategy for Allowing Development to Continue
11	The cladding and coating material is stable under ambient conditions (dry air, 0.1 MPa, room temperature, various humidities).	Y	Long-Term observation
14	The cladding and coating process provides acceptable control of dimensions and geometry (e.g., diameter, surface finish, straightness, ovality, uniformity of thickness, pellet end geometry, etc., as applicable).	Y	Performance testing has shown.
17	The cladding and coating process does not lead to the formation of mixed wastes. (Goal)	Y	No waste generation
30	The coatings will be deposited uniformly over substantially the entire exterior cladding surface.	Y	Fabrication specification can be met commercially.
35	Fuel rod handling and insertion into grids will not degrade cladding or coating performance.	Y	Performance testing has shown.
46	The cladding and coating process will, in principle, be capable of producing full-length cladding tubes.	Y	Commercially shown
47	The cladding and coating composition will not challenge the available supplies of an isotope, element, or material. (Goal)	Y	Commercially available
48	Each fuel rod will be capable of being marked with a unique, legible identifier	Y	Fabrication specification can be met.
65	The cost of the cladding and coating process is comparable to that of present fuels. (Goal)	N	More expensive
68	The cladding and coating process has an acceptable scrap rate. (Goal)	Y	No waste generation
69	Subsequent cladding and coating processing steps will not cause unacceptable degradation of materials prepared previously. (Goal)	Y	No chemical reactions

Table 4: Cladding and Coating Electrophoretic Deposition Process (TiO_2)

Technical Element 4: Cladding and Coating Electrophoretic Deposition Process (TiO_2) Manufacturing Gate Review Evaluation for EATF Discovery Phase			
RTM No.	Manufacturing Requirements / Goals	Y/N	Basis, Supporting Documentation, and Mitigation Strategy for Allowing Development to Continue
11	The cladding and coating material is stable under ambient conditions (dry air, 0.1 MPa, room temperature, various humidities).	Y	Long-Term observation
14	The cladding and coating process provides acceptable control of dimensions and geometry (e.g., diameter, surface finish, straightness, ovality, uniformity of thickness, pellet end geometry, etc., as applicable).	Y	Performance testing has shown.
17	The cladding and coating process does not lead to the formation of mixed wastes. (Goal)	Y	No waste generation
30	The coatings will be deposited uniformly over substantially all of the exterior cladding surface.	Y	Fabrication specification can be met commercially.
35	Fuel rod handling and insertion into grids will not degrade cladding or coating performance.	Y	Performance testing has shown.
46	The cladding and coating process will, in principle, be capable of producing full-length cladding tubes.	Y	Commercially shown
47	The cladding and coating composition will not challenge the available supplies of an isotope, element, or material. (Goal)	Y	Commercially available
48	Each fuel rod will be capable of being marked with a unique, legible identifier	Y	Fabrication specification can be met.
65	The cost of the cladding and coating process is comparable to that of present fuels. (Goal)	N	More expensive
68	The cladding and coating process has an acceptable scrap rate. (Goal)	Y	No waste generation
69	Subsequent cladding and coating processing steps will not cause unacceptable degradation of materials prepared previously. (Goal)	Y	No chemical reactions

Table 5: Cladding and Coating Cold-Spray Process (Ti_2AlC)

Technical Element 5: Cladding and Coating Cold-Spray Process (Ti_2AlC) Manufacturing Gate Review Evaluation for EATF Discovery Phase			
RTM No.	Manufacturing Requirements / Goals	Y/N	Basis, Supporting Documentation, and Mitigation Strategy for Allowing Development to Continue
11	The cladding and coating material is stable under ambient conditions (dry air, 0.1 MPa, room temperature, various humidities).	Y	Long-Term observation
14	The cladding and coating process provides acceptable control of dimensions and geometry (e.g., diameter, surface finish, straightness, ovality, uniformity of thickness, pellet end geometry, etc., as applicable).	Y	Performance testing has shown.
17	The cladding and coating process does not lead to the formation of mixed wastes. (Goal)	Y	No waste generation
30	The coatings will be deposited uniformly over substantially all of the exterior cladding surface.	Y	Fabrication specification can be met commercially.
35	Fuel rod handling and insertion into grids will not degrade cladding or coating performance.	Y	Performance testing has shown.
46	The cladding and coating process will, in principle, be capable of producing full-length cladding tubes.	Y	Commercially shown
47	The cladding and coating composition will not challenge the available supplies of an isotope, element, or material. (Goal)	Y	Commercially available
48	Each fuel rod will be capable of being marked with a unique, legible identifier	Y	Fabrication specification can be met.
65	The cost of the cladding and coating process is comparable to that of present fuels. (Goal)	N	More expensive
68	The cladding and coating process has an acceptable scrap rate. (Goal)	Y	No waste generation
69	Subsequent cladding and coating processing steps will not cause unacceptable degradation of materials prepared previously. (Goal)	Y	No chemical reactions

Table 6: Molybdenum Cladding

Technical Element 6: Molybdenum Cladding Manufacturing Gate Review Evaluation for EATF Discovery Phase			
RTM No.	Manufacturing Requirements / Goals	Y/N	Basis, Supporting Documentation, and Mitigation Strategy for Allowing Development to Continue
11	The cladding material is stable under ambient conditions (dry air, 0.1 MPa, room temperature, various humidities).	Y	Observed
14	The cladding manufacturing process provides acceptable control of dimensions and geometry (e.g., diameter, surface finish, straightness, ovality, uniformity of thickness, pellet end geometry, etc., as applicable).	Y	Demonstrated
17	The cladding manufacturing process does not lead to the formation of mixed wastes. (Goal)	Y	None
35	Fuel rod handling and insertion into grids will not degrade cladding performance.	Y	Assumes over clad
46	The cladding process will, in principle, be capable of producing full-length cladding tubes.	Y	To be demonstrated
47	The cladding composition will not challenge the available supplies of an isotope, element, or material. (Goal)	Y	No rare materials
48	Each fuel rod will be capable of being marked with a unique, legible identifier.	Y	Commercially performed on Zircaloy
65	The cost of the cladding process is comparable to that of present fuels. (Goal)	N	More Expensive
68	The cladding process has an acceptable scrap rate. (Goal)	N	Needs to be developed
69	Subsequent cladding processing steps will not cause unacceptable degradation of materials prepared previously. (Goal)	Y	Compatible with Zircaloy

2.0 RECOMMENDATIONS BASED ON MANUFACTURING GATE REVIEW

The manufacturing gate review was held as planned on 20 September 2013. The following persons participated as members of the review board:

Veronique Garat (AREVA)
Adam Howell (AREVA) (Secretary)
Ben Howell (Duke)
Jim Lemons (TVA)
Kevin McCoy (AREVA)
Rose Montgomery (TVA)
Paul Murray (AREVA) Chairman
John Strumpell (AREVA)
Suresh Yagnik (EPRI)

John Guerci (Dominion) had also been invited to participate but was unable to attend.

Presentations were made by Jim Tulenko and Ghatu Subhash, University of Florida (UF), Ben Hauch, University of Wisconsin (UW), Liz Hoffman, Savannah River National Laboratory (SRNL), and Bo Cheng, Electric Power Research Institute (EPRI). After each presentation, the board met in closed session to discuss the strengths and weaknesses of each research project. The following subsections provide comments from the board on the various approaches.

The portions of the Requirements Matrix applicable to Manufacturing were also evaluated and the results are supplied in Table 1 through Table 6.

2.1. UO_2-SIC FUEL FABRICATION BY SPARK PLASMA SINTERING (UNIVERSITY OF FLORIDA)

The presenters discussed silicon carbide powder (SiC(p)) and silicon carbide whiskers (SiC(w)) as potential additives for increasing the thermal conductivity (TC) of fuel pellets. The primary claimed advantages of an increased TC are (1) decreased cracking of the fuel pellets, (2) reduced fuel swelling, (3) decreased stored heat in the pellets at the time of Large Break Loss of Coolant (LOCA) initialization, and (4) greatly reduced fission gas release (FGR). The presenters also asserted that spark plasma sintering (SPS) could result in reduced fabrication costs; they estimated a cost of $1.33 per pellet for SPS versus $4.30 for conventional sintering, capital costs excluded. It was claimed that the results produced to date satisfied all the applicable requirements and goals in the requirements traceability matrix.

The board had some concerns regarding the work:

1. Decreased cracking may contribute to retention of fission gas, but the size of the benefit is not clear. Cracking results from thermal stresses, which are reduced by an increase in TC, but thermal stresses can also be reduced by reducing the linear power density, and studies of conventional pellets have not shown a strong effect of power density on cracking.

2. Reduced fuel swelling maintains a gap between the pellet and cladding for a longer period. That is beneficial in controlling pellet-cladding interaction. The thermal benefits are less clear. A larger pellet-cladding gap means a larger temperature

drop across the gap, but if the FGR is reduced, the TC of the gas will be higher because the effects of released xenon and krypton will be smaller.

3. It is reasonable to expect that the claimed increases in TC, if realized, will produce a large reduction in FGR. A key question is whether the increase in TC will be sustained until end of life. Direct implantation of fission products, implantation of knock-on atoms, and neutron irradiation effects all have the potential to degrade the SiC.

4. The claimed cost advantages during manufacturing of the pellets need to be carefully quantified. The costs for conventional pellet processing are unrealistically high, and the costs for SPS do not include capital cost.

5. The SiC takes up a substantial volume of the pellet and thus displaces fuel. As a result, the uranium loading and energy extraction per fuel assembly will be reduced.

The board concluded that the research is viable but has the following recommendations for Year 2:

1. Production work should focus on providing high-quality pellets for irradiation in the ATR. Producing usable pellets is essential for continued work on this approach.

2. A close investigation of how TC degrades with irradiation and the impact of TC improvement on potential for cracking is in order. Since cracking could be a threshold effect, a study to look at an equivalent linear power decrement for introduction of SiC compared to conventional pellets could add some insight.

3. A deeper economic analysis of fabrication costs is in order. The analysis should include capital costs, equipment maintenance costs (e.g., die replacement), and any other costs that are associated with SPS (e.g., costs of graphite felt).

4. Scaling up production by SPS is NOT recommended at this time.

2.2. COATINGS APPLIED BY ELECTROPHORETIC DEPOSITION

The presenter described work at the UW. Work to date has included electrophoretic deposition (EPD) of coatings, measurements of critical heat flux (CHF), consolidation of coatings (by sintering or laser surface treatment), wear and scratch testing, and autoclave testing.

Advantages of EPD are that (1) it produces thin, uniform coatings (typically 10 to 15 µm thick), (2) it is a well-established technique that is used commercially at large scales, and (3) it can be used to deposit a wide variety of coatings. Claimed benefits are an increase in the CHF and possibly increased resistance to high-temperature oxidation in steam. The requirements and goals in the requirements traceability matrix were not explicitly addressed. An increase in oxidation resistance is possible but has not been demonstrated yet.

Difficulties were encountered in depositing some of the candidate coating materials, especially alumina.

The board had some concerns regarding the work:

1. Consolidation of the coatings is a key problem in manufacturing that has not been successfully addressed yet. Tests with laser treatment have resulted in either too little or too much energy absorption, with the coatings being either inadequately consolidated or ablated. The alternative is low-temperature furnace sintering. The fineness of the deposited particles may make this approach feasible, though the temperatures that cause changes to the microstructure of cladding are low in comparison to those typically used for sintering. It is not clear that long; low-temperature heat treatments will provide a solution, because longer heat treatment times may also promote changes to the cladding.

2. There is the possibility that the increase in CHF will be lost during irradiation. Even in PWRs, parts of the fuel undergo nucleate boiling, and that raises questions about the possibility that crud will be deposited over the coating and degrade its performance.

3. An increase in CHF is welcome, but it does not provide a large benefit during the long accidents that are of interest to EATF.

The board concluded that the research is possibly viable but has the following recommendations for year 2:

1. Work should focus on producing well-consolidated coatings. The presenter suggested yttria-stabilized zirconia (YSZ) and TiO_2 as promising coating materials, and the board accepts that suggestion. Work on all other coatings should stop immediately. Reducing the number of coating materials is recommended so that more effort can be put into making high-quality coatings of the two chosen materials.

2. If well-consolidated, adherent coatings can be produced, the effects of the consolidation treatment on the microstructure of the substrate should be investigated.

3. An additional gate review is recommended for March 2014 to determine whether progress is being made in coating consolidation or the work should be terminated.

4. Related work (such as quench testing, CHF testing, and laser engraving) is NOT recommended at this time until the next gate review is passed.

2.3. MAX PHASE COATINGS APPLIED BY SPRAY PROCESSES

The presenter discussed the application of MAX phase coatings by high-velocity oxy-fuel (HVOF) and cold spray (CS) processes. HVOF was tested and found to present some difficulties: the powder caused an energetic excursion, and the composition of the deposited coating was substantially different from that of the original powder. In addition, microcracks were observed in HVOF coatings, even though the samples were handled gently. No additional work on HVOF deposition is planned. It should be noted that the cracks could have been formed during handling of the samples.

Cold spray coatings provided better retention of the original composition and, for properly chosen spray conditions, lower porosity. Both processes provided good adhesion and good scratch resistance.

It was claimed that the results produced to date satisfied all the applicable requirements and goals in the requirements traceability matrix except that of cost. Coating is an additional step and requires additional materials, so it will necessarily increase the cost of the cladding.

The board had some concerns regarding the work:

1. The coatings are typically thick, about 200 µm. The desired range is a few micrometers. The thickness means that the coating takes up a substantial volume in the core of a reactor and will affect the thermal hydraulic performance of the fuel assembly. The surface of the Zircaloy surface is also "roughened" by the application of the coating material. Therefore, the coating must fill in these peaks and troughs and this sets the minimum coating thickness.

2. Roughening of the substrate provides a mechanical bond with the coating, but a metallurgical bond is needed to prevent steam oxidation of the substrate. It is also possible that water or steam will penetrate through the coating and cause delamination.

3. Coupons of coated Zircaloy sheet showed discoloration on their uncoated faces. The discoloration suggests that the substrate reached a relatively high temperature, and its heat treatment may have been affected.

The board concluded that the research is possibly viable but has the following recommendations for Year 2:

1. Work should focus on CS application only.

2. The effect of the coating process on the microstructure of the substrate should be investigated. Annealing or phase change in the substrate is not desirable.

3. It is important to understand whether oxidation of the substrate is caused by penetration of steam or water through the coating or by transport under the coating from the edges. This question can be answered by metallography of a lightly oxidized sample.

4. The coating thickness must be dramatically reduced from what is currently seen.

5. Testing of flat coupons progressing to rods should proceed.

2.4. MOLYBDENUM ALLOY FOR FUEL CLADDING

In consideration of EPRI joining the AREVA EATF team in the next phase of the program, the board reviewed the progress of EPRI to date in their self-funded development program.

The performance of zirconium alloys in severe accidents is limited by their loss of strength at high temperature and by hydrogen generation in high-temperature, oxidizing environments. Molybdenum alloys are being investigated for fuel cladding because they provide superior strength at high temperatures. A common concern about molybdenum is that it will oxidize to volatile MoO_3 at high temperatures, but tests showed surprising resistance to that. In any case, oxidation could be addressed by applying an outer coating of zirconium or a FeCrAl alloy. The outer layer could be applied by coating techniques (physical vapor deposition, vacuum plasma spray, etc.) or by coextrusion. Molybdenum has a thermal neutron capture cross section comparable to that of FeCrAl, so there will be a neutronic penalty unless the molybdenum is depleted in Mo-95.

The requirements and goals in the requirements traceability matrix were not explicitly addressed.

This work was funded by EPRI and the board passed on the comments directly on this work.

APPENDIX D

Results of Gate Review #2
for the
Phase 1A Final Report for
Enhanced Accident Tolerant Fuels

Prepared by:
AREVA Federal Services, LLC

TABLE OF CONTENTS

1.0 SUMMARY 1

LIST OF TABLES

Table 1: Manufacturing Gate Review Evaluation for EATF Discovery Phase Form 3
Table 2: Completed Manufacturing Gate Review Evaluation for EATF Discovery Phase Form 6

1.0 SUMMARY

A gate review board was convened on April 10, 2014 to review progress on the cladding coatings. The review board's agenda is provided in Attachment A, along with the checklist for each Technical Element. The meeting minutes are provided in Attachment B. In summary, the EPD coatings were dropped and work on the cold spray (CS) MAX phase coating was continued.

ATTACHMENT A – GATE REVIEW AGENDA

Proposed EATF Gate Review
April 10, 2014

AGENDA

I. Session (8:30 – 9:00 am)

Review Board Preparation/Instructions

II. Session Topics (9:00 am)

Presentation by Team Members of:

1. The technologies that they developed, including composition, manufacturing techniques, process parameter, and sensitivities
2. Tests and test results
3. Judgments of whether the technology will meet the other applicable gate review criteria
4. Summary of anticipated enhanced accident tolerance benefits
5. Scoring of each technology by the Gate Review Board
6. Collection of scores, adjustments, final verdict on each technology

III. Presentations

The following elements should be addressed by your presentation to the Gate Review Board, which is scheduled for 30 minutes (or less).

1. Describe the process and optimizations investigated.
2. Provide a summary of test results.
3. Address the attached checklists based on the Manufacturing Design Criteria.
4. What technologies should be carried forward in this program, and why.
5. What are the next steps? What remains to be done to be ready for performance testing of coated cladding? What development and performance testing do you recommend in year 2?

Table 1: Manufacturing Gate Review Evaluation for EATF Discovery Phase Form

Cladding Coating; Process and Material: Cold Spray MAX Phase Manufacturing Gate Review Evaluation for EATF Discovery Phase			
RTM No.	Manufacturing Requirements / Goals	Y/N	Basis, Supporting Documentation, and Mitigation Strategy for Allowing Development to Continue
11	The cladding and coating material is stable under ambient conditions (dry air, 0.1 MPa, room temperature, various humidities).		
14	The cladding and coating process provides acceptable control of dimensions and geometry (e.g., diameter, surface finish, straightness, ovality, uniformity of thickness, pellet end geometry, etc., as applicable).		
17	The cladding and coating process does not lead to the formation of mixed wastes. (Goal)		
30	The coatings will be deposited uniformly over substantially all of the exterior cladding surface		
35	Fuel rod handling and insertion into grids will not degrade cladding or coating performance.		
46	The cladding and coating process will, in principle, be capable of producing full-length cladding tubes.		
47	The cladding and coating composition will not challenge the available supplies of an isotope, element, or material. (Goal)		
48	Each fuel rod will be capable of being marked with a unique, legible identifier.		
65	The cost of the cladding and coating process is comparable to that of present fuels. (Goal)		
68	The cladding and coating process has an acceptable scrap rate. (Goal)		
69	Subsequent cladding and coating processing steps will not cause unacceptable degradation of materials prepared previously. (Goal)		

ATTACHMENT B – GATE REVIEW MEETING MINUTES

EATF Cladding Coatings Gate Review
April 10, 2014
AREVA Offices, Charlotte, NC

The cladding coating gate review was held at the AREVA offices in Charlotte, NC on April 10, 2014, beginning at 8:00am. The following board members were present:

John Guerci - Dominion
Kevin McCoy - AREVA
Rose Montgomery - TVA
Jim Lemons - TVA
Michele Pleasants - AREVA
Paul Murray - AREVA
John Strumpell - AREVA
Suresh Yagnik (via phone) - EPRI

The following were also in attendance to make presentations or observe:

Kumar Sridharan – UW
Brenda Garcia-Diaz - SRNL
Luke Olsen - SRNL
Jeremy Bischoff - AREVA
Mike Morrell - AREVA

The board reviewed progress against the manufacturing gate review criteria for the cladding coatings. Other concepts being investigated by the AREVA team (pellets with additives and alternative cladding concepts) were not reviewed. It should be noted that the objective of the manufacturing gate review is to establish that the concept is basically manufacturable; in many cases, at this early stage of development, the detailed supporting evidence for full-scale manufacturability is not available. However, where it can be logically construed that the concept is manufacturable, this was noted for the record. For example, Criterion 35 requires that fuel rod handling and grid insertion not degrade the cladding or coating performance; while full length rods have not been inserted into a grid under typical manufacturing conditions; scratch testing has been performed with similar scratch loads applied.

The board agreed to the following recommendations with respect to manufacturability of the coating concepts:

1. Investigations of EPD coatings will be discontinued owing to the inability to meet the project specifications with respect to manufacturability.

2. Cold spraying of MAX phase coatings is promising and work should be continued, with the following task prescribed to further substantiate the viability of the concept:

a) It is recommended that coating be applied to small tubular samples (both open and closed end) (rather than on flat coupons as has been done so far) and tested to assess edge effects and viability of applying coatings on actual cladding.

3. Either the coating is applied as the cladding is manufactured, and the end plugs and weld areas are uncoated, or the coating is applied after rod loading. The resulting vulnerabilities of each approach should be investigated. The effect of having uncoated ends needs to be investigated, or a method for coating the end caps and welds should be provided and investigated.

4. Polishing may be required to achieve thickness and surface roughness objectives. The size of the sprayed particles greatly influences the deposition layer of the coating so different sizes should be considered to reduce the overall coating thickness.

5. The effects of rod flexing needs to be investigated. It should be noted that handling restrictions are currently imposed to maintain straightness of the rod; a good objective would be to demonstrate that these current restrictions will maintain coating integrity. If they are not, a new handling restriction should be defined. This information may be developed based on analytical work or lab experiments. These investigations should be done on a coated rod of sufficient length.

6. A cost analysis including materials and manufacturing costs needs to be completed. In support of this, the scrap rate needs to be estimated.

7. The board also discussed the general performance evidence available, and recommended that additional information be supplied for the coatings that will be further investigated:

   a. The diffusivity of aluminum in Zircaloy should be measured at several temperatures and any change in microstructure identified.
   b. Discussion during the review noted that the best result would occur for a coating with a thermal conductivity very near, or greater than, the substrate thermal conductivity. Additional data from the literature should be supplied to substantiate the objective, or more testing and analyses must be completed, or both.
   c. The oxidation kinetics of the coating itself under the accident conditions should be established to further substantiate any benefits of the concept (improvement over the Zircaloy kinetics).
   d. Tensile testing should be completed to determine the threshold for detrimental effects on the coating and substrate.
   e. The compatibility of the various oxides and eutectics should be established.

8. Further optical microscopy images are requested to substantiate the claim that the microstructure over the majority of the substrate is unaffected by the coating application.

9. It is known that there will be uncoated areas on the cladding. AREVA needs to establish how much coating must be intact during the accident scenario to achieve any improvement.

Table 2: Completed Manufacturing Gate Review Evaluation for EATF Discovery Phase Form

Cladding Coating; Process and Material: Cold Spray MAX Phase Manufacturing Gate Review Evaluation for EATF Discovery Phase			
RTM No.	Manufacturing Requirements / Goals	Y/N	Basis, Supporting Documentation, and Mitigation Strategy for Allowing Development to Continue
11	The cladding and coating material is stable under ambient conditions (dry air, 0.1 MPa, room temperature, various humidities).	Y	Long-Term observation and testing under ASTM G2 conditions.
14	The cladding and coating process provides acceptable control of dimensions and geometry (e.g., diameter, surface finish, straightness, ovality, uniformity of thickness, pellet end geometry, etc., as applicable).	Y - Coupons N - Rods	Corrosion and LOCA testing have shown uniform protection.
17	The cladding and coating process does not lead to the formation of mixed wastes. (Goal)	Y	No waste generation.
30	The coatings will be deposited uniformly over substantially all of the exterior cladding surface	Y - Coupons N - Rods	Fabrication specification can be met commercially.
35	Fuel rod handling and insertion into grids will not degrade cladding or coating performance.	Y	Scratch testing only.
46	The cladding and coating process will, in principle, be capable of producing full-length cladding tubes.	N	Not demonstrated yet.
47	The cladding and coating composition will not challenge the available supplies of an isotope, element, or material. (Goal)	Y	Commercially available
48	Each fuel rod will be capable of being marked with a unique, legible identifier.	N	Not demonstrated yet.
65	The cost of the cladding and coating process is comparable to that of present fuels. (Goal)	N	Need to perform a cost analysis.
68	The cladding and coating process has an acceptable scrap rate. (Goal)	N	Not evaluated yet.
69	Subsequent cladding and coating processing steps will not cause unacceptable degradation of materials prepared previously. (Goal)	N	Needs to be evaluated.

APPENDIX E

UO_2-Composite LWR Fuel Pellets with Increased Thermal Conductivity Fabricated by Spark Plasma Sintering for the Phase 1A Final Report for Enhanced Accident Tolerant Fuels

Principal Investigators:

James S. Tulenko, Materials Science and Engineering
Ghatu Subhash, Mechanical and Aerospace Engineering

Prepared by:
AREVA Federal Services, LLC

TABLE OF CONTENTS

1.0 INTRODUCTION 1
2.0 SPARK PLASMA SENTERING 1
3.0 UO_2-SIC COMPOSITE FUEL 2
4.0 UO_2 –CR_2O_3 DOPED PELLETS 7
5.0 MASTER SINTERING CURVES FOR UO_2 AND UO_2 – SIC COMPOSITES 9
6.0 PRODUCTION OF PELLETS INTENDED FOR IRRADIATION IN THE ATR 12
7.0 EFFECT OF MIXING ON SINTERING BEHAVIOR 13
8.0 SPS DIE TOOLING FOR SMALL FUEL PELLET 26
9.0 CONCLUSIONS AND FUTURE WORK 29
10.0 REFERENCES 29

LIST OF TABLES

Table 1: Attributes of sintered UO_2 – Cr_2O_3 pellets 7
Table 2: Pellet types and quantities to be fabricated for irradiation in the ATR 12
Table 3: Dimensional statistics for8.2 mm pellets 13
Table 4: Dimensional statistics for 12.5 mm fuel pellets 13
Table 5: Mixing method, Particle Size and Sintered Density 16
Table 6: Mixing method and Sintered Density 18
Table 7: Mixing methods with resultant sintered densities 19
Table 8: Mixing Method with Sintered Density 20
Table 9: Average density for UO_2 pellets sintered at 1150°C for 5 minutes and 40MPa 26
Table 10: Difference in average density of sintered pellets for a die OD of 0.944” 27

LIST OF FIGURES

Figure 1: Dr. Sinter 1030 system and schematic representation of sintering chamber [2] 2
Figure 2: UO_2 – 10vol% SiC composite pellets produced by both conventional sintering (1600°C) and SPS (1400°C) 3
Figure 3: Relative density of UO_2 – 10vol%SiC composite pellets sintered by conventional sintering and SPS at various maximum temperatures 4
Figure 4: Polished surfaces of high density UO_2 – 10vol%SiC composites sintered by SPS showing uniform dispersion of A) SiC whiskers & B) SiC particles 4
Figure 5: Microstructures of UO_2 – SiC composites sintered at 1500°C 5
Figure 6: Thermal conductivity of various sintered UO2 – 10vol%SiC pellets 6
Figure 7: Comparison of XRD spectra of UO_2 – 70 vol % SiC pellets sintered by SPS and conventional sintering at 1600°C. The peaks contained in dotted circles refer to USi1.88 phase 6
Figure 8: Sintered pellet density as a function of chromia concentration 8
Figure 9: Graph of axial variance of grain size in dope UO_2 pellets sintered at 1600°C for 30 seconds 8
Figure 10: Evolution of relative density as a function of temperature for UO_2 and UO_2-SiC composite 9
Figure 11: ρ-lnΘ curves for selected value of activation energy 10
Figure 12: Mean residual squares for various estimated activation energy values. The minimum value provides the activation energy for a given powder 10
Figure 13: Master sintering curve for pure UO_2 with activation energy of 140 KJ/mol and UO_2-SiC with activation energy of 420 KJ/mol 11
Figure 14: Comparison of predicted relative densities of UO_2 and UO_2-SiC pellets and densities measured by isothermal heating method 11
Figure 15: 17x17 sized pellets intended for irradiation in the ATR 12
Figure 16: Differential Volume Plot: Batches mixed without Steel Balls 15
Figure 17: Differential Volume Plot: Batches mixed with Steel Balls 15
Figure 18: EDS Spectra: Diamond Particles mixed 120 minutes 17
Figure 19: Differential Volume Plot: Batches mixed with and without Deca 17
Figure 20: Differential Volume Plot: Batches mixed with Diamond Particles 19
Figure 21: SEM Images of Raw Powder 21
Figure 22: SEM Images: UO_2 Powder mixed without balls but with Decafluoropentane 22
Figure 23: UO_2 Powder mixed with steel balls and with decaflouropentane 23
Figure 24: SEM images illustrating excess mixing aid in powder 24
Figure 25: SEM Images: The need for a mixing aid 25
Figure 26: SEM Images: Mixing Aid related failure 25
Figure 27:"Lipped punch" used to try to reduce the current density in the punches 27
Figure 28: Lipped punch (at the top of the die) and die combination loaded into the SPS furnace 28

1.0 INTRODUCTION

Current commercial light water reactor (LWR) technology utilizes uranium dioxide (UO_2) almost exclusively for fuel pellets. UO_2 has the advantage of having a high melting point, enhanced oxidation resistance, as well as a history of operational and fuel cycle data. A major shortcoming for UO_2 is a low thermal conductivity which can lead to large radial temperature gradients and high centerline temperatures. As a result, fuel pellet cracking and release of gaseous fission products can occur during normal operation. In an effort to enhance the safety of LWRs the U.S. Department of Energy (DOE) introduced the Enhanced Accident Tolerant Fuels (EATF) program. Fuels with enhanced accident tolerance are defined by the DOE as "fuels, which in comparison with standard UO_2 – zircaloy systems, can tolerate loss of active cooling in the reactor core for a considerably longer time period while maintaining or improving the fuel performance during normal operations" [1].

The proposed accident tolerant fuel design by the University of Florida (UF) introduces a high thermal conductivity additive to UO_2. The additive materials employed are silicon carbide (SiC) (whiskers and powder) and diamond (powder). SiC has been shown to increase the thermal conductivity of the pellets by up to 40%. Increasing the thermal conductivity of the fuel allows for a decrease in fuel temperature as well as a more uniform radial temperature gradient through the pellet. Moreover, the decreased temperature gradient reduces thermal stresses and cracking in pellets [2]. In addition, during accident scenarios, an increase in thermal conductivity decreases the amount of stored thermal energy and reduces the peak cladding temperature. FRAPCON simulations for fuel with increased thermal conductivity reveal an ~ 250 °C decrease in fuel centerline temperature. Additionally, the increase in thermal conductivity allows for about an ~ 100 °C decrease in average fuel temperature. These decreases allow for improved loss of coolant accident (LOCA) response and with minimal fission gas release (FGR) can yield improved accident response.

Conventional pressing and sintering methods for UO_2 composite fuel pellets yielded a pellet density < 90% theoretical density (%TD). To achieve the industry standard of ~96.5%TD the advanced manufacturing process of Spark Plasma Sintering (SPS) had to be utilized. Composite UO_2 fuels fabricated using SPS have routinely achieved densities up to 98%TD [2] with a greatly improved thermal conductivity.

2.0 SPARK PLASMA SENTERING

Spark Plasma Sintering (SPS) or Field Assisted Sintering Technique (FAST) is an advanced manufacturing process that allows the rapid sintering of a variety of materials, particularly difficult-to-sinter ceramics and metals. Due to the fact that conventional sintering methods were not able to achieve industry standards for the advanced composite UO_2 fuels, SPS was utilized.

SPS is characterized by a high amperage pulsed DC current passing through a conductive graphite mold while simultaneous mechanical pressure is applied to the ends of the mold. The graphite mold consists of a cylindrical die and two punches. The powder is placed in the die cavity and punches are inserted on both sides. The entire die assembly is placed in the SPS sintering chamber. Figure 1 shows a schematic representation of the SPS chamber and the Dr. Sinter 1030 system utilized in this research. The current applied to the mold flows both through the punch and die and the powder loaded in the mold. The application of this current sinters the powder via multiple mechanisms including plasma activation, Joule heating, and resistive heating

[3]. The pressure applied to the mold helps compress the sample while maintaining a set outer diameter (OD). This process promotes the rapid heating and densification of the sample on the order of minutes versus several hours with conventional methods. Fast heating rates and high mechanical pressures help reduce porosity and facilitate uniform densification. The entire process is done within a vacuum to ensure that chemical reactions and oxidation are controlled.

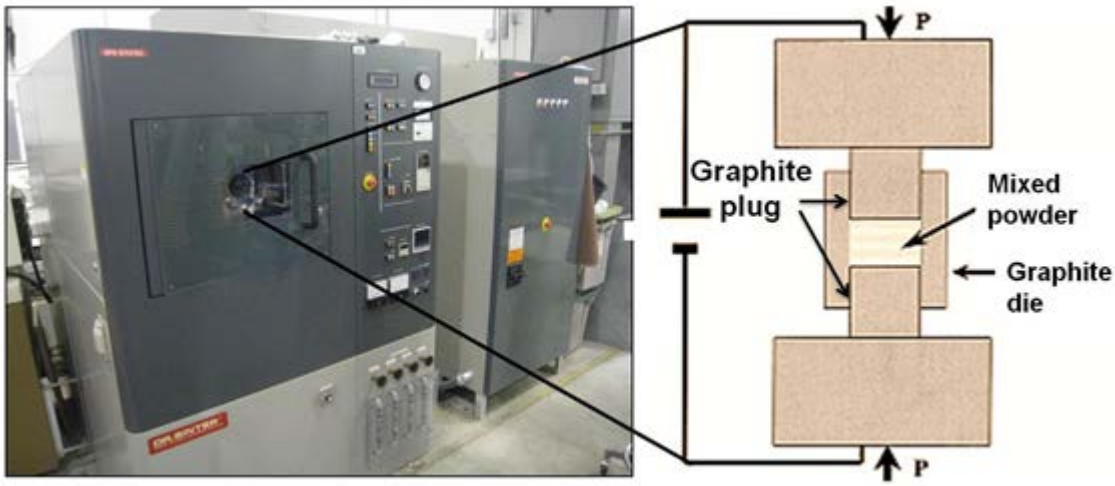

Figure 1: Dr. Sinter 1030 system and schematic representation of sintering chamber [2]

Utilizing SPS requires the control of many different sintering parameters. In particular, temperature ramp up and cool down rate, hold time, maximum temperature, and axial pressure can be varied in order to produce different results. SPS has the ability to reduce processing time and save energy relative to that of conventional sintering methods, while achieving unique densification results.

In the current project the UF has conducted SPS processing of UO_2 – SiC, UO_2 – Diamond, and enriched (4.95% UO_2) material with and without addition of a grain growth enhancer, Cr_2O_3. UF has also developed the M theory for 15x15 dimension pellets which allows UF to identify SPS conditions that are required to achieve a desired density in a pellet.

3.0 UO_2-SIC COMPOSITE FUEL

Silicon carbide (SiC) was the initial 2nd phase additive chosen for the accident tolerant composite fuels. SiC has long been considered a prime candidate for use as a fuel matrix material, cladding, and as a fuel-particle diffusion barrier. This is due to a low neutron cross section, high thermal conductivity, chemical stability (strong resistance to oxidation in air and air moisture environments), and high melting temperature. SiC also has the advantage of being non-toxic over alternatives such as beryllium oxide [2]. Both SiC particles and whiskers were considered for the fuel.

Both conventional sintering and SPS techniques were undertaken for the UO_2-SiC composites. For conventional sintering, green body pellets were made by pressing the blended UO_2 - SiC powder at 200 MPa for 10 minutes in a stainless steel die. The die walls were lubricated with a film of stearic acid to prevent fracture of the green body pellets while being taken out. The die

and pellet diameters were 12.5 mm. The green body pellets were then sintered in an alumina tube furnace with a ramp rate of 2.6 °C/min until the temperature reached 1600 °C where it was held for 4 hours. To maintain a hyper-stoichiometric state, an ultrahigh purity (UHP) Ar gas atmosphere, with a continuous flow rate of 2 liter/min, was used during the sintering process.

Spark plasma sintering was performed in a Dr. Sinter® SPS-1030 system. For SPS, the blended material was loaded into a diameter graphite die. The inner die surface was covered by a thin graphite foil to prevent a reaction of the powder with the graphite die wall. Cylindrical graphite punches were inserted into both ends of the die. The end of each punch that contacts the powder was coated with an aerosol graphite spray to prevent reaction of the punch and the powder. The ramp up/down rate was set at 100 °C/min and the hold time at the maximum temperature was 5 minutes. An axial pressure of 40 MPa was applied at the beginning of hold time. The maximum sintering temperature was set at 1400 °C, 1500 °C, and 1600 °C for different pellets.

It was found through a series of trials that the optimal SiC fraction for the greatest increase in thermal conductivity was 10 volume percent. Figure 2 shows sintered disks of UO_2 – 10 vol%SiC (both whiskers and particles). Figure 3 shows that, SPS processing produces much higher density pellets relative to that of conventional. It was found that conventional sintering was not feasible for the composite fuels due to the very low densities of the fuels relative to the industry standard of ~96.5% theoretical density.

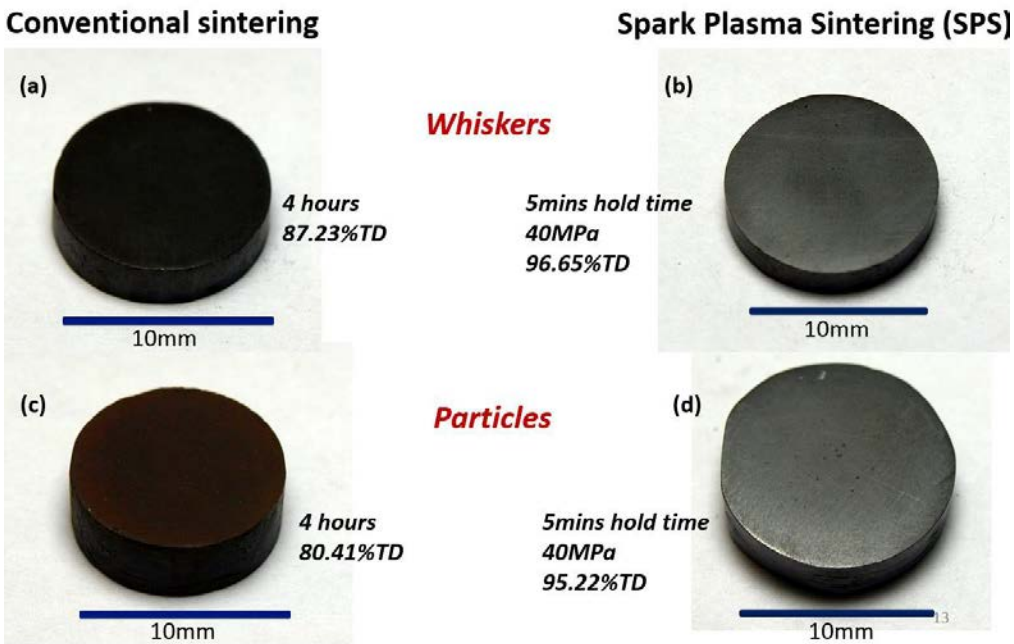

Figure 2: UO_2 – 10vol% SiC composite pellets produced by both conventional sintering (1600°C) and SPS (1400°C)

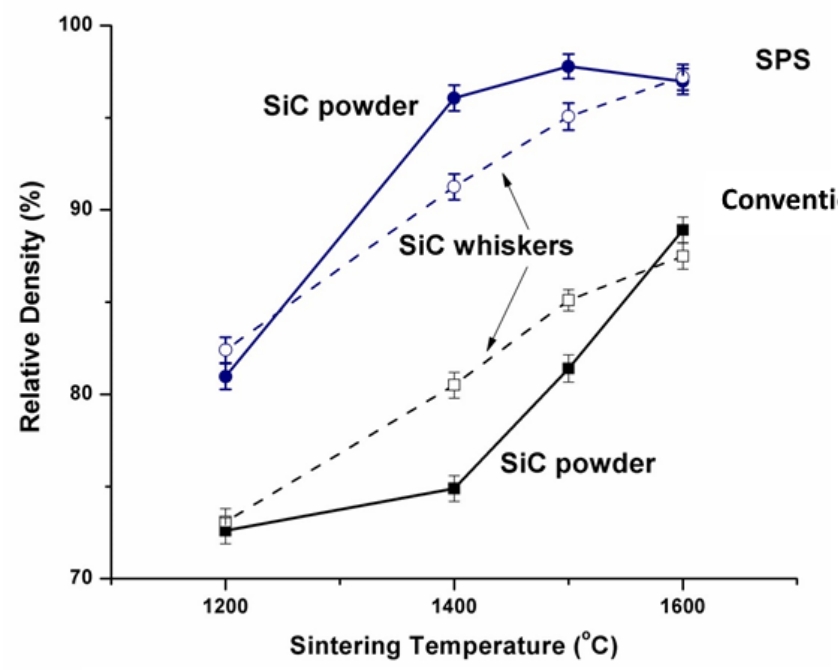

Figure 3: Relative density of UO_2 – 10vol%SiC composite pellets sintered by conventional sintering and SPS at various maximum temperatures

Figure 4 reveals the distribution of SiC whiskers and particles within the UO_2 matrix. Both the whiskers and particles are seen to be uniformly distributed without any agglomeration. In addition, the micrographs in Figure 5 show that SPS sintered pellets have much more favorable interfacial contact than conventionally sintered pellets.

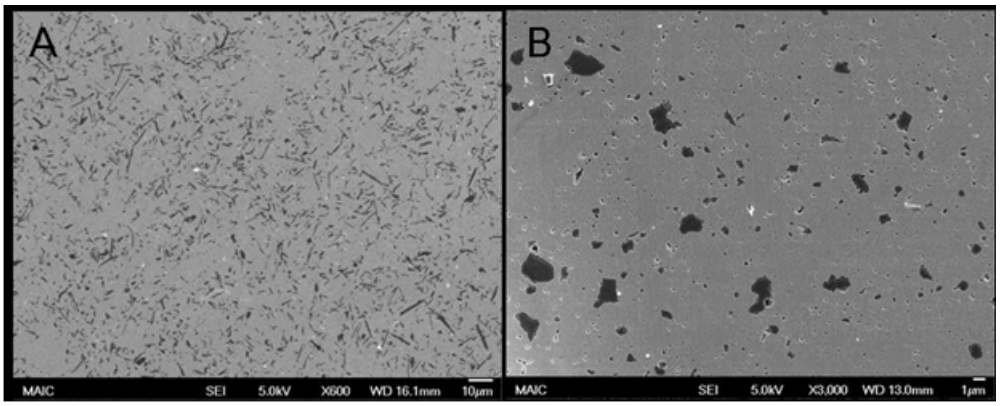

Figure 4: Polished surfaces of high density UO_2 – 10vol%SiC composites sintered by SPS showing uniform dispersion of A) SiC whiskers & B) SiC particles

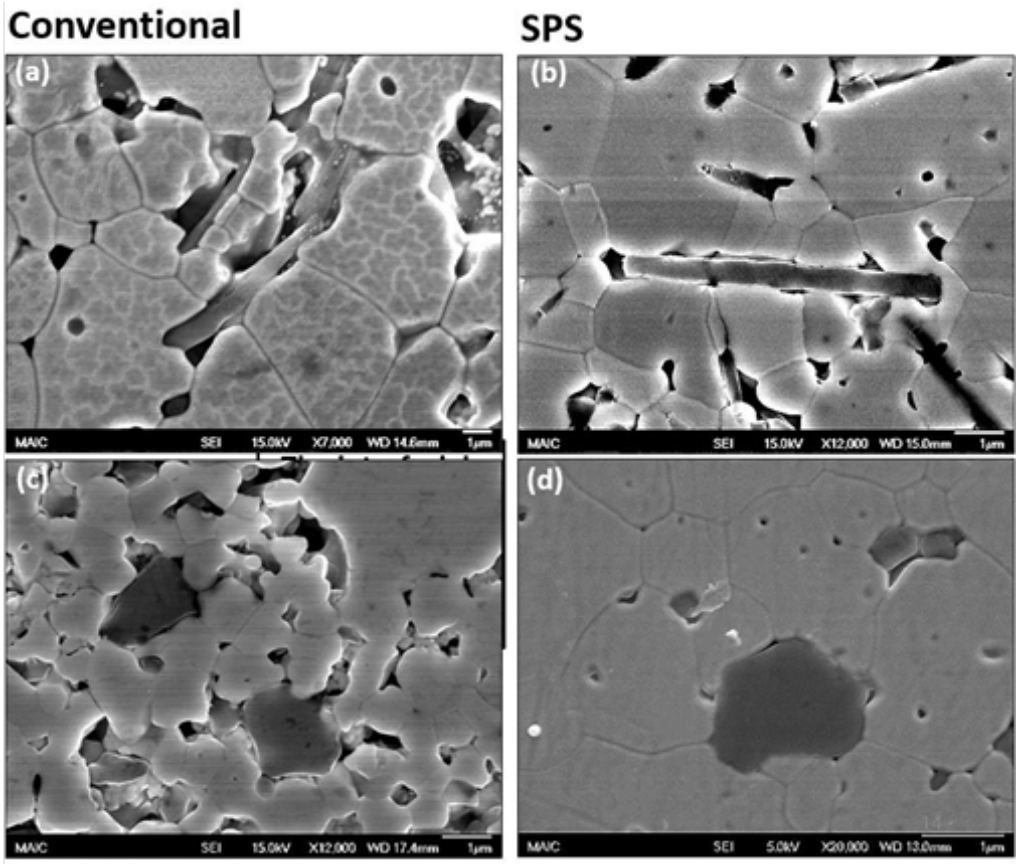

Figure 5: Microstructures of UO_2 – SiC composites sintered at 1500°C

In Figure 5 Subfigs A) & C) are sintered by conventional sintering for a 4 hour hold time while B) and D) are sintered by SPS for a 5 min. hold time.

Using laser flash analysis, thermal diffusivity and heat capacity were measured, and thermal conductivity was calculated. Figure 6 shows that, in general, as the sintering temperature increased, the thermal conductivity increased. The thermal conductivity is up to 60% greater than that of pure UO_2. This increase allows for increased accident tolerance in a loss of coolant accident, and decreased fuel centerline temperature of ~ 250 °C. In contrast, the thermal conductivity of conventionally sintered UO_2 – 10vol%SiC pellets was lower than that of pure UO_2 measurements.

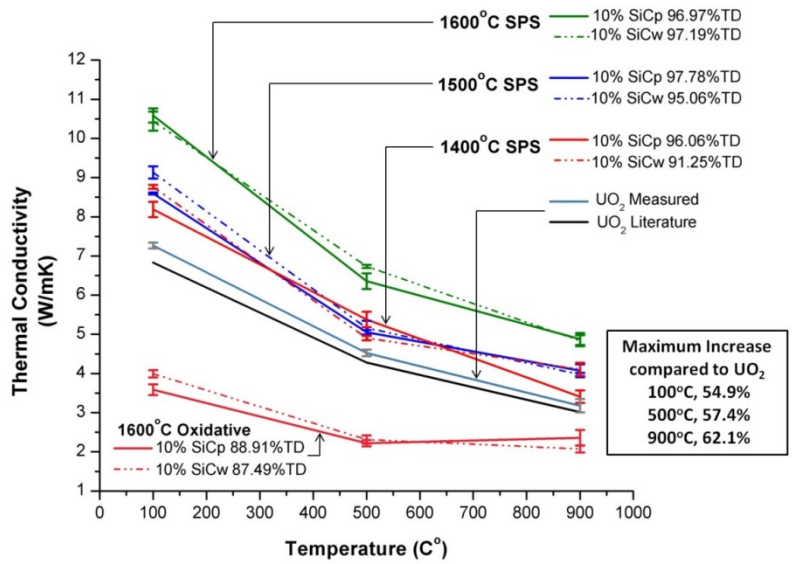

Figure 6: Thermal conductivity of various sintered UO2 – 10vol%SiC pellets

Controlling chemical reactions between SiC and UO_2 during the high temperature sintering process is critical to the fabrication of dense UO_2-SiC pellets, because the formation of various reaction products at the UO_2 and SiC interface may lead to poor thermal properties. In our study XRD analysis was used to determine the reaction products at the interface. Figure 7 shows two XRD spectra obtained from UO_2-10vol%SiC pellets sintered at 1600 °C for 4 hours and at the same temperature by SPS for 5 minutes hold time. A $USi_{1.88}$ peak was clearly seen in the oxidative sintered pellet, but no such reaction product was detected on the pellet fabricated by SPS.

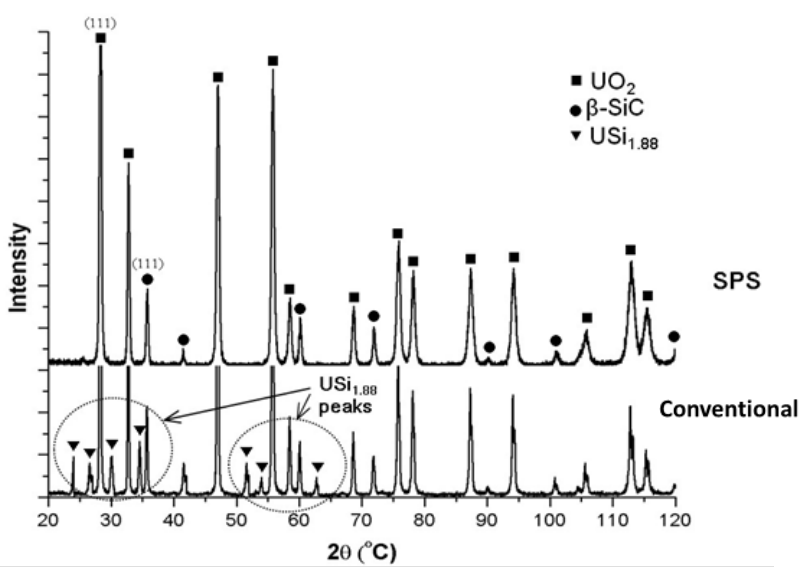

Figure 7: Comparison of XRD spectra of UO_2 – 70 vol % SiC pellets sintered by SPS and conventional sintering at 1600°C. The peaks contained in dotted circles refer to USi1.88 phase

4.0 UO_2 –CR_2O_3 DOPED PELLETS

It has been shown that an increase in a fuel's grain size can decrease the rate of FGR. To promote grain growth, a dopant of chromia (Cr_2O_3) was proposed. SPS was used to fabricate Cr_2O_3 doped UO_2 at different dopant levels and the resulting pellets were characterized. Table 1 lists the pellets and their densities, grain size, and sintering parameters.

Doping Amount mCr_2O_3/mUO_2 (µg/g)	Temperature (^0C)	Hold Time (min)	Pellet Condition	Density (%TD)	Average Grain Size (µg)
0	1450	20	Good	98.7	5±0.6
1000	1450	20	Good	97.5	4±0.4
1500	1450	20	Good	97.3	5±1.2
2000	1450	20	Good	97.3	5±0.7
0	1600	40	Crumbled	-	-
0	1600	20	Crumbled	-	-
1000	1600	20	Crumbled	-	-
1500	1600	20	Crumbled	-	-
2000	1600	20	Crumbled	-	-
0	1600	0.5	Good	97.6	4.1
1000	1600	0.5	Good	97.4	14.3
1500	1600	0.5	Good	97.5	41.7
2000	1600	0.5	Good	95.8	4.3

Table 1: Attributes of sintered UO_2 – Cr_2O_3 pellets

The influence of the Cr_2O_3 concentration on the density of the sintered pellets was studied. The results of this study are shown in Figure 8. As shown in the graph, the density of the sintered UO_2 – chromia pellet generally decreased as doping amount was increased. In particular, there was a large drop in density when going from 1500ppm by mass to 2000 ppm by mass for the sample held for 30 seconds.

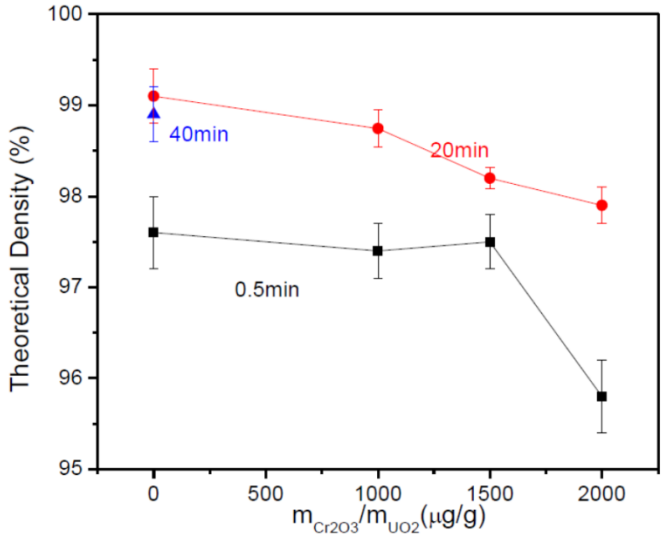

Figure 8: Sintered pellet density as a function of chromia concentration

The grain sizes of the pellets were investigated to try to achieve the high grain size of 41 μm seen previously (Table 1). It was found that the grain size was large at the end of the pellet and that there was a large gradient in grain size along the length of the pellet. This fact is evident in the graph of grain size versus distance from pellet surface seen in Figure 9. Although there is a significant drop in grain size in the interior of the pellet, the doped pellets still were able to achieve grain sizes much higher than pure UO2. It was determined that 1500ppm by mass was the optimal level of chromia dopant for promoting grain growth in UO2 pellets sintered by SPS.

.

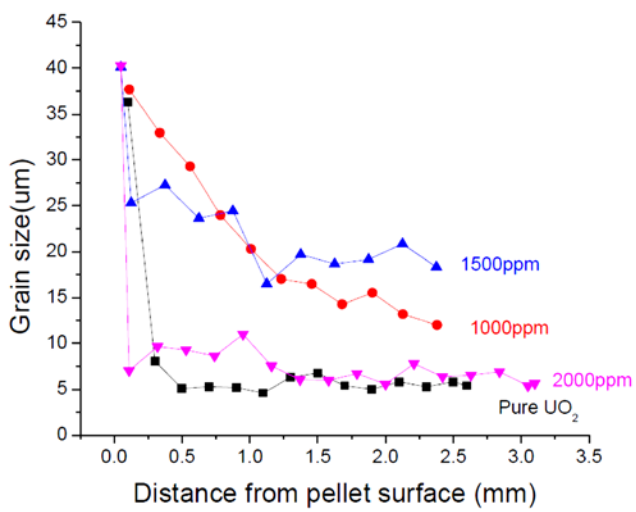

Figure 9: Graph of axial variance of grain size in dope UO_2 pellets sintered at 1600°C for 30 seconds

5.0 MASTER SINTERING CURVES FOR UO_2 AND UO_2 – SIC COMPOSITES

The master sintering curve (MSC) describes the empirical relationship between the evolution of densification and the microstructure. In the MSC, material microstructure parameters and thermal parameters are separated, and two characteristic parameters are defined - the densification parameter $\Phi(\rho)$ and the work of sintering $\Theta(t,T)$. The curve showing the relationship between $\Phi(\rho)$ (or alternately, $\Theta(t,T)$) and density (ρ) is then defined as the MSC.

Two different sets of heating schedules were used. The constant heating rate method was used to construct the MSC and the isothermal method was used to validate the constructed curve.

The time-dependent relative densities for UO_2 and UO_2 with SiC particles are plotted versus temperature in Figure 10. The instantaneous relative density is dependent on the heating rate for a given powder, but all densification curves have the regular sigmoidal shape.

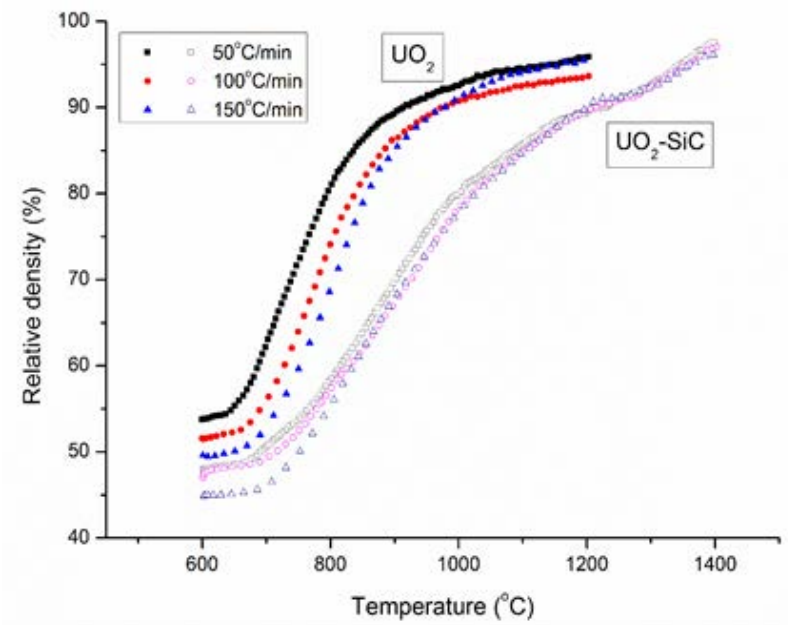

Figure 10: Evolution of relative density as a function of temperature for UO_2 and UO_2-SiC composite

To calculate the work of sintering ($\Theta(t,T)$), determination of the activation energy Q is essential. For an appropriate value of Q, the MSC is independent of heating path, thus the ρ-lnQ curves with different heating rates should converge to a single curve. The ρ-lnΘ curves of UO_2 with selected Q values for all heating profiles are shown in Figure 11.

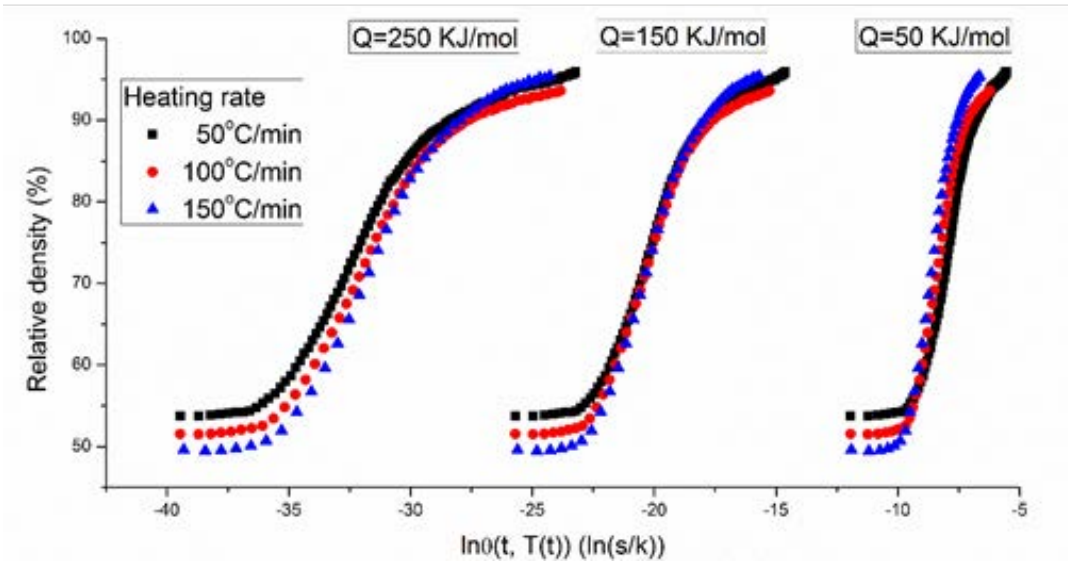

Figure 11: ρ-lnΘ curves for selected value of activation energy

To quantify the convergence, a polynomial curve fit was made and the mean of residual squares was calculated. Figure 12 reveals the mean residual squares with different assumed values of Q, from which the minimum is identified when Q=140KJ/mol for pure UO_2, and Q=420 KJ/mol for UO_2- SiC composite.

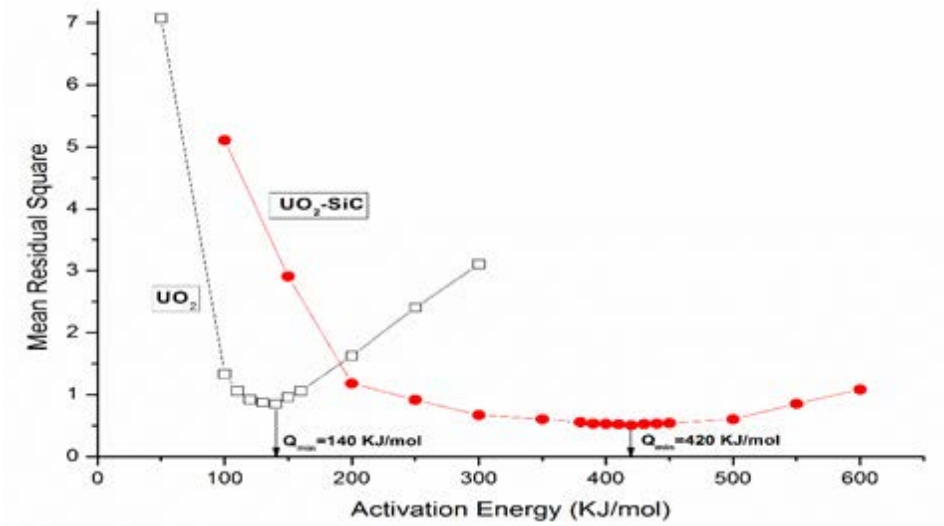

Figure 12: Mean residual squares for various estimated activation energy values. The minimum value provides the activation energy for a given powder

The MSCs for UO_2 and UO_2-SiC were then constructed (Figure 13). Despite a threefold difference in heating rates, a single curve has been obtained by converging the individual curves.

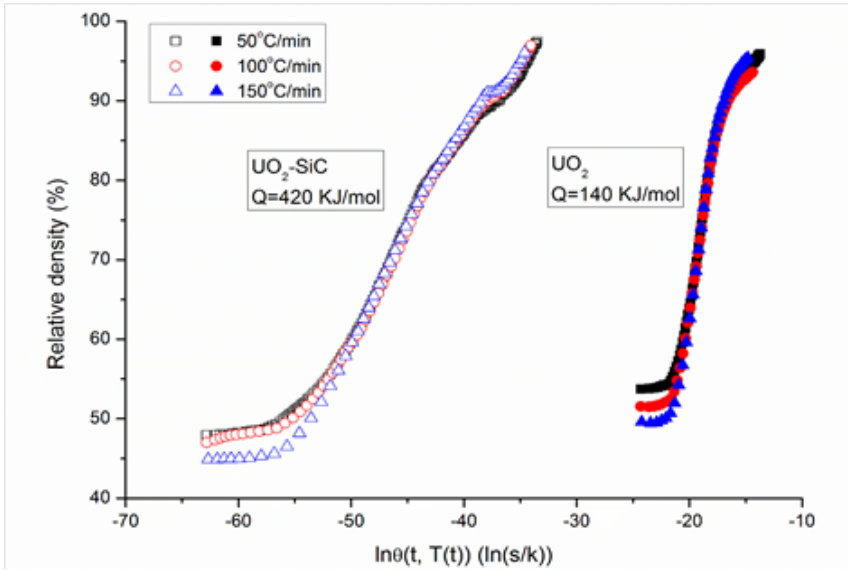

Figure 13: Master sintering curve for pure UO_2 with activation energy of 140 KJ/mol and UO_2-SiC with activation energy of 420 KJ/mol

The validity of the constructed MSC was verified by a few experimental runs with the isothermal sintering method (Figure 14). Despite the rather different heating profiles, the experimentally measured relative densities align closely with the constructed MSCs, confirming the validity of the MSCs derived from the earlier experiments.

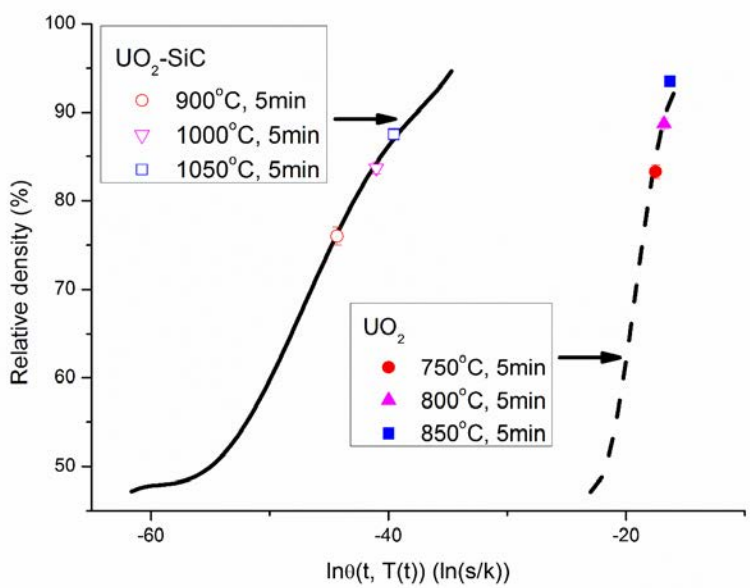

Figure 14: Comparison of predicted relative densities of UO_2 and UO_2-SiC pellets and densities measured by isothermal heating method

MSC theory has been applied successfully to UO_2 and UO_2-SiC composite ceramics sintered by SPS. Utilizing just one temperature and time dependent parameter (Θ), the densification process was quantified. The activation energy for SPS has been determined to be 140 kJ/mol for UO_2 and 420 kJ/mol for UO_2-SiC composite. It should be noted that the MSC work done in Phase 1a was for pellets with a diameter of 12.5 mm. MSCs will also be constructed for pellets with a diameter of 8.2 mm.

6.0 PRODUCTION OF PELLETS INTENDED FOR IRRADIATION IN THE ATR

In accordance with the EATF project, the UF fabricated pellets with enriched UO_2 intended for irradiation in the Advanced Test Reactor (ATR). Work was done to fabricate, characterize, and maintain quality control of ATR sized fuel pellets. The ATR requires pellets with a diameter of ~8.2 mm, much smaller than the 12.5 mm pellets that had been fabricated previously. Additionally, the UF felt that UO_2 – Diamond pellets also had favorable thermal properties and should be included in irradiation tests. Based on this, the pellets in Table 2 were fabricated for irradiation in the ATR. The rodlets in the ATR are composed of 8 enriched pellets and 2 blanket pellets. The production quantities allowed for 3 extra pellets of each type for archival purposes. Figure 15 shows the fabricated ATR pellets as well as a comparison of the two pellet sizes.

Pellet Type	Quantity
Blanket	15
Base	19
SiCw	19
Diamond	19

Table 2: Pellet types and quantities to be fabricated for irradiation in the ATR

Figure 15: 17x17 sized pellets intended for irradiation in the ATR

Shown in Table 3 are statistics regarding the dimensions of small-diameter fuel pellets. Likewise, in Table 4 are comparative statistics of the dimensions of previously fabricated large-diameter pellets. Diameter control approaches that required for commercial pellets.

During the production of the ATR pellets many challenges were encountered. In particular the transitioning from 12.5 mm pellets to 8.2 mm pellets proved difficult. The sintering profiles defined for the larger pellets were not applicable for the smaller one, and sintering parameters had to be actively determined during production. Many of the smaller pellets were seen to delaminate, break, and chip. Many factors were thought to have caused these issues including pre-sintering powder preparation (mixing, drying, particle size), and the die tooling and are being investigated.

Number of samples measured	98
Sample Mean Diameter	0.3223”
Standard Deviation	0.0006”
95% Confidence Interval	(0.3222”, 0.3224”)

Table 3: Dimensional statistics for8.2 mm pellets

Number of samples measured	50
Sample Mean Diameter	0.4908”
Standard Deviation	0.002”
95% Confidence Interval	(0.4902”, 0.4914”)

Table 4: Dimensional statistics for 12.5 mm fuel pellets

7.0 EFFECT OF MIXING ON SINTERING BEHAVIOR

The effect of mixing additives into UO_2 powder was studied to better understand the failure modes experienced during the production of pellets for the ATR. The possibility that the mixing procedure may contribute to negative effects was first proposed when pellets with SiC powder failed to sinter. These pellets were fabricated from powder that was mixed two separate times. The first mixture was enriched UO_2 with Cr_2O_3, mixed for one hour and intended for use in base pellets. The Cr_2O_3 addition was later deemed unnecessary, and this powder was remixed with SiC powder for one hour in an attempt to not waste the enriched stock. All of these pellets failed to sinter. Unlike other pellet failures which had surface issues, the silicon carbide particle (SiC(p)) pellets failed in the bulk. Additional inspection of once-mixed powders showed the possibility of similar failures. Furthermore, mixed powders, depleted UO_2 powders, and enriched UO_2 powders exhibited different sintering behavior. For these reasons, the effect of the powder mixing process on sintering behavior was studied.

Additives are mixed into the UO_2 powder using simple mechanical mixing. The powders are weighed and placed in plastic trays. The size of any one mixing batch is limited to 20 grams because of the size of the mixing vial. The powders are the placed in a zirconia vial and a mixing aid is added to promote a uniform dispersion of the additive. For SiC additives, three small steel balls were also added. For diamond additives, no steel balls were used. The vial top is sealed with

tape and placed in a plastic bag. This is all done to prevent contamination. The vial is then placed in a 3D ball miller. For the ATR project, any single batch was mixed for one hour. The previously mentioned SiC(p) batches were mixed two separate times for an hour each. After the one hour mixing is completed, the powder is removed and placed in beakers. The powder comes out slightly wet from the mixing aid. For this reason the powder is dried at least 24 hours in air before being sintered.

The parameters of the mixing process studied were the effects of mixing time, steel balls, and mixing aid on pellet sintering behavior. The effect of mixing time on particle size, pellet density, and structural stability was examined. The effect of the mixing aid on dispersion of additives, pellet density, and structural stability was examined. It should be noted that ATR pellet fabrication exposed other issues such as the change in pellet diameter.

The effect of mixing time on particle size was studied. Twenty-gram powder batches were prepared with only depleted UO_2 powder. These batches were mixed for 15, 30, 60, and 120 minutes. For each mixing time, batches were mixed with and without the addition of steel balls. All batches were mixed with the use of the mixing aid. After drying, the particle size of each batch was measured with the use of laser light scattering. After particle size was measured, each batch was sintered via SPS.

Full size 12.5 mm pellets were fabricated. The hold temperature was 1150 °C. The hold time was 5 minutes. The heating and cooling rate was 100 °C/min. Density of each pellet was measured via the Archimedes method. Also SEM was performed on all mixed powders and a few fracture surfaces of broken pellets. Raw unmixed powder was also analyzed as a control. Particle size was measured via a Coulter LS320 analyzer, which measures particle sizes from 40 nm to 2,000 µm by laser light scattering (LS). It is based on the principle that light intensity scattered from particles is a function of scattering angle, particle size, shape, incident wavelength, and response of the material to light. Calculations assume the particles are spherical.

A graph of particle size measurements for samples mixed without the use of steel balls is shown in Figure 16. In this figure, Raw_01 is raw unmixed powder, A15 is powder mixed for 15 minutes, A30 is powder mixed for 30 minutes, and so on. The Y-axis is the volume percent, thus meaning for A15 powder, 11% of the powder volume is taken up by 38 µm particles. There is no visible trend for these batches of powder. The average size of a single particle is about 650 nm. There is a consistent size reduction from the raw powder. This is expected, as these large particles are just agglomerates of smaller particles.

A graph of particle size measurements for samples mixed with the use of steel balls is shown in Figure 17. In this figure Raw_01 is raw unmixed powder, B15 is powder mixed for 15 minutes, B30 is mixed for 30 minutes, and so on. The Y-axis is volume percent meaning for B30 powder, 6.5% of the powder volume is taken up by 10 µm particles. There is an obvious visible trend for these batches of powder. The average size of a single particle is about 600 nm. There is a consistent size reduction from raw powder. The steel balls break up UO_2 agglomerates. After 60 minutes there is no further size reduction; however, there is a slow approach to the expected distribution around 600 nm. This implies there are still agglomerates after 120 minutes.

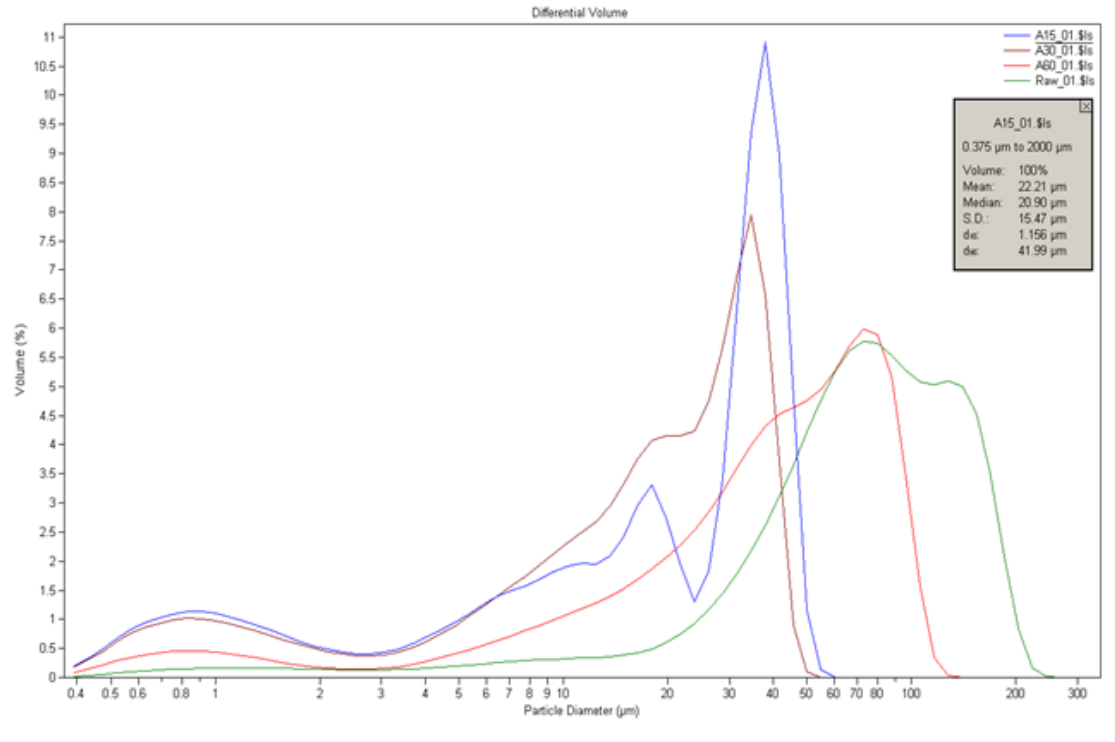

Figure 16: Differential Volume Plot: Batches mixed without Steel Balls

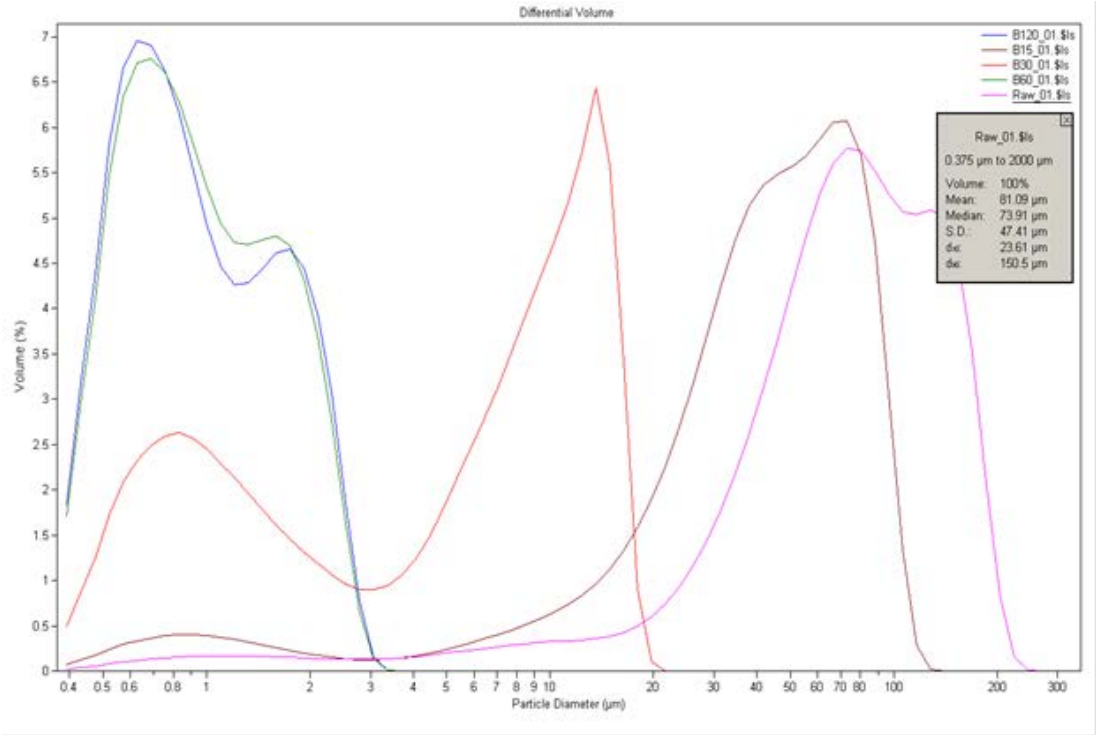

Figure 17: Differential Volume Plot: Batches mixed with Steel Balls

Mixing Method	Mean Size um(dV)	Mean Size nm(dN)	% Theoretical Density
RAW	81.1	711.0	98.0
W/O 15	22.2	656.0	91.1**
W/O 30	19.3	656.0	95.7
W/O 60	44.4	651.0	97.4
W/O 120	53.85	640.0	92.9*
W 15	45.8	656.0	96.5
W 30	6.65	641.0	96.7*
W 60	1.09	605.0	95.7
W 120	1.04	598.0	94.7*

Table 5: Mixing method, Particle Size and Sintered Density

Table 5 compares mixing method, particle size and sintered density. Single asterisks denote pellets that broke upon removal. The double asterisk is for a pellet that survived removal but broke upon later inspection. There is no clear effect of particle size on sintered density. Literature suggests smaller particle size leads to greater density but may require more sintering time [5], but both batches mixed for 120 minutes yielded pellets that broke and had lower densities, whereas raw powder produced the highest density pellet.

In addition to particle size, the effect of the mixing aid was investigated. Regardless of particle size, powder that was exposed to the mixing aid for two hours, always yielded pellets that suffered bulk failure. This fact led to the investigation of the mixing aid. The mixing aid is Decafluoropentane (Deca) with a formula $C_5H_2F_{10}$. The boiling point of Deca is 55 °C; it has a flash point of 125 °C and a vapor pressure 30.12 kPa. There is very little data on degradation and reactivity of this compound. Deca will quickly evaporate in air at room temperature.

EDS measurements were taken on samples that were mixed with Deca for 2 hours. These measurements showed no contamination in powders after mixing. An EDS spectrum for diamond particles and UO_2 mixed with Deca for 120 minutes is shown in Figure 18. There were no noticeable peaks except for those expected. To examine if the mixing aid was required, powder was mixed without adding Deca. Figure 19 compares the particle size of that batch and the particle size of powder mixed with Deca. The red line denotes powder mixed for 60 minutes without Deca, and the blue line denotes powder mixed for 60 minutes with Deca. The particle size is smaller without the Deca; however, particle size changes have not been confirmed to lead to pellet failure. Pellets were fabricated with powder mixed in the mill without the use of Deca and compared with pellets than used Deca. Pellets were fabricated from powder mixed without Deca for 60 and 120 minutes.

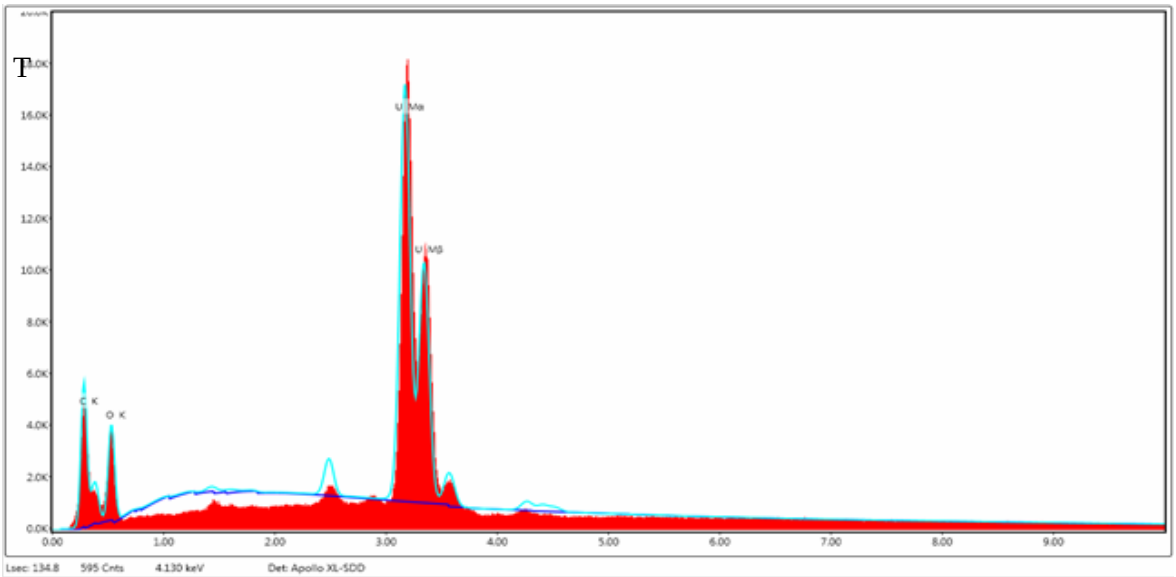

Figure 18: EDS Spectra: Diamond Particles mixed 120 minutes

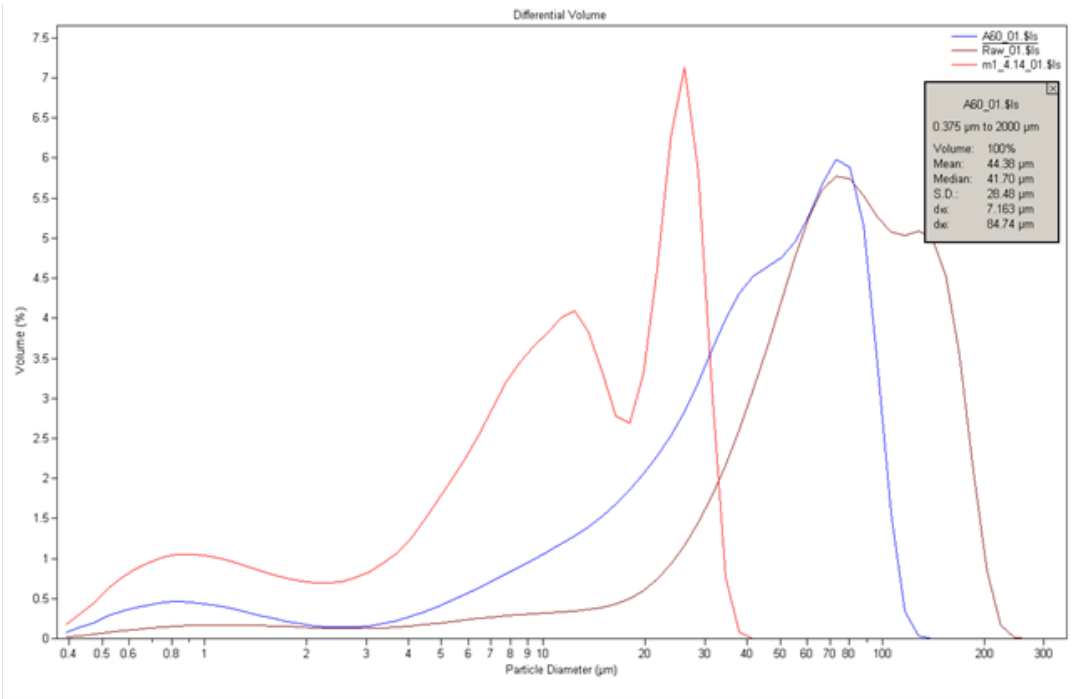

Figure 19: Differential Volume Plot: Batches mixed with and without Deca

Mixing Method	% Theoretical Density
Raw	98.0
With Deca No Balls 60 min	97.4
With Deca No Balls 120 min	92.9*
With Deca With Balls 60 min	95.7
With Deca With Balls 120 min	94.7*
Without Deca No Balls 60 min	96.3
Without Deca No Balls 120 min	96.5

Table 6: Mixing method and Sintered Density

Densities of different mixing methods are compared on Table 6. The only pellet fabricated from powder mixed for 120 minutes that remained intact was mixed without Deca. Both pellets fabricated without Deca remained intact and achieved over 96% TD. The need for Deca was then investigated for powder mixed with additive. Since the SiC(p) pellets always failed and the silicon carbide whisker (SiC(w)) pellets were not optimal, diamond additive was studied first.

First the effect on particle size of mixing diamond particles with UO_2 was investigated. For these measurements, UO_2 powder was mixed with 10 volume percent diamond with an average size of 12 µm. The powders were mixed for 60 minutes with Deca but no steel balls. The particle size measurements for two batches mixed for 60 minutes are shown in Figure 20. The line marked "Raw_01" is for UO_2 powder mixed without balls but with Deca for 60 minutes. The bimodal distribution was interesting but has not been investigated. The diamond particles may break up UO_2 agglomerates.

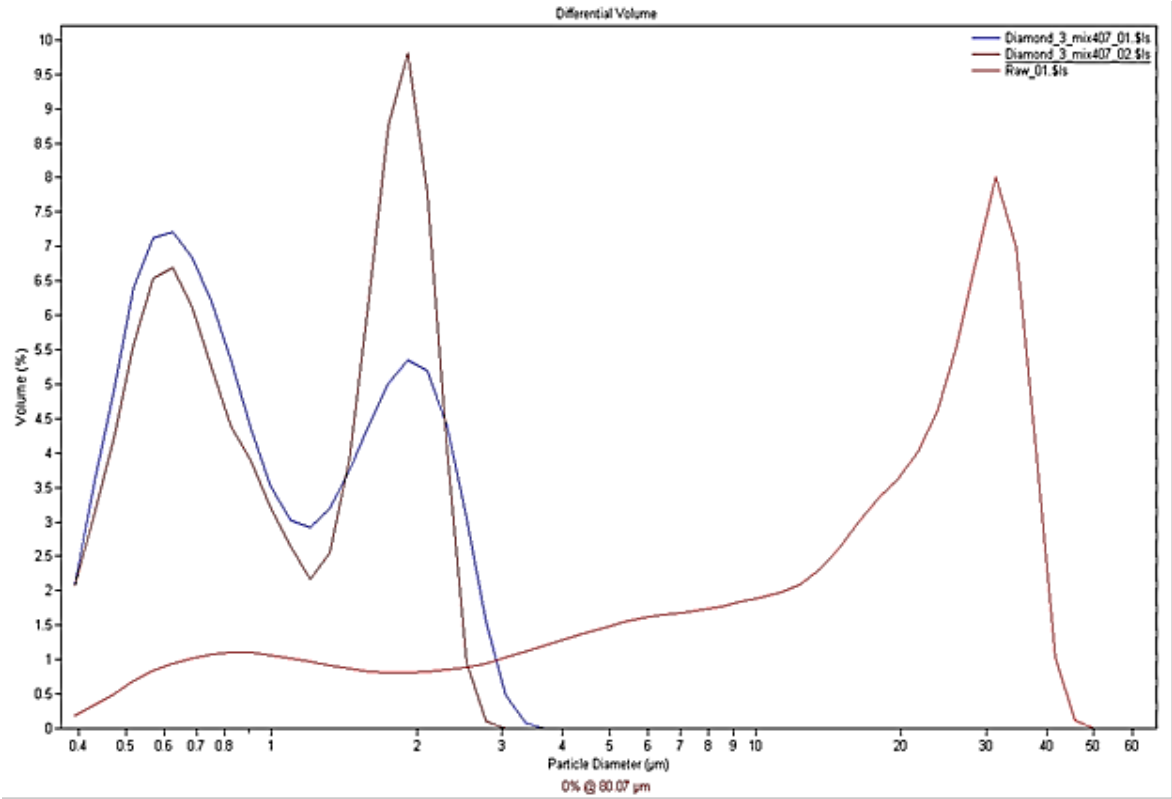

Figure 20: Differential Volume Plot: Batches mixed with Diamond Particles

Diamond Pellet	%Theoretical density
Raw	98.0
No Deca 30 min	97.5
No Deca 60 min	95.0*
No Deca 120 min	89.7*
NB W Deca 120 min	94.3

Table 7: Mixing methods with resultant sintered densities

Since particle size did not explain sintering behavior, the rest of the diamond additive pellets were just sintered and further examined. Table 7 displays the mixing method with resultant densities. Asterisks indicate that the pellet broke upon removal. As shown from the chart, pellets fabricated with powders mixed without Deca performed poorly. Two of three pellets broke. This may be due to nonuniform dispersion of diamond particles. The diamond particles mixed with Deca for 120 minutes gave low density, but the pellets were intact.

At this point it was assumed that Deca was necessary but was not fully removed after mixing. To investigate its removal and to test a possible solution, powders mixed for 120 minutes were heated for 12 hours at 50 °C. This temperature is near the boiling point of Deca and should encourage evaporation. To ensure that oxidation of the powder did not occur, each batch was weighed before and after heating. Pellet sintering behavior was compared and SEM was performed to see the difference in powder morphology. No mass change was seen after heating, which suggests no oxidation occurred.

Mixing Method	%TD
W/O balls with Deca 120 minutes	92.9*
W/O balls with Deca 120 minutes heated	96.8
W/O balls with Deca 120 minutes ****	95.8
Dia Particles with Deca 120 minutes	94.3
Dia Particles with Deca 120 minutes heated	95.9

Table 8: Mixing Method with Sintered Density

Table 8 shows a comparison of densities for different mixing methods. For both pure UO_2 powder and UO_2 with diamond, heating the powder produced better results. These results indicate there may be an undetected contamination of the mixing aid. A different approach was sued for the sample marked with four asterisks. For that sample the powder was sintered at 1150 °C but with a 15 minute hold time instead of 5 minutes. The pellet was intact but its density was still lower than that of pellets made from heated powder. It is obvious that the mixing aid leads to suboptimal sintering performance. SEM images below show more of these effects.

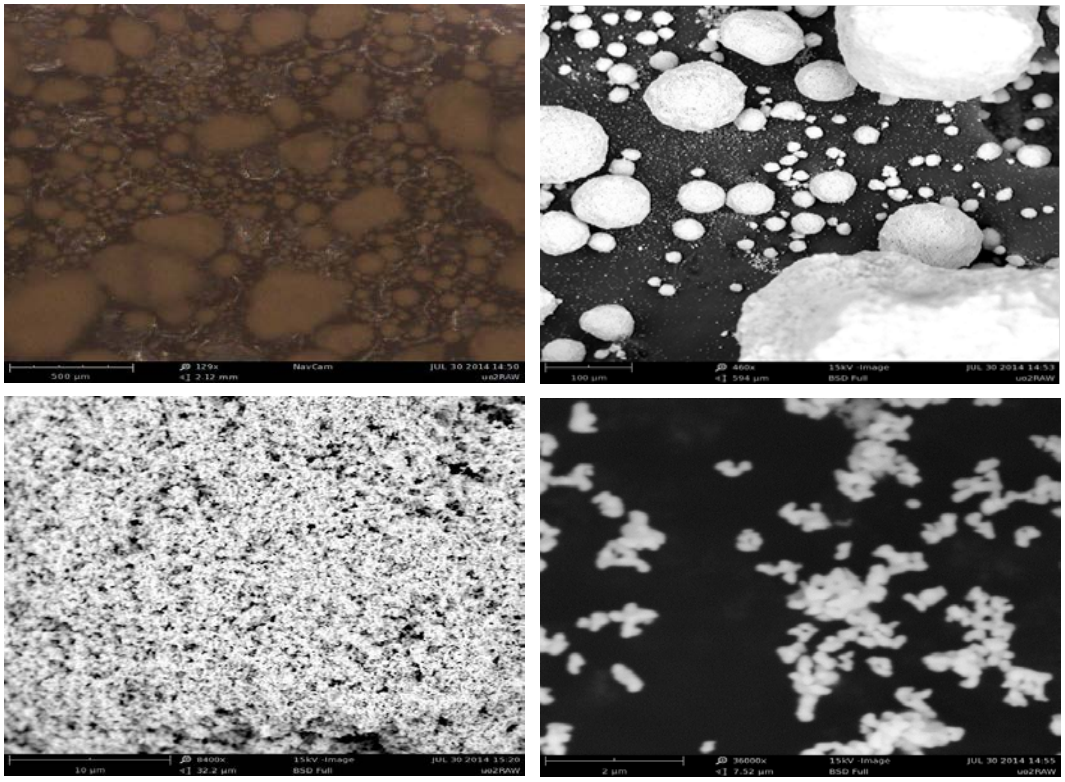

Figure 21: SEM Images of Raw Powder

The picture in the top left of Figure 21 is an optical image of raw UO_2 powder. It looks as expected, with a few large agglomerates and many small particles. The rest of the images are back scattered electron images. They show large agglomerates as seen in the top right image. The agglomerates are made up of many of the smaller particles, as is shown in the lower left image. The bottom right image shows the true scale of each particle. These images show the powder is very dry and fine. There is very little adhesion between two agglomerates. These powders produced the highest density pellets.

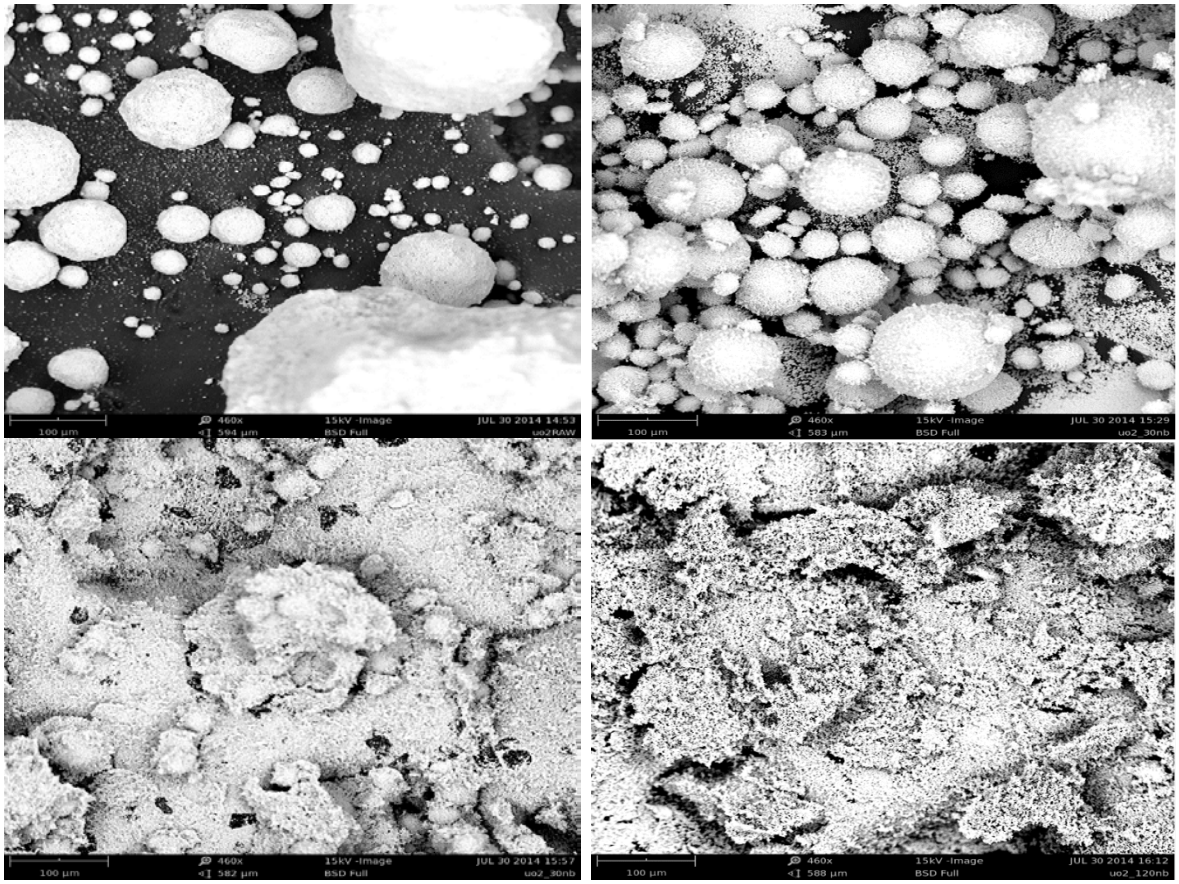

Figure 22: SEM Images: UO_2 Powder mixed without balls but with Decafluoropentane

Figure 22 shows raw powder in the top left, mixed for 15 minutes in the top right, mixed for 60 minutes in the bottom left and mixed for 120 minutes in the bottom right. All images are at the same magnification. The morphology completely changes. The powder begins very fine and structured and degrades to a muddied agglomeration of small particles. It is not surprising that the above powders exhibit different sintering behavior. The black spots in the 60 minute sample were not identified but may have just been the carbon tape under each sample. There is significant cohesion between particles in the 60 minute and 120 minute samples.

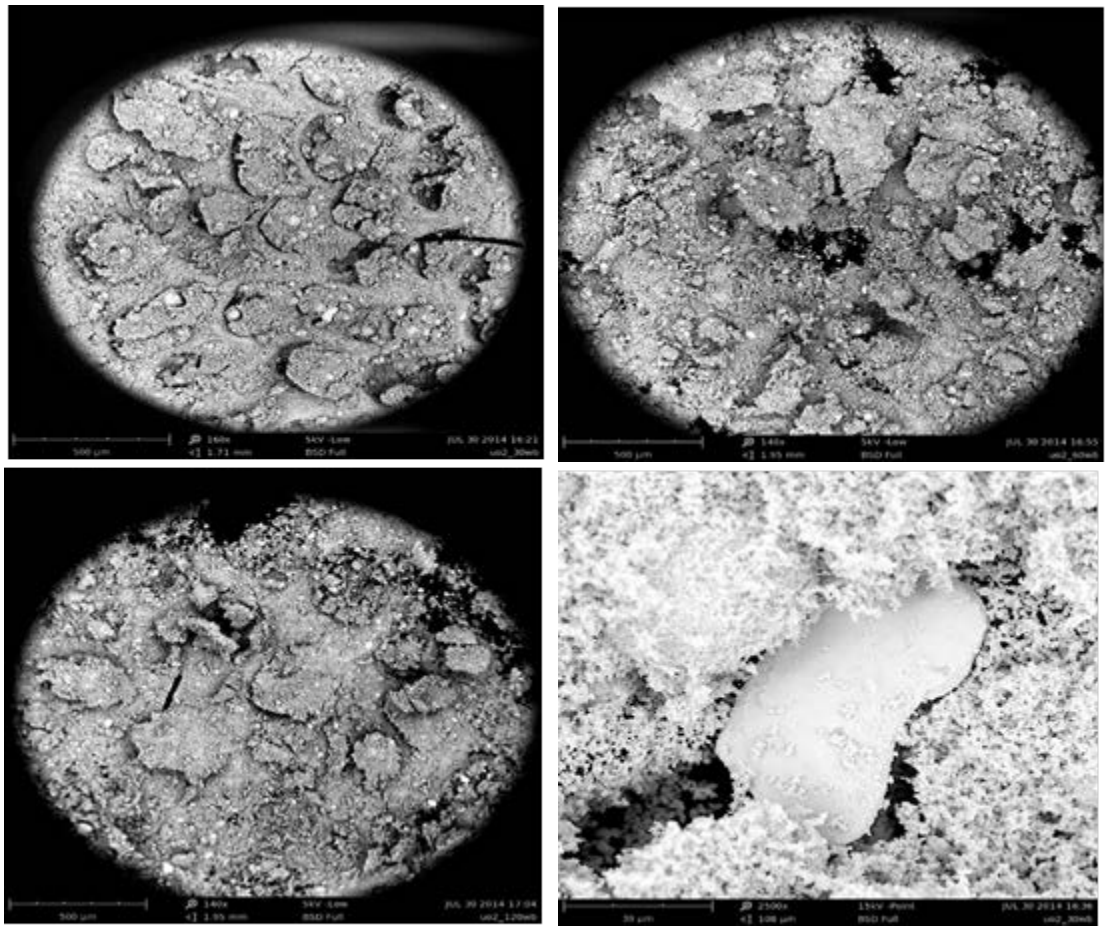

Figure 23: UO_2 Powder mixed with steel balls and with decaflouropentane

Figure 23 shows powder samples mixed with Deca and steel balls. Mixing times are 30 minutes (top left); 60 minutes (top right), and 120 minutes (bottom left). The fine raw powder again degrades to a more cohesive mat of particles. Degradation is seen after 30 minutes of mixing, versus 60 minutes for a sample mixed without balls. The reduction in particle size enhances adhesion of particles. Also there are shiny particles in these samples. One of these is shown in the bottom right image. This was from the 30 minute sample. Energy-dispersive spectroscopy (EDS) was inconclusive, but the particle appeared to be Urania.

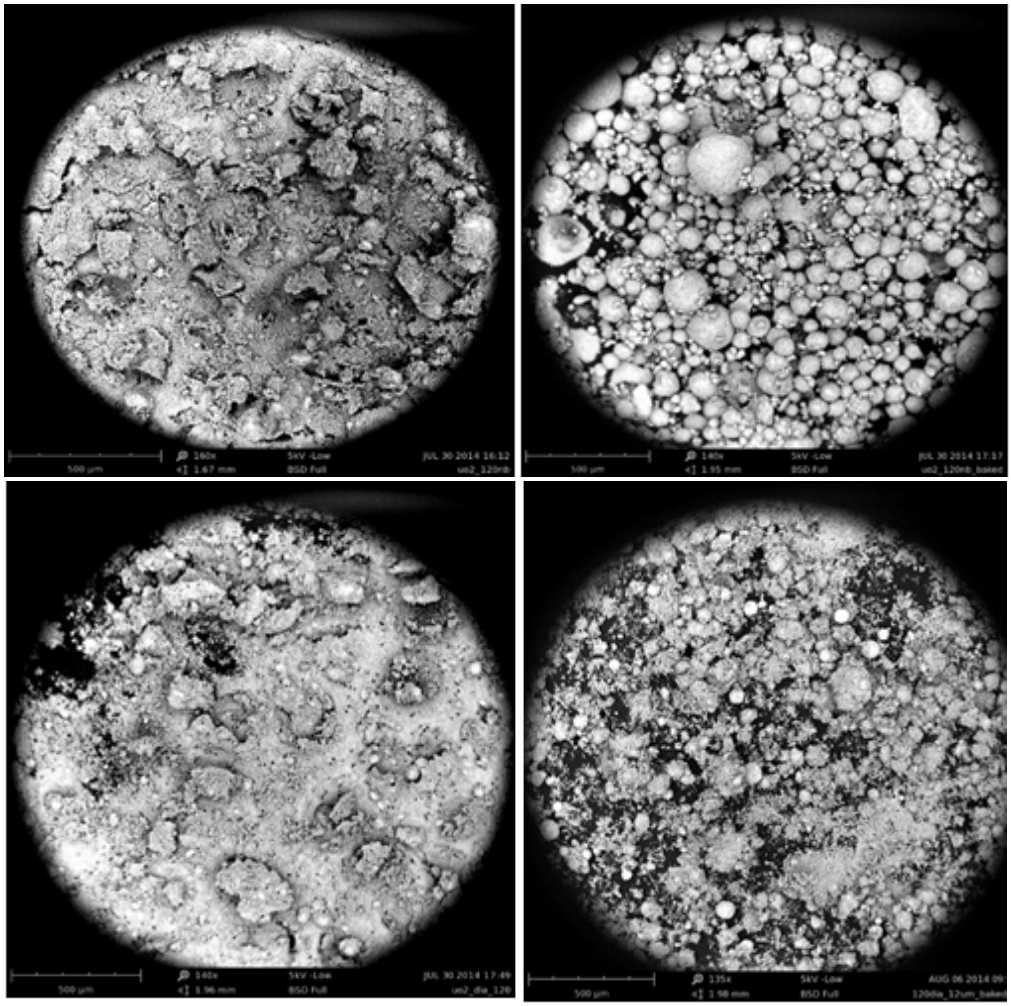

Figure 24: SEM images illustrating excess mixing aid in powder

Figure 24 illustrates the effect of excess mixing aid. The powders shown on the left were mixed for two hours. The top image shows UO_2 and the bottom UO_2 with diamond additive. The powders shown on the right were the same as those on the left but were heated overnight at 50 °C. The powders shown on the right are finer and are more organized. Also, diamond particles seem to be more uniformly distributed in the right image, but it is not clear if there is a significant effect.

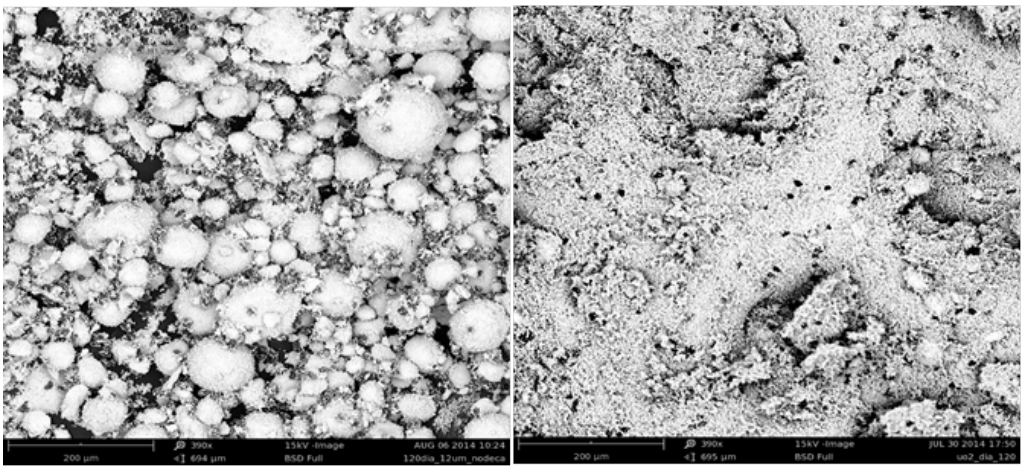

Figure 25: SEM Images: The need for a mixing aid

Figure 25 shows the need for the mixing aid. The left image is for UO_2 and diamond additive mixed for 120 minutes without Deca. The powder shown in the right image is similar but was mixed with Deca. The diamonds are the black spots and appear more evenly distributed in the right image. In the left image, the diamond particles seem to be clumping. That interpretation is supported by the first image in Figure 26. This image is of a fractured pellet made from powder mixed without Deca for 60 minutes. On the surface there is much more than ten volume percent diamond. This image shows that the mixing aid is required to distribute diamond particles into the UO_2 matrix.

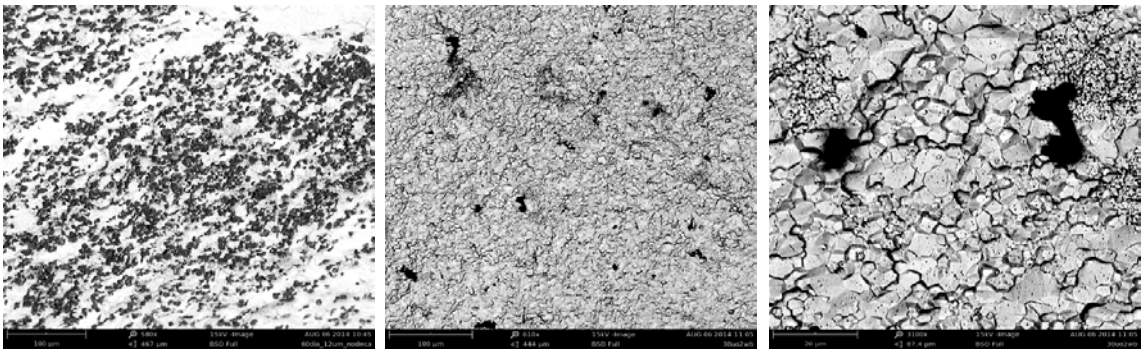

Figure 26: SEM Images: Mixing Aid related failure

The second and third images in Figure 26 show the fracture surface of a pellet fabricated with UO_2 powder mixed with steel balls for 30 minutes. The dark spots were not positively identified. EDS measurements were inconclusive; no signal was detected. These spots could be voids or contaminants. Either could lead to pellet failure and future work must be done to identify their nature. This pellet was over 96% dense so contamination is suspected. Something below the EDS detection limit is a possibility.

In conclusion, the effects of the mixing process on the sintering behavior of powder were investigated. The effect of mixing time on particle size depends on the use of steel balls or particles. With steel balls or diamond particles, the large UO_2 agglomerates are broken up into roughly 600 nm particles. With added mixing time, a single peak distribution around 600 nm is attainable. The effect of particle size on density in inconclusive. Particle size does not seem to have a direct effect on pellet structural stability. The effect of mixing aid is clearer. The mixing aid does not completely evaporate in air. This may be due to porosity and surface interactions with the UO_2. The powder with diamond particles was affected less. A simple solution may be to heat the powder to encourage evaporation. Powder oxidation should still not occur at 50 °C. Mixing aid is required to distribute additives uniformly.

The exact nature of the failure mode introduced by mixing aid should be investigated. Features of special interest are the dark spots on SEM images and the bright spots in the powders mixed with steel balls. Furthermore, the effect of mixing time on other powder properties such as surface area and porosity may provide a greater understanding of sintering behavior and failure mechanisms. Also, a determination of the effect of mixing time on the thermal conductivity of the pellets would be informative. Interfacial bonding is the largest variable that may be altered. Further investigation on removal of mixing aid after mixing is also planned

8.0 SPS DIE TOOLING FOR SMALL FUEL PELLET

A major problem incurred during the manufacturing of the ATR pellets was that the graphite die and punch used in SPS was not able to reach high temperatures without failure. A large current is necessary to achieve high temperatures required for sintering. Because of the small diameter of the pellets, there was a large local current density in the punches. This large current density created very high temperature zones and caused the punches to deform and bow. This phenomenon was observed at about 1400 °C. To try to overcome this problem in future SPS processing, a study was conducted on the die size and on the punch shape.

Mechighel et al. [6] showed that the joule heating in the punches is about 100 times higher than in the samples at the center of the die. This was due to the small diameter of the punches and the resulting high resistance. It was hypothesized that the desired temperatures could be attained with less current if a smaller die OD were used. The current density in the punches would also be reduced. To test this idea, graphite dies with OD of ~2”, ~1.5”, ~1” and ~0.5” were made. If the sintering parameters were held constant, the pellet density increased as the die OD increased. The results are shown in Table 9. The increase was not significant enough at higher ODs to justify the increase in current, voltage, and consequently power consumption.

Die OD	Average Density (%TD)
~2”	98.1% (Majority of Pellets were in
~1.5”	97.7%
~1”	96.6%
~0.5”	95.3%

Table 9: Average density for UO_2 pellets sintered at 1150°C for 5 minutes and 40MPa

Recall that the temperature of the sample is measured from the exterior of the die wall, which means that more current flow is required for a larger die to reach the same temperature as a smaller die. As a result, the current density in the punches was too high with a large die, and the samples within larger dies see an actual temperature that is much higher than in the smaller dies. This causes chips and cracks due to high thermal radial gradients during sintering. Because of this, the smallest die OD is the most favorable. However, to maintain a safe loading of the sample in the SPS furnace the die OD was increased to 0.944 inch to withstand pressures of the sample on the die wall. That OD is three times the pellet diameter. Use of these smaller dies enabled the successful sintering of high density pellets with SiC whiskers or with diamond particles, as shown in Table 10.

Pellet Type	Average Density (%TD) (die OD = ~1.5", ATR production)	Average Density (%TD) (die OD = 0.944")
UO_2 – SiC Whiskers (1400 °C)	94.4%	95.6%
UO_2 – Diamond (1350 °C)	95.3%	96.1%
UO_2 (1150 °C)	96.5%	97.1%

Table 10: Difference in average density of sintered pellets for a die OD of 0.944"

A novel punch shape was also used to try to mitigate the problem of high current density. A "lipped" punch was designed as shown in Figure 27 to try to direct more of the current through the die wall as opposed to directly through the sample.

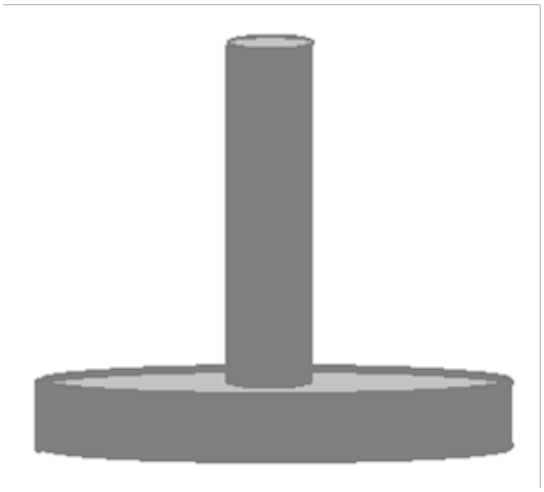

Figure 27: "Lipped punch" used to try to reduce the current density in the punches

The "lip" of the punch was the same diameter as the die OD, and the length was such that the sample would be centered in the die. A regular cylindrical punch would be placed at the other end of the die so that pressure could be applied during sintering. An image of the lipped punch and die loaded into the SPS furnace can be seen in Figure 28. Pellets were sintered at 1150 °C for 5 minutes and 40 MPa to a density of up to 99% TD. All pellets sintered with the lipped punches were shown to have a larger relative density than those sintered with regular cylindrical punches.

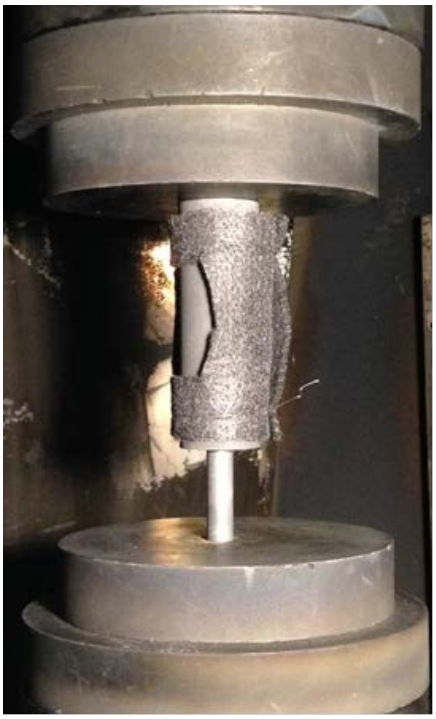

Figure 28: Lipped punch (at the top of the die) and die combination loaded into the SPS furnace

Further work is to be completed in Phase 1B regarding this novel punch idea. Material characterization needs to be performed to ensure that the pellets produced have uniform microstructure throughout the pellet regardless of the asymmetrical set up.

9.0 CONCLUSIONS AND FUTURE WORK

The University of Florida has successfully proven that the SPS process is physically viable for the sintering of composite fuels. UF was able to fabricate and characterize UO_2 – composite pellets at 12.5 mm diameter and conclude that high density, high thermal conductivity pellets were achievable. A MSC was constructed for 12.5-mm pellets for both UO_2 and UO_2 – SiC. Work is underway to create an MSC for 8.2-mm pellets for both pure UO_2 and UO_2 – composites. The production of 8.2-mm pellets for irradiation in the ATR exposed many challenges. Because of this, work was done to determine the cause of defects in many of the smaller pellets. Mixing time, mixing agent, particle size, and powder drying were investigated to determine their effect on sintering behavior. In addition, novel concepts of punch shapes and die sizes were studied to determine their influence on sintering and pellet quality. Further work is to be completed in the area of 8.2-mm fuel pellets, and the determination of the economic viability of the SPS process will be investigated.

10.0 REFERENCES

1. F. Goldner, “Development Strategy for Advanced LWR Fuels with Enhanced Accident Tolerance,” Office of Fuel Cycle R&D. DOE. June 12, 2012.

2. S. Yeo et al. “Enhanced Thermal Conductivity of Uranium Dioxide – Silicon Carbide Composite Fuel Pellets Prepared by Spark Plasma Sintering,” Journal of Nuclear Materials, 433, 66-73 (2013).

3. L. Ge et al. “Densification of Uranium Dioxide Fuel Pellets Prepared by Spark Plasma Sintering (SPS),” Journal of Nuclear Materials, 435, 1-9 (2013).

4. Z. Chen et al. “Master Sintering Curves for UO_2 and UO_2 – SiC Composites Processed by Spark Plasma Sintering,” Journal of Nuclear Materials, Under Review.

5. Diouf, S., and A. Molinari. "Densification mechanisms in spark plasma sintering: effect of particle size and pressure." Powder Technology 221 (2012): 220-227.

6. F. Mechighel et al. “Study of thermo-electric and mechanical coupling during densification of a polycrystalline material using COMSOL” COMSOL Conference. 2008, Hannover.

APPENDIX F

Electrophoretic Deposition (EPD) Coatings for the Phase 1A Final Report for Enhanced Accident Tolerant Fuels

Principal Investigator: Kumar Sridharan

Prepared by:
AREVA Federal Services, LLC

TABLE OF CONTENTS

1.0 BACKGROUND OF ELECTROPHORETIC DEPOSITION 1
2.0 EPD WORK PERFORMED AT UW-MADISON 3
2.1. COATING OPTIMIZATION 3
2.2. EPD COATING OF TUBES 5
2.3. HEAT TREATMENTS 6
2.4. LASER SURFACE TREATMENTS OF EPD COATINGS 7
2.5. MECHANICAL TESTING 18
2.6. QUENCH TEST DESIGN WORK 20
2.7. LITERATURE REVIEW ON COATING MATERIALS AND METHODS FOR NUCLEAR FUEL CLADDING .. 23
3.0 CONCLUSIONS 25
4.0 REFERENCES 25

LIST OF TABLES

Table 1: Initial Parameters for EPD Coatings Investigated in this Study 3
Table 2: Y_2O_3 Optimization 4
Table 3: Heat Treatments 7
Table 4: EPD coating deposition matrix for the 1st round of laser sintering 8
Table 5: EPD coating deposition matrix for the 2nd round of laser sintering 10
Table 6: Laser parameter sets for vendor trial #2. Parameter sets 6, 10, and 12 gave the most promising visual characteristics ... 10
Table 7: Parameter sets used during laser sintering trial #3 with the collaborating vendor (QCW: Quasi-continuous Wave; CW: Continuous Wave) 13
Table 8: Parameter sets used for the fourth laser sintering experiment, performed with a UW research group 16
Table 9: Scratch Test Measurement Results 18
Table 10: Pin-on-Disk Initial Parameters 19
Table 11: EPD Pin-on-Disk Results 19

LIST OF FIGURES

Figure 1: (a) Schematic illustration of the EPD process and (b) coaxial electrode EPD configuration developed at the University of Wisconsin to coat the outer surface of Zircaloy-alloy claddings 1
Figure 2: Increased TEA Concentration. Figure 2a) shows the coating surface after increasing the TEA concentration from 1 to 2 drops and Figure 2b) shows the coating surface after increasing the TEA concentration from 1 to 6 drops 3
Figure 3: Change in Solvent. Figure 3 shows the coating surface of Y_2O_3 where 3a) is the original solvent of acetyl acetone 3b) is a 1:1 ratio of acetone: ethanol and 3c) is a 3:1 ratio of acetone: ethanol. 4
Figure 4: The detail design of the tube-geometry coating apparatus and the fabricated apparatus. The titanium tube and the Zircaloy tube sample serve as electrodes, electrically isolated via HDPE mounting blocks and connected via external wires (not shown) to a DC power supply. 5
Figure 5: EPD coated tubes before and after heat treatment. Titanium (60-80nm) nanoparticles dispersed in acetylacetone solvent were deposited on SS316 tube using a 30V applied voltage for 150 seconds. 6
Figure 6: SEM micrograph of laser-surface-treated TiO_2 EPD coating (vendor trial #3). Localization of the surface treatment is evident, as are cracks in the coating material. 8
Figure 7: Optical micrographs of TiO_2 (left) and Y_2O_3 (right) after processing with various laser powers. At high energy, 100% ablation and localized re-melting of the Zircaloy-4 occurs. As energy decreases, the amount of remelting observed decreases. All coating is ablated at laser powers of 40W or higher, with some remnant coating observed at 30W. At 20W, both TiO_2 and Y_2O_3 had the highest amount of retained coating after laser treatment. 9
Figure 8: TiO_2 with (left) and without (right) the post-deposition baking process. Best results from the processing are seen in parameter sets 6, 10, and 12. 11
Figure 9: From left to right, post-laser-treated samples of Y_2O_3, YSZ, Al_2O_3, and Ti EPD-coated Zircaloy-4. The above 4 samples were not subjected to the 200°C post-deposition baking treatment. 11
Figure 10: A high-magnification (90 KX) image of TiO_2 after processing by laser condition 10. The individual nanoparticles are largely unaffected and do not show the desired level of intergrowth. 12
Figure 11: A high-magnification (90 KX) image of the 8% YSZ coated sample after processing by laser condition 10. Individual nanoparticles do not show sintering behavior. 12
Figure 12: "Normal" TiO_2 coating prior to laser surface treatment. The above coating has been baked for 2h at 200°C to drive out any remnant liquids from the deposition process. 15
Figure 13: YSZ coating following laser surface treatment at an aggressive parameter set. Pockets of densification are observed, but it is evident that further optimization is required to prevent ablation and complete melting. 15
Figure 14: A 50 KX image of standard-thickness TiO_2 after laser processing. A desired effect of laser processing, enhanced particle interconnectivity, is most prominent in the lower right but is apparent throughout the image. 15
Figure 15: A 10 KX image of thick-deposited TiO_2 after laser processing. This microstructure is characteristic of resolidified nanoparticles, and represents the upper limit of desired laser surface treatment effects. 16
Figure 16: YSZ EPD coatings after having undergone 3 different continuous – wave laser energies (0.8, 1.5, 4.95 W respectively). All conditions lead to ablation. 17
Figure 17: FIB-milled cross-section view of parameter set #6 from the intra-university laser sintering collaboration. Coating thickness was reduced from >12μm to 1 μm or less, and subsurface cracking of the Zircaloy-4 substrate is evident in the processed region. 17
Figure 18: Scratch Test Results. Figure 18 shows SEM images from scratch testing done at a load of 150g where 18a) is bare zirconium 18b) is laser treated TiO_2 and 18c) is laser treated YSZ. 18
Figure 19: Pin-on-Disk Parameters. Figure 19 shows the depth profile of the initial parameter on bare zirconium where 19a) is 60 minutes at a load of 10 grams and 19b) is 120 minutes at a load of 10 grams. 19
Figure 20: EPD Pin-on-Disk. Figure 20 shows the wear tracks from the rotating pin-on-disk wear testing where 20a) is the heat treated (700°C 6 hours + 600°C 200 hours) TiO_2 sample 20b) is the heat treated (700°C 6 hours + 600°C 200 hours) YSZ sample 20c) is the laser treated TiO_2 sample 20d) is the laser treated YSZ sample. 20
Figure 21: The schematic designs of quenching facility. This was the initial design for the quench test apparatus. 21
Figure 22: Quench test schematic. A potential new designs for fixturing a thin-walled tube to a supporting structure for controlled-position quench testing. In this design, all threads are located in the thermal load material, which has thermocouple locations and a resting lip to secure the bottom of the sample. 22
Figure 23: Finite element simulation for end-cap. Development of the bottom gap when using a metallic (SS, Al, Cu) thermal load to support the Zircaloy-4 tube sample during the ramp to quenching temperature. Total gap length (top and bottom) is estimated to be 0.65 – 1.7 mm, depending on the material. 22
Figure 24: Heat flux comparison. Comparison of heat flux computed for the same event by literature (left) and UW (right) heat flux codes. The in-development UW code shows similar behavior but has room for improvement. 23

1.0 BACKGROUND OF ELECTROPHORETIC DEPOSITION

Electrophoretic deposition (EPD) is a colloidal processing technique which has been used to fabricate micro-laminate and functionally graded materials, ceramic matrix/ceramic-fiber composites, and thermal barrier coatings [1, 2]. EPD is similar in many ways to electroplating, with the difference that electroplating uses an ionized solution whereas EPD uses a colloidal suspension comprised of small particles (≤ 100nm) of the coating material dispersed in a liquid. As a result of introduction of certain additives in the liquid, the nano-particles acquire a surface charge in the colloidal suspension and are directed and deposited on an electrode by an electric field. In keeping with terminology used in recent literature we define nanofluid as a fluid with a homogeneous dispersion of nanoparticles. Figure 1 shows a schematic illustration of the EPD process for coating test flats of Zircaloy-alloy as well as a co-axial electrode configuration developed at the University of Wisconsin (UW) for coating the outer surfaces of the claddings sections.

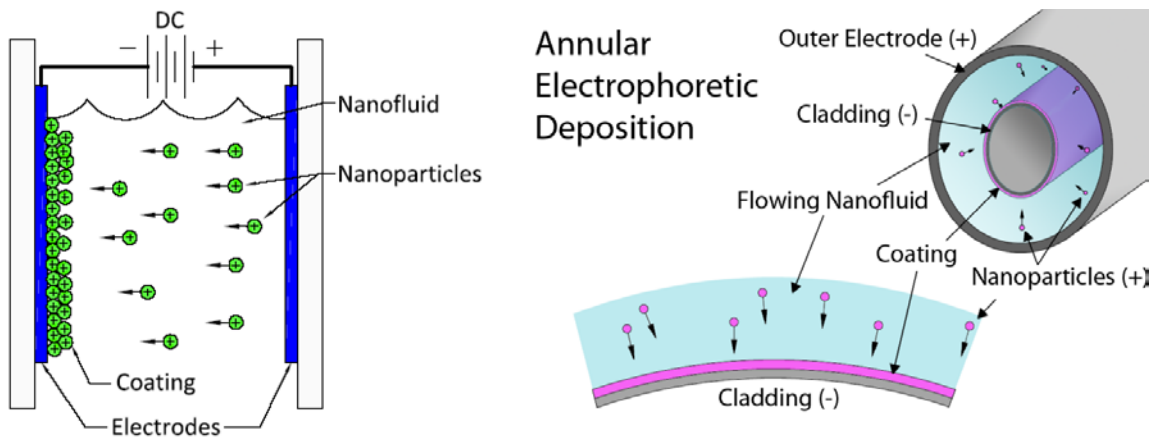

1a) 1b)

Figure 1: (a) Schematic illustration of the EPD process and (b) coaxial electrode EPD configuration developed at the University of Wisconsin to coat the outer surface of Zircaloy-alloy claddings

Electrophoretic deposition (EPD) combines two processes: electrophoresis and deposition. During electrophoresis charged particles suspended in a solvent are accelerated under the influence of an electrical field toward an electrode of opposite polarity. During deposition, the particles assemble on the electrode to form a coating [3 - 6]. Water is not commonly used as a solvent as it undergoes hydrolysis when more than 1.2 V is applied [7]. This causes bubbles to be trapped within the deposit unless special procedures are adopted. For these reasons, organic solvents are commonly used for EPD.

In order to obtain a stable colloid, a high surface charge/zeta potential is required to induce a high repulsive force between particles [8, 9]. Zeta potential is the electrokinetic potential in colloidal systems. From a theoretical standpoint, the zeta potential is the electrical potential at the interfacial double layer (DL), i.e. the location of the slipping plane relative to a point in the bulk fluid away from the interface. In other words, this is the potential difference between the dispersion medium and the stationary layer of fluid attached to the dispersed particle. A general, but simplified equation for the weight of coating deposited, w (proportional to coating thickness), in an EPD process as first determined by Hamaker is as follows [10]:

$$w = f\frac{2}{3}C\varepsilon_o\varepsilon_r\zeta\left(\frac{1}{\eta}\right)\left(\frac{E}{L}\right)t \qquad \textbf{Equation (1)}$$

In this equation "C" is the particle concentration, "ε0" the permittivity of free space, "εr" the relative permittivity of the solvent, "ζ" the zeta potential, and "f" the related correction factor with a value between 0 and 1 accounting for the fact that not all particles brought to the electrode are incorporated in the deposit. "η" is the viscosity of the suspension medium, "E" the applied electric field strength, "L" the distance between the electrodes and "t" is the deposition time.

The charge adsorbed on the particles increases the repulsive energy between the particles which minimizes particle agglomeration. Also, since the particles are more highly charged, they will be more affected by the applied electric field. The particles in a nanofluid can acquire charge by several mechanisms including, selective adsorption of ions onto the solid particle from the liquid and electron transfer between the solid and liquid phase due to differences in work function forces between neighboring particles.

Several methods for charging oxides in organic solvents have been discussed in literature. In each case, a reaction occurs between the solvent and oxide particles or additive to cause the production of positive ions which in most cases are protons. These ions are then adsorbed onto the particles' surface and the charged particles are available to be influenced by the applied electric field and undergo electrophoresis. In the widely investigated yttria-stabilized zirconia (YSZ) EPD coating deposition for YSZ nanoparticles in acetylacetone (ACAC) liquid, the dipole of the –OH group on the YSZ surface tends to capture protons from ACAC to form a positive charge on the particle surface, as shown in Equation (2). Moreover, the chemical reaction between YSZ and ACAC (Equation 3) is also thought to release a large number of protons. Both of these assist in creating a positive zeta potential for particles [10].

$$(Zr{-}OH)_{surface} + CH_3COCH_2COCH_3 \rightarrow (Zr-OH_2)^+{}_{surface} + (CH_3CO)_2CH^- \qquad \textbf{Equation (2)}$$

$$ZrO_2 + 4ACAC \rightarrow Zr(ACC)_4 + 2H^+ + 2OH \qquad \textbf{Equation (3)}$$

The addition of acetic acid and triethanolamine (TEA) into ACAC suspensions has also been studied. The particle zeta potential increased through further adsorption of protons ionized by the acid. Addition of iodine to organic nanofluid suspensions has been investigated where it has been found that protons were produced when iodine reacted with ACAC (equation 5) and ethanol (Equation 6).

$$CH_3CH_2COCH_2COCH_2CH_3 + I_2 \leftrightarrow ICH_2CH_2COCH_2COCH_2CH_2I + 2H^+ \qquad \textbf{Equation (4)}$$

$$CH_3CH_2COCH_2COCH_2CH_3 + I_2 \leftrightarrow ICH_2CH_2COCH_2COCH_2CH_2I + 2H^+ \qquad \textbf{Equation (5)}$$

2.0 EPD WORK PERFORMED AT UW-MADISON

Initially five nanoparticles were used to make EPD coatings; Ti, TiO_2, YSZ, Y_2O_3, and Al_2O_3. Throughout this phase of the project these coatings were heat treated and mechanically tested to determine the feasibility of EPD coatings. Mechanical tests included scratch tests and rotating pin-on-disk wear testing. Indicators of an improved coating included particle sintering, absence of microcracks in coating, a decrease in scratch width, and a smaller wear track. Prior to coating optimization a set of parameters were created to consistently produce coatings between 10 and 15 µm, which was a predetermined target range. Table 1 shows the initial coating parameters for each of the five nanoparticles. Table 1 shows the initial voltage and time parameters for various coating nanoparticles to create a coating that is between 10 and 15 µm in thickness on a flat sample using acetyl acetone as a solvent and one drop of TEA.

Nanoparticle	Voltage (V)	Time (seconds)
Ti (60-80 nm)	20	130
TiO_2 (50 nm)	20	110
YSZ (200-300 nm)	20	230
Y_2O_3 (32-36 nm)	20	190
Al_2O_3 (40-80 nm)	20	150

Table 1: Initial Parameters for EPD Coatings Investigated in this Study

2.1. COATING OPTIMIZATION

The Y_2O_3 nanoparticle when observed under an SEM was shown to have microcracks in the coating. In order to optimize the coating the initial coating parameters for Y_2O_3 were changed. First the amount of TEA, a charging additive, was increased to two, three, four, five, and six drops. However, the microcracks were still present and could be seen under an optical microscope. Figure 2 shows some of the microcracks present in the Y_2O_3 coatings.

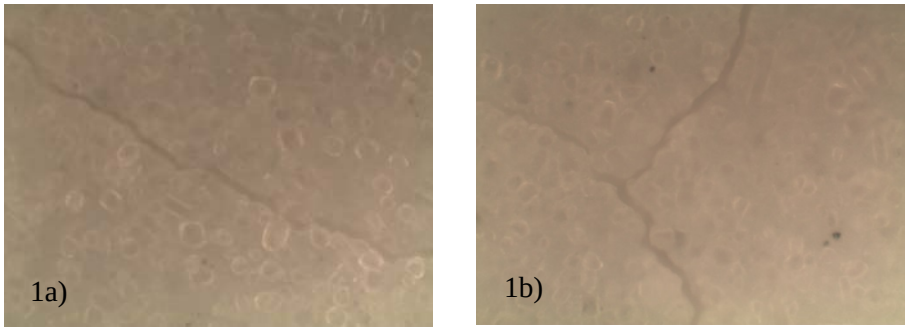

Figure 2: Increased TEA Concentration. Figure 2a) shows the coating surface after increasing the TEA concentration from 1 to 2 drops and Figure 2b) shows the coating surface after increasing the TEA concentration from 1 to 6 drops

The next parameter that was changed was the solvent of the nanoparticle solution. Combinations of acetone and ethanol were tried because acetone has a low surface tension but a high evaporation rate, while ethanol has a high surface tension but a low evaporation rate. The original time and voltage conditions were used for this round of experiments. Table 2 shows the results from changing the solvent of the nanoparticle solution to optimize the Y_2O_3 coating. The solution completely made of acetone did not stay in suspension after sonication; therefore, it was not used to make a coating.

Ratio (Acetone:ethanol)	Average coating thickness (μm)	150g scratch test (μm)	Coating Penetration	100g scratch test (μm)	Coating Penetration
1:1	7	107.25±2.21	Yes	106.2±5.73	Yes
1:0	X	X	X	X	X
0:1	16	150.32±6.87	Yes	135.12±1.7	Yes
1:3	17	105.78±5.09	No	105.16±4.31	Yes
3:1	23	128.66±2.89	Yes	126.83±3.13	Yes

Table 2: Y_2O_3 Optimization

After scratch testing and SEM imaging it was determined that the coatings made with 1:1 and 3:1 ratios of acetone:ethanol were the best coatings. The criteria for determining which parameters created the best coating were scratch width and uniform thickness of the coating. Even though the coating made with the 1:3 (acetone:ethanol) had the smallest scratch width the coating was not uniform over the entire sample.

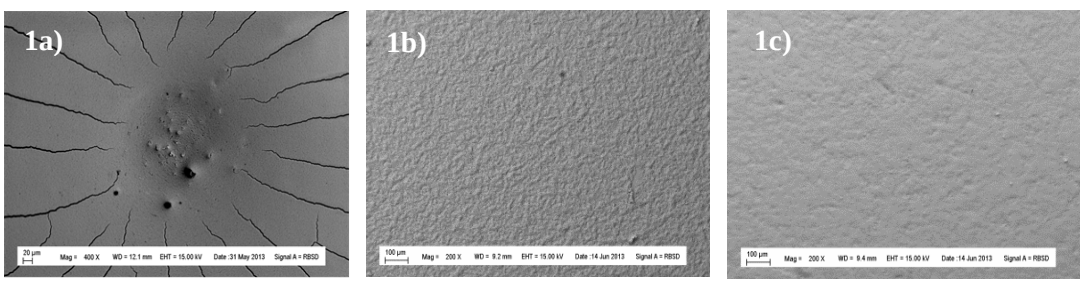

Figure 3: Change in Solvent. Figure 3 shows the coating surface of Y_2O_3 where 3a) is the original solvent of acetyl acetone 3b) is a 1:1 ratio of acetone: ethanol and 3c) is a 3:1 ratio of acetone: ethanol.

After the Y_2O_3 optimization no microcracks were present in any of the as deposited samples. In order to try and sinter the nanoparticles, low temperature (below 700°C) and laser sintering techniques were tested. In order to save time and resources, the preliminary results from the low temperature and laser sintering were used to narrow the possible nanoparticles down to YSZ and TiO_2. These two coatings showed the most promise in particle sintering capabilities and mechanical integrity.

Following the use of only YSZ and TiO_2 coatings the initial coating parameters were reevaluated. The YSZ coating was no longer coating evenly and the coating thickness was below the target range of 10-15µm. Increasing the voltage and time causes the coating thickness to increase, which was thought to help create a uniform coating. Therefore increased combinations of YSZ and TiO_2 were tested until a combination fell within the target range. The combination that provided the desired thickness was 30 V for 320 seconds (determined on July 29, 2013).

After a few months of using the previously stated conditions, the EPD parameters were once again reevaluated. The parameters previously used were found to be inconsistent and the coatings were thicker than desired. For the following months of the project the coating parameters were continuously monitored and optimized. The first few changes began with changing the time and voltage. After these attempts were shown to be unsuccessful the solvent was changed. Based off the improvement in the Y_2O_3 optimization, a 1:1 and 3:1 ratios of acetone:ethanol were tested. This change initially showed some improvement in the coatings, but consistently acquiring the desired coating thickness of 10-15 µm still continued to be a challenge.

2.2. EPD COATING OF TUBES

In addition to coating flat samples, tubes were also coated using the EPD process. This substrate geometry is more representative because nuclear fuel claddings are tube-shaped. Since the substrate geometries are different, a new coating apparatus was needed. Figure 4 shows the design schematics and the fabricated apparatus used for coating tubes. In addition to a different coating apparatus, the voltage and deposition time was increased because the tube sample has a larger surface area than the flat substrate used.

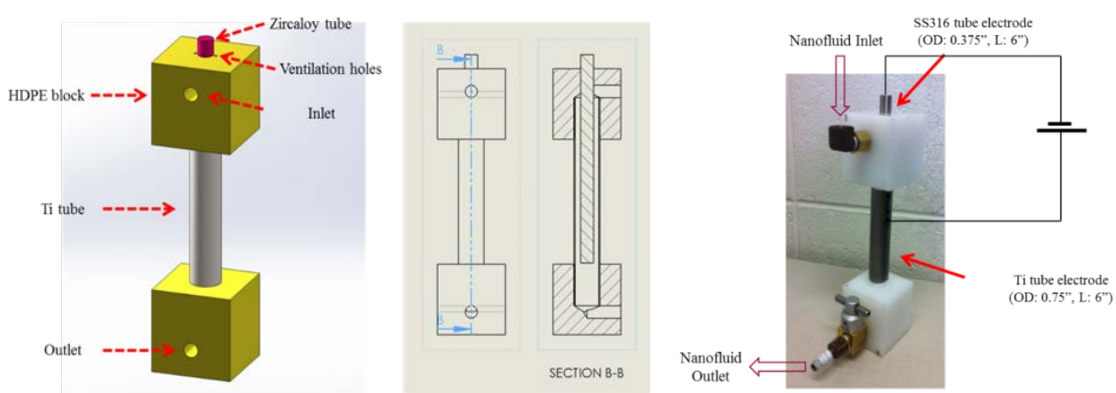

Figure 4: The detail design of the tube-geometry coating apparatus and the fabricated apparatus. The titanium tube and the Zircaloy tube sample serve as electrodes, electrically isolated via HDPE mounting blocks and connected via external wires (not shown) to a DC power supply.

A Zircaloy tube sample is placed coaxially within a titanium tube in a vertical orientation. The vertical titanium tube (counter electrode, nanoparticle reservoir wall) is electrically isolated from the coaxially-mounted sample via HDPE mounting blocks. Coating is deposited by supplying a DC voltage through external wires to the sample and counter electrode as shown in Figure 4. For the first set of tube coatings, Titanium (Ti) was used.

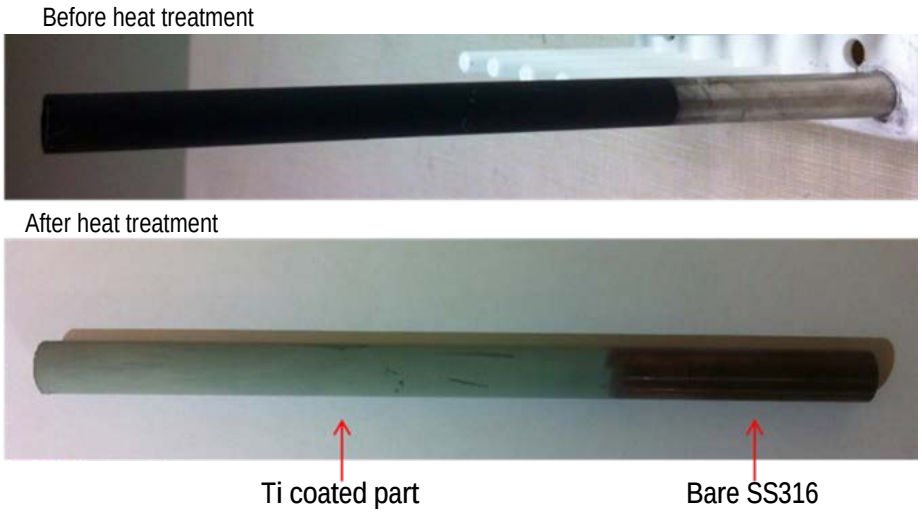

Figure 5: EPD coated tubes before and after heat treatment. Titanium (60-80nm) nanoparticles dispersed in acetylacetone solvent were deposited on SS316 tube using a 30V applied voltage for 150 seconds

The resultant coating was thick and visible to the naked eye. To avoid microstructure changes in a Zircaloy substrate the heat treatment was at a low temperature for a long period of time (400°C for 100 hours); however, the first tube samples had a SS316 substrate. This first round of heat treatment was performed in an air environment and showed promising results. When the sample was heat treated there was better adhesion between the Ti coating and the substrate than before the heat treatment.

2.3. HEAT TREATMENTS

Three types of heating environments were used throughout this phase of the project; an air furnace, an air furnace where the samples were encapsulated in borosilicate glass and backfilled with argon, and a hot press furnace. During the beginning stages of the project the hot press furnace was broken, so the only option was an air furnace. However, by using an air furnace the substrates are more likely to oxidize, causing the coating to separate and fall off. Encapsulating the samples in borosilicate glass and backfilling with argon was supposed to provide an environment to minimize oxidation while using the air furnace. There was little to no improvement in the coating by encapsulation since the tubes occasionally cracked and in order to place the samples in the tube some samples would slide over each other. When the samples slid over one another pieces of the coating would be removed and the sliding would apply additional stresses to the coating.

When the hot press furnace was fixed a vacuum environment could be achieved to help eliminate oxygen in the air and decrease oxidation. Unfortunately, the coatings had difficulty adhering to the Zicaloy-4 substrate. Temperatures were increased to try and show sintering effects, but no significant results were seen. Table 3 shows the different heat treatments that were used in the air furnace (HT01-HT08) and the hot press furnace (HT09-HT11). In Table 3 T stands for temperature, while t stands for time.

Heat Treatment Name	T (°C)	T (°C)	t (hr)	T (°C)	t (hr)	T (°C)	t (hr)	T (°C)	t (hr)	T (°C)	t (hr)	T (°C)	t (hr)	T (°C)	t (hr)	T (°C)	t (hr)
HT00	25	#N/A															
HT01	25	400	2	400	99	400	99	25	4								
HT02	25	500	2	500	99	500	99	25	4								
HT03	25	200	2	200	2	500	2	500	99	500	99	25	4				
HT04	25	200	2	200	2	700	4	700	3	500	2	500	99	500	99	25	6
HT05	25	200	2	200	2	700	4	700	3	25	8						
HT06	25	200	2	200	2	700	4	700	3	600	2	600	99	600	99		
HT07	25	200	2	200	2	700	4	700	3	600	2	600	99	600	99	25	8
HT08	25	200	2	200	2	700	4	700	6	600	2	600	99	600	99	25	8
HT09	20	20	5 min	1050	1.50	1050	0:00	20	1.50	20	5 min						
HT10	20	20	5 min	850	1:11	850	16	20	1:11	20	5 min						
HT11	10	10	1 min	900	1	900	6	850	5 min	850	24	50	55 min				

Table 3: Heat Treatments

2.4. LASER SURFACE TREATMENTS OF EPD COATINGS

Laser surface treatment is of particular interest as a possible coating densification process due to the localized nature of thermal exposure [D4], not achievable with furnace-based sintering methods. UW explored laser surface treatments with two partnerships, firstly with a Wisconsin company and secondly with another UW research group, both of whom specialize in laser treatments and/or research. In the first partnership, three sample exchanges were made, each a testing a variety of process parameters. Unfortunately, a successful combination of parameters could not be determined for EPD-coated substrates. The parameters modified were the laser operation mode (quasi-continuous wave, QCW, or continuous wave, CW), raster speed, and average power. When in QCW mode, the additional parameters of duty cycle and cycle frequency were modified. An extremely sensitive threshold between essentially “no effect” and “complete ablation” was discerned for most settings, with only one parameter set producing visible modifications of the EPD coating without any ablation. SEM characterization of this parameter set (Figure 6) indicates that, even then, laser sintering of current EPD coatings occurs only in hyper-local regions of the treated area. Characterization of other parameter sets indicates that regions neighboring the sintered areas may be ablated instead. Following is a more detailed examination of significant findings from the laser sintering investigation.

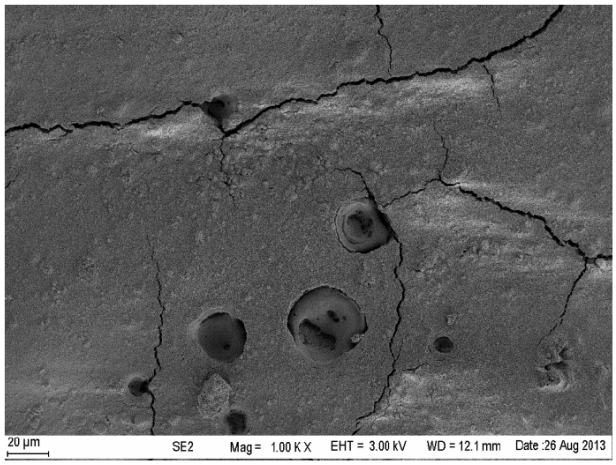

Figure 6: SEM micrograph of laser-surface-treated TiO_2 EPD coating (vendor trial #3). Localization of the surface treatment is evident, as are cracks in the coating material.

In the first trial, 10 samples were provided to the collaborating industrial vendor, and a general description of the desired effect was conveyed, in addition to compositional and topological information. The vendor treated the samples with a focused IPG QCW AC 150/1500 laser running at 500Hz, 100ipm, and 10% Duty Cycle in QCW mode. Between passes, the wattage output of the system was adjusted, based on the results of the previous pass. As evidenced in the results for TiO_2 and Y_2O_3 (Figure 7), permissible results were only seen at the 20W setting. All higher power settings resulted in coating loss and even re-melted Zircaloy layers.

#	Nanoparticle	Concentration (wt. %)	Deposition time (s)	Voltage (V)	Avg. Thickness (µm)
1	Bare	-	-	-	-
2	Ti (60-80nm)	0.5	120	20	11.7
3	Ti (60-80nm)	0.5	130	20	12.2
4	TiO_2 (250nm)	0.5	100	20	7.5
5	TiO_2 (250nm)	0.5	90	20	6.6
6	Y_2O_3 (32-36nm)	0.5	190	20	13.5
7	Y_2O_3 (32-36nm)	0.5	180	20	11.5
8	YSZ (200-300nm)	0.5	220	20	9.5
9	YSZ (200-300nm)	0.5	220	20	9.5
10	Al_2O_3 (40-80nm)	0.5	150	20	12
11	Al_2O_3 (40-80nm)	0.5	150	20	14.5
12	Bare	-	-	-	-

Table 4: EPD coating deposition matrix for the 1st round of laser sintering.

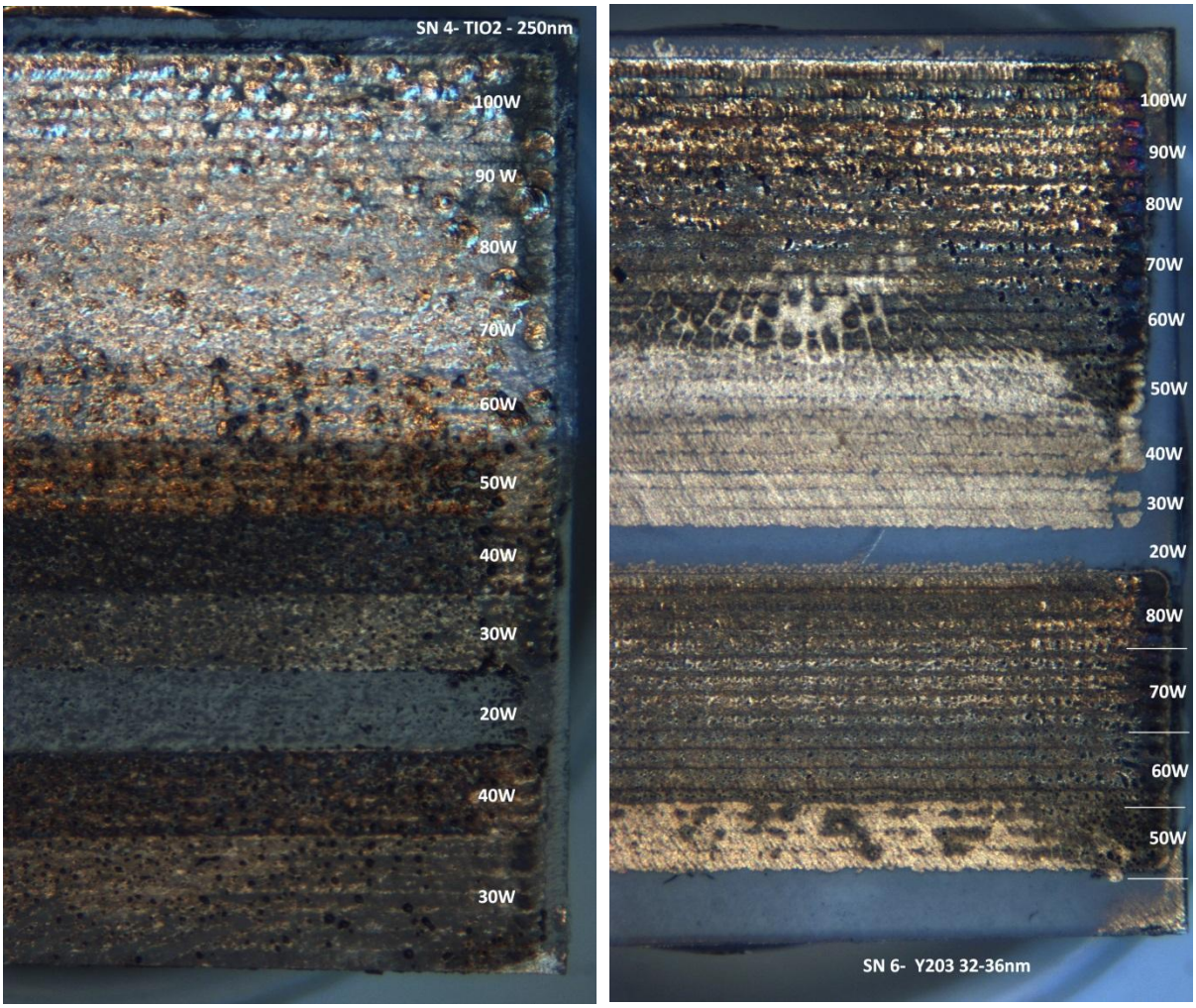

Figure 7: Optical micrographs of TiO_2 (left) and Y_2O_3 (right) after processing with various laser powers. At high energy, 100% ablation and localized re-melting of the Zircaloy-4 occurs. As energy decreases, the amount of remelting observed decreases. All coating is ablated at laser powers of 40W or higher, with some remnant coating observed at 30W. At 20W, both TiO_2 and Y_2O_3 had the highest amount of retained coating after laser treatment.

For the second trial with the vendor, the sub-20W power regime was explored. The possible presence of remnant volatiles from the EPD process was tested by treating half the samples with a two hour, 200°C post-deposition baking process.

Table 5 indicates the composition and topography of the samples sent for laser processing. To achieve the lower power output of the QCW laser in trial 2, the vendor modified the peak power, laser frequency, and duty cycle (Table 6). The travel speed and focused spot size remained unchanged from the first trial, at 100 inches/minute and 329 µm respectively.

#	Nanoparticle	Concentration (wt. %)	Deposition time (s)	Voltage (V)	Avg. Thickness (µm)	Baked (2hr 200C)
1	TiO_2 (250nm)	0.5	110	20	14.5	Y
2	TiO_2 (250nm)	0.5	110	20	14.5	N
3	Y_2O_3 (32-36nm)	0.5	190	20	20.5	Y
4	Y_2O_3 (32-36nm)	0.5	190	20	20.5	N
5	YSZ (200-300nm)	0.5	250	20	12.8	Y
6	YSZ (200-300nm)	0.5	250	20	12.8	N
7	Al_2O_3 (40-80nm)	0.5	160	20	11.3	Y
8	Al_2O_3 (40-80nm)	0.5	160	20	11.3	N
9	Ti (60-80nm)	0.5	130	20	10.8	Y
10	Ti (60-80nm)	0.5	130	20	10.8	N

Table 5: EPD coating deposition matrix for the 2nd round of laser sintering

Set #	Average Power (W)	Peak Power (W)	Frequency (Hz)	Duty Cycle (%)	Avg. Pulse Intensity (mJ)
1	15	150	250	10	6
2	15	150	250	5	3
3	15	150	192	10	7.8
4	15	150	192	5	3.9
5	10	100	250	10	4
6	10	100	250	5	2
7	10	100	192	10	5.2
8	10	100	192	5	2.6
9	7.5	75	250	10	3
10	7.5	75	250	5	1.5
11	7.5	75	192	10	3.9
12	7.5	75	192	5	1.95

Table 6: Laser parameter sets for vendor trial #2. Parameter sets 6, 10, and 12 gave the most promising visual characteristics

After the testing was completed, it was determined that the baking process was largely ineffective at improving the sample condition following a laser treatment, as the baked samples typically chipped and flaked more than the as-deposited samples. Comparison of the treated areas with the indicated parameters sets reveals that when the average laser power was less than 2 mJ energy per pulse, the most coating was retained on the sample surface. It was determined that the best potential for success lay with the TiO_2 and YSZ coatings, and the other coatings would no longer be investigated.

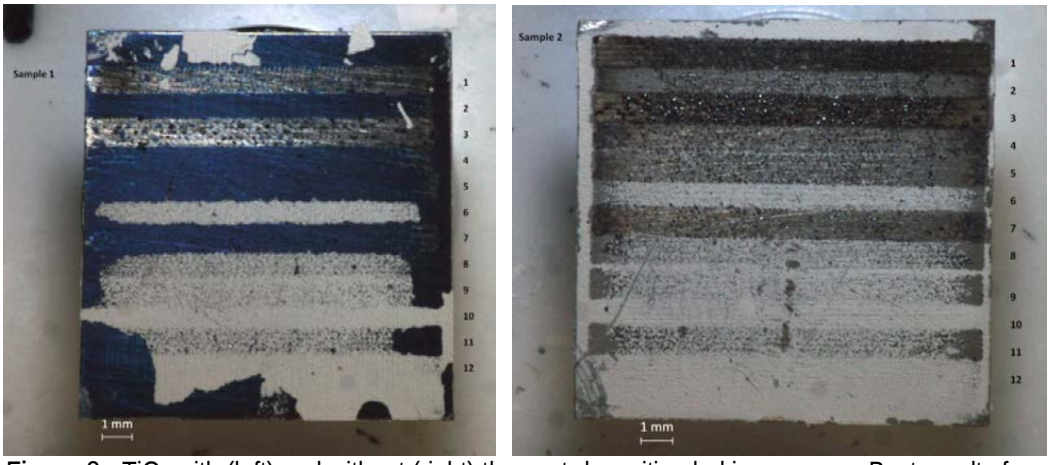

Figure 8: TiO_2 with (left) and without (right) the post-deposition baking process. Best results from the processing are seen in parameter sets 6, 10, and 12.

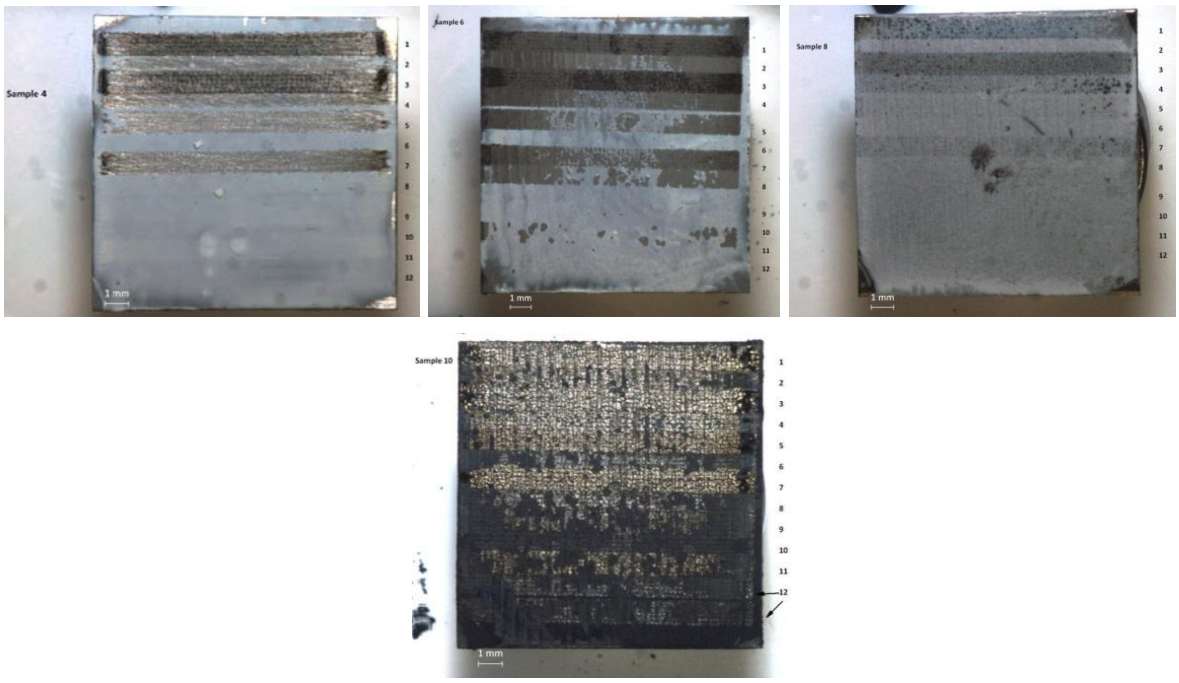

Figure 9: From left to right, post-laser-treated samples of Y_2O_3, YSZ, Al_2O_3, and Ti EPD-coated Zircaloy-4. The above 4 samples were not subjected to the 200°C post-deposition baking treatment.

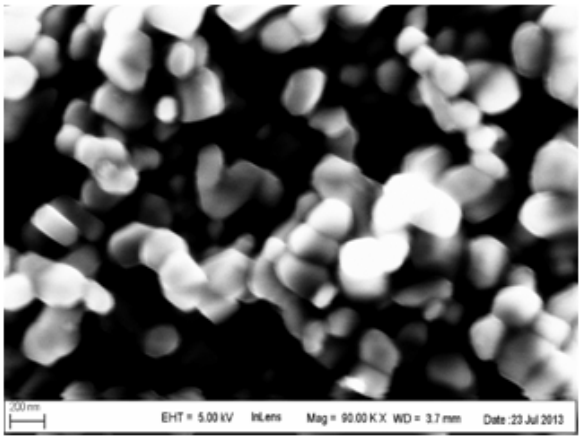

Figure 10: A high-magnification (90 KX) image of TiO_2 after processing by laser condition 10. The individual nanoparticles are largely unaffected and do not show the desired level of intergrowth.

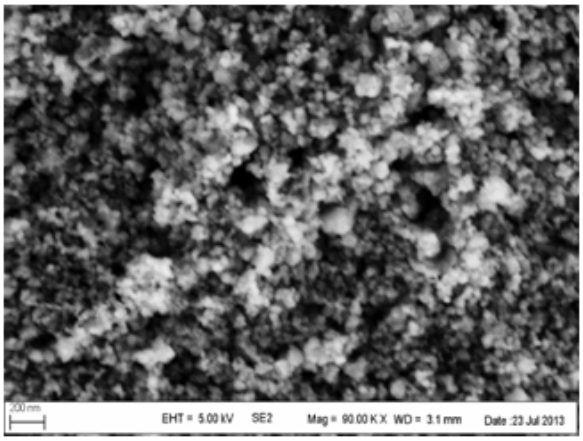

Figure 11: A high-magnification (90 KX) image of the 8% YSZ coated sample after processing by laser condition 10. Individual nanoparticles do not show sintering behavior.

The final collaboration with the vendor company involved 16 samples of EPD-coated Zircaloy-4, all of which had been treated with the 200°C post-coating bakeout. Half of the samples were coated with TiO_2, and the remaining 8 samples were coated with YSZ. Two of each coating's samples were intentionally coated with an excess of material to test the hypothesis that the initial deposits were not thick enough to withstand any initial transients during the laser treating process. All samples were baked for two hours at 200°C to drive out potential remnant volatile liquids. Of the six "normal" thickness coatings, two were used to test a different laser processing conditions. After exhausting potential parameters, the best condition was then applied to the remaining samples to demonstrate repeatability and transferability of the laser parameter set to multiple samples. Of the two "thick" coatings, one was used in a similar manner before applying the chosen parameter set to the other sample.

Table 7: Parameter sets used during laser sintering trial #3 with the collaborating vendor (QCW: Quasi-continuous Wave; CW: Continuous Wave)

Set #	Avg Power (W)	QCW Frequency (Hz)	Travel Speed (ipm)	QCW Duty Cycle (%)	# Passes	Notes	Coating
1	12	300	20	9	1	Power below threshold	Normal TiO_2
2	25	300	20	9	1	No effect observable	Normal TiO_2
3	25	300	20	7	1		Normal TiO_2
4	12	100	20	9	1	Power below threshold	Normal TiO_2
5	25	100	20	9	1		Normal TiO_2
6	25	100	20	7	1		Normal TiO_2
7	25	300	20	9	1		Normal TiO_2
8	25	100	20	9	1		Normal TiO_2
9	150	CW mode	20	CW mode	1	Welding/ablation observed	Normal TiO_2
10	100	CW mode	20	CW mode	1	Welding/ablation observed	Normal TiO_2
11	100	CW mode	100	CW mode	1	Welding/ablation observed	Normal TiO_2
12	85	CW mode	100	CW mode	3	No effect observable	Normal TiO_2
13	90	CW mode	100	CW mode	3	Minor spotting	Normal TiO_2
14	95	CW mode	100	CW mode	1	Welding/ablation	Normal TiO_2
15	80	CW mode	100	CW mode	1		Normal TiO_2
16	80	CW mode	50	CW mode	1		Normal TiO_2
17	80	CW mode	35	CW mode	3	No effect observable	Normal TiO_2
18	85	CW mode	30	CW mode	3		Normal TiO_2
19	85	CW mode	10	CW mode	1	Minor spotting	Normal TiO_2
20	85	CW mode	20	CW mode	1	Minor spotting	Normal TiO_2
21	85	CW mode	25	CW mode	2		Normal TiO_2
22	85	CW mode	25	CW mode	1		
23	25	100	25	9	1	Spotting	

Set #	Avg Power (W)	QCW Frequency (Hz)	Travel Speed (ipm)	QCW Duty Cycle (%)	# Passes	Notes	Coating
24	15	100	25	9	1	No spotting/ablation	
25	15	50	25	9	1		
26	20	50	25	9	1	Ablation	Normal TiO_2
27	15	100	25	9	1	Used for remaining normal TiO_2 samples	Normal TiO_2
28	50	250	100	10	1	Ablation	Normal TiO_2
29	20	250	100	10	1	Little effect observable	Normal TiO_2
30	25	250	100	10	1	50% ablation	Normal TiO_2
31	22	250	100	10	1	Promising	Thick TiO_2
32	22	250	100	5	1	Little effect observable	Thick TiO_2
33	22	125	100	10	1	Less promising	Thick TiO_2
34	20	125	100	10	1	Promising	Thick TiO_2
35	22	250	100	10	1	Used for remaining thick TiO_2 sample	
36	35	250	100	10	1	Ablation	Normal YSZ
37	25	250	100	10	1	Little effect observable	Normal YSZ
38	27	250	100	10	1	Little effect observable	Normal YSZ
39	30	250	100	10	1	Ablation	Normal YSZ
40	27	250	100	10	1	Ablation	Normal YSZ
41	25	250	100	10	1	No ablation	Normal YSZ
42	25	250	100	10	1	Used for remaining normal YSZ samples	
43	30	250	100	10	1	Partial ablation	Thick YSZ
44	27	250	100	10	1	Partial ablation	Thick YSZ
45	25	500	100	10	1	Little effect observable	Thick YSZ
46	30	500	100	10	1	Promising	Thick YSZ
47	30	500	100	10	1	Used for remnant thick YSZ test sample and half the other thick YSZ sample	

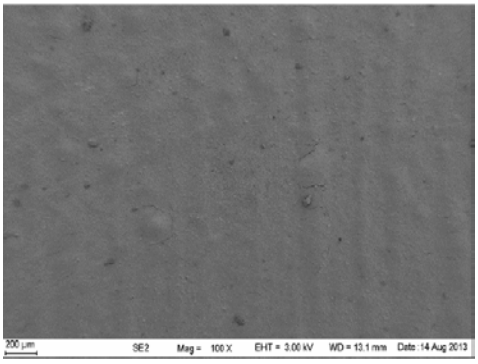

Figure 12: "Normal" TiO_2 coating prior to laser surface treatment. The above coating has been baked for 2h at 200°C to drive out any remnant liquids from the deposition process.

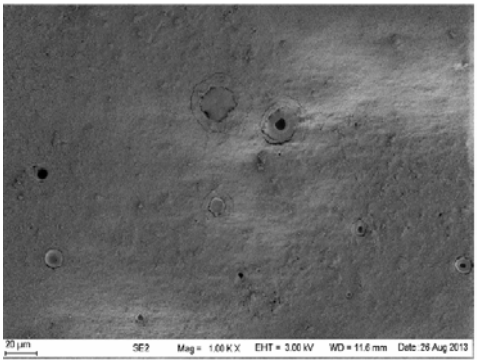

Figure 13: YSZ coating following laser surface treatment at an aggressive parameter set. Pockets of densification are observed, but it is evident that further optimization is required to prevent ablation and complete melting.

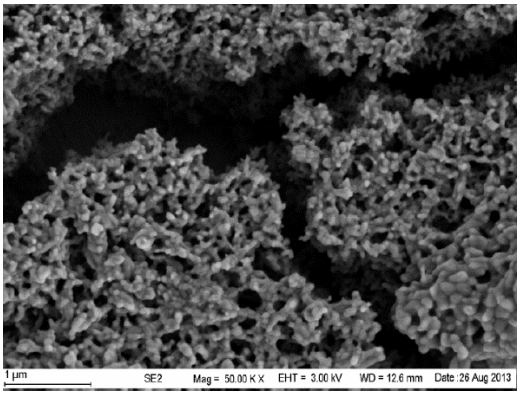

Figure 14: A 50 KX image of standard-thickness TiO_2 after laser processing. A desired effect of laser processing, enhanced particle inter-connectivity, is most prominent in the lower right but is apparent throughout the image.

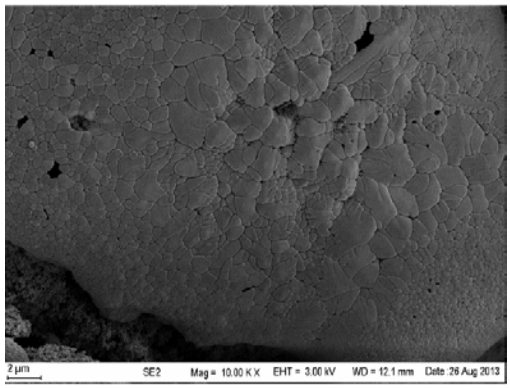

Figure 15: A 10 KX image of thick-deposited TiO_2 after laser processing. This microstructure is characteristic of resolidified nanoparticles, and represents the upper limit of desired laser surface treatment effects.

Effort to improve the post-laser sintering coating was postponed from September 2013 to February 2014, at which time UW collaborated with an on-campus group with a laser capable of lower power output and variable spot sizing. In the previous experiments, it was thought that the initial transient of energy could be sufficient to vaporize some or all of the coating material, resulting in non-uniform sintering behavior, coating disruption, and overexposure of the substrate Zircaloy-4. Use of a continuous wave laser operating at low power should reduce coating stresses associated with the energy transient in comparison to an equivalent average wattage QCW mode, potentially promoting a sintering response instead of vaporization or melting.

Expt #	Operation Mode	Target Power (W)	Spot Size (µm)	Travel speed (ipm)	Passes	Notes
1	CW	0.80	30	11.8	1	Spotting / Sparking seen
2	CW	0.80	30	2.4	1	Less frequent sparking
3	CW	1.50	30	11.8	1	Sparking
4	CW	1.50	30	2.4	1	
5	CW	0.80	30	11.8	3	Sparking only on first pass
6	CW	9.70	100	11.8	1	Constant light emission from sample
7	CW	4.95	100	11.8	1	Near-constant light emission
8	CW	5.00	100	23.6	1	
9	CW	5.00	100	47.2	1	
10	CW	5.00	100	118.1	1	

Table 8: Parameter sets used for the fourth laser sintering experiment, performed with a UW research group

The results from the intra-university collaboration were not as promising as hoped. The "sparking" / "spotting" behavior observed at the laser-coating interaction site was confirmed with SEM to be due to offgassing and vaporization. Imaging of the parameter sets did reveal that condition 6 presented the most unique region yet. This region was analyzed using FIB methods, and it was discovered that not only did most of the coating vaporize, but the substrate was cracked beneath the coating layer. Damage to the treated region from parameter set #6 was observed that could only have been caused by the SEM electron beam, indicating that the coating was even more fragile than the as-deposited condition.

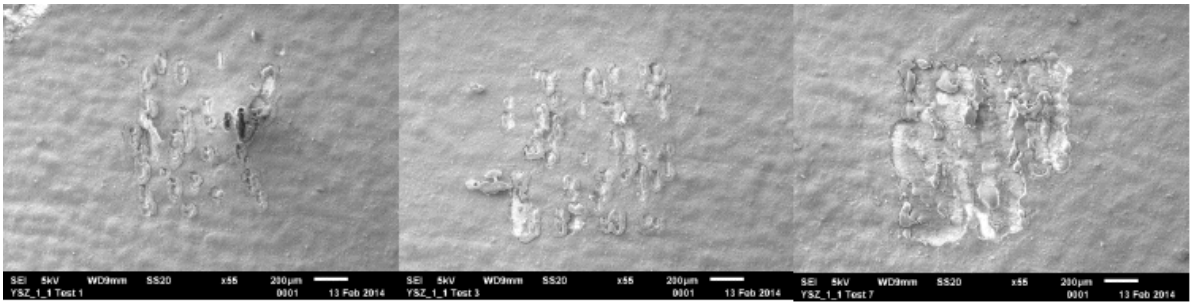

Figure 16: YSZ EPD coatings after having undergone 3 different continuous – wave laser energies (0.8, 1.5, 4.95 W respectively). All conditions lead to ablation.

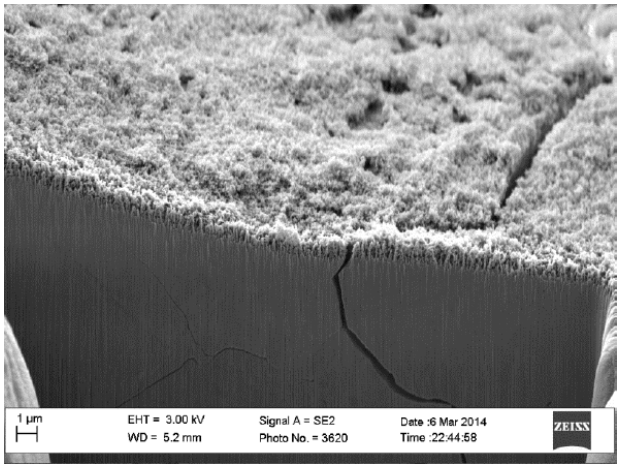

Figure 17: FIB-milled cross-section view of parameter set #6 from the intra-university laser sintering collaboration. Coating thickness was reduced from >12µm to 1 µm or less, and subsurface cracking of the Zircaloy-4 substrate is evident in the processed region.

2.5. MECHANICAL TESTING

The mechanical testing performed on the EPD samples, for both heat treated and laser sintered samples, included scratch testing and rotating pin-on-disk wear testing. For scratch testing, the sample is secured in the base underneath the end of the lever. A diamond indenter is used to apply the load in a concentrated location and a counterweight was used to balance the lever holding the indenter. Then an applied load was added, usually 100 or 150 grams. The base could then be moved at a constant speed creating a scratch in the coating. Multiple measurements of each scratch on a specimen were performed using an SEM. Table 9 shows the results of scratch test done at 150g for bare zirconium and the UW-Madison Laser Treatment (LS).

Coating Material	Scratch Width @ 150g (±µm)
Bare Zircaloy	42.99 ± 2.09
TiO_2	163.4 ± 5.70
YSZ	146.7 ± 12.5

Table 9: Scratch Test Measurement Results

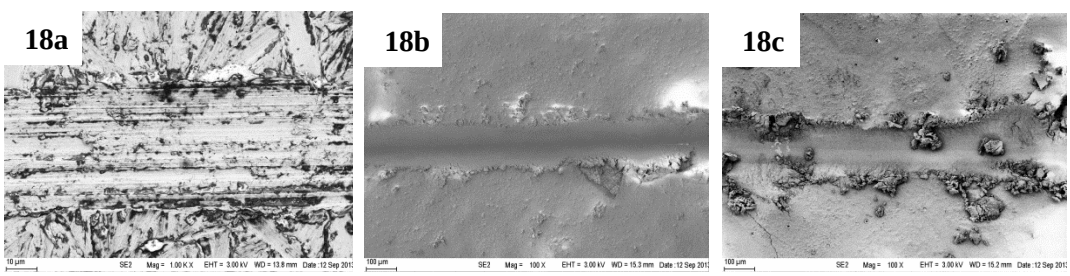

Figure 18: Scratch Test Results. Figure 18 shows SEM images from scratch testing done at a load of 150g where 18a) is bare zirconium 18b) is laser treated TiO_2 and 18c) is laser treated YSZ.

For rotating pin-on-disk wear testing, the sample is secured on a rotating disk underneath the end of a lever. Instead of a diamond indenter, a ruby (Al_2O_3) stylus is used. Once the load is applied, 10, 25, or 49.95 grams, the device can be turned on to turn the disk at a constant rate. The rotating pattern creates a circular wear track. The wear tracks were analyzed using a white light interferometer (Zygo New View) in addition to SEM imaging. With the Zygo an annulus stitch of the wear track, including the depth profile, can be obtained. Depth measurements in 8 different directions along the wear track were taken and compiled to determine the average depth, width, and volume loss of the wear track. Table 10 shows the different initial experiment parameters that were performed on a bare zirconium sample.

Condition	Test Duration (min)	Load (g)	Est. Rotations	Avg. Volume Lost (mm^3)
1	60	25	8,798.40	0.0420
2	60	49.95	8,798.40	0.0663
3	60	10	8,798.40	0.0170
4	30	25	4,399.20	0.0138
5	30	49.95	4,399.20	0.0272
6	30	10	4,399.20	0.0066
7	120	10	17,596.80	0.0222

Table 10: Pin-on-Disk Initial Parameters

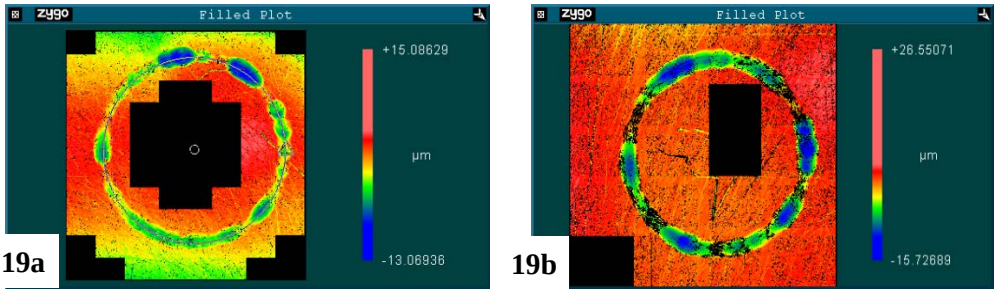

Figure 19: Pin-on-Disk Parameters. Figure 19 shows the depth profile of the initial parameter on bare zirconium where 19a) is 60 minutes at a load of 10 grams and 19b) is 120 minutes at a load of 10 grams.

After analysis on bare zirconium, condition 3 (10 g for 60 min) was chosen as the standard for wear track testing. Lower loads for longer periods of time were deemed to be a more realistic model. The time could be increased if improvement in the EPD coatings was seen. Unfortunately, the EPD coatings were not developed enough to improve performance under rotating pin-on-disk wear testing. Table 11 shows the results from pin-on-disk wear testing for the UW-Madison laser treatment (LS) and UW-Madison furnace treatment samples (HT), which was done at 700˚C for 6 hours plus 600˚C for 200 hours, on a stainless steel 316 substrate.

Treatment	Coating Material	Avg. Width (±µm)	Avg. Depth (±µm)	Avg. Volume Lost (mm^3)
HT	TiO_2	673.21 ± 44.43	13.65 ± 1.30	0.0937
HT	TiO_2	695.65 ± 64.92	11.31 ± 1.61	0.0822
HT	YSZ	640.40 ± 88.89	11.32 ± 4.73	0.0743
HT	YSZ	621.90 ± 40.96	11.89 ± 2.52	0.0794
LS	TiO_2	590.79 ± 49.29	4.926 ± 3.13	0.0352
LS	TiO_2	646.54 ± 80.47	4.564 ± 3.67	0.0346
LS	YSZ	653.14 ± 72.17	6.021 ± 3.03	0.0455
LS	YSZ	603.85 ± 70.91	4.452 ± 6.84	0.0321

Table 11: EPD Pin-on-Disk Results

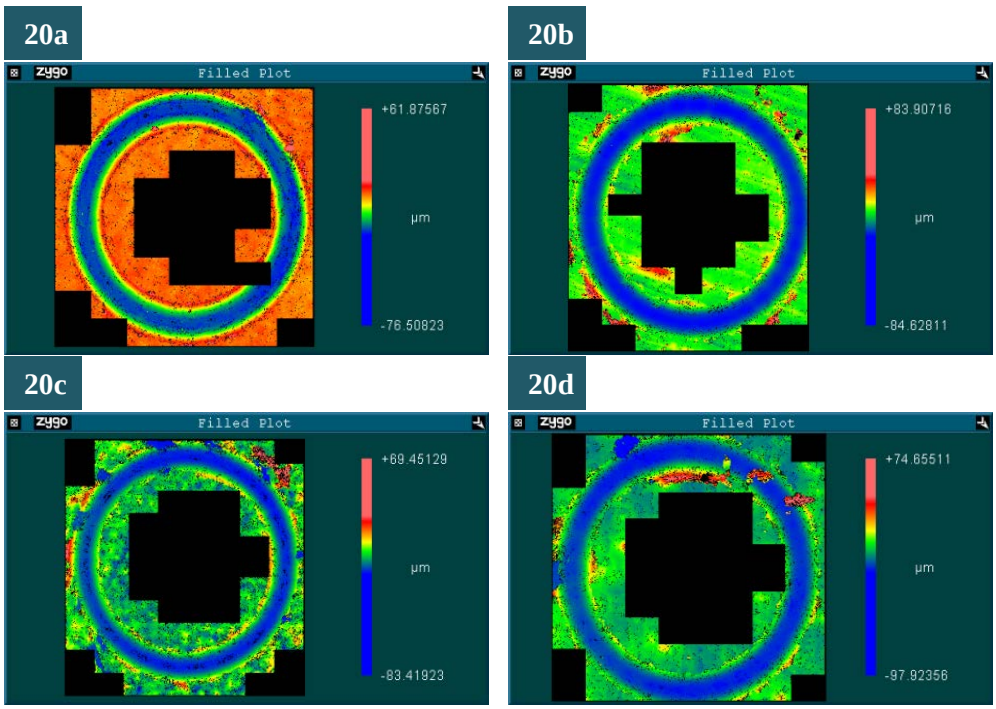

Figure 20: EPD Pin-on-Disk. Figure 20 shows the wear tracks from the rotating pin-on-disk wear testing where 20a) is the heat treated (700°C 6 hours + 600°C 200 hours) TiO_2 sample 20b) is the heat treated (700°C 6 hours + 600°C 200 hours) YSZ sample 20c) is the laser treated TiO_2 sample 20d) is the laser treated YSZ sample.

2.6. QUENCH TEST DESIGN WORK

It has been previously shown that nanoparticle coatings have increased the critical heat flux (CHF), reduced the cooling time, and increased the surface temperature of the minimum heat flux. The increase in CHF causes the temperature where bubbles form a film on the surface to increase. This helps the metal from overheating, since the film decreases the efficiency of heat transfer and the film would form at a higher temperature if the CHF increases. An increase in the surface temperature of the minimum heat flux means that the film that builds up along the sample surface collapses quicker. A way to test and confirm this phenomenon is to perform a quench test. Figure 21 shows the design schematics of a quench test apparatus that was designed for possible experiments.

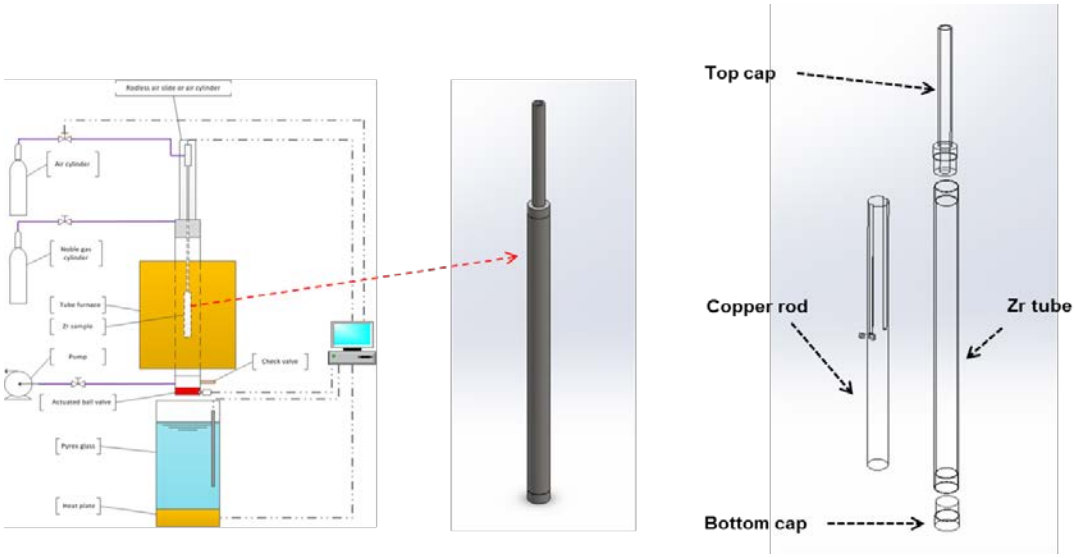

Figure 21: The schematic designs of quenching facility. This was the initial design for the quench test apparatus.

The quench test apparatus consists of the Zircaloy tube sample, a tube furnace, quenching pool, compressed gas cylinders (1 air, 1 inert), and a data acquisition system. A copper rod fitted with a thermocouple fills the Zircaloy tube sample, serving as a thermal load that extends the quench time and also measures the temperature of the sample during the experiment. The tube sample starting temperature is 500°C. An inert gas such as Helium or Argon flows inside the furnace during heat-up to prevent undesirable surface oxidation. An air-driven sliding rod pushes the sample down when the sample reaches the specified 500°, immersing it into the saturated water pool. The temperature of the sample is recorded by the thermocouple simultaneously. It was expected that there would be a distinct difference in temperature histories for the uncoated and nanoparticle-coated Zircaloy tubes.

The design depicted in Figure 21 utilized a thread interface in order to secure the sample to the insertion rod, but it was suspected this threading step may damage the thin-walled tubes. The design was modified to consolidate the bottom end-cap and instrumented thermal load, with the sample then mounted as a sleeve on the thermal load (Figure 22). A lip between the inner rod and the bottom end-cap prevents the sample from sliding off and water from infiltrating the instrumented cavity. The sample assembly is then attached to the insertion rod at the top, by means of a threaded hole in the thermal load rod. Successful implementation of this new design requires selection of materials that approximate the thermal expansion of the sample, such that no gaps open up during the heating or cooling stages of the experiment.

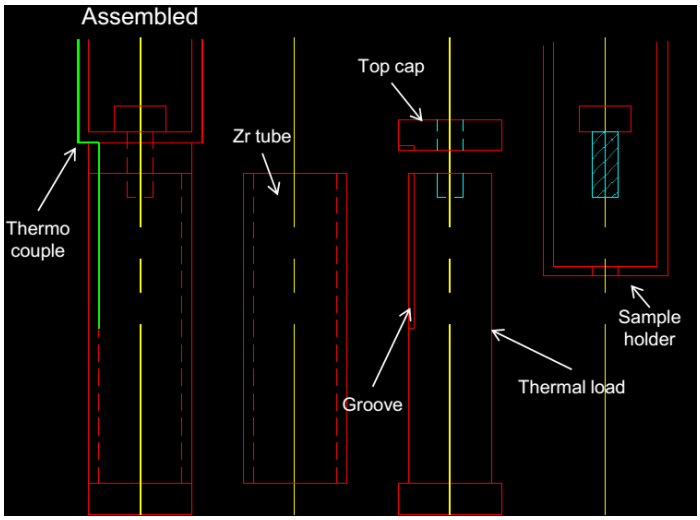

Figure 22: Quench test schematic. A potential new designs for fixturing a thin-walled tube to a supporting structure for controlled-position quench testing. In this design, all threads are located in the thermal load material, which has thermocouple locations and a resting lip to secure the bottom of the sample.

Finite element simulations of several common materials in varied geometries were performed to examine the likely behavior of the sample assembly during an experiment. Results (Figure 23) indicate that conventional metallic materials will not work for the thermal load/end-cap assembly without introducing a gap at temperature, but ceramics hold promise. The simulations also indicate the choice of thermal load diameter is critical in order to prevent yielding of the sample tube during ramp or quench stages.

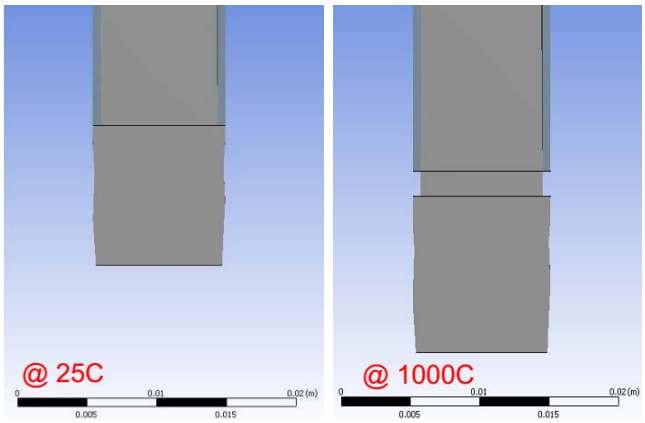

Figure 23: Finite element simulation for end-cap. Development of the bottom gap when using a metallic (SS, Al, Cu) thermal load to support the Zircaloy-4 tube sample during the ramp to quenching temperature. Total gap length (top and bottom) is estimated to be 0.65 – 1.7 mm, depending on the material.

Literature data was manually converted into time-temperature data for use as a validation/demo data set of a 1-D inverse heat transfer code. A comparison between UW's implementation with the literature implementation was then performed (Figure 24). It is suspected that increasing the uniformity of the input data's "time-step" will improve performance of the UW code. Other known and desired code improvements include incorporation of temperature dependence for material density and heat capacity.

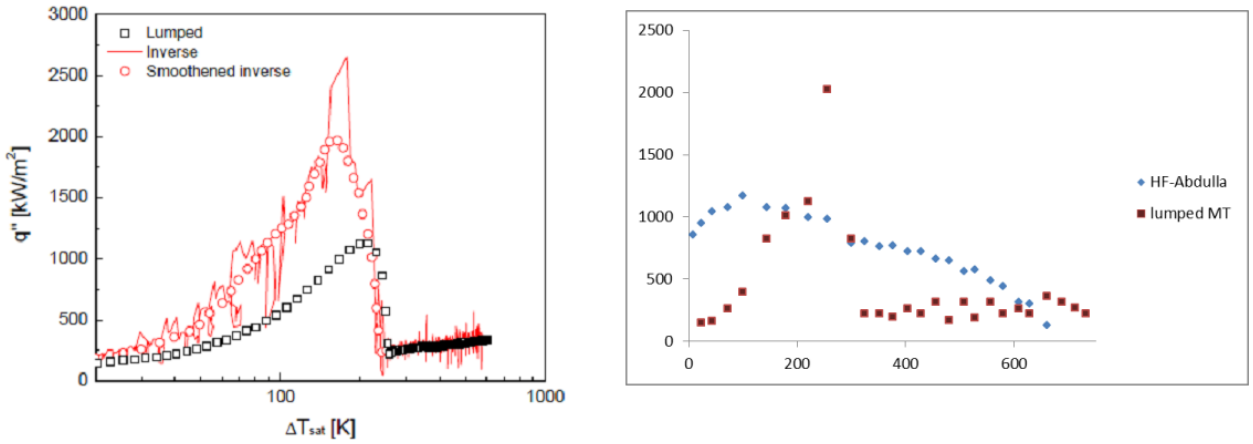

Figure 24: Heat flux comparison. Comparison of heat flux computed for the same event by literature (left) and UW (right) heat flux codes. The in-development UW code shows similar behavior but has room for improvement.

A refined design for the quench testing apparatus was completed. The design was also studied using finite element analysis. Even though the design work was completed, fabrication of the quench test apparatus was not started. In addition to the design work, there was work on an inverse heat transfer code that was compared to results from literature.

2.7. LITERATURE REVIEW ON COATING MATERIALS AND METHODS FOR NUCLEAR FUEL CLADDING

The study of the surface modification for improving the mechanical integrity and corrosion resistance of a fuel cladding exposed in a high temperature environment has been conducted actively. The zirconium based alloys have been widely used in nuclear fuel in light water reactors (LWRs) because of their very low thermal neutron absorption cross-section and excellent high temperature water corrosion resistance. In a loss-of-coolant-accident, however, the Zircaloy alloys easily oxidize in a high temperature steam environment and they lose its intrinsic mechanical properties due to hydriding [11]. Moreover, the cladding oxidation reaction gives rise to an increase in fuel temperature and it is accompanied by hydrogen production, which was shown in Fukushima nuclear accident [12].

Therefore, most of the study has been focused on fabricating a protective surface layer on commercial Zircaloy alloys or possible cladding materials [10-25]. Kim et al. [13] and Khatkhatay et al. [14] deposited thin TiN film (~1μm) on stainless steel bars and tubes by using pulsed laser deposition (PLD). The TiN films had excellent adhesion properties, high surface hardness, and diffusion barrier characteristics. Multilayered TiN coatings on Ti46Al8Nb alloy surface have also been successfully prepared by the hollow cathode discharge method. The layers had good adhesion to the substrate and wear resistance by the microstructure optimization [15]. Silicon carbide (SiC) coatings also are a potential method to reduce oxidation and hydriding in fuel cladding [16, 17]. Al-Olayyan et al. [16] made SiC thin layer by Chemical Vapor Deposition (CVD) on a Zircaloy-4 substrate with various surface roughness conditions. During scratch test experiments, SiC coatings had high adhesion to the substrate without cracks and delamination. In addition, molybdenum disilicide ($MoSi_2$) has been tried to check its feasibility as a promising coating material due to its high temperature mechanical properties and oxidation resistance [18-20]. Reisel et al. [18] sprayed $MoSi_2$ powers by high velocity oxyfuel spraying technique (HVOF) onto a polished carbon steel substrate. The coating showed a large value of surface hardness from 8.1GPa to 10.5GPa depending on porosity. During oxidation at 1500˚C for 28h, the MoSi2 coatings formed a protective SiO_2 layer on the surface, which showed a very small mass change. $MoSi_2$ oxidation protective coatings on molybdenum substrate were prepared using air plasma spraying technique (APS) by Wang et al. [19]. Although the coating surface had some microcracks, pores, and spherical features, a large bonding strength was measured while tensile load was applied. The $MoSi_2$ coated Mo substrate exhibited good oxidation resistance at 1200˚C. Also, deposition of thin chromium oxide coatings (Cr_2O_3) (~4μm) on low carbon steel substrates was performed by reactive radio frequency magnetron sputtering. Annealing at a higher temperature of 500˚C led to a significant improvement in mechanical properties of the coatings such as hardness, adhesion, and wear resistance due to the formation of crystalline Cr_2O_3 phase [21]. Cerny et al. [22] prepared protective Cr_2O_3 films on AISI 316 stainless steel by Plasma Assisted Chemical Vapor Deposition (PACVD). The films decreased high temperature oxidation at 700-1000˚C for up to the test period of 1000h and exhibited a satisfactory adhesion to the steel substrate. Firouzdor et al. [23-25] fabricated diffusion protective coatings on T91 ferritic steel by titanium, titania, yttrium stabilized zirconia nanofluid-based EPD technique, respectively. Each coating had optimal deposition condition and post-heat treatment condition to achieve target coating thickness (~10μm) as well as excellent mechanical integrity of the coating.

Mn+1AXn (MAX) phase materials have been actively explored since the mid-1990s because of their exceptional oxidation resistance and mechanical properties. There are about 60 MAX phases with at least 9 discovered in the last five years alone [26]. Some aluminum containing MAX phases, Ti_2AlC, Ti_3AlC_2, and Cr_2AlC performed as a promising oxidation barrier due to the formation of a dense, spall resistant, and adherent alumina (Al_2O_3) layer during oxidation tests in air. The Cr_2AlC had better oxidation resistance compared with Ti_2AlC and Ti_3AlC_2 at all oxidation temperature under 1200˚C [27]. However, in terms of practical application, Ti_2AlC is the most attractive material due to high Al concentration, the thermal expansion coefficient match with Al_2O_3, and lower density. It is also significant to choose an appropriate coating method to build a desired MAX phase layer on substrates. Preliminary investigations using physical vapor deposition or thermal spray deposition technique have been studied. In addition, Rech at al. [28] studied the feasibility of the cold spray deposition of Ti_2AlC on Al and steel substrate. They found the substrate hardness plays a major role in the quality of the

coatings. Unlike HVOF spraying process, the cold spray does not induce substantial phase transformation and avoids degradation. Successful studies on Ti-Al-C MAX phase coatings have been performed at the U W in collaboration with Savannah River National Laboratory (SRNL) [29]. Finally, MAX phase materials containing Al, Nb_2AlC, Ta_2AlC, and $(TiNb)_2AlC$ appear to be promising candidates.

3.0 CONCLUSIONS

The EPD method of depositing coatings on both flat surfaces and tubes proved to be capable of yielding very uniform and then coatings. However, none of the heat treatment methods, including furnace and laser, could sinter the coating sufficiently without affecting the microstructure of the Zircaloy cladding. Therefore, the EPD process was eliminated from further development.

4.0 REFERENCES

[1] "Application of Electrophoretic and Electrolytic Deposition Techniques in Ceramic Processing", Boccaccini, A and Zhitomirsky, I. 2002, Current Opinion in Solid State & Materials Science, pp. 251-260.

[2] "Electrophoretic Deposition Forming of Porous Alumina Memebranes", Chen, C.Y., Chen, S.Y. and Liu, D.M. 9, 1999, Acta Materialia, Vol. 47, pp. 2717-2726.

[3] "Electrophoretic Deposition of Materials", Van der Biest, O.O. and Vandeperre, L.J. 1999, Annual Review of Material Science, Vol. 29, pp. 327-352.

[4] "Electrophoretic Deposition from Aqueous Suspensions for Near-Net Shape Manufacturing of Advanced Ceramics and Glasses – Applications", Tabellion, J and Clasen, R. 2004, Journal of Materials Science, Vol. 39, pp. 803-811.

[5] "Functionally Graded Ceramic/Ceramic and Metal/Ceramic Composites by Electrophoretic Deposition", Sarkar, P., Datta, S and Nicholson, S. 1997, Composites Part B, Vol. 28, pp. 49-56.

[6] "Nickel-Alumina Functionally Graded Materials by Electrophoretic Deposition", Nagarajan, N. and Nicholson, P.S. 11, 2004, Journal of the American Ceramic Society, Vol. 87, pp. 2953-2057.

[7] "A Review on Fundamentals and Applications of Electrophoretic Deposition (EPD)", Besra, L., Liu, M. 2007, Progress in Materials Science, Vol. 52, pp. 1-61.

[8] Hunter, Robert J. Zeta, Potential in Colloid Science: Principles and Applications. London and New York : Academic Press, 1981. 0123619602.

[9] "Zeta Potential, An Introduction in 30 Minutes", Malvern Instruments.

[10] "The Influence of pH on Particle Packing in YSZ Coating Electrophoretically Deposited from a Non-Aqueous Suspension", Xu, H., Shapiro, I.P. and Xiao, P. 2010, Journal of the European Ceramic Society, Vol. 30, pp. 1105-1114.

[11] Wei, J., Frankel, P., Blat, M., Ambard, A., Comstock, R., Hallstadius, L., Lyon, S., Cottis, R., and Preuss, M, Autoclave study of zirconium alloys with and without hydride rim, Corrosion Engineering, Science and Technology, vol.47, pp. 516-528, 2012.

[12] Pint, B., Terrani, K., Brady, M., Cheng, T., Keiser, J, High temperature oxidation of fuel cladding candidate materials in steam-hydrogen environments, Journal of Nuclear Materials, vol. 440, pp. 420-427, 2013.

[13] Kim, I., Khatkhatay, F., Jiao, L., Swadener, G., Cole, J., Gan, J., Wang, H, TiN-based coatings on fuel cladding tubes for advanced nuclear reactors, Journal of Nuclear Materials, vol. 429, pp. 143-148, 2012.

[14] Khatkhatay, F., Jian, J., Jiao, L., Su, Q., Gan, J., Cole, J., Wang, H., Diffusion barrier properties of nitride-based coatings on fuel cladding, Journal of Alloys and Compounds, vol. 580, pp. 442-448, 2013.

[15] Yu, Z., Hu, J., Niu, Y., Wei, J., Yang, Y., Adhesion performance and wear resistance of multilayered TiN coating deposition by hollow cathode discharge method, Key Engineering Materials, Vol. 531-532, pp. 342-345, 2013.

[16] Al-Olayyan, Y., Fuchs, G., Baney, R., Tulenko, J., the effect of Zircaloy-4 substrate surface condition on the adhesion strength and corrosion of SiC coatings, Journal of Nuclear Materials, vol. 346, pp. 109-119, 2005.

[17] Pint, B., Terrani, K., Brady, M., Cheng, T., Keiser, J., High temperature oxidation of fuel cladding candidate materials in steam-hydrogen environments, Journal of Nuclear Materials, vol. 440, pp. 420-427, 2013.

[18] Reisel, G., Wielage, B., Steinhauser, S., Morgenthal, I., Scholl, R., High temperature oxidation behaviour of HVOF-sprayed unreinforced and reinforced molybdenum disilicide powders, Surface and Coatings Technology, vol.146-147, pp. 19-26, 2001.

[19] Wang, Y., Wang, D., Yan, J., Sun, A., Preparation and characterization of molybdenum disilicide coating on molybdenum substrate by air plasma spraying, Applied Surface Science, vol. 284, pp. 881-888, 2013.

[20] Zhao, X and Ye, Z., Microstructure and wear resistance of molybdenum based amorphous nanocrystalline alloy coating fabricated by atmospheric plasma spraying, Surface & Coatings Technology, vol. 228, pp.S266-S270, 2013.

[21] Pang, X., Gao, K., Luo, F., Yang, H., Qiao, L., Wang, Y., Volinsky, A., Annealing effects on microstructure and mechanical properties of chromium oxide coatings, Thin Solid Films, vol. 516, pp. 4685-4689, 2008.

[22] Cerny, F., Pitter, J., Konvickova, S., Jech, V., High temperature oxidation protective chromium-based coatings prepared by IBAD and PACVD methods, Surface & Coatings Technology, vol. 203, pp. 2566-2570, 2009.

[23] Firouzdor, V., Brechtl, J., Wilson, L., Semerau, B., Sridharan, K., Allen, T., Development of titanium diffusion barrier coatings for mitigation of fuel-cladding chemical interactions, Surface & Coatings Technology, vol. 219, pp. 59-68, 2013.

[24] Firouzdor, V., Brechtl, J., Wilson, L., Semerau, B., Sridharan, K., Allen, T., Development of Yttrium Stabilized Zirconia (YSZ) diffusion barrier coatings for mitigation of Fuel-Cladding Chemical Interactions, Journal of Nuclear Materials, vol. 438, pp. 268-277, 2013.

[25] Firouzdor, V., Brechtl, J., Hauch, B., Sridharan, K., Allen, T., Electrophoretic deposition of diffusion barrier titanium oxide coatings for nuclear reactor cladding applications, Applied Surface Science, vol. 282, pp. 798-808, 2013.

[26] P. Eklund, M. Beckers, U. Jansson, H. Hogberg, L. Hultman, The Mn+1AXn phases: Materials science and thin-film processing, Thin Solid Films, vol. 518, pp. 1851-1878, 2010

[27] D. Tallman, B. Anasori, M. Barsoum, A Critical Review of the Oxidation of Ti2AlC, Ti_3AlC and Cr_2AlC in Air, Materials Research Letters, Vol. 1, pp. 115-125, 2013

[28] S. Rech, A. Surpi, S. Vezzu, A. Patelli, A. Trentin, J. Glor, J. Frodelius, L. Hultman, P. Eklund, Cold-spray deposition of Ti2AlC coatings, Vacuum, vol. 94, pp. 69-73, 2013

[29] B. Garcia-Diaz, L. Olson, C. Verst, R. Sindelar, E. Hoffman, B. Hauch, B. Maier, and K. Sridharan, “MAX Phase Coatings for Accident Tolerant Nuclear Fuel”, proc. Trans. American Nuclear Society Conf., Reno, NV, 2014.

APPENDIX G

MAX Phase Coatings Evaluation
for the
Phase 1A Final Report
for Enhanced Accident Tolerant Fuels

Prepared by:
AREVA Federal Services, LLC
Savannah River National Laboratory (SRNL)
University of Wisconsin (UW)

TABLE OF CONTENTS

1.0 INTRODUCTION 1
2.0 SELECTION OF MAX PHASE CARBIDE POWDERS AND COATING PROCESS 1
2.1. MAX PHASE CARBIDE POWDER SELECTION 1
2.2. SPRAY COATINGS PROCESS SELECTION 1
2.3. MAX COATING ZIRCALOY SUBSTRATES FOR PERFORMANCE TESTING 3
3.0 CHARACTERIZATION OF MAX POWDER & SPRAY COATED MAX POWDER ON ZIRCALOY SUBSTRATES PRIOR TO PERFORMANCE TESTING 5
3.1. CHARACTERIZATION OF MAX POWDER 5
3.2. CHARACTERIZATION OF SPRAY-COATED SUBSTRATES PRIOR TO TESTING 6
4.0 PERFORMANCE TESTING - MECHANICAL (PHYSICAL) 11
4.1. SCRATCH ADHESION TESTING 12
4.2. WEAR TESTING 13
5.0 PERFORMANCE TESTING – CORRISION/OXIDATION: INITIAL SCOPING TESTS AND EXTENDED OPERATIONAL CONDITIONS (AUTOCLAVE) 15
5.1. INITIAL SCOPING TESTS 16
5.2. REACTOR OPERATIONAL TESTING – ASTM G2 CONDITIONS 23
6.0 CHEMICAL/OXIDATION PERFORMANCE TESTING AT LOCA CONDITIONS (STEAM REACTOR) 42
6.1. INITIAL TESTING – LOCA CONDITIONS 42
7.0 FUTURE TESTING 51
8.0 SUMMARY OF CONCLUSIONS 51
8.1. MATERIAL 51
8.2. SPRAY METHODS 52
8.3. PERFORMANCE TESTING RESULTS 52
8.4. NORMAL OPERATING CONDITIONS ASTM-G2 TESTING 53
8.5. LOCA CONDITION TESTING 53
8.6. OVERALL CONCLUSIONS 54

LIST OF TABLES

Table 1: Spray Coatings Process. 2
Table 2: Surface Roughness values for MAX spray coatings, as measured via optical profilometry. 9
Table 3: Rotating Pin-on-Disc test results for spray-coated samples prepared for the Manufacturing GR. No results could be measured for the sample produced by HVOF spraying. All samples tested with a 10 g load for 120 minutes. 14
Table 4: Manufacturing GR Recommendations. 15
Table 5: Measured oxide thicknesses of various surfaces after 3 days of 400°C, 1500 psi steam exposure. Measurements collected are based on point-to-point interpolations within SEM imaging software, with minimum 5 measurements per reported quantity. 24
Table 6: Mass measurements of the three ASTM G2 condition samples. The higher weight gain of the sprayed coupons is not surprising given the capability of the coating to oxidize and the high free energy of formation for both TiO_2 and Al_2O_3. 26
Table 7: The table shows coating thickness statistics for representative 4-pass, 6-pass, and 9-pass samples. A vendor estimate indicated each pass should deposit ~10 μm MAX phase. The 9-pass thickness is less than expected due to sloughing off of outer coating layers. Future sprayings will be designed to provide a maximum of 4 to 5 passes to minimize sloughing off..... 30
Table 8: Measured oxide thicknesses for sintered and non-sintered Ti_2AlC coatings after a 72-hour G2 autoclave test. 38

LIST OF FIGURES

Figure 1: Illustration of the cold-spray process and equipment. 3
Figure 2: Coupon Size for Corrosion/Adhesion Testing. 4
Figure 3: Autoclave Coupon in Holder Post Design for Corrosion Testing. 4
Figure 4: Tube Samples. 4
Figure 5: Maxthal 211 Particle Size Distribution (Volume). 5
Figure 6: X-Ray Diffraction of Maxthal Powder 211 (Ti_2AlC). 6
Figure 7: Top-View SEM of MAX Powder (Ti_2AlC): HVOF Spray (180 μm thick) on left and CS (200 μm thick) on right – 500X. 7
Figure 8: Cross-Sectional View SEM of MAX Powder (Ti_2AlC): HVOF Spray (180 μm thick) on left and CS (200 μm thick) on right. Light grey area is Zircaloy-4 and dark area is MAX. 7
Figure 9: High Magnification (3340 X) Top-View SEM of MAX Powder (Ti_2AlC): HVOF Spray (180 μm thick). 7
Figure 10: XRD of HVOF MAX Coating (Ti_2AlC). 8
Figure 11: XRD of CS MAX Coating (Ti_2AlC). 8
Figure 12: (A) Ti_2AlC / Zircaloy-4 CS – Prior to Testing (Mag. = 500X). 10
Figure 13: Thermal diffusivity measurements at varying temperature for Ti_2AlC CS spray coated Zircaloy-4. 11
Figure 14: Nanovea Mechanical Tester Initial Testing: Ti_2AlC MAX-Phase HVOF Coated Zircaloy-4 on left and Ti_2AlC MAX- Phase Cold-Spray Coated Zircaloy-4 on right. 13
Figure 15: Wear track result for the polished cold-sprayed MAX phase. Wear tracks were minimal for Zircaloy-4 and the polished cold-sprayed Ti_2AlC-coated sample as shown in this figure. 14
Figure 16: Autoclave Corrosion Testing Sequence @ G2 Conditions (i.e. Extended Operating Conditions). 16
Figure 17: University of Wisconsin Corrosion/Oxidation Testing at supercritical conditions (144 hours, 500 C, 3600 psia); Top 3 coupons after testing: Ti_2AlC MAX-Phase Cold-Spray coated Zircaloy-4 and HVOF- coated Zircaloy-4, and uncoated Zircaloy-4, labeled "As-Received". Bottom 2 coupons are coated coupons prior to test. 17
Figure 18: The cold-sprayed Ti_2AlC coating, HVOF-coated sample (both coating and substrate), and attached portion of the Zircaloy-4 control sample, as removed from the autoclave following conclusion of the 7-day test. The cold-sprayed Zircaloy-4 substrate and the control Zircaloy-4 substrate were later retrieved from within the autoclave test section. 18
Figure 19: Front and back of samples removed from the autoclave after the 7-day test. The chip in the CS coating above the hole is due to handling after removal from the autoclave. The HVOF-sprayed Zircaloy-4 is discolored relative to the control. A grey splotching is observed on the back of the delaminated coatings. The control sample was not flipped over to image its backside. 18
Figure 20: "Reassembled" Zircaloy-4 substrate previously coated with cold-sprayed Ti_2AlC, following the 7-day, 500°C, 3600 psi exposure to pure water. At left is an untested coupon with the cold-sprayed Ti_2AlC coating. 19
Figure 21: Side view of the HVOF sample illustrating the delamination and curvature of the sample. The samples as received from SRNL were not flat, but were also not as curved. 19
Figure 22: Cross section image of exposed HVOF coated MAX powder (Ti_2AlC) coupon @ 500 C, 3600 psia, 144 hrs, characterized in cross-sectional SEM micrographs by Drexel University. A slightly thicker Zircaloy-4 layer is underneath the coating than on the other side. 20
Figure 23: Exposed HVOF coated MAX powder (Ti_2AlC) coupon @ 500 C, 3600 psia, 144 hrs, characterized in top view SEM micrographs by Drexel University. 21
Figure 24: High-magnification micrograph of the HVOF-sprayed MAX phase indicating the EDS regions studied. The dark grey regions are a mixture of TiO_2 and Al_2O_3 oxides, while the light grey sections are un-oxidized Ti_2AlC. The black regions are voids / epoxy resin. 21
Figure 25: EDS spectra for the light grey (top) and dark grey (bottom) portions of the HVOF-sprayed MAX phase. The top spectrum is consistent with un-oxidized HVOF-sprayed MAX phase, while the bottom spectrum is indicative of the presence of some mixed oxide. 22
Figure 26: XRD spectra of the MAX phase coatings before and after the 7-day test. The HVOF coating (bottom middle) begins with considerably more TiC phase present (36, 42° peaks) than Ti_2AlC (13, 40°) – in other words, CS (top) deposits a truer Ti_2AlC MAX phase coating. Both coatings are significantly altered during the test. 23
Figure 27: The oxide layer present on the unsprayed test Zircaloy-4 coupon is small. 25

Figure 28: The interface between the cold-sprayed MAX phase and the Zircaloy-4 substrate is oxidizing despite presence of the external layer. Evidence of preliminary steps towards coating delamination is visible. 25
Figure 29: Beginning stages of coating delamination are observable in the cold-sprayed sample. Uneven thinning of the coating is also observed. 26
Figure 30: Cold-sprayed Ti_2AlC MAX phase on a Zircaloy-4 flat after rough grinding with SiC papers to a calculated thickness of 50 μm. 27
Figure 31: Collected EDS Spectrum from the plan view imaging of cold-sprayed Ti_2AlC on Zircaloy-4. No evidence of Zircaloy-4 is detected through the coating. 28
Figure 32: Before (l) and After (r) autoclave testing under G2 conditions. The bottom corner of the post-autoclave HVOF coating (top right) separated from the substrate. 28
Figure 33: SEM micrograph of the innermost coating-substrate interface of the thinned, cold-sprayed Ti_2AlC sample. Interface oxidation is readily apparent, and a through-thickness crack in the coating is visible. 29
Figure 34: EDS Spectral maps for Oxygen, Aluminum, and Titanium in the post-autoclave, thinned CS sample. Intensities are mapped as counts per pixel. 29
Figure 35: As-received cross-section of a 4-pass sample. The thinner-sprayed coating has significantly poorer surface roughness and thickness uniformity than the ground sample. 30
Figure 36: Higher magnification examination of a 4-pass sample shows significant intra-coating cracking. However, nearly all cracks are parallel to the interface. An aluminum-rich oxide particle is observed at right, and was likely embedded during an Al2O3 grit blasting surface preparation step before the coating was applied. 31
Figure 37: Higher magnification examination of a 4-pass sample shows significant intra-coating cracking. However, nearly all cracks are parallel to the interface. An aluminum-rich oxide particle is observed at right, and was likely embedded during an Al_2O_3 grit blasting surface preparation step before the coating was applied. 31
Figure 38: Higher magnification examination of the 9-pass sample also shows coating cracks within the externalities of the coating. 32
Figure 39: CS 4p, CS 6p, and CS 9p following removal from the autoclave following a 12h test at 400°C, 1500psi. Yellowing of the coatings is observable. 33
Figure 40: Post-autoclave XRD spectra for the three "thin-sprayed" cold-sprayed Ti_2AlC. The number of passes does not influence phase evolution during the test. 33
Figure 41: SEM image from the CS-4p sample after 12h autoclave testing. It is difficult to discern what oxidation occurred during the test and what was imparted during the Al_2O_3 grit blasting step preceding manufacture. 34
Figure 42: SEM image from the CS-4p sample after 12h autoclave testing. It is difficult to discern what oxidation occurred during the test and what was imparted during the Al_2O_3 grit blasting step preceding manufacture. 34
Figure 43: SEM image from the CS-6p sample after 12h autoclave testing. Only a minor amount of the from-edge oxidation is noted. 35
Figure 44: SEM image from the interior of the CS-6p sample after autoclave testing. A crack in the coating runs from the exposed surface to the interface, and at the junction site interfacial oxidation is observed. 35
Figure 45: The vacuum hot press furnace used for sintering of cold-spray and HVOF coatings. 36
Figure 46: Plan view SEM image of a cold-sprayed sample that was ground down to a nominal 50μm thickness and then sintered 16 hours at 850°C. 37
Figure 47: XRD spectra for the cold-sprayed samples as a function of sintering time and temperature. 37
Figure 48: SEM micrograph of the coating-substrate interface of the Ti_2AlC sample treated at 850°C for 16 hours. Interface oxidation is again less apparent than the non-sintered case, yet still present. 38
Figure 49: Edge-protected SRNL coupons in alumina crucibles prior to furnace sintering. At far right is a crucible of Ti sponge that was also included as an upstream oxygen gettering agent. 39
Figure 50: Edge-protected SRNL coupons after the furnace sintering at 1300°C for 3 hours. All cold-sprayed Ti_2AlC samples are intact, but the HVOF sample has fragmented at the corner. 39
Figure 51: 2D x-ray diffraction pattern and total integrated intensity for the coating side of (l) the sintered cold-sprayed sample and (r) the sintered HVOF-sprayed sample, taken prior to autoclave exposure. 39
Figure 52: Sample coupons mounted and ready for the autoclave test. Samples were edge-protected (EP) and one cold-sprayed (CS) sample was sintered (S) for 3h @ 1300°C prior to autoclave testing. 40
Figure 53: Sample coupons/remnants after the autoclave test. Samples were edge-protected (EP) and one cold-sprayed (CS) sample was sintered for 3h @ 1300°C prior to autoclave testing. This sintered sample did not survive the autoclave test; pictured above is the epoxy that coated its edges. 40
Figure 54: Left and Right edges of an edge-protected sample cross-section. The protective quality of the treatment is mixed – good protection in the image at left, but significant gaps in the image at right. 40

Figure 55: Left and Right edges of an edge-protected sample cross-section following the sintering treatment of 3h @ 1300°C. The cross section makes it plain that edge protection, at least for this sample, was a failure. Significant diffusion between coating and substrate is detected in the sintered sample. 41
Figure 56: 2D x-ray diffraction pattern and total integrated intensity for the coated side of the (l) cold-sprayed sample, and (r) HVOF-sprayed sample after G2 testing. As expected from the differing spray processes, the spectra are not equivalent. 41
Figure 57: Photo of the steam reactor test apparatus used for LOCA conditions. 43
Figure 58: Heating Profile during Reactor Steam Testing. 43
Figure 59: Actual Exposure Time for three test coupons Reactor Steam Testing. 44
Figure 60: Illustration of the analysis method used by SRNL. 44
Figure 61: Relative weight gain for coated and uncoated Zircaloy-4 samples at 1100°C at approximately 240 seconds in steam at atmospheric pressure. 45
Figure 62: Optical Microscope of the edge of HVOF Sprayed Ti_2AlC coated Zircaloy-4 (~450 μm) after LOCA Testing (1100°C, 4 minutes). 46
Figure 63: SEM of a Center-Cut HVOF Sprayed Ti_2AlC coated Zircaloy-4 (~450 μm) after LOCA Testing (1100°C, 4 minutes). 47
Figure 64: SEM/EDS analysis of the interface between a Ti_2AlC HVOF coating and the Zircaloy-4 substrate. 47
Figure 65: High magnification SEM micrograph of oxide layer that forms on the HVOF coating. 48
Figure 66: SEM image of the Ti_2AlC coated Zircaloy-4 sample after oxidation at 1100°C. 49
Figure 67: Low magnification micrograph of Zircaloy-4 with the cold-spray coating after testing at LOCA conditions. 49
Figure 68: SEM/EDS analysis of the interface between a Ti_2AlC cold-spray coating and the Zircaloy-4 substrate. 50

1.0 INTRODUCTION

Cladding coatings are expected to be a significant accident enhancement technology. Coatings have the potential to protect the Zircaloy cladding against major oxidation during Design Basis (DB) and Beyond Design Basis Events (BDBE) and therefore reduce hydrogen generation during these events. The challenge is to find a material and fuel rod application process for that material that can yield a coating that is compatible with the Zircaloy material, including thermal conductivity and thermal expansion. It must yield a coating that can withstand the processes of manufacturing and shipping, and perform well in normal operation, provide accident enhancement during DB accidents and Beyond Design Basis (BDB) accidents. Many coatings and application processes were evaluated during this Discovery Phase of Enhanced Accident Tolerant Fuel (EATF) development and the AREVA Gate Review (GR) process has selected MAX Phase coatings applied by the Cold Spray (CS) process. This material and the application process will be described in detail, along with the work performed to finally arrive at this decision.

Savannah River National Laboratory (SRNL)/University of Wisconsin (UW) evaluated compounds from the MAX Phase class of carbides as a spray-applied coating material to make Zircaloy reactor fuel cladding more resistant to high water temperature and steam conditions. MAX Phase coatings have demonstrated promise to provide increased utility reaction time under accident conditions while having fewer validation requirements than a new stand-alone cladding material. The EATF Discovery Phase goal was to develop MAX Phase coatings and spray technologies for light water reactor (LWR) Zircaloy claddings and then evaluate the effectiveness of these coatings under normal and accident conditions.

2.0 SELECTION OF MAX PHASE CARBIDE POWDERS AND COATING PROCESS

2.1. MAX PHASE CARBIDE POWDER SELECTION

"MAX" is an acronym for a set of compounds with the chemical formula $M_{n+1}AX_n$, where n = 1, 2, or 3, and where M = early transition metal, A = group A element, and X = carbon or nitrogen. In consultation with Drexel University, SRNL selected the carbide powder compounds, Ti_2AlC and Ti_3AlC_2/Ti_3SiC_2 as MAX Phase coating candidates based on their good thermal conductivity, elevated temperature ductility, fracture toughness, weldability, high temperature mechanical stability, chemical stability, and high resistance to chemical attack.

SRNL and UW are using spray methods to produce coatings of a MAX Phase, specifically Ti_2AlC for fuel cladding. Advantages of the sprayed MAX Phase include a relatively high resistance to elevated temperature oxidation, a high thermal conductivity and a coefficient of thermal expansion that is close to that of zirconium.

2.2. SPRAY COATINGS PROCESS SELECTION

Spray coating methods investigated by SRNL/UW included the high velocity oxy-fuel (HVOF) and the CS processes which are discussed in this section along with the results. Following technical and capability evaluations of potential coating vendors, ASB Industries was selected to do the sample coating.

Spray coating methods used by SRNL/UW included the HVOF and CS processes and are described in the Table 1. Difficulties were encountered with the HVOF process both within the coating/substrate and in the spray application method. First, there was discoloration on the back surfaces of the samples, indicating that the Zircaloy-4 substrate had been heated to high temperatures and the composition of the deposited coating was substantially different from that of the original powder. Second, the process sometimes caused energetic combustion of the coating material. In addition, microcracks were observed in the HVOF coatings despite careful handling. Therefore, later work focused on cold-spray coatings.

Cold-spray coatings oxidized less and had lower porosity when using proper CS parameters and techniques (see). Both processes provided good adhesion and durable surface characteristics as shown by good scratch resistance. The results produced to date satisfied all the applicable requirements and goals in the requirements traceability matrix except that of cost. Coating is an additional step and requires additional materials, so it will necessarily increase the cost of the cladding. However, there may be some cost reduction factors related to the total fuel cycle cost with improved safety margin and, for some fuel designs, replacement of current surface treatment processes.

Spray Process	Description
HVOF	Previous successful applications of the HVOF process provided confidence that it would be a viable candidate for the EATF cladding coating application. In this process, the coating material in powder form is injected into the stream from a controlled feeder, where it is heated and accelerated as it is exiting the nozzle. The material stream impacts the work surface to form a solid homogenous coating. The HVOF velocity is much higher than other application methods and results in higher quality coatings in terms of bond, wear, and corrosion.
Cold-Spray	CS is a relatively new process that does not heat up the powders and, therefore, maintains the chemistry of the MAX powders and their superior properties after deposition onto a substrate. CS is a high kinetic thermal energy coating process. It follows the trend of increasing particle spray velocity and reducing particle temperature as with the HVOF process but to a more extreme level. The CS process uses the energy stored in high pressure compressed gas to propel fine powder particles at very high velocities (500 - 1500 m/s). Compressed gas (usually nitrogen or helium) is fed via a heating unit to the gun where the gas exits through a specially designed nozzle (Laval type convergent-divergent nozzle typically) at very high velocity. Compressed gas is also fed via a high pressure powder feeder to introduce powder material into the high velocity gas jet. The powder particles are accelerated and moderately heated to a preset velocity and temperature where on impact with the cladding surface they deform and bond to form a coating. As with the other processes a fine balance of particle size, density, temperature and velocity is important for producing the desired coating properties.

Table 1: Spray Coatings Process.

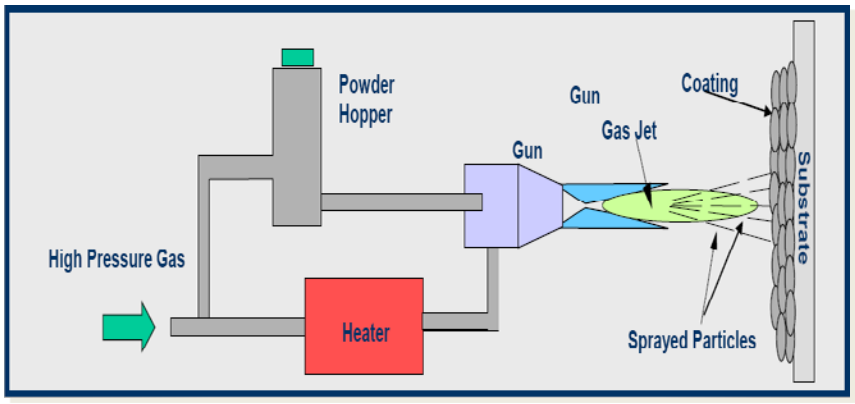

Figure 1: Illustration of the cold-spray process and equipment.

2.3. MAX COATING ZIRCALOY SUBSTRATES FOR PERFORMANCE TESTING

Performance testing was initially done using small coupons to facilitate a wide range of testing before testing of down-selected technologies was performed on tubular coated cladding samples. These material forms are described in this section.

2.3.1. STRIP SAMPLES

A strip of Zircaloy-4 substrate was coated prior to being cut into coupons using electrical discharge machining (EDM) to prevent any compromise to the integrity of the coating. Only one face of the strip was coated and the strip was 0.5 mm thick. Schematics for the coupon size and the actual coupon test assembly are shown in Figure 2 & Figure 3. The surface patterns around the bolts in this photograph suggest a possible effect of the bolted sample holder. Therefore, future oxidation corrosion tests were conducted such that impact from the sample holder were minimized or even eliminated.

The spray equipment deposition parameters were optimized to obtain the desired thickness and density attributes. The spray vendor provided the following MAX powder coated strips (each strip provides 14 coupons):

- 2 HVOF– 450 µm thick coating
- 1 HVOF– 180 µm thick coating
- 2 Cold-Spray – 150 - 200 µm thick coating

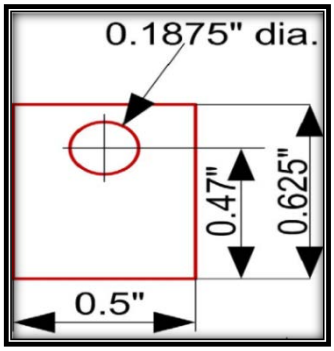

Figure 2: Coupon Size for Corrosion/Adhesion Testing.

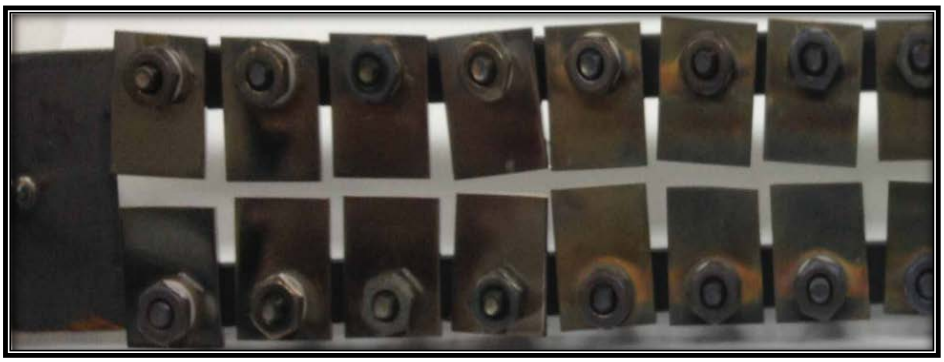

Figure 3: Autoclave Coupon in Holder Post Design for Corrosion Testing.

2.3.2. TUBE SAMPLES

Standard production samples of zircaloy cladding wer supplied by AREVA from their fuel manufacturing plant. A typical sample is shown in Figure 4.

Figure 4: Tube Samples

3.0 CHARACTERIZATION OF MAX POWDER & SPRAY COATED MAX POWDER ON ZIRCALOY SUBSTRATES PRIOR TO PERFORMANCE TESTING

Characterization of the Ti_2AlC spray-coated coupons was developed using Scanning Electron Microscopy (SEM). Also, additional characterization was performed to evaluate the impact that spray coating had on the Zircaloy-4 substrate since it was recognized that application of the coating at high temperature can affect the Zircaloy-4 substrate micro-structure.

3.1. CHARACTERIZATION OF MAX POWDER

MAX Phase powder used in this testing is commercially available and identified as Maxthal 211 Aluminum Titanium Carbide (Ti_2AlC Powder). It is available at a size of d90 = 25 µm / d50 = 10 µm (i.e., 90% of the particles are below 25 µm in size and 50% of the particles are below 10 µm). The particle size distribution (PSD) was measured to confirm the size of the particles and is shown in Error! Reference source not found**.** The PSD was based upon laser light scattering (diffraction) which depends upon analysis of the "halo" of diffracted light produced when a laser beam passes through a dispersion of particles. The lasers were calibrated using ASTM E1458-92 for verification that the laser diffraction particle sizing instrument was operating within tolerance limit specifications. The results of the PSD analysis indicate that over 50% volume was less than 13 µm.

The composition and structure of the MAX powder was characterized using X-ray diffraction (XRD). The XRD patterns are presented in Figure 6. The XRD patterns how that in addition to the Ti_2AlC, the powder consisted of Ti_3AlC_2 and a small amount of TiC. Analysis of a pure substance is required to determine the percentage of each of the components.

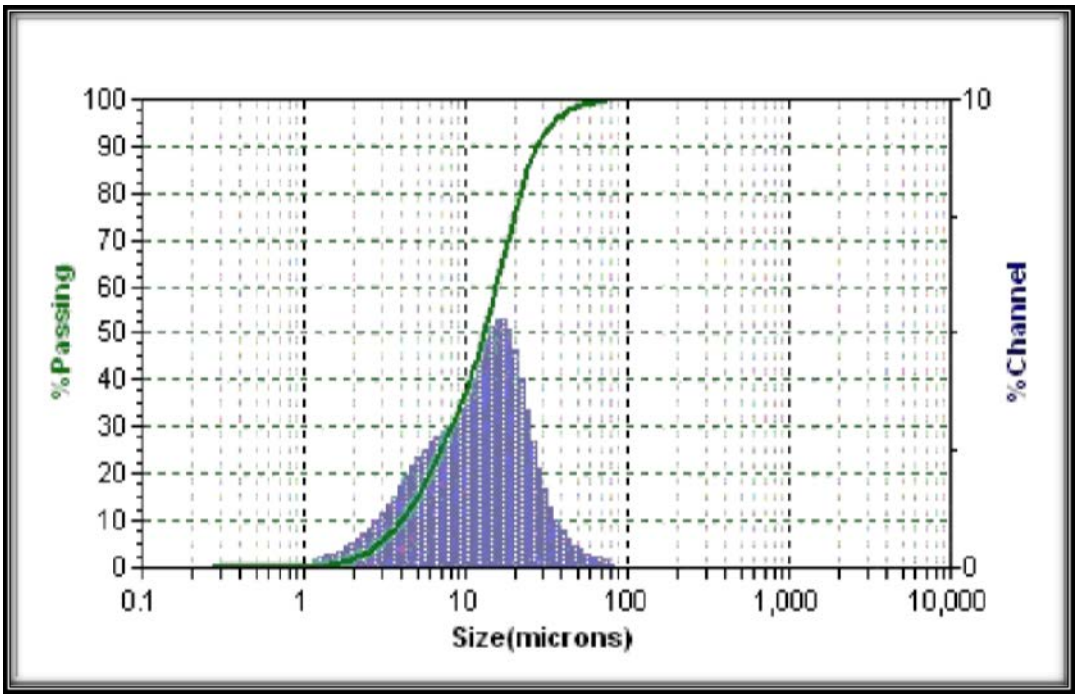

Figure 5: Maxthal 211 Particle Size Distribution (Volume).

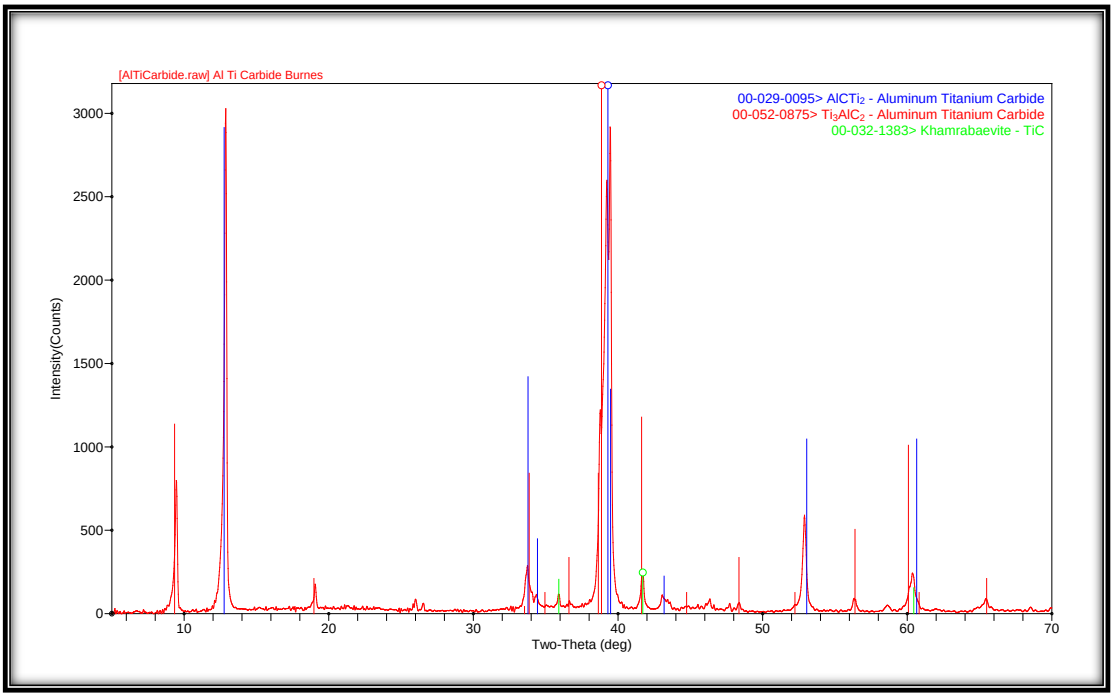

Figure 6: X-Ray Diffraction of Maxthal Powder 211 (Ti_2AlC).

3.2. CHARACTERIZATION OF SPRAY-COATED SUBSTRATES PRIOR TO TESTING

3.2.1. SCANNING ELECTRON MICROSCOPE (SEM) MICROGRAPHS

The Ti_2AlC HVOF and CS MAX coupons were characterized using SEM, by Drexel University under contract to SRNL, and the micrographs are shown in Figure 7, Figure 8 and Figure 9. The top-view SEM micrograph of the HVOF coating shows more porosity in the coating than that of the CS as shown in Figure 7. The cross-sectional SEMs also confirmed that the HVOF process resulted in a more porous coating as shown in Figure 8. Also, Al_2O_3 grains were observed at the interface for both spray processes. The dark spots at the interface, especially visible for the CS sample, are Al_2O_3 grit blast used in surface preparation. Altering the surface preparation technique can minimize the potential of alumina grit entrapment at the interface. Cracks in the HVOF coated samples can be seen at higher SEM magnifications as shown in Figure 9. The XRD patterns in Figure 10 and Figure 11 confirm that the HVOF sprayed MAX coating is mostly TiC with not Ti_3AIC_2 while the CS coatings shows mostly Ti_2AIC and Ti_3AIC_2 MAX Phase powders.

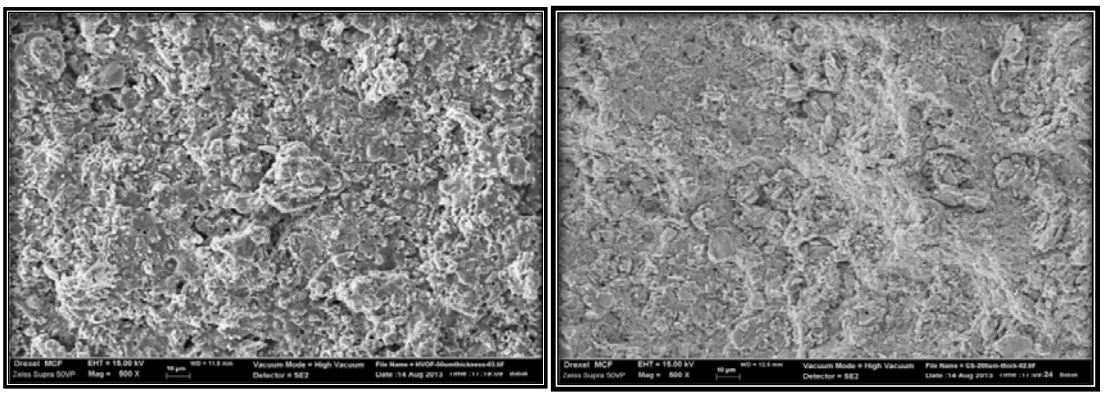

Figure 7: Top-View SEM of MAX Powder (Ti_2AlC): HVOF Spray (180 μm thick) on left and CS (200 μm thick) on right – 500X.

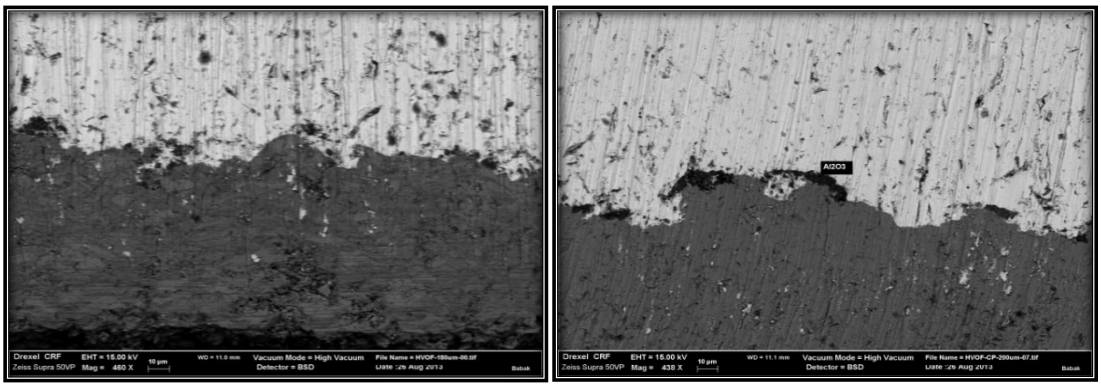

Figure 8: Cross-Sectional View SEM of MAX Powder (Ti_2AlC): HVOF Spray (180 μm thick) on left and CS (200 μm thick) on right. Light grey area is Zircaloy-4 and dark area is MAX.

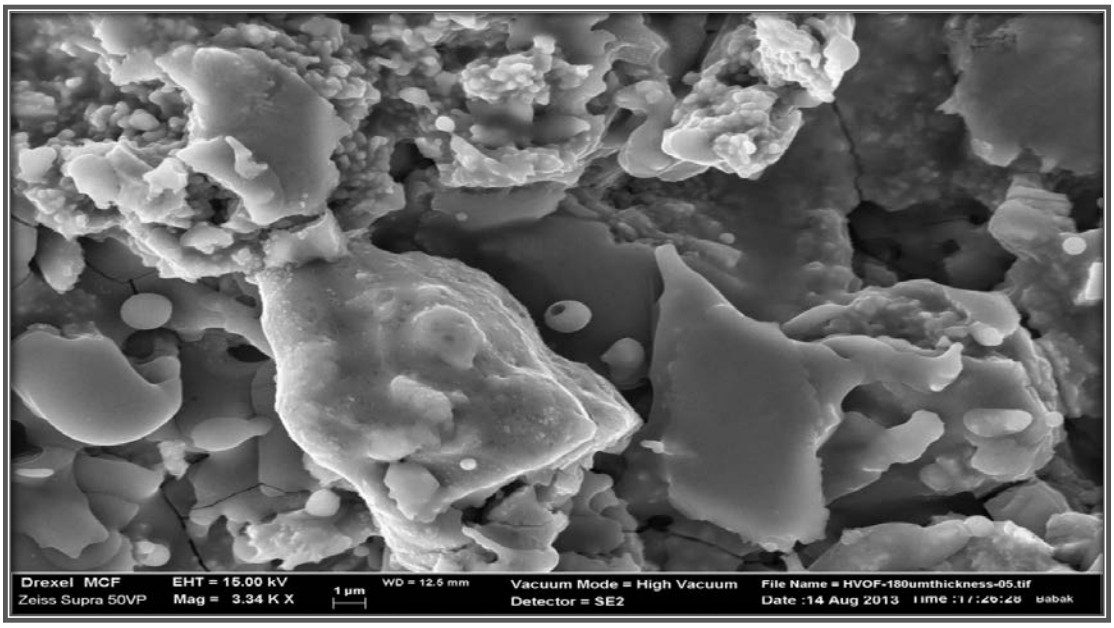

Figure 9: High Magnification (3340 X) Top-View SEM of MAX Powder (Ti_2AlC): HVOF Spray (180 μm thick).

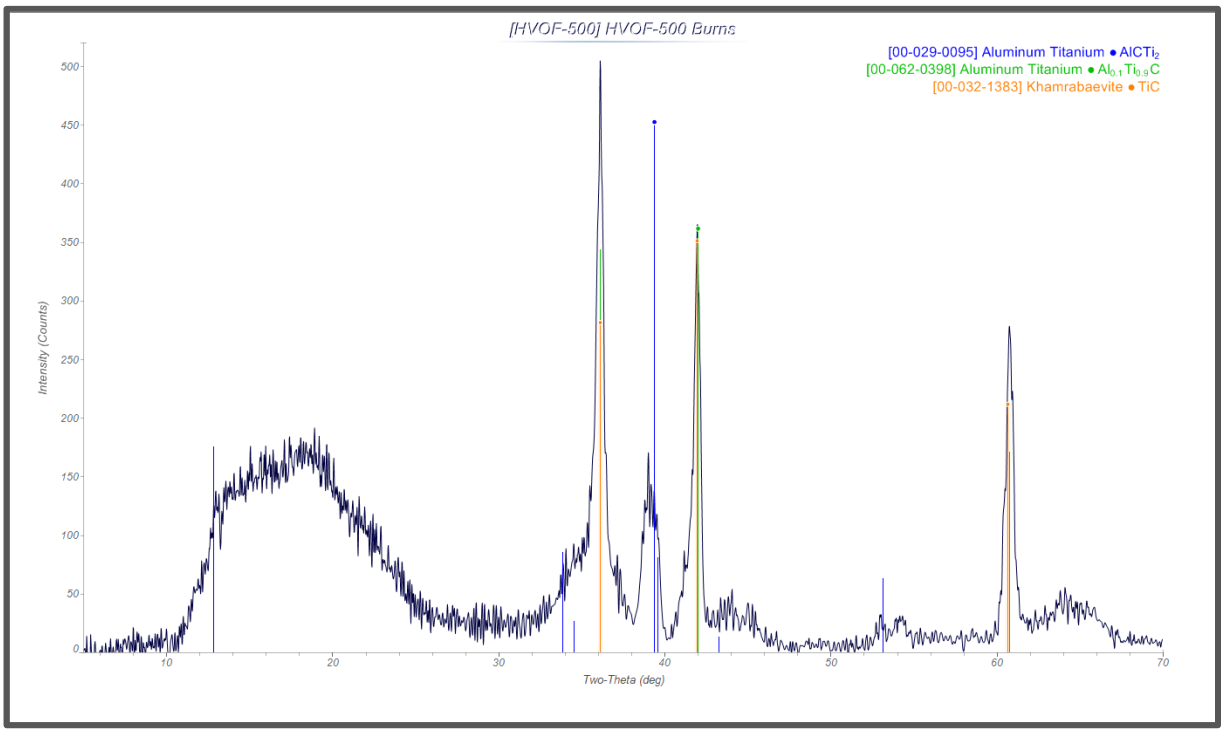

Figure 10: XRD of HVOF MAX Coating (Ti_2AlC).

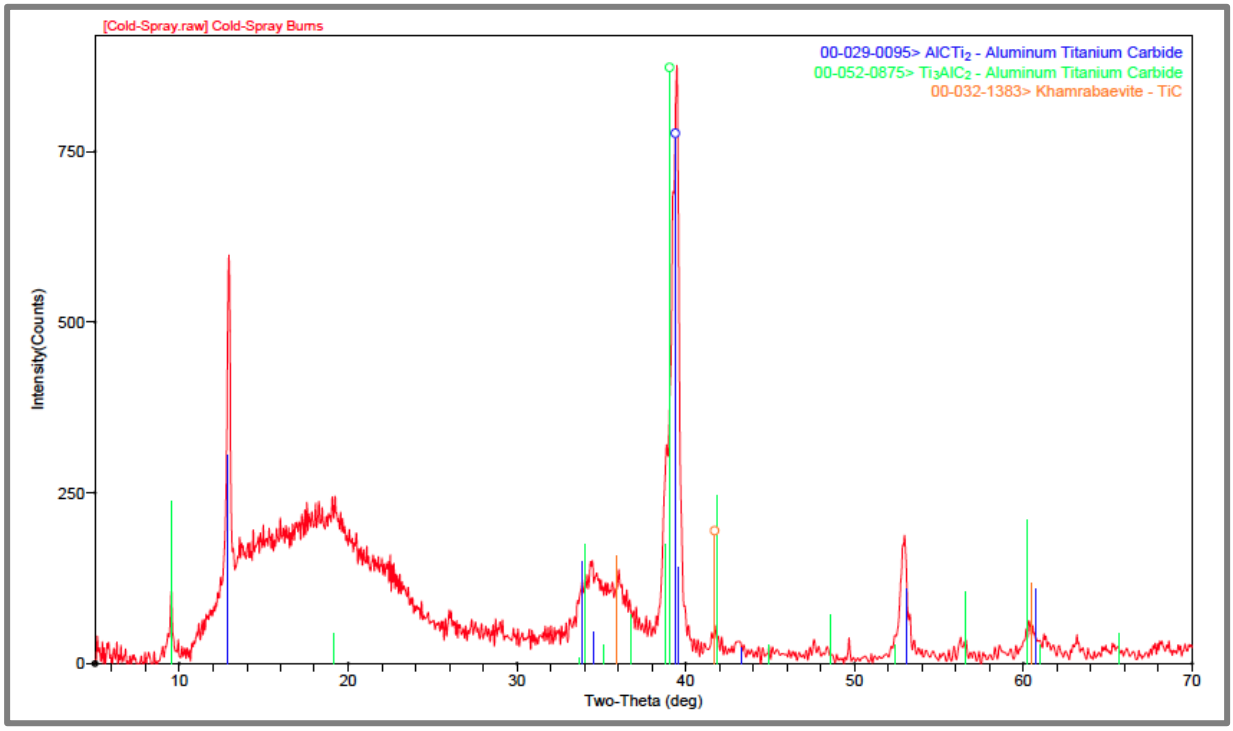

Figure 11: XRD of CS MAX Coating (Ti_2AlC).

In Summary, the presence of Al_2O_3 grains observed at the interface for both spray processes as shown in the figures in this section reveal that the spray coating surface blasting preparation is leaving residual Al_2O_3 at the interface. Future work will ensure that surface preparation techniques are revised to minimize and even eliminate interface/substrate entrapment of Alumina particles.

3.2.2. SURFACE ROUGHNESS

A summary of surface roughness measurements for the HVOF and cold-spray samples is given in Table 2. The surface roughness will impact core pressure drop and heat transfer characteristics in a nuclear reactor along with affecting rod handling, loading, and wear interactions. The measurements in the table indicate that the surface roughness of the coating exceeds current fuel rod design limits which are nominally nearer to the bare sheet sample roughness. Subsequent evaluation will include coating processing to reduce roughness and improved coating thickness uniformity.

Treatment / Coating	Image Zoom	Grid Size	Size X (mm)	Size Y (mm)	R_a (µm)	R_{rms} (µm)
Zircaloy-4 (400 grit)	1	2x2	1.3	0.97	0.4475	0.6186
HVOF MAX	0.5	4x4	2.51	1.87	4.8249	6.1199
CS MAX	0.5	4x4	2.51	1.87	9.2748	11.5865

Table 2: Surface Roughness values for MAX spray coatings, as measured via optical profilometry.

3.2.3. ADDITIONAL CHARACTERIZATION OF MAX SPRAYED SUBSTRATES PRIOR TO PERFORMANCE TESTING

Ti_2AlC coated Zircaloy-4 coupons using CS technology was sent to Drexel University for characterization. The SEM micrographs in Error! Not a valid bookmark self-reference. (a-c) which show the microstructure of a Ti_2AlC cold-spray coating on Zircaloy-4 provide evidence to support the conclusion that there is minimal effect of CS processes on Zircaloy-4 microstructures from the spray process itself. The microstructure of the substrate after coating has a microstructure that is typical for recrystallized Zircaloy-4 that is the as-received, pre-coated condition. Therefore, the CS coating has a minimal effect on the microstructure of the substrate in the bulk. However, it is noted that in Error! Not a valid bookmark self-reference. (a-c) it shows that a dark interface was etched out creating a probable Al-rich layer in the three increasing SEM magnifications.

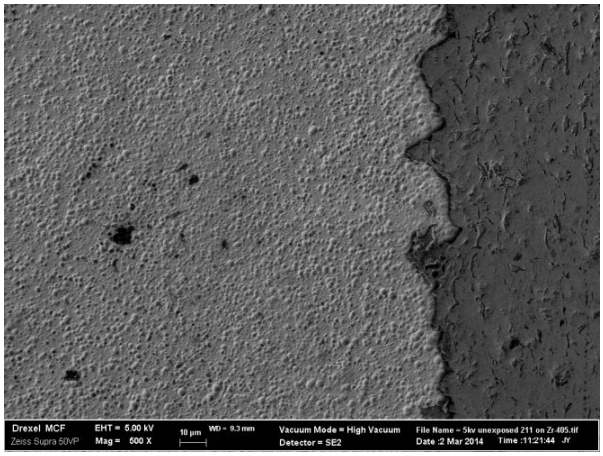

Figure 12: (A) Ti_2AlC / Zircaloy-4 CS – Prior to Testing (Mag. = 500X).

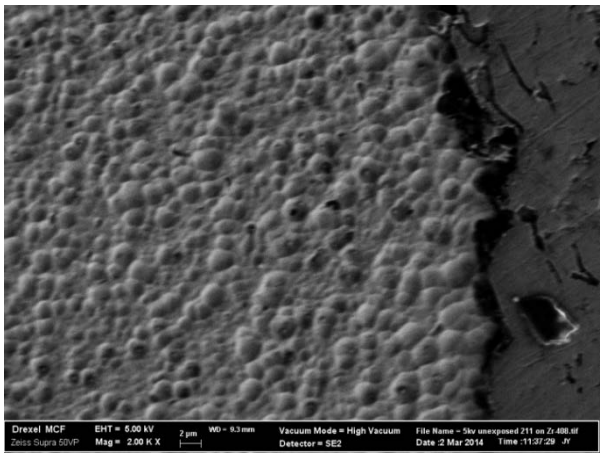

Figure 12: (B) Ti_2AlC / Zircaloy-4 CS – Prior to Testing (Mag. = 2000X). Dark area at the interface is Al-rich layer that was etched out during spraying.

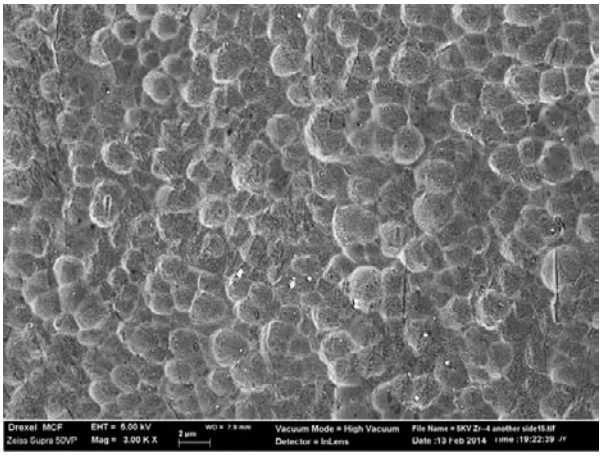

Figure 12 (c): Ti_2AlC / Zircaloy-4 CS – Prior to Testing (Mag. = 3000X). Figure represents Zircaloy-4 after coating and far away from the interface.

3.2.4. THERMAL DIFFUSIVITY IN MAX COATINGS

Maintaining high thermal diffusivity for oxidation resistant coatings on nuclear fuel is important to ensure that they perform normally during normal operation and in accident scenarios. The thermal diffusivity of a 200 micron cold-sprayed Ti_2AlC coating was measured by laser flash analysis. Figure 13 presents the thermal diffusivity comparison of the Ti_2AlC coated sample with literature data for the base Zircaloy-4 alloy and pure Ti_2AlC. Ti_2AlC has a thermal diffusivity that is higher than the base Zircaloy-4 substrate with no coating. The coated sample has a similar thermal conductivity to the literature data for Zircaloy-4. Since thermal resistances in series are additive, the thermal diffusivity for the coated sample must be lower than the base substrate. Therefore, the data in Figure 1 showing similar thermal conductivity is as good as can be expected for a Ti_2AlC coated Zircaloy-4 substrate. These results show that high thermal diffusivity of Ti_2AlC is retained when applied as a coating and likely other MAX Phases have heat transfer properties that allow them to be used as coatings for nuclear fuel with minimal impact on heat transfer.

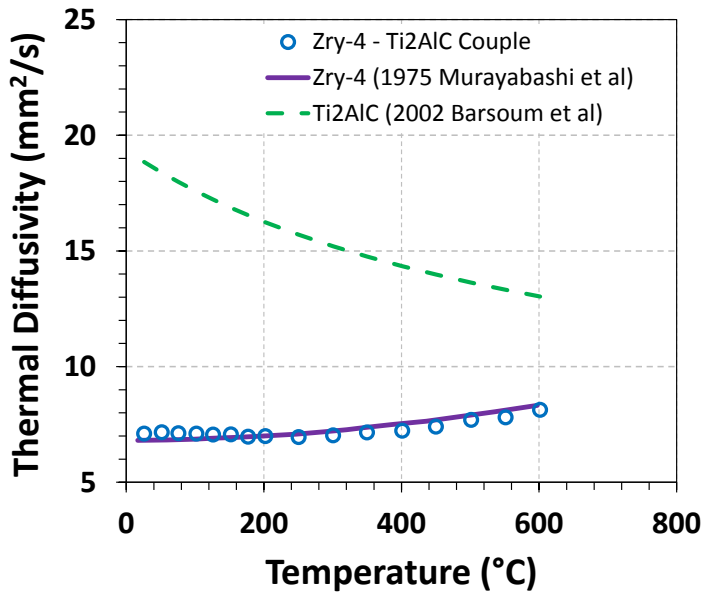

Figure 13: Thermal diffusivity measurements at varying temperature for Ti_2AlC CS spray coated Zircaloy-4.

4.0 PERFORMANCE TESTING - MECHANICAL (PHYSICAL)

Testing of the MAX Phase Ti_2AlC coated Zircaloy-4 substrate was conducted by both SRNL and the UW to characterize the mechanical and performance properties. One of the primary mechanical concerns about coatings is the presence of discontinuities. Discontinuities come in at least three types. First, there could be intrinsic defects, porosity that extends through the entire thickness of the coating. Second, there could be defects that are produced during the life of the fuel, such as scratches and wear. Third, there could be intentional discontinuities. The fuel fabricator could intentionally leave the end plugs and the extreme ends of the cladding tube uncoated. Such a design would allow for a more flexible coating process because the tube could be coated prior to fuel loading which would allow more processing options.

Therefore, evaluation testing of the physical performance is needed to confirm that the future product will meet the nuclear fuel manufacturer's requirements. These evaluations include the following:

- Measurement of cladding coating thickness variations
- Scratch test to confirm the ability of the cladding coating and/or cladding to withstand manufacturing and handling operations and to evaluate the integrity of the cladding coating bonding
- Wearing of the cladding coating and/or cladding due to vibrations and fretting

Wear testing was performed at UW while SRNL performed mechanical adherence testing using a Nanovea Scratch Tester under unirradiated conditions. MAX coatings are designed to perform under conditions of high load and temperature. By using scratch testing it was possible to determine relative coating hardness and resistance to coating damage related to mechanical interactions. In general, coating resistance to any significant penetration is a prime concern. If the coating is breached during rod handling / assembly loading or wear during operation, a path for water to the interface is made with subsequent coating peeling becomes of immediate concern. Information on coating resistance to scratching relative to bare cladding and oxide coated cladding is necessary to address this concern. Most fuel designs have rod to grid contact points that can produce an axial scratch in the rod during loading; this is not a major issue with bare cladding but can be for coated cladding

In general, both HVOF and CS coatings performed well in scratch and wear testing. The initial coatings were considerably thicker (i.e., 200-250 µm) and inherently had a higher mechanical integrity due to the specifics of the coating processes. Additional physical characterization has not been performed on "ground" or thinner sprayed coatings (i.e., 50 µm). Also testing has not been performed on tubes.

4.1. SCRATCH ADHESION TESTING

Scratch adhesion testing assesses mechanical integrity, failure modes, and practical adhesion strength of a specific hard ceramic coating on a given metal or ceramic substrate.

For EATF MAX coatings, the scratch adhesion test measurements were conducted by a technique based upon ASTM C1624. The process of scratching was simulated in a controlled and monitored manner to observe adhesive or cohesive failures and to measure scratch depth versus load. In this application, the Nanovea Mechanical Tester in its micro scratch testing mode was used to measure the load required to cause failure to a MAX coating on a flat Zircaloy-4 substrate. A 20 µm spherical diamond stylus was used at progressive loads ranging from 0.1 N to 200 N to scratch the coating. Initial testing was based upon a progressive increasing load up to this maximum applied pressure.

SRNL and UW are currently working with AREVA to define the maximum pressure that should be anticipated during fuel fabrication including assembly loading, normal reactor operation, and off-normal events. Current planning calls for future testing based on a design-basis scratch of 50 N applied load. The initial testing has shown that the Ti_2AlC MAX coatings applied by both HVOF and Cold-Spray hold up beyond the 50 N design-base scratch load.

SRNL and UW have used initial testing performed on MAX-coated Zircaloy-4 specimens to develop testing protocols. Pictures of the Ti_2AlC MAX-Phase HVOF coated Zircaloy-4 and the cold-spray samples in Figure 14, show six or more scratches at 5 mm lengths. It was determined that the proximity of the scratches to each other (i.e., 1 mm separation) impacted the failure rates of the coatings. Future testing protocols will ensure sufficient separation between the scratches to mitigate scratch tester-induced failures.

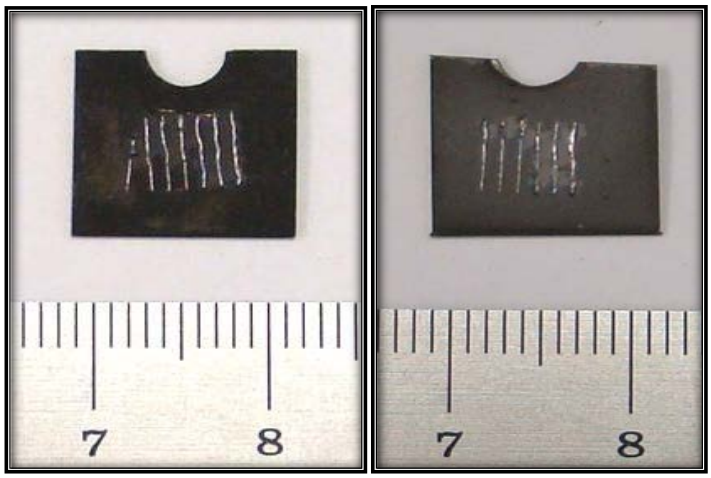

Figure 14: Nanovea Mechanical Tester Initial Testing: Ti_2AlC MAX-Phase HVOF Coated Zircaloy-4 on left and Ti_2AlC MAX-Phase Cold-Spray Coated Zircaloy-4 on right.

For the HVOF-coated Zircaloy-4, the coating appeared to partially spall off about 1/3 of the way through scans that progressively increased loading. This partial spalling is estimated to occur at 66 N based upon the overall range in force from ~0.5 N of force to 200 N. For the cold-spray coated Zircaloy-4, the coating appeared to spall off at a position corresponding to approximately 150 N.

The controlled scratches produced by the abrasion tester can be examined later by SEM to aid in interpretation of the results. Scratch adhesion testing in conjunction with SEM will provide a method of analyzing single-point wear mechanisms of coated systems through an assessment of the deformation and fracture produced.

4.2. WEAR TESTING

Both HVOF and cold-spray coatings performed well in mechanical wear testing. The coatings were considerably thicker than other coatings such as EPD and inherently had a higher mechanical integrity due to the specifics of the coating processes.

Wear testing of each coating type was performed after polishing the as-received coating with 400 grit SiC paper. The polished surface condition is more representative of bulk properties as it removes the large, inherent roughness of the as-coated surface stemming from individual splat geometries. Given the hardness of the Ti_2AlC material, polishing the coating surface prior to wear testing also prevents the surface from artificially degrading the ruby stylus.

No coating failures occurred as a result of 150 N scratch testing or 10 g, 120 minute pin-on-disc wear testing. Wear tracks and scratches observed were minimal for Zircaloy-4 and the polished cold-sprayed Ti_2AlC-coated sample as shown by the test data in Table 3 and in Figure 15. Wear track width and depth as reported were measured using a white-light optical interferometer / profilometer. The profilometer measurements were collected along a circular track at 45° increments with 8 measurements being made ranging between 26.5 µm and 87.3 µm with the average being 47.7 µm for the CS Ti_2AlC coupon. This shows that the CS coating provides 10 times more wear resistance than the present have Zircaloy-4.

Sample	Avg. Width (µm)	Avg. Depth (µm)
AR Zircaloy-4	475.75	4.55
CS Ti_2AlC	47.66	0.41
HV Ti_2AlC	*0	*0

Table 3: Rotating Pin-on-Disc test results for spray-coated samples prepared for the Manufacturing GR. No results could be measured for the sample produced by HVOF spraying. All samples tested with a 10 g load for 120 minutes.

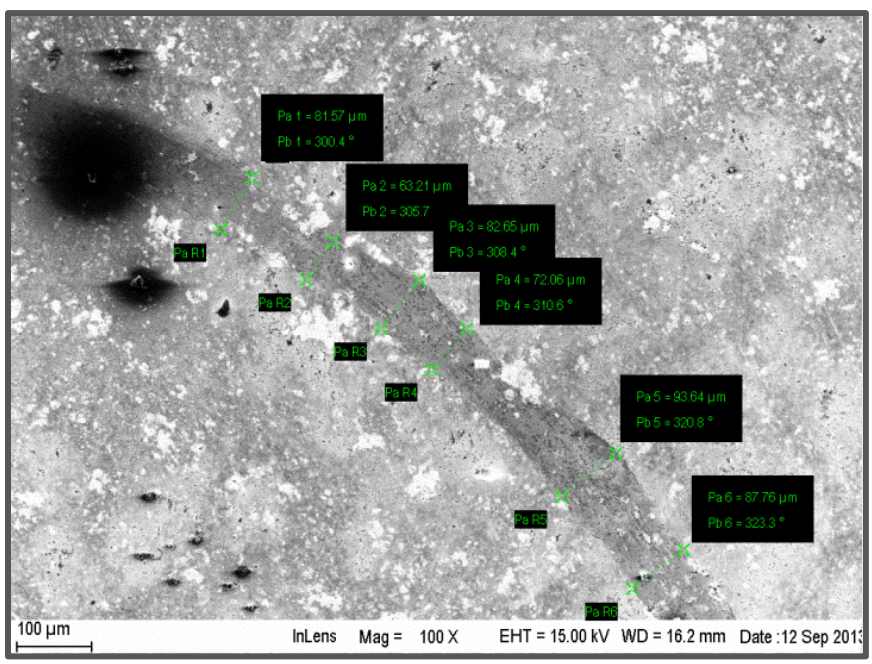

Figure 15: Wear track result for the polished cold-sprayed MAX Phase. Wear tracks were minimal for Zircaloy-4 and the polished cold-sprayed Ti_2AlC-coated sample as shown in this figure.

5.0 PERFORMANCE TESTING – CORRISION/OXIDATION: INITIAL SCOPING TESTS AND EXTENDED OPERATIONAL CONDITIONS (AUTOCLAVE)

Oxidation test conditions and parameters were designed to evaluate short duration accidents such as a large break loss of coolant accident (LOCA) conditions representing a large reactor water coolant line break (i.e., "Large-Break Design Basis Event"). SRNL and UW collaborated with AREVA to define temperature, pressure, and time of exposure test parameters for design basis (Large break and Small break LOCAs).

Initial scoping tests of the Ti_2AlC coated coupons, described in Section 5.1, were conducted under supercritical conditions (500°C water at 3600 psi in 144 hours) to accelerate oxidation without a reference point of when the coating would fail. After these initial tests, AREVA directed that testing be conducted at ASTM G2 conditions (400°C and 1500 psi in 72 hours). Tests at G2 conditions, described in Section 5.2, were used to evaluate cladding coating performance under normal operating conditions. Tests at LOCA conditions representing large DBE are discussed in Section 6.0.

Subsequent testing at G2 conditions was driven by recommendations resulting from the GRs and follow-on biweekly AREVA-led team conference calls after Phase I Testing was completed. Table 4 includes the recommendations on future MAX Phase testing parameters from the Manufacturing GR held on 20 September 2013. A schematic of the progression of MAX Phase testing at G2 conditions is shown in Figure 16.

Topic	Concern	Recommendation
Coating Thickness	HVOF and cold-spray coatings are typically around 200 µm thick. The desired range thickness is around 25 microns. Reducing coating thickness is necessary because the coating has a neutronics penalty. In addition, the thickness means that the coating takes up a substantial volume in the core of a reactor and will affect the thermal hydraulic performance of the fuel assembly.	The coating thickness must be dramatically reduced from typical commercial thicknesses. Coatings are to be ≤ 50 µm
"Roughened" Surface forming metallurgical bond	The surface of the Zircaloy-4 surface is also roughened by the application of the coating material. Therefore, the coating must fill in these peaks and troughs and this sets the minimum coating thickness. It is also possible that water or steam penetrates through the coating resulting in oxidation at the clad- coating interface which then causes delamination.	Roughening of the substrate provides a mechanical bond with the coating, but a metallurgical bond is needed to prevent steam oxidation of the substrate.
Coated Zircaloy Discoloration	HVOF coated coupons of Zircaloy-4 sheet showed discoloration on their uncoated faces. The discoloration suggests that the substrate reached a relatively high temperature, and its heat treatment may have been affected.	The effect of the coating process on the microstructure of the substrate should be investigated. Annealing or phase change in the substrate is not desirable.
SPRAY Method	HVOF coatings do not perform well and the coating process has safety concerns	Work should focus on CS applications.
Oxidation of Substrate	It is important to understand whether oxidation of the substrate is caused by penetration of steam or water through the coating or by transport under the coating from the edges. This question can be answered by metallography of a lightly oxidized sample.	Metallography should be performed on samples after oxidation testing to evaluate diffusion of oxygen beneath the coating.

Table 4: Manufacturing GR Recommendations.

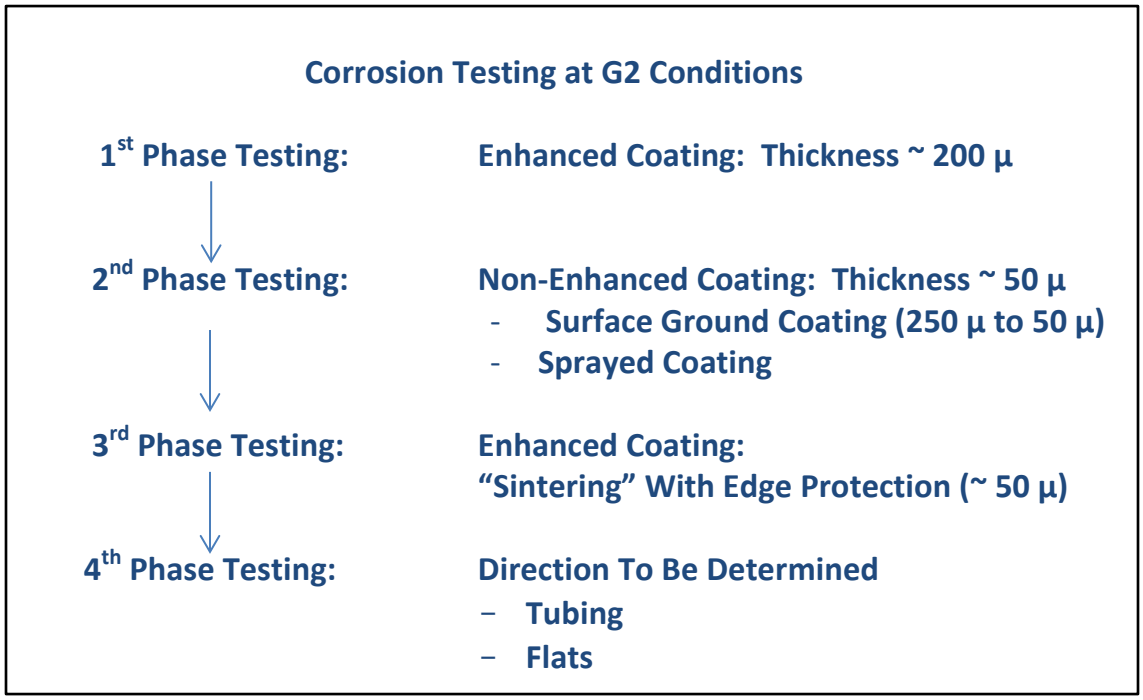

Figure 16: Autoclave Corrosion Testing Sequence @ G2 Conditions (i.e. Extended Operating Conditions).

The rationale behind the thickness of MAX Phase coatings was changed after the initial scoping tests and 1st Phase testing as the AREVA Team recognized that some of the concepts under consideration for the EATF coatings come with penalties that offset the benefits. Some of the penalties to employing coatings included:

- Reduction in the overall thermal conductivity,
- Thick coatings will displace a significant volume of water in the fuel assembly design and result in an increased flow resistance and increased pressure drop through the core, and
- Impact on reactor neutronics

AREVA directed that the coating thickness be reduced to a maximum of 50 µm after the initial and 1st Phase testing. The testing was driven by conclusions from the GRs and the recommendations resulting from the reviews. Other recommendations from later reviews included a recommendation for "edge protection". This recommendation was made so that it could be understood whether oxidation of the substrate is caused by penetration of steam or water through the coating or by transport under the coating from the edges.

5.1. INITIAL SCOPING TESTS

Initial corrosion/oxidation scoping tests of Ti_2AlC MAX-coated Zircaloy-4 were conducted in a pressurized autoclave system at supercritical conditions. The rationale behind the initial process parameterizations was to accelerate oxidation without a reference point of when the

coating would fail. However, the supercritical conditions chosen (144 hours, 500 °C, 3600 psi) were not representative of nuclear reactor design-basis accident environments. Subsequent testing was designed to be representative of both accelerated operating conditions and design-base accident environments.

In the initial scoping tests, three coupons were tested: Ti_2AlC MAX-Phase Cold-Spray coated Zircaloy-4 and HVOF- coated Zircaloy-4, and uncoated as-received Zircaloy-4. Standard purified water was used, with approximately 5-7 ppb dissolved oxygen. A single sample was chosen from the each of supplied HVOF and cold-spray Ti_2AlC coatings, and a sample of untreated, as-received Zircaloy-4 from AREVA was included as a reference.

Images of the coated materials subjected to these tests are provided in Figures 17-21. Figure 17 shows the exposed coatings (top 2 from left to right) and the uncoated Zircaloy-4 coupons and compares them to the bottom unexposed coated coupons. From all the figures, it is apparent that at prolonged supercritical conditions failure will occur on both the coated and uncoated sides of the Zircaloy-4 substrate. More realistic extended operating conditions that are characteristic in actual reactor operations and LOCA conditions were defined later by AREVA. In Phase 1 Testing, these conditions were implemented.

In summary, though the initial scoping tests revealed poor corrosion results after 144 hours at 500°C and 3600 psi, the high pressure may have been a significant factor that accelerated corrosion. The very high pressure would enhance the water permeation at the clad-coating interface and may be the primary reason for the poor corrosion resistance resulting in accelerated oxidation at the interface which then caused the delamination shown in the figures in this section. Future test designs can be made to determine the impact of various factors on the coating performance including reactor pressures. Therefore, this section should be used for information only at this point and not used in determination of the performance of MAX coatings.

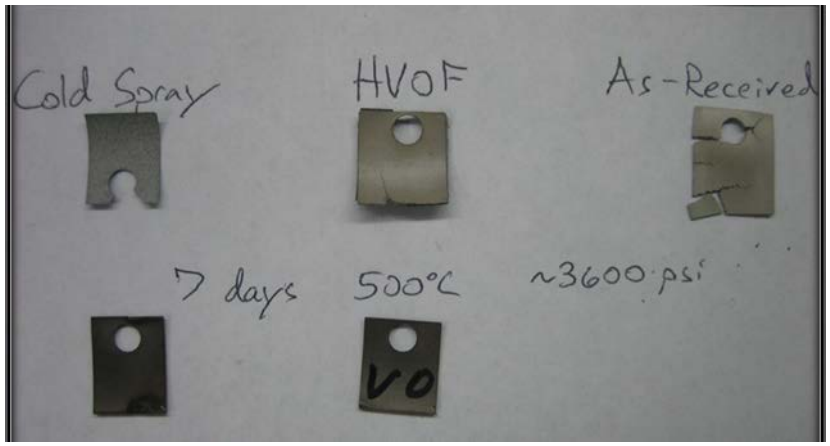

Figure 17: University of Wisconsin Corrosion/Oxidation Testing at supercritical conditions (144 hours, 500 C, 3600 psia); Top 3 coupons after testing: Ti_2AlC MAX-Phase Cold-Spray coated Zircaloy-4 and HVOF- coated Zircaloy-4, and uncoated Zircaloy-4, labeled “As-Received”. Bottom 2 coupons are coated coupons prior to test.

Figure 18: The cold-sprayed Ti_2AlC coating, HVOF-coated sample (both coating and substrate), and attached portion of the Zircaloy-4 control sample, as removed from the autoclave following conclusion of the 7-day test. The cold-sprayed Zircaloy-4 substrate and the control Zircaloy-4 substrate were later retrieved from within the autoclave test section.

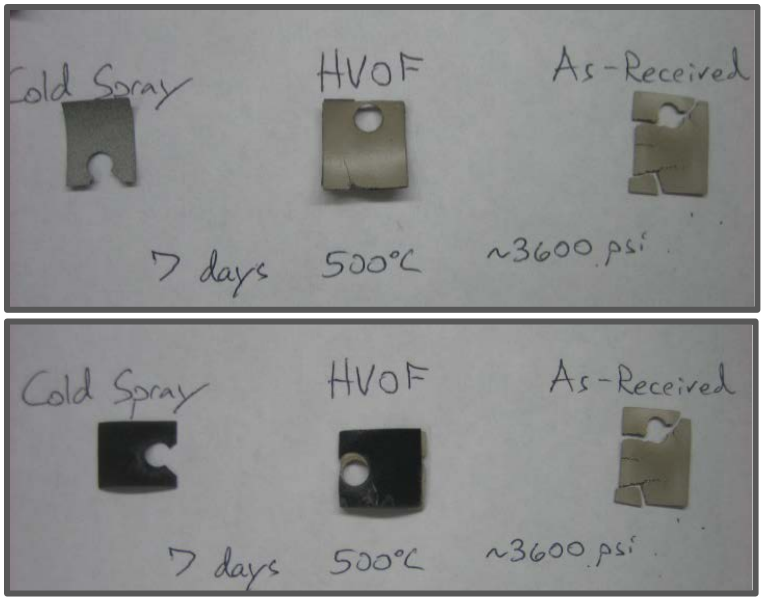

Figure 19: Front and back of samples removed from the autoclave after the 7-day test. The chip in the CS coating above the hole is due to handling after removal from the autoclave. The HVOF-sprayed Zircaloy-4 is discolored relative to the control. A grey splotching is observed on the back of the delaminated coatings. The control sample was not flipped over to image its backside.

Figure 20: "Reassembled" Zircaloy-4 substrate previously coated with cold-sprayed Ti_2AlC, following the 7-day, 500°C, 3600 psi exposure to pure water. At left is an untested coupon with the cold-sprayed Ti_2AlC coating.

Figure 21: Side view of the HVOF sample illustrating the delamination and curvature of the sample. The samples as received from SRNL were not flat, but were also not as curved.

All substrates show oxide growth on all sides and cracks emanating from substrate edges. Using the autoclave for the G2 tests, it is not clear at what testing time the delamination of the coating from the substrate occurred. The root cause of the delamination could not be definitively determined, but potential reasons for delamination include: 1) the natural growth of the oxide layer on the substrate, 2) dissolution of the adhesion layer between the coating and the sample, and 3) thermal expansion stresses. Natural growth of ZrO_2 would indicate that the coatings did not provide any protection to the substrate in the tested condition, either due to coating imperfections or formation of non-protective TiO_2 instead of Al_2O_3.

The following figures**,** Figures 22-24**,** show the exposed HVOF coated MAX powder (Ti_2AlC) coupons characterized in both top and cross-sectional SEM micrographs by Drexel University under contract to SRNL. The cross-sectional SEM micrographs revealed that both the uncoated and coated sides of the Zircaloy-4 substrate were heavily oxidized, and even to a greater degree on the coated side. The top-view SEM micrograph for the HVOF coating shows formation of oxides (lighter portions) and high porosity in the coating surface.

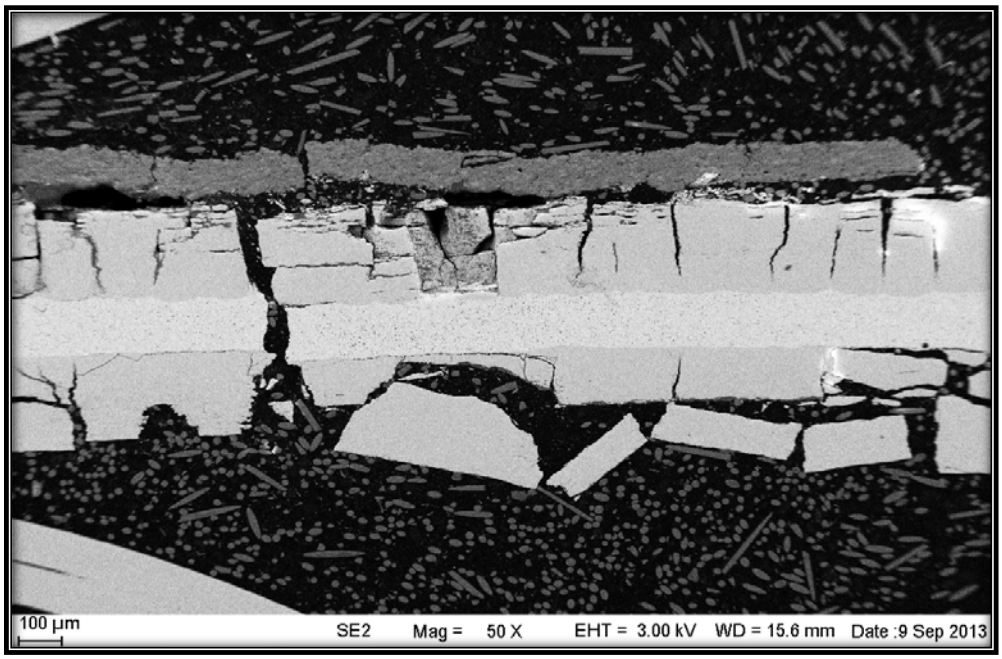

Figure 22: Cross section image of exposed HVOF coated MAX powder (Ti_2AlC) coupon @ 500 C, 3600 psia, 144 hrs, characterized in cross-sectional SEM micrographs by Drexel University. A slightly thicker Zircaloy-4 layer is underneath the coating than on the other side.

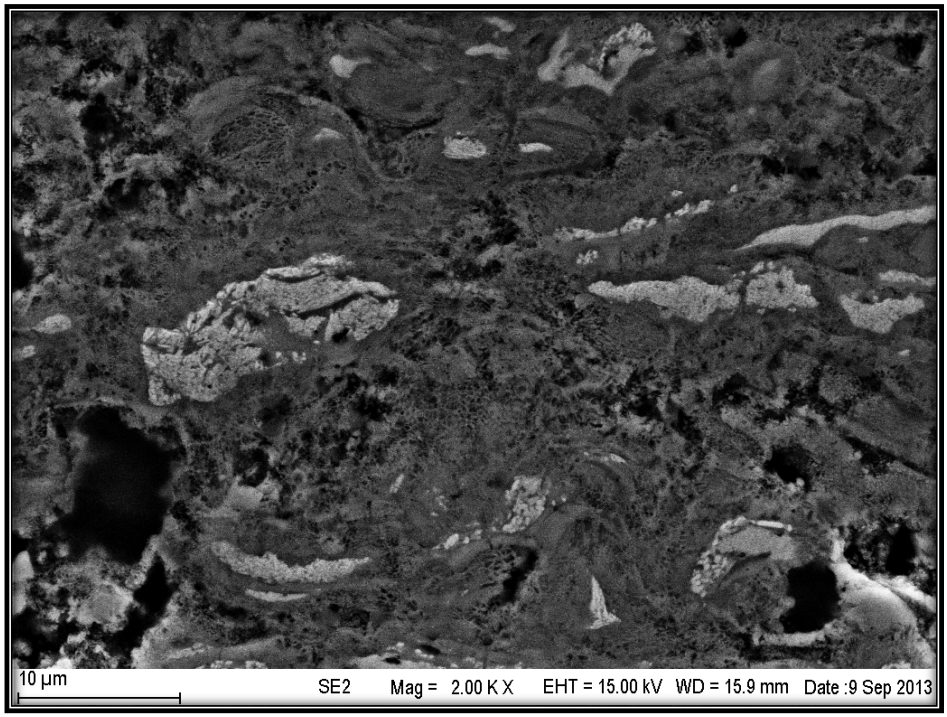

Figure 23: Exposed HVOF coated MAX powder (Ti_2AlC) coupon @ 500 C, 3600 psia, 144 hrs, characterized in top view SEM micrographs by Drexel University.

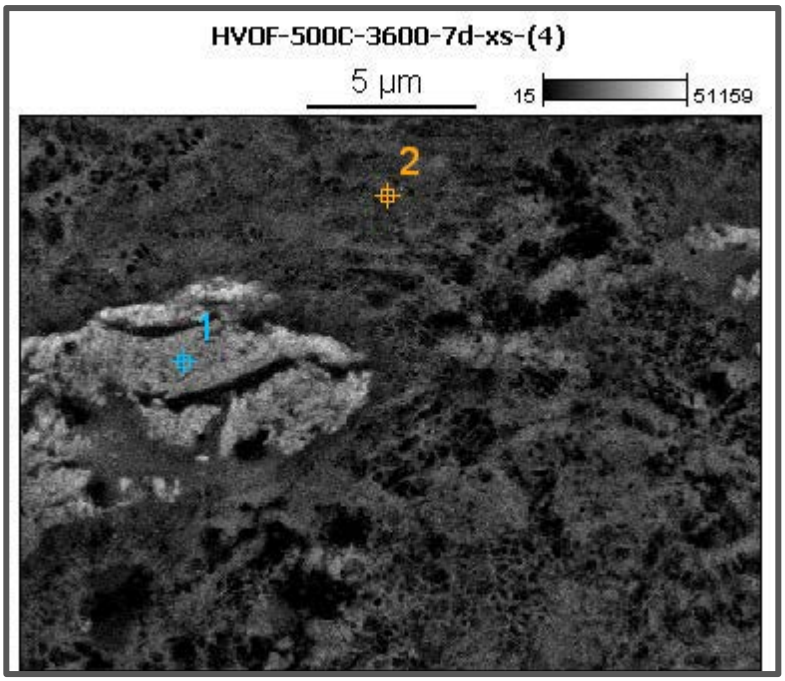

Figure 24: High-magnification micrograph of the HVOF-sprayed MAX Phase indicating the EDS regions studied. The dark grey regions are a mixture of TiO_2 and Al_2O_3 oxides, while the light grey sections are un-oxidized Ti_2AlC. The black regions are voids / epoxy resin.

It was expected that the MAX Phase coatings will improve the resistance of the Zircaloy substrate to the corrosive conditions of the autoclave, as Ti_2AlC has been shown to form a coherent, protective Al_2O_3 oxide layer in high-temperature oxidizing environments. However, in this autoclave exposure this benefit was not realized. Delamination of both HVOF and CS coatings occurred, resulting in exposed Zircaloy substrate, with delamination of the cold-sprayed sample being more severe than in the HVOF-sprayed sample. The cold-sprayed Zircaloy-4 substrate completely separated from the sample holder, while the HVOF-sprayed coating remained lightly attached to its substrate above the mounting screw. The control Zircaloy-4 sample also broke off of the sample holder during the test. Both MAX Phase coatings were quite brittle and exhibited grey spots on the coating side that was previously attached to their respective substrates, which was confirmed by EDS to be remnant substrate material. In Figures 25-26, EDS analysis of the HVOF coating in cross section shows that it has oxidized considerably, and XRD spectra of both coatings confirm there was a significant change in the coating composition during the test.

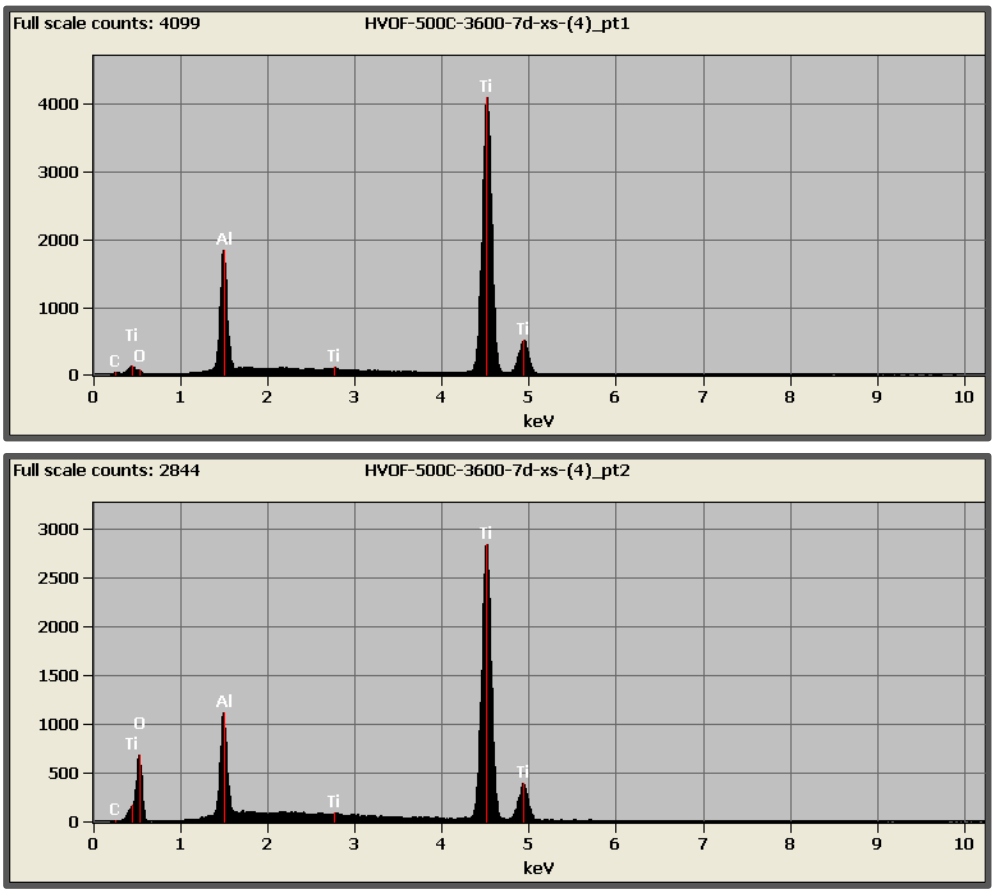

Figure 25: EDS spectra for the light grey (top) and dark grey (bottom) portions of the HVOF-sprayed MAX Phase. The top spectrum is consistent with un-oxidized HVOF-sprayed MAX Phase, while the bottom spectrum is indicative of the presence of some mixed oxide.

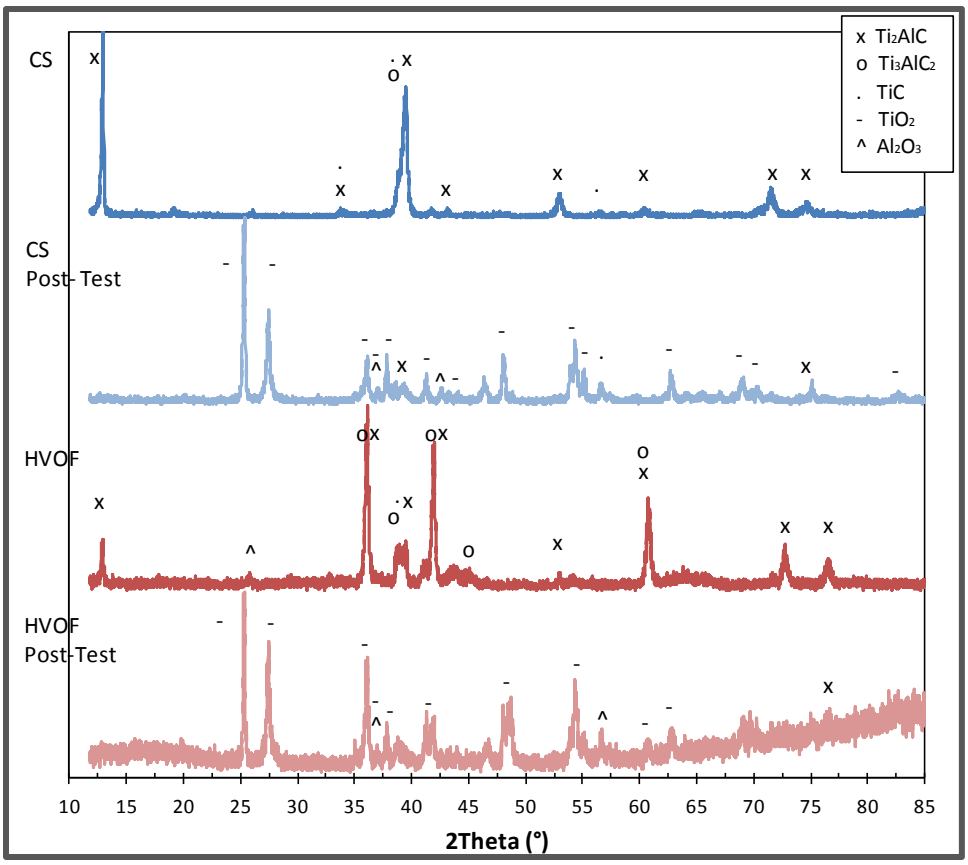

Figure 26: XRD spectra of the MAX Phase coatings before and after the 7-day test. The HVOF coating (bottom middle) begins with considerably more TiC phase present (36, 42° peaks) than Ti_2AlC (13, 40°)–in other words, CS (top) deposits a truer Ti_2AlC MAX Phase coating. Both coatings are significantly altered during the test.

5.2. REACTOR OPERATIONAL TESTING – ASTM G2 CONDITIONS

5.2.1. 1ST PHASE TESTING – ENHANCED COATING: THICKNESS ~ 200 µ

In the first phase of testing, as with the supercritical condition exposure, one sample from each group was tested at ASTM G2 conditions because of the limited number of coated coupons available for future testing. Therefore, this testing is considered exploratory and further testing is recommended and needed for repeatability purposes. The G2 conditions of 400°C and 1500 psi are considerably more representative of normal operating reactor conditions than the supercritical conditions used in the preliminary test. The coatings were optimized in that the thicknesses prior to testing were an approximate average of 200 µm thick and the size of the Ti_2AlC powder particles used to coat were an average of 13 µm as shown in Figure 27.

Again, it was expected that the thermal spray coatings would serve in a protective manner, preventing oxygen from reacting with the substrate zirconium. Unlike the supercritical test, only the HVOF sample delaminated, and it did not disconnect from its substrate until it was being weighed after the test. No samples fell off of the sample

holder during the test, and no debris was generated inside of the autoclave as a result of Zircaloy-4 cracking / pulverizing. After removal and separation, the HVOF-sprayed coating was found to be as brittle as after the supercritical test. Also, as was with the supercritical water test, the previously-covered Zircaloy-4 interface was lighter than the fully-exposed backside.

SEM imaging in Figure 27, Figure 28, and Figure 29 of sample cross sections has determined that the interfaces of all samples have begun to oxidize, including the innermost regions of the interface between the CS coating and the Zircaloy-4. Table 5 shows that oxide thickness measurements of the sprayed surfaces are oxidizing at a rate higher than the unsprayed test coupon, with the HVOF-sprayed sample oxidizing more than the CS sample. The unsprayed side of the HVOF sample is also oxidizing more rapidly than the unsprayed test coupon, though this is not true for the CS sample. These observations are consistent with the observations made of the supercritical condition samples. Mass change measurements, shown in Table 6, suggest that more oxidation (of MAX and/or base material) is observed on the sprayed coupons as opposed to the bare control sample. However, this does not discriminate between oxidation of the coating and that of the base material.

Sample	Coated Side (if applicable) (µm)	Not Coated Side (if applicable) (µm)
Zircaloy-4 ZrO2 layers	--	1.4 ± 0.5
HVOF-sprayed Zircaloy-4 Oxide layer	4.2 ± 1.3	2.3 ± 0.4
Cold-Spray Zircaloy-4 Oxide layer	3.1 ± 0.9	1.4 ± 0.3

Table 5: Measured oxide thicknesses of various surfaces after 3 days of 400°C, 1500 psi steam exposure. Measurements collected are based on point-to-point interpolations within SEM imaging software, with minimum 5 measurements per reported quantity.

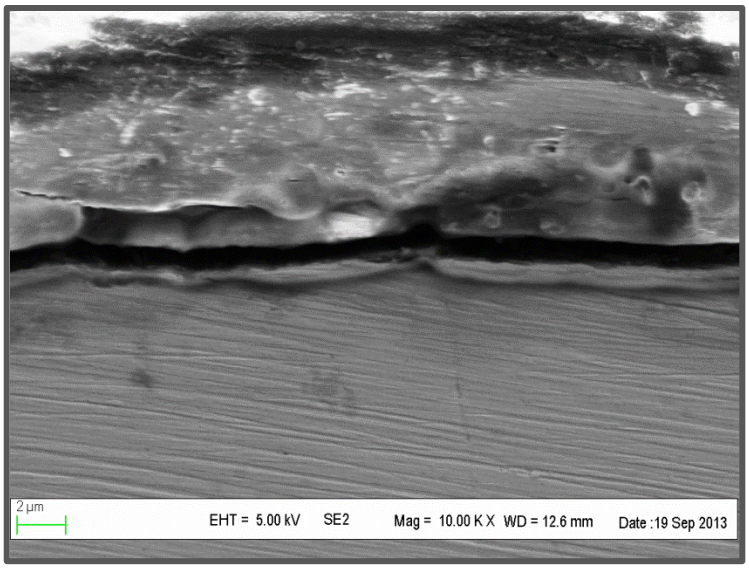

Figure 27: The oxide layer present on the unsprayed test Zircaloy-4 coupon is small.

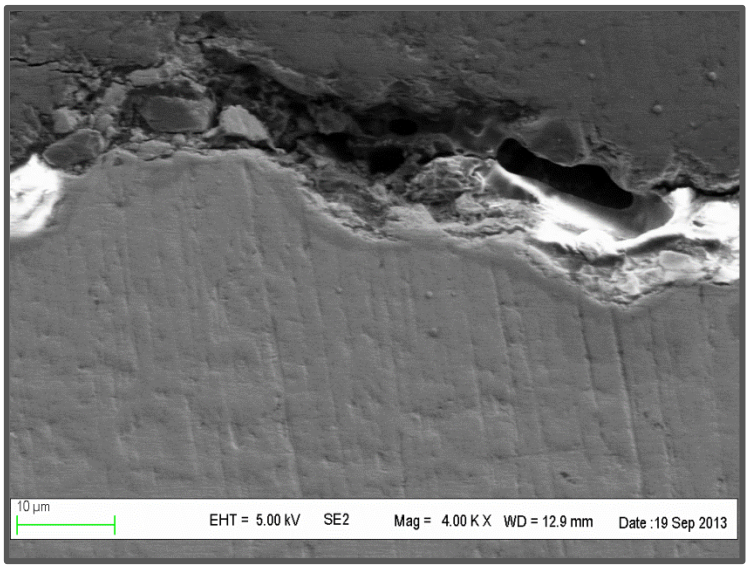

Figure 28: The interface between the cold-sprayed MAX Phase and the Zircaloy-4 substrate is oxidizing despite presence of the external layer. Evidence of preliminary steps towards coating delamination is visible.

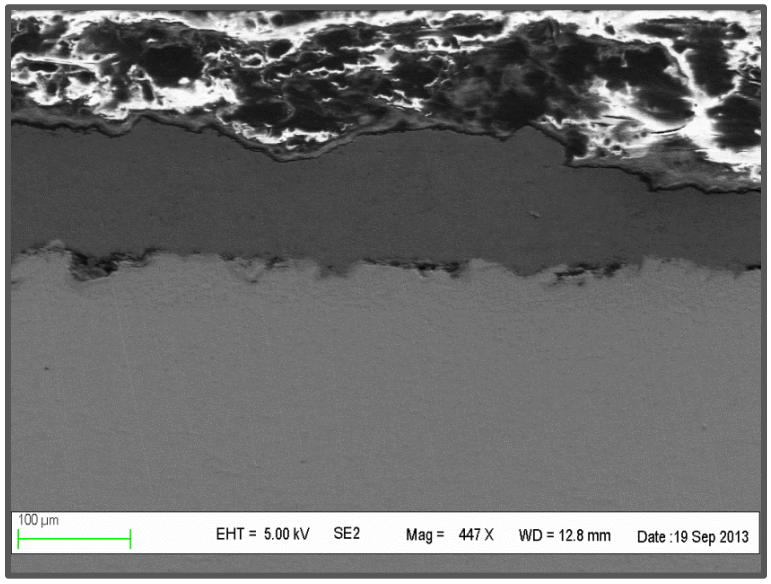

Figure 29: Beginning stages of coating delamination are observable in the cold-sprayed sample. Uneven thinning of the coating is also observed.

Sample	Pretest (g)	Post-test (g)	Delta (g)
SRNL Cold-Spray MAX	0.6373	0.6445	0.0072
SRNL HVOF MAX	0.6166	0.6209	0.0043
UW Zircaloy-4 Control	0.6892	0.6898	0.0006

Table 6: Mass measurements of the three ASTM G2 condition samples. The higher weight gain of the sprayed coupons is not surprising given the capability of the coating to oxidize and the high free energy of formation for both TiO_2 and Al_2O_3.

5.2.2. 2ND PHASE TESTING – COATING: THICKNESS 50 µ, AVG

The coating thickness of the initial samples received from SRNL in July 2013 for autoclave testing were considerably thicker than the 50 µm maximum thickness recommendation currently in place, which was specified after the September 2013 GR. Two approaches exist to reduce the thickness of the sprayed MAX-Phase coating: a) grind away portions of thick coatings until the coating thickness is within tolerance; or b) spray thinner coatings.

Each approach has positive and negative aspects. Grinding of thicker coatings will likely be expensive and generate a significant waste stream at an industrial scale. However, because coating accumulation is a successive, layer-by-layer process, the first layers to deposit, the ones that remain after grinding, are the stronger and denser layers compared to the outer layers. The increased strength and density may confer an increase in coating protectiveness compared to coatings sprayed to be under 50 µm thickness, as the final layer on the thinner-sprayed coatings will not have been subjected to the impacts and compaction as the underlying layers. Samples of the targeted thickness were produced using both methods and tested at UW-Madison.

5.2.2.1. SURFACE GOUND COATING: 50 µ, AVG THICKNESS

The coating was ground to 50 µm thickness with the SEM image shown in Figure 30 and was monitored at three points along its curvature at a resolution of 0.1 µm. Ground coatings were then imaged in the SEM to verify that the substrate was not visible through the coating, as shown in Figure 31.

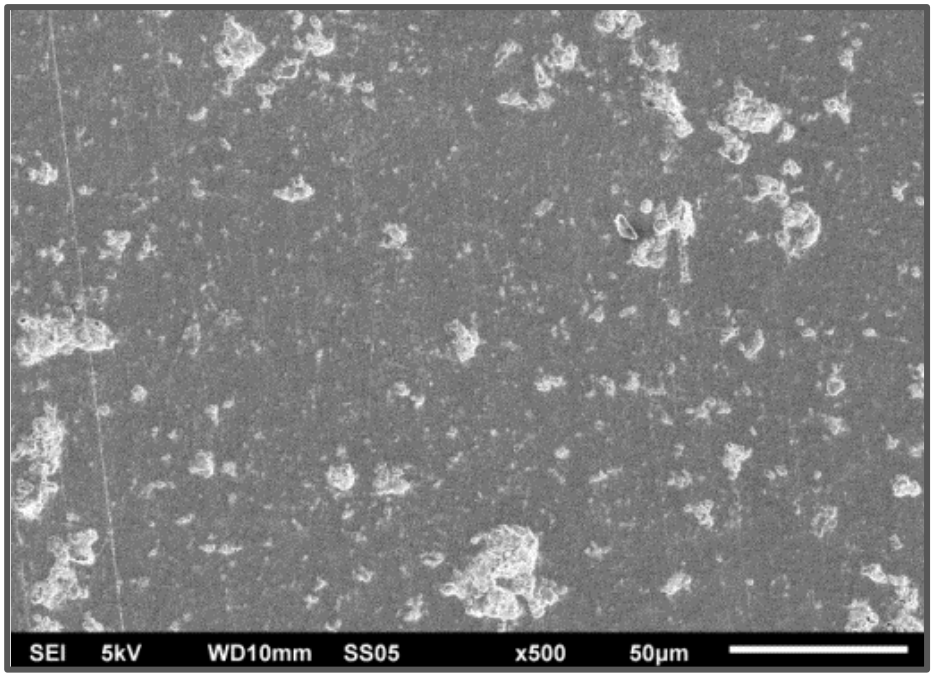

Figure 30: Cold-sprayed Ti_2AlC MAX Phase on a Zircaloy-4 flat after rough grinding with SiC papers to a calculated thickness of 50 µm.

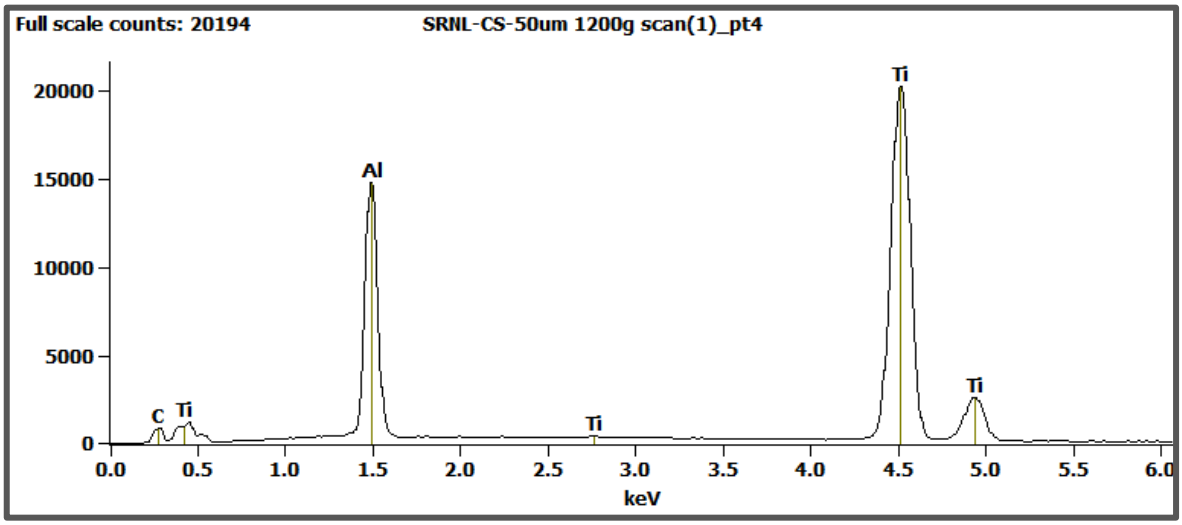

Figure 31: Collected EDS Spectrum from the plan view imaging of cold-sprayed Ti_2AlC on Zircaloy-4. No evidence of Zircaloy-4 is detected through the coating.

After G2 testing, HVOF coatings remained monolithic, embrittled, and delaminated from the Zircaloy-4 substrate as shown in Figure 32. A cross-sectional image taken near the CS sample midpoint (Figure 33) reveals the density of the ground coatings. There are no cracks running in the plane of the coated MAX Phase. The average coating thickness pictured is 49 ± 3 µm MAX Phase material. However, there are cracks running through the coating thickness, and oxidized regions are clearly visible. Future spray coating work will employ techniques to minimize the impact of grit blasting with the resulting entrapment which should optimize interface quality.

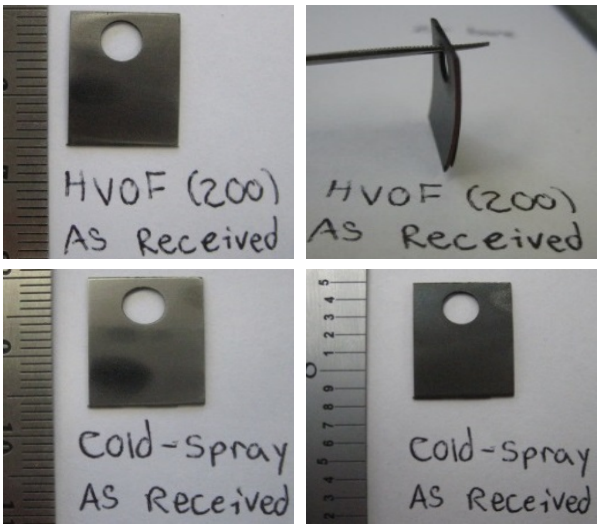

Figure 32: Before (l) and After (r) autoclave testing under G2 conditions. The bottom corner of the post-autoclave HVOF coating (top right) separated from the substrate.

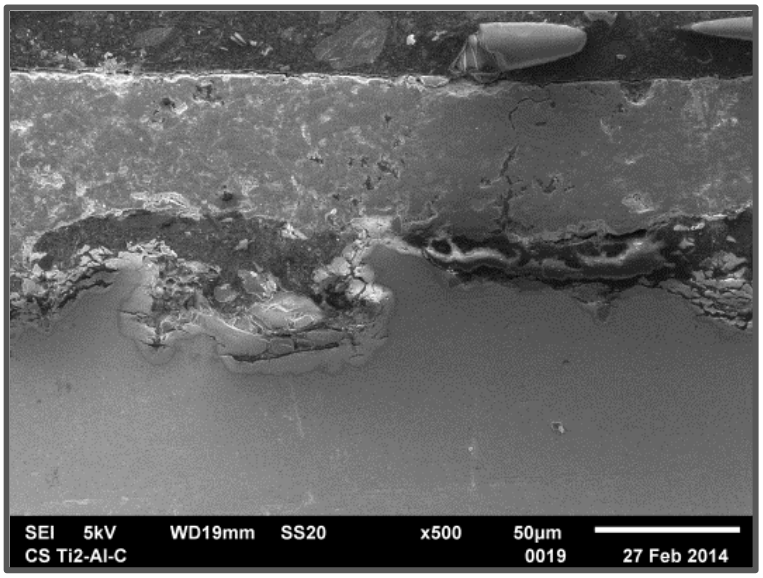

Figure 33: SEM micrograph of the innermost coating-substrate interface of the thinned, cold-sprayed Ti_2AlC sample. Interface oxidation is readily apparent, and a through-thickness crack in the coating is visible.

Analysis of this same region via EDS (Figure 34) leads to interesting information regarding the composition of the oxide that forms along the interface. Rather than the expected high ZrO_2 content, a large amount of Al_2O_3-based oxide is observed. High levels of carbon are detected, indicating zirconium carbide may have formed in addition to alumina. The EDS maps also indicate that oxygen has permeated the coating, forming aluminum and titanium oxides.

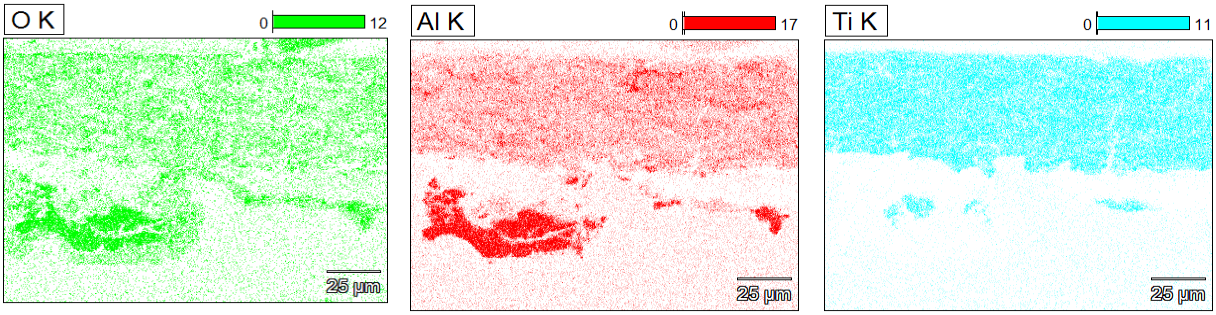

Figure 34: EDS Spectral maps for Oxygen, Aluminum, and Titanium in the post-autoclave, thinned CS sample. Intensities are mapped as counts per pixel.

5.2.2.2. SPRAYED COATING: 50 µ, AVG THICKNESS

Sixteen Zircaloy-4 coupons coated with Ti_2AlC by a commercial vendor under contract with SRNL were delivered to UW-Madison in June 2014. Of these coupons, fifteen belonged to a new spray program targeted at spraying thinner, denser coatings, in which a variable number of passes (4, 6, or 9) were performed using the same spraying parameters as the original program in early 2013. The remaining sample was coated in the original spray program, and is available as a reference sample for behavioral comparison.

A single sample of each of the 3 groups was mounted and viewed in cross section. All were found to be considerably wavier than the ground coatings, but as the number of passes increased the apparent waviness decreased. All possessed cracks ran parallel to the interface. Measurements of the coating thickness were collected using ImageJ to generate the statistics of Table 7. In all samples, large Al-rich oxides are found along the interface. It is likely that these are the byproduct of a surface preparation step (Al_2O_3 grit blasting) that occurred prior to the CS deposition. Figures 35-38 show various SEM micrographs of cross-sections of the 3 groups prior to exposure.

Sample	Avg. Ti_2AlC Thickness (µm)	Uncertainty (µm)	Number passes
CS-4p AR	44.2	±5.9	4
CS-6p AR	57.8	±14.1	6
CS-9p AR	38.5	±13.7	9

Table 7: The table shows coating thickness statistics for representative 4-pass, 6-pass, and 9-pass samples. A vendor estimate indicated each pass should deposit ~10 µm MAX Phase. The 9-pass thickness is less than expected due to sloughing off of outer coating layers. Future sprayings will be designed to provide a maximum of 4 to 5 passes to minimize sloughing off.

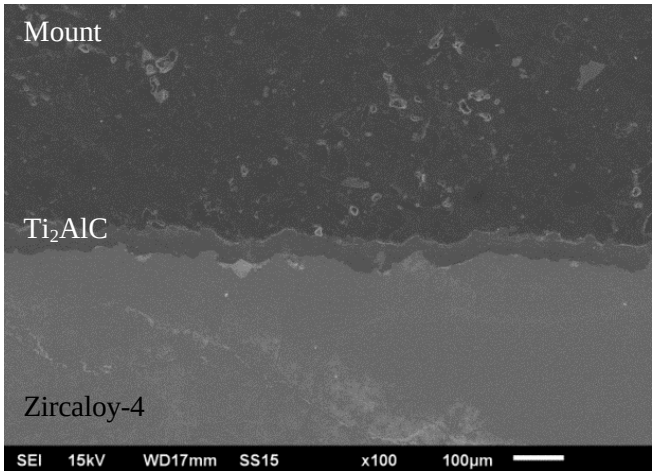

Figure 35: As-received cross-section of a 4-pass sample. The thinner-sprayed coating has significantly poorer surface roughness and thickness uniformity than the ground sample.

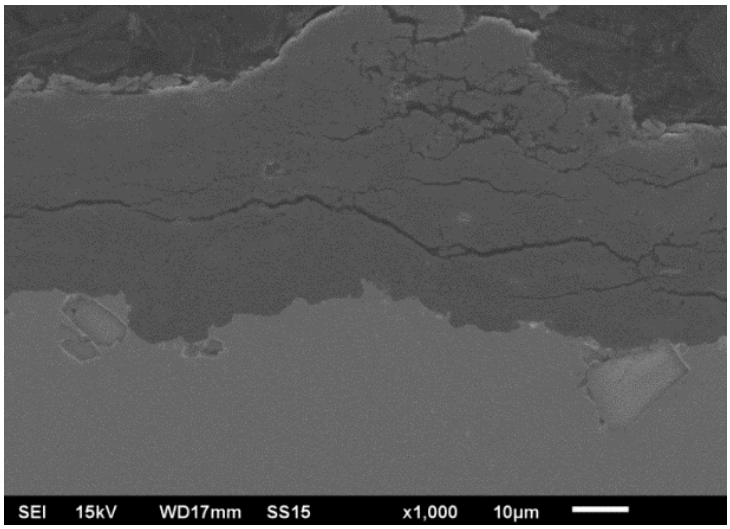

Figure 36: Higher magnification examination of a 4-pass sample shows significant intra-coating cracking. However, nearly all cracks are parallel to the interface. An aluminum-rich oxide particle is observed at right, and was likely embedded during an Al2O3 grit blasting surface preparation step before the coating was applied.

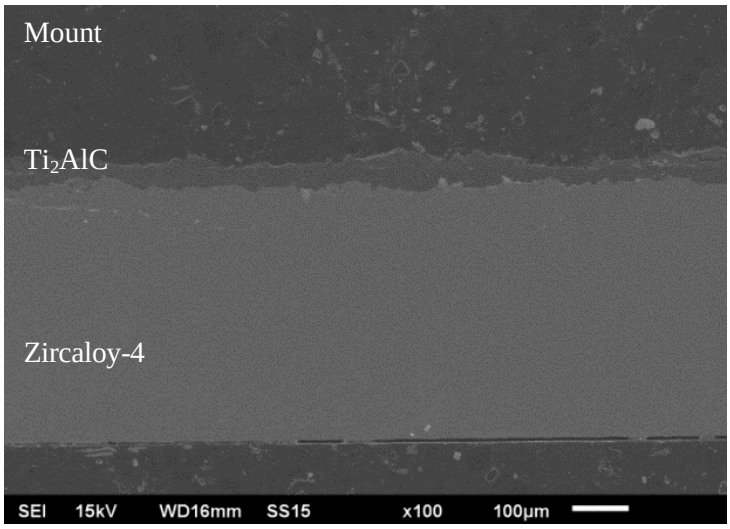

Figure 37: Higher magnification examination of a 4-pass sample shows significant intra-coating cracking. However, nearly all cracks are parallel to the interface. An aluminum-rich oxide particle is observed at right, and was likely embedded during an Al_2O_3 grit blasting surface preparation step before the coating was applied.

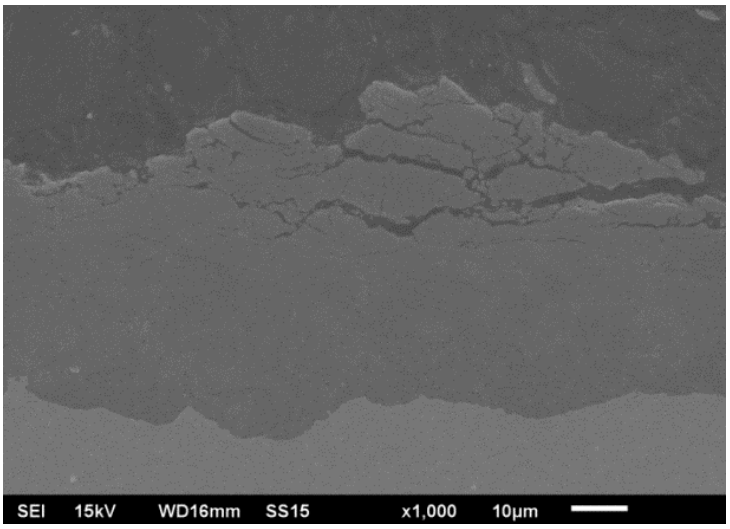

Figure 38: Higher magnification examination of the 9-pass sample also shows coating cracks within the externalities of the coating.

One sample each of CS-4p, CS-6p, and CS-9p were autoclave tested for a short duration of just 12h at 400°C and 1500psi (Figure 39). This short duration was chosen such that, if oxidation of the substrate interface occurred primarily by inward edge oxidation, it would not likely be complete in 12 hours. In this case, the cross section images of tested samples would show roughly consistent edge oxidation behavior. If the oxidation of the interface is due to defects in the bulk of the coating, the amount of oxide detected in the central region should decrease with increasing number of passes, as any cracks or defects get sealed off from the interface and/or external coating surface.

There is no qualitative or quantitative difference in the collected XRD spectra for the varied passes (Figure 39). There is no comparable sample of the original spray batch for the 12-hour G2 condition autoclave test, so it is not known if the 4p, 6p, and 9p samples oxidize differently as a function of time compared to the samples tested in the 72-hour exposures.

It is difficult to tell if the tested samples are representative of the samples in the past, or even if the results allow for the discrimination between oxidation mechanisms. It is clearly evident from SEM photographs (Figures 41-44) that the coatings are highly defected in even the as-received state. The presence of alumina grit blast residue underneath the coating poses a considerable challenge to correctly interpreting the oxidation of the substrate in the post-test condition. What is clear is that there is oxygen diffusion/ steam permeation along cracks and pores that leads to oxidation of the underlying Zircaloy-4.

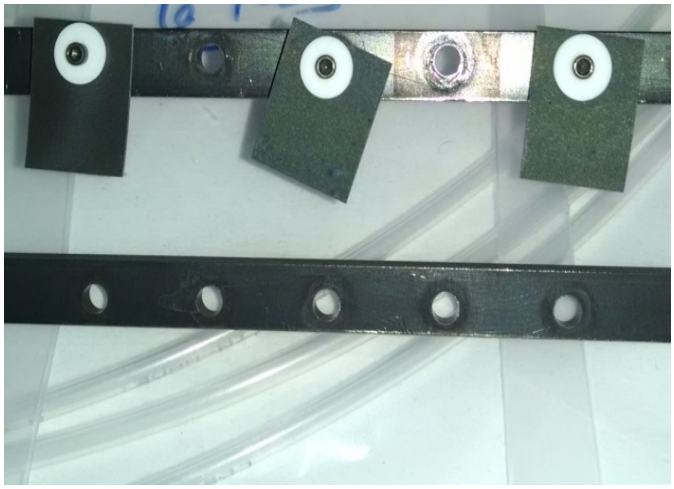

Figure 39: CS 4p, CS 6p, and CS 9p following removal from the autoclave following a 12h test at 400°C, 1500psi. Yellowing of the coatings is observable.

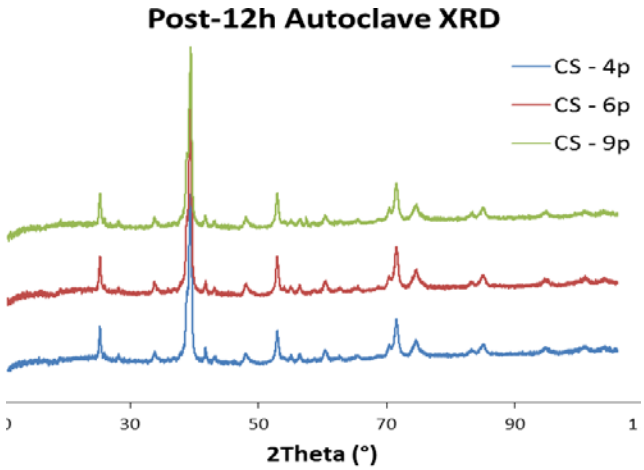

Figure 40: Post-autoclave XRD spectra for the three "thin-sprayed" cold-sprayed Ti_2AlC. The number of passes does not influence phase evolution during the test.

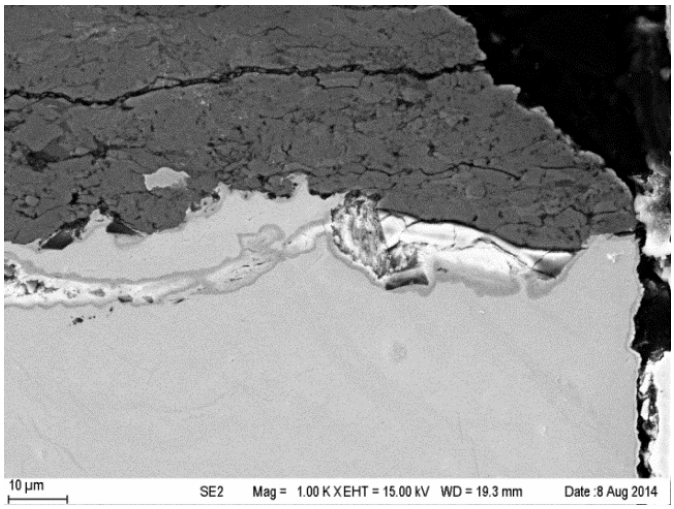

Figure 41: SEM image from the CS-4p sample after 12h autoclave testing. It is difficult to discern what oxidation occurred during the test and what was imparted during the Al_2O_3 grit blasting step preceding manufacture.

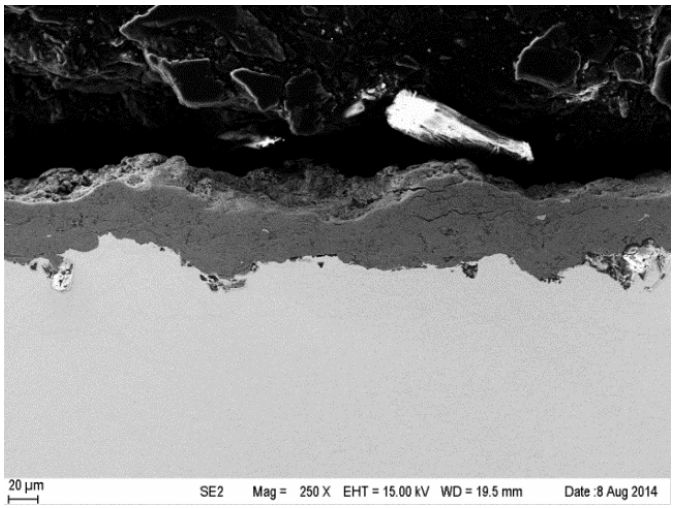

Figure 42: SEM image from the CS-4p sample after 12h autoclave testing. It is difficult to discern what oxidation occurred during the test and what was imparted during the Al_2O_3 grit blasting step preceding manufacture.

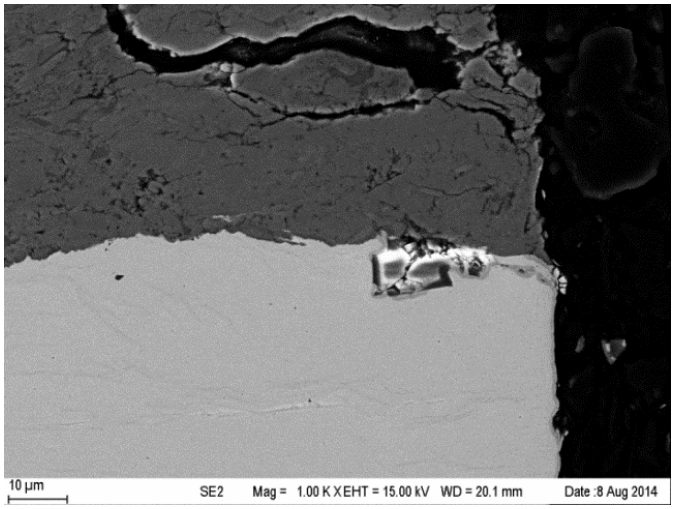

Figure 43: SEM image from the CS-6p sample after 12h autoclave testing. Only a minor amount of the from-edge oxidation is noted.

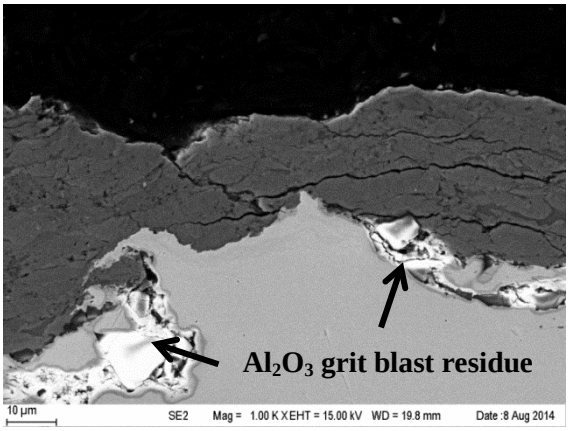

Figure 44: SEM image from the interior of the CS-6p sample after autoclave testing. A crack in the coating runs from the exposed surface to the interface, and at the junction site interfacial oxidation is observed.

In summary, conclusions from this work are:

1) Surface grinding is a potential process option that should be further evaluated.
2) Surface roughness of ground samples should be measured along with coating thickness variability.
3) Alumina blast media impacts should be evaluated and appropriate media/process changes made.

Subsequent discussions with the spray vendor have resulted that techniques to reduce the alumina blast media impacts will be employed on the next phase of spray coating of tubes.

Other significant changes in spray coating will be made to improve the density and hence the performance of the thinner coatings required for reactor operation. Changes are being made at the Vendor site for an upgraded spray system that delivers higher carrier gas velocities which are known and proven to improve the coating density and reducing the porosity to minimize oxygen diffusion through the coating.

5.2.3. 3RD PHASE TESTING - SINTERED & EDGE PROTECTION

Two methods of reducing the oxygen ingress into the coating-substrate interface were explored in the third phase of testing: a) pre-test sintering of the coupons; b) application of oxidation-resistant epoxy to exposed edges of the sample prior to autoclave testing. Investigation of these additional post-coating treatments was recommended following the September 2013 GR, in order to determine if oxygen detected within the central region of the post-autoclave samples diffused from the exposed edges of the samples or through the coating. It is recognized that water/steam pressure could have been a significant oxygen transport mechanism, and therefore, will be evaluated in future testing.

Sintering is a technique commonly used in powder metallurgy and ceramics manufacturing to remove excess grain boundaries, promote powder consolidation, and reduce porosity. As a bulk diffusion process, sintering requires a non-trivial duration of high-temperature exposure. The small particle size of the raw MAX phase powder and the presence of intra-coating cracks / voids in as-received material suggested sintering of cold-sprayed MAX Phases could reduce defect pathways within the coating that otherwise would allow easy oxygen transport to the substrate.

Two furnaces were used to perform sintering experiments at UW-Madison. The first is a vacuum hot press furnace, capable of 10-5 Torr vacuum and temperatures in excess of 1700°C (Figure 45). The second is an MTI GSL-1600X, and was used due to equipment availability conflicts.

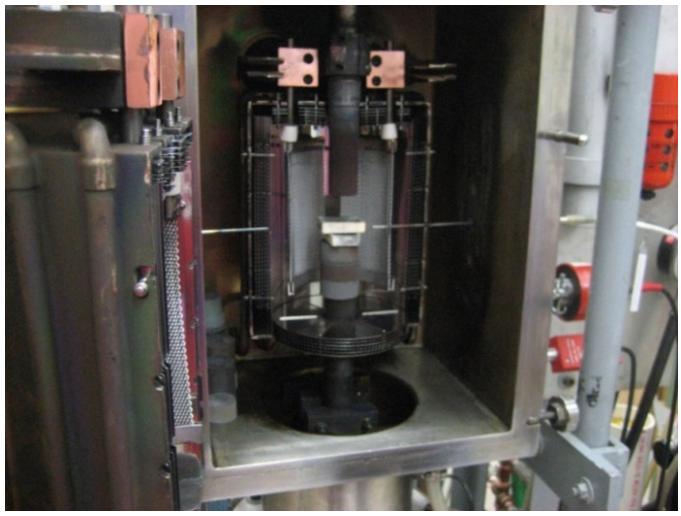

Figure 45: The vacuum hot press furnace used for sintering of cold-spray and HVOF coatings.

Initial sintering time and temperature were driven by UW's work with EPD coatings. One HVOF-sprayed and one cold sprayed sample were thus sintered for 4 hours at 1050°C and another set for 16 hours at 850°C. (Figure 46 and Figure 48)

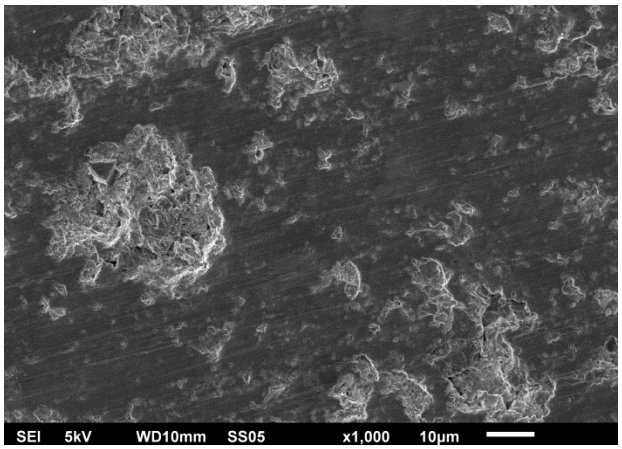

Figure 46: Plan view SEM image of a cold-sprayed sample that was ground down to a nominal 50µm thickness and then sintered 16 hours at 850°C.

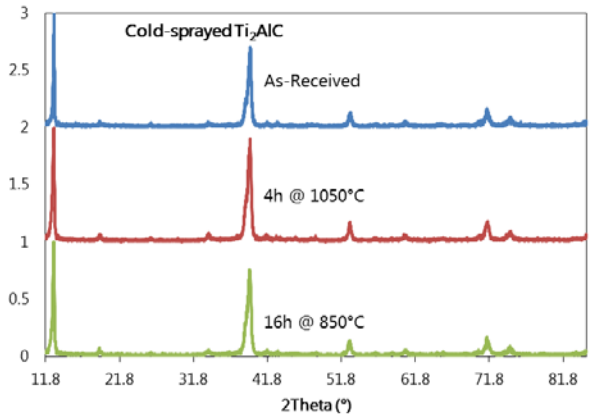

Figure 47: XRD spectra for the cold-sprayed samples as a function of sintering time and temperature.

The sintered samples were also tested with non-sintered samples in a 72 hour, 400°C, 1500 psi autoclave exposure. Less oxidation of the interface was observed in both heat treated cold-spray samples, but more oxidation of the uncoated Zircaloy-4 was observed, probably due to the significant microstructure changes to the Zircaloy-4 base material with the high temperature heat treatment (Table 8).

Region	Coated side (µm)	±	Uncoated Sides (µm)	±
CS ht#1 Zircaloy-4 oxide layer	3.13	1.79	4.42	1.01
CS ht#2 Zircaloy-4 oxide layer	3.50	3.01	5.34	1.90
CS Zircaloy-4 control oxide layer	9.00	9.23	14.11	4.76
HV ht#1 Zircaloy-4 oxide layer	4.62	1.75	1.91	0.78
HV ht#2 Zircaloy-4 oxide layer	8.71	3.97	5.11	2.47
Zircaloy-4 controls oxide layer	n/a	n/a	1.80	1.41

Table 8: Measured oxide thicknesses for sintered and non-sintered Ti_2AlC coatings after a 72-hour G2 autoclave test.

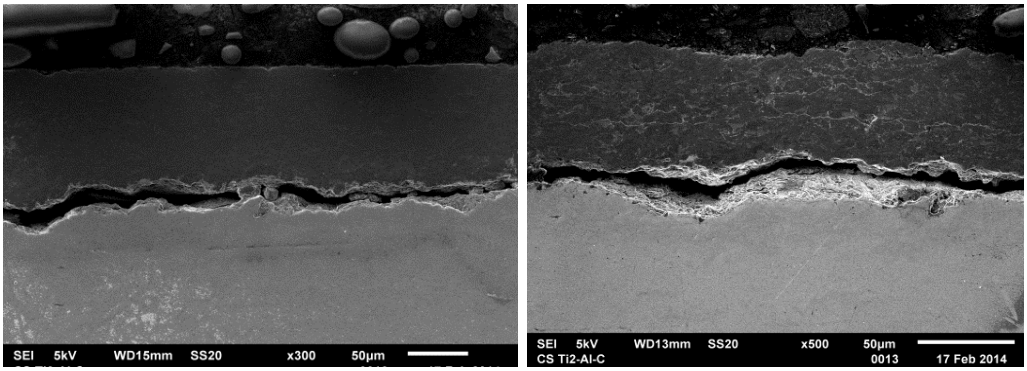

Figure 48: SEM micrograph of the coating-substrate interface of the Ti_2AlC sample treated at 850°C for 16 hours. Interface oxidation is again less apparent than the non-sintered case, yet still present.

An oxidation resistant epoxy was selected to serve as a barrier to oxygen entry from the exposed coating-sample interface during autoclave testing to test the hypothesis that oxygen located in the central region of post-autoclave samples diffused along the interface from the edge rather than through the coating. Past work with the silica-based epoxy indicated it had a service temperature limit of 1400°C. It was not known if the epoxy would be compatible with the high pressure within the autoclave. This epoxy was combined with an aggressive sintering experiment of 3 hours at 1300°C, a treatment found in literature to result in effective sintering of Ti_2AlC without decomposing it into binary compounds (Figures 49 – 56). The MTI-GSL-1600X furnace was used for this sintering experiment, with a flowing argon cover gas of 215-353 cm³ per minute. This cover gas flow was found to be insufficient because there was oxygen present that caused oxidation during the sintering process.

Figure 49: Edge-protected SRNL coupons in alumina crucibles prior to furnace sintering. At far right is a crucible of Ti sponge that was also included as an upstream oxygen gettering agent.

Figure 50: Edge-protected SRNL coupons after the furnace sintering at 1300°C for 3 hours. All cold-sprayed Ti_2AlC samples are intact, but the HVOF sample has fragmented at the corner.

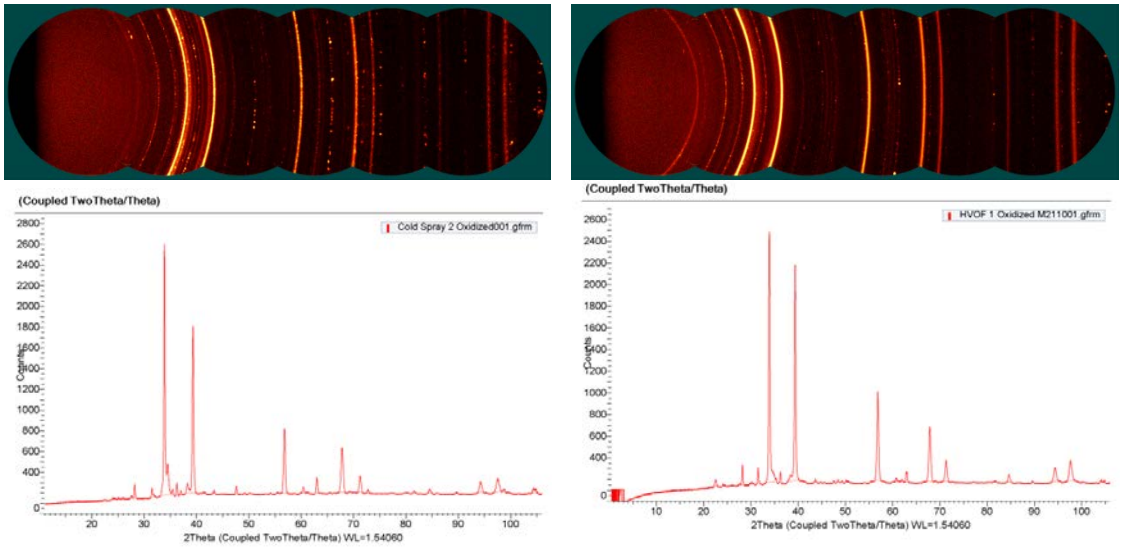

Figure 51: 2D x-ray diffraction pattern and total integrated intensity for the coating side of (l) the sintered cold-sprayed sample and (r) the sintered HVOF-sprayed sample, taken prior to autoclave exposure.

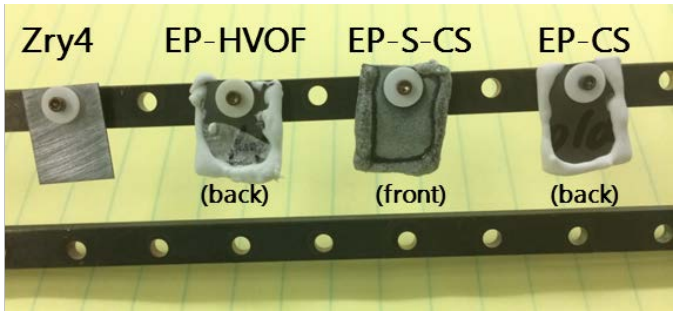

Figure 52: Sample coupons mounted and ready for the autoclave test. Samples were edge-protected (EP) and one cold-sprayed (CS) sample was sintered (S) for 3h @ 1300°C prior to autoclave testing.

Figure 53: Sample coupons/remnants after the autoclave test. Samples were edge-protected (EP) and one cold-sprayed (CS) sample was sintered for 3h @ 1300°C prior to autoclave testing. This sintered sample did not survive the autoclave test; pictured above is the epoxy that coated its edges.

The high temperature epoxy that was not included in the sintering experiment was found to be incapable of withstanding the pressure of the 72h G2 autoclave test; it can be removed with light cleaning actions. The high temperature epoxy that was sintered was able to withstand the autoclave experiment.

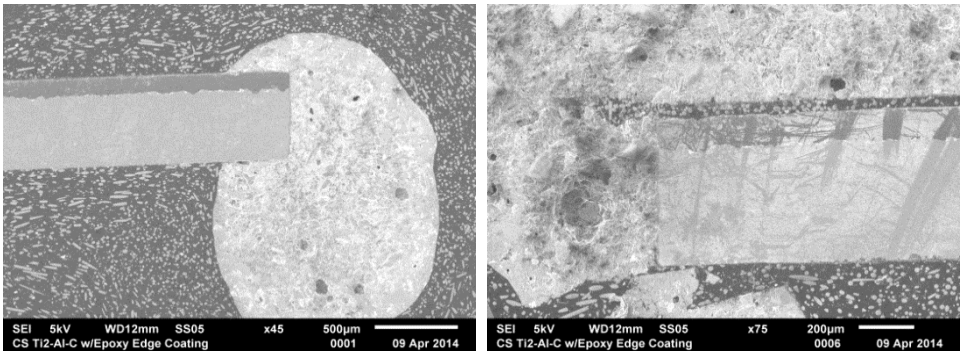

Figure 54: Left and Right edges of an edge-protected sample cross-section. The protective quality of the treatment is mixed – good protection in the image at left, but significant gaps in the image at right.

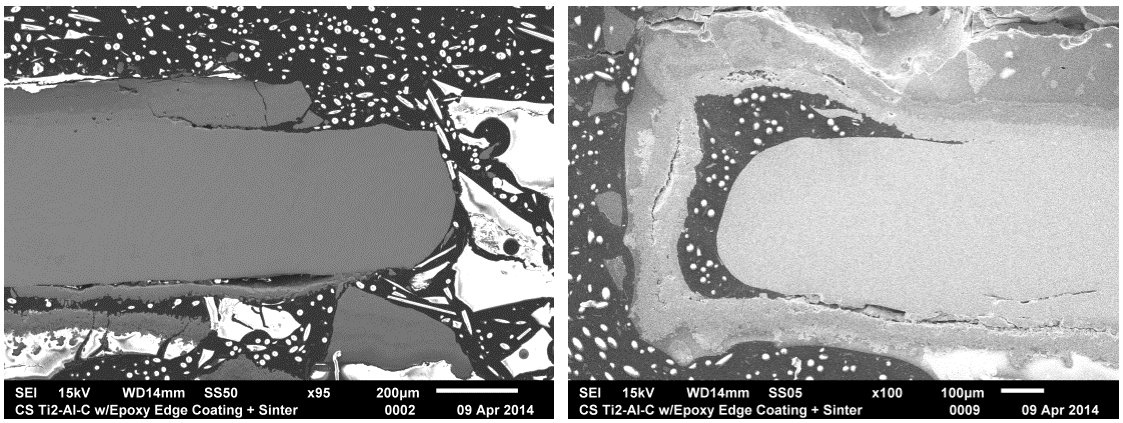

Figure 55: Left and Right edges of an edge-protected sample cross-section following the sintering treatment of 3h @ 1300°C. The cross section makes it plain that edge protection, at least for this sample, was a failure. Significant diffusion between coating and substrate is detected in the sintered sample.

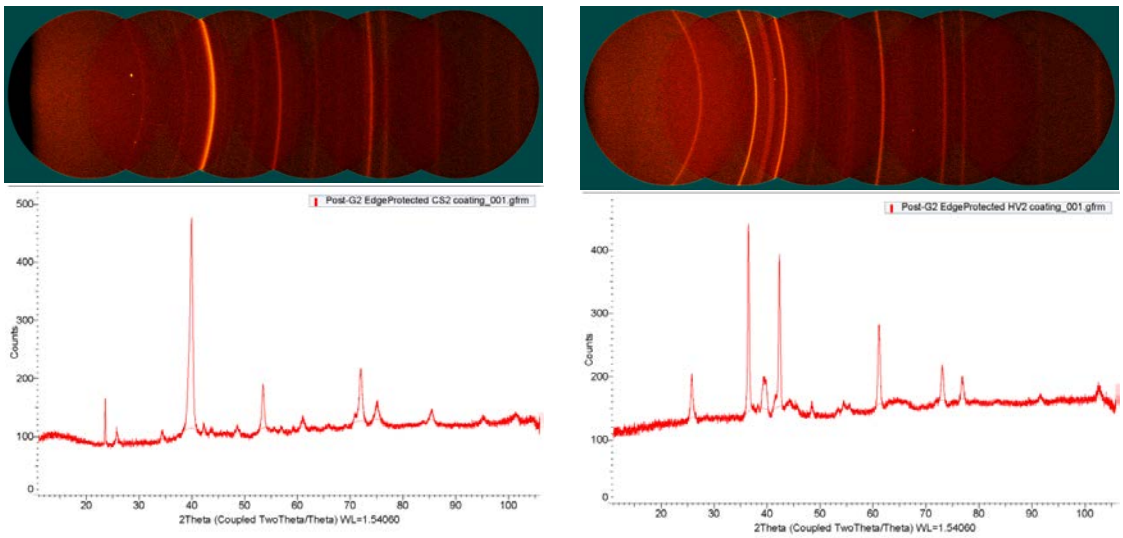

Figure 56: 2D x-ray diffraction pattern and total integrated intensity for the coated side of the (l) cold-sprayed sample, and (r) HVOF-sprayed sample after G2 testing. As expected from the differing spray processes, the spectra are not equivalent.

In conclusion, sintering of the coated material is not a preferred process and has significant impacts on the base Zircaloy-4 performance.

6.0 CHEMICAL/OXIDATION PERFORMANCE TESTING AT LOCA CONDITIONS (STEAM REACTOR)

6.1. INITIAL TESTING – LOCA CONDITIONS

6.1.1. METHODOLOGY / PROCESS / GOAL

Cladding oxidation at LOCA conditions is an important metric in evaluating how cladding will withstand an accident scenario and decreasing cladding oxidation under these conditions is one of the main metrics of the DOE ATF program. At LOCA conditions, cladding temperatures may exceed 1000°C for seconds to minutes, depending on the specific accident cause. To simulate the reactor conditions of a temporary severe condition due to a loss of coolant from a large-pipe break, the AREVA team (in Appendix P) has defined LOCA conditions as exposure of the cladding to 1100°C for 4 minutes at 1 atm with steam. These tests determine the oxidation resistance of coated flat coupons and tube sections at the LOCA conditions. These studies determined the overall weight gain due to oxidation and used metallography along with SEM and electron dispersive X-ray (EDS) to examine changes to the cladding and coating during oxidation.

6.1.2. LOCA TESTING OF MAX COATED ZIRCALOY-4

LOCA testing was conducted in the test reactor system shown in Figure 58. The test apparatus consists of the Zircaloy cladding sample rod holder, a vertical tube furnace, steam boiler, an inert gas purge system, and a data acquisition system. LOCA testing to simulate a reactor cooling water large-pipe break was conducted at 1100°C for 4 minutes. The following three sample coupons were tested with the coated coupon coating thicknesses ranging from ~200 to 450 µm:

- Uncoated Zircaloy-4
- HVOF spray-coated Zircaloy-4 coupon (~450 µm) with a Ti_2AlC coating
- Cold-Spray coated Zircaloy-4 coupon (~200 µm) with a Ti_2AlC coating

The control system maintains and records the temperatures in the test chamber in which the coupons are exposed and the heating profile results are shown in Figure 58 for the 3 samples that were tested. Figure 59 records the actual time that the three coupons were exposed to the LOCA conditions.

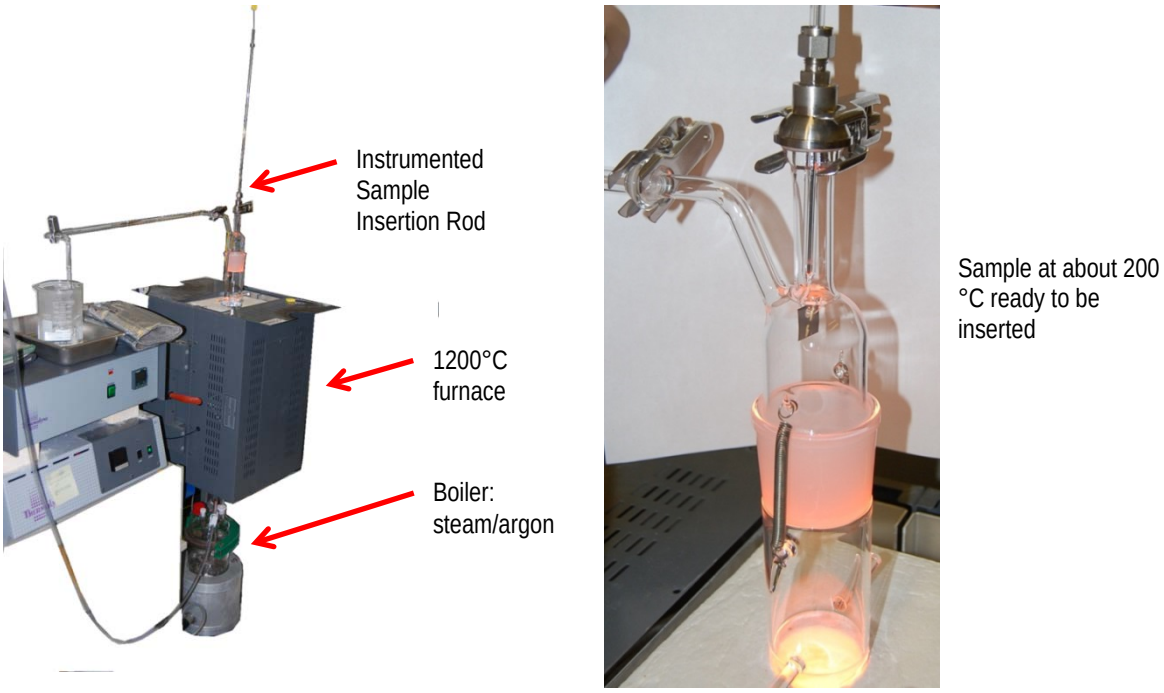

Figure 57: Photo of the steam reactor test apparatus used for LOCA conditions.

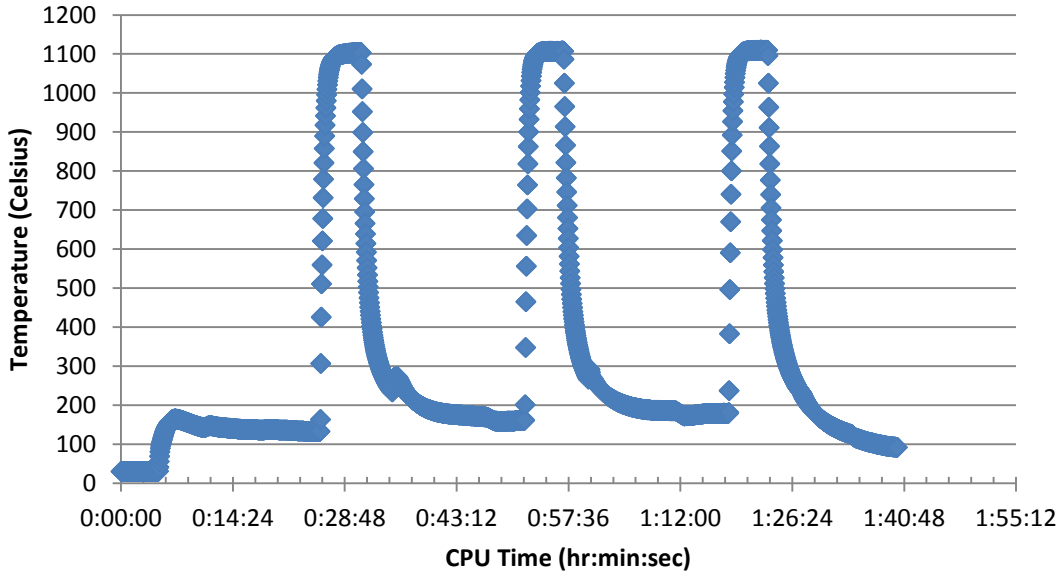

Figure 58: Heating Profile during Reactor Steam Testing.

Start/stop counting at 1090 °C (temperatures soon thereafter reached ≥1100 °C)

- Uncoated Zircaloy: **268** seconds (1104 °C=T_{Max})
- HVOF Coated Zircaloy (~450 µ): **256** seconds (1108 °C=T_{Max})
- ColdSpray Coated Zircaloy (~200 µ): **253** seconds (1110 °C=T_{Max})

Figure 59: Actual Exposure Time for three test coupons Reactor Steam Testing.

6.1.3. ANALYSIS OF LOCA RESULTS AND SAMPLES

RELATIVE WEIGHT GAIN ANALYSIS

There is no standardized protocol for evaluating the oxidation response of coated cladding samples. However, the oxidation of uncoated cladding has been extensively characterized on an area basis. Therefore, SRNL has utilized the coated area of cladding samples along with the oxidation of both coated and uncoated samples at the same conditions to analyze cladding oxidation behavior. Figure 60 provides an overview of the analysis technique used by SRNL in evaluating the oxidation performance of coated cladding samples.

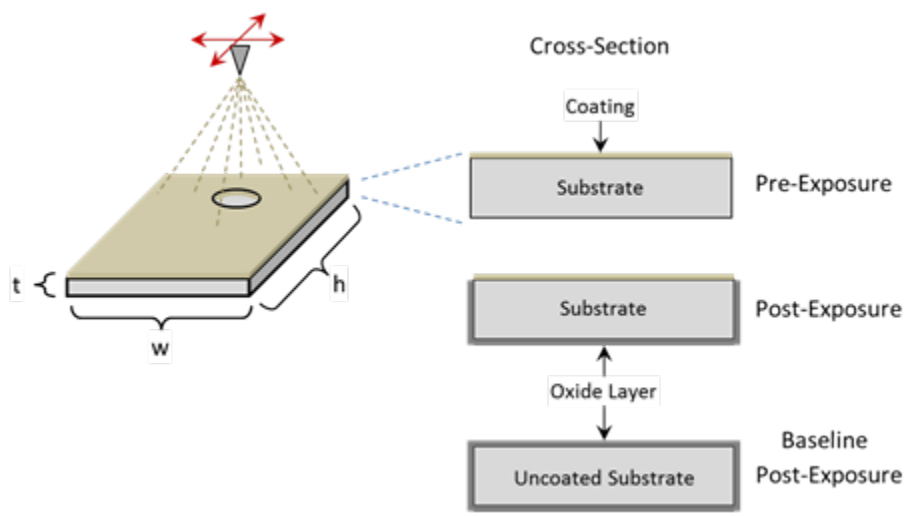

Figure 60: Illustration of the analysis method used by SRNL.

Figure 60 illustrates that the cladding substate is coated on one side and the other sides of the sample are allowed to oxidize normally. The weight gain of the coated sample can be compared to the weight gain in the uncoated sample. If the coating does not allow oxidation of the cladding surface area below the coating and does not oxidize itself, then the maximum percentage weight gain reduction should be equal to the percentage of coated area. In other words, if 45% of a samples surface is coated, then a 45% reduction in the weight gain for the coated sample versus the uncoated sample should be expected.

The weight gain for the uncoated Zircaloy-4, Ti_2AlC HVOF, and Ti_2AlC cold-spray coated and samples are shown in Figure 61. Both the HVOF and the cold-spray coated Zircaloy-4 samples had 45% of the sample surface area coated. The Ti_2AlC HVOF sample had a weight gain 55% less than the uncoated Zircaloy-4 sample. The Ti_2AlC cold-spray sample had a weight gain that was 57% less than the coated sample. The fact that the percent reduction in weight gain for the coated sample decreased the weight gain by a greater percentage than the uncoated sample is very promising. The larger percent reduction in the weight gain for the coated samples was likely due to the samples being in the reactor around 15 seconds longer than anticipated and in slight inequalities in the sample removal procedure.

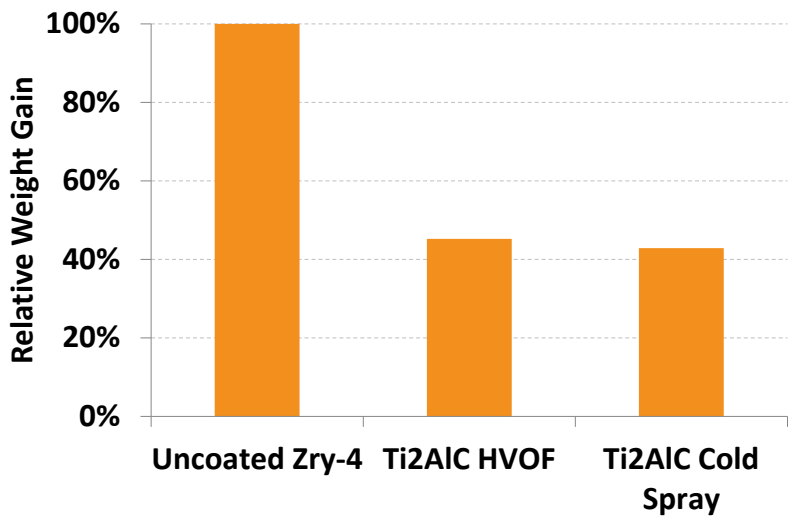

Figure 61: Relative weight gain for coated and uncoated Zircaloy-4 samples at 1100°C at approximately 240 seconds in steam at atmospheric pressure.

HVOF SPRAYED TI_2ALC COATED ZIRCALOY-4 (~450 µM)

Figure 62 shows an optical micrograph of HVOF Ti_2AlC coated Zircaloy-4 sample after oxidation. The edges of the substrate show that there is significant oxidation at the edges of the sample and there appears to be some delamination of the HVOF coating at the edges. This suggests that the HVOF coating is not bound well to the substrate at the edges. This edge delamination during the LOCA tests is one indication that the HVOF coating process may not create a strong enough bond between the surface and the coating at all locations. However, further analysis was

conducted to understand the performance of the HVOF coating in regions where the edge effects are not as important.

SEM images of a center-cut HVOF sprayed Ti_2AlC coated Zircaloy-4 specimen with coating thickness of ~450 µm after oxidation at 1100°C with steam for 4 minutes are shown in Figure 62. This center cut sample is intended to evaluate the performance of the coating away from the edges of the sample. The sample oxidized normally on the uncoated surfaces of the flat sample that were exposed to the steam. The SEM images showed that the Zircaloy-4 substrate did not oxidize significantly beneath the HVOF Ti_2AlC coating and the coating remained well-adhered to the surface. The images showed that there was no significant diffusion of steam beneath the edges of the coating. This result suggests that at the coating thicknesses observed, that the coating adheres well to the surface and blocks lateral diffusion even though the bond at the surface is mostly a mechanical bond.

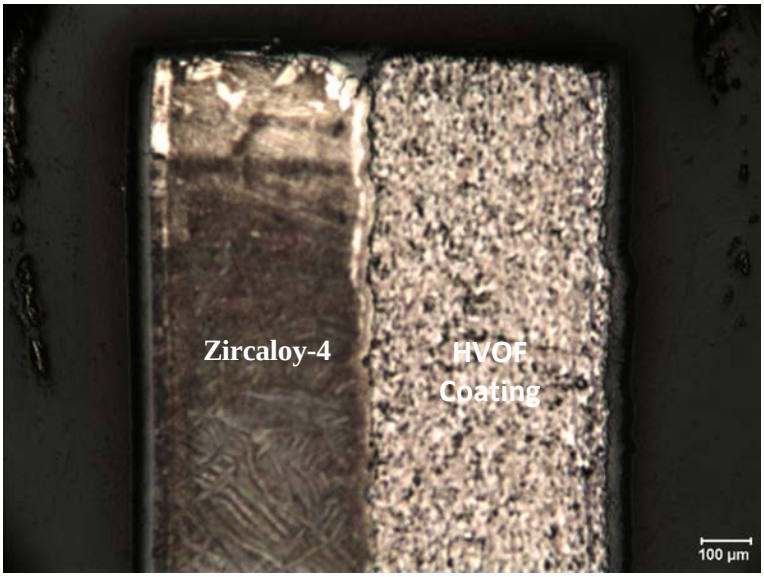

Figure 62: Optical Microscope of the edge of HVOF Sprayed Ti_2AlC coated Zircaloy-4 (~450 µm) after LOCA Testing (1100°C, 4 minutes).

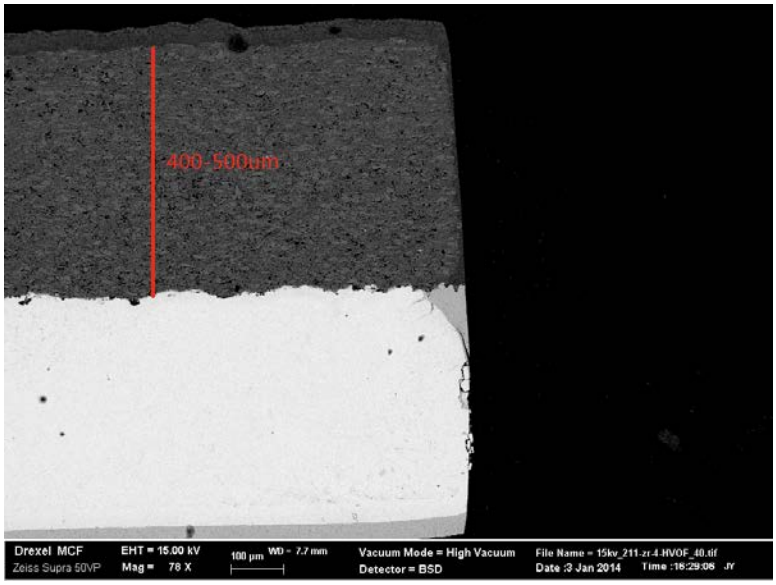

Figure 63: SEM of a Center-Cut HVOF Sprayed Ti_2AlC coated Zircaloy-4 (~450 µm) after LOCA Testing (1100°C, 4 minutes).

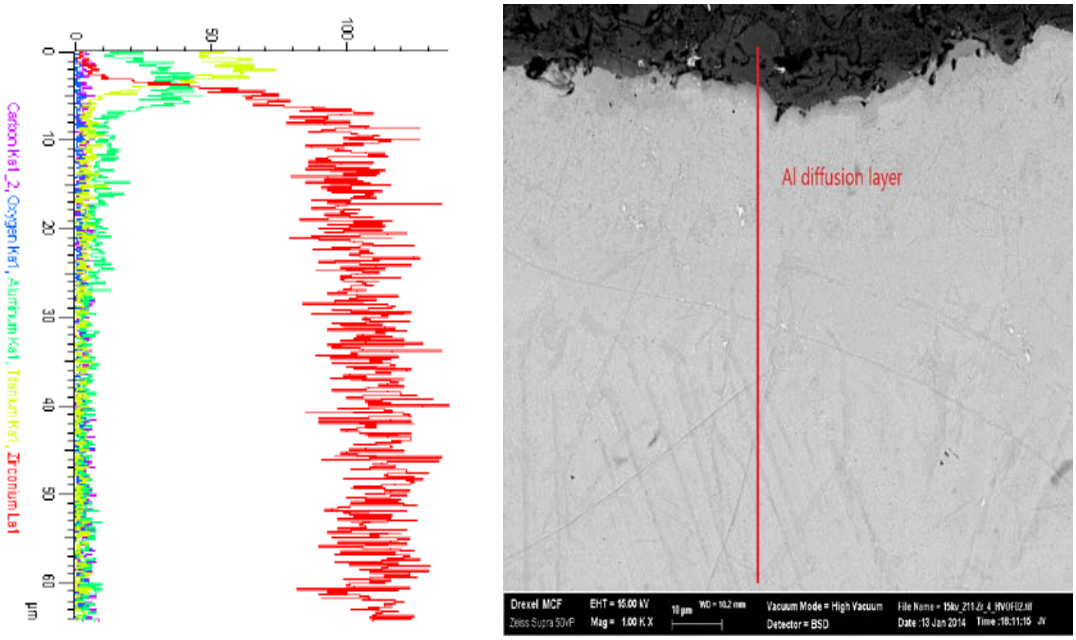

Figure 64: SEM/EDS analysis of the interface between a Ti_2AlC HVOF coating and the Zircaloy-4 substrate.

Figure 64 shows SEM/EDS analysis of the HVOF Ti_2AlC coating after testing at LOCA conditions. This figure shows some Al diffusion from the Ti_2AlC coating into the Zircaloy-4 substrate. The diffusion of Al occurs in a 5-10 µm layer at the substrate surface. Upon oxidation, a ZrO_2 layer, with a thickness of approximately 40 µm, was formed on all uncoated Zircaloy surfaces. A 40-50 µm oxide layer, however, was also found on the coating (Figure 65). This oxide layer was comprised of TiO_2 and Al_2O_3. No oxygen was detected at the coating/substrate interface confirming that at least for the oxidation conditions tested, the coatings did protect the substrate.

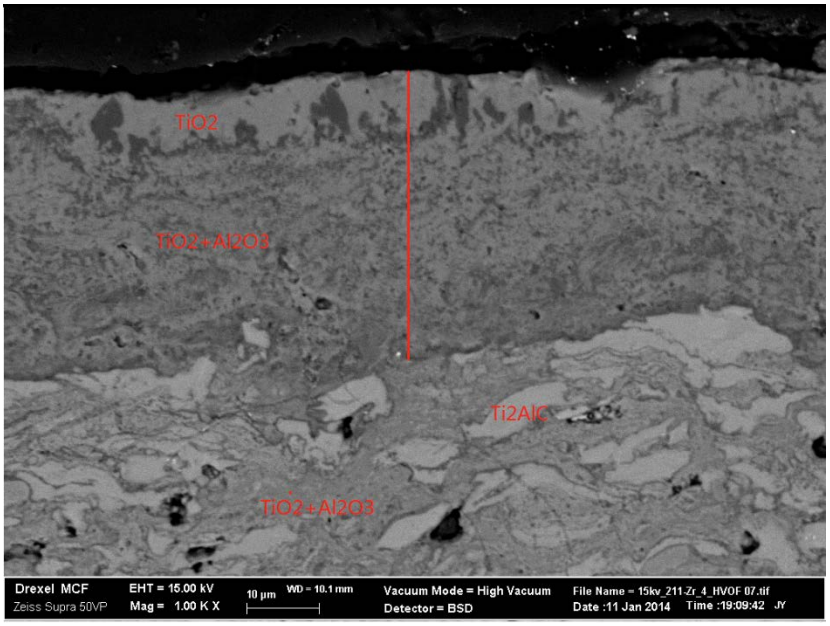

Figure 65: High magnification SEM micrograph of oxide layer that forms on the HVOF coating.

COLD-SPRAY TI_2ALC COATED ZIRCALOY-4 (~200 µM):

Figure 66 shows SEM images of the edges of a Ti_2AlC coated Zircaloy-4 specimen after oxidation at 1100°C with steam for 4 minutes. Unlike the HVOF Ti_2AlC coating, the Ti_2AlC cold-spray coated sample oxidized normally on the uncoated surfaces of the flat sample that were exposed to the steam. The SEM images showed that the Zircaloy-4 substrate did not oxidize significantly beneath the MAX coating and remained well adhered to the surface. The images showed that there was no significant diffusion of steam beneath the edges of the coating. This result suggests that the coating adheres well to the surface and blocks lateral diffusion even if the bond at the surface is mostly a mechanical bond.

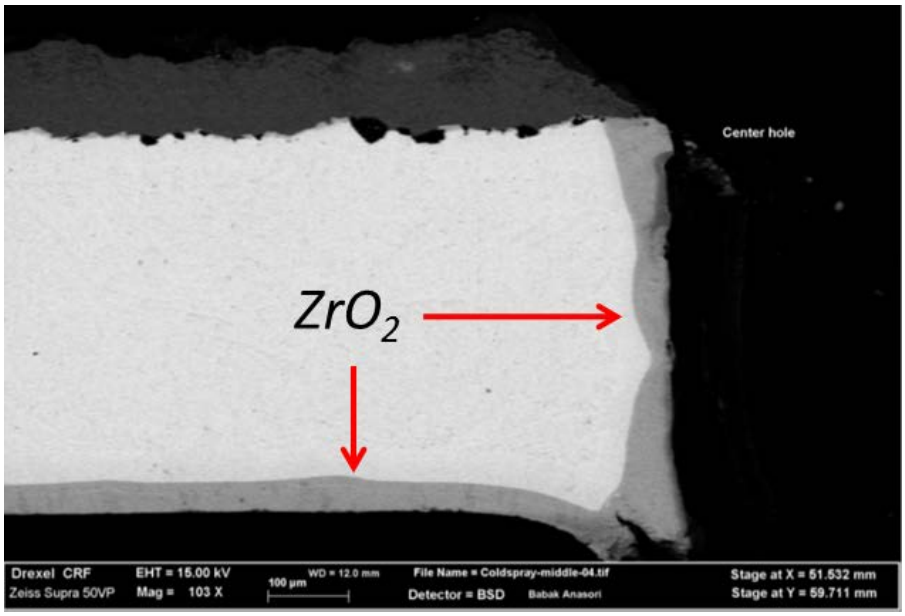

Figure 66: SEM image of the Ti_2AlC coated Zircaloy-4 sample after oxidation at 1100°C.

The weight gain results in Figure 61 coupled with the SEM images in Figure 66 that show no oxidation under the coating indicate that Ti_2AlC is providing an effective barrier against oxidation of the underlying substrate.

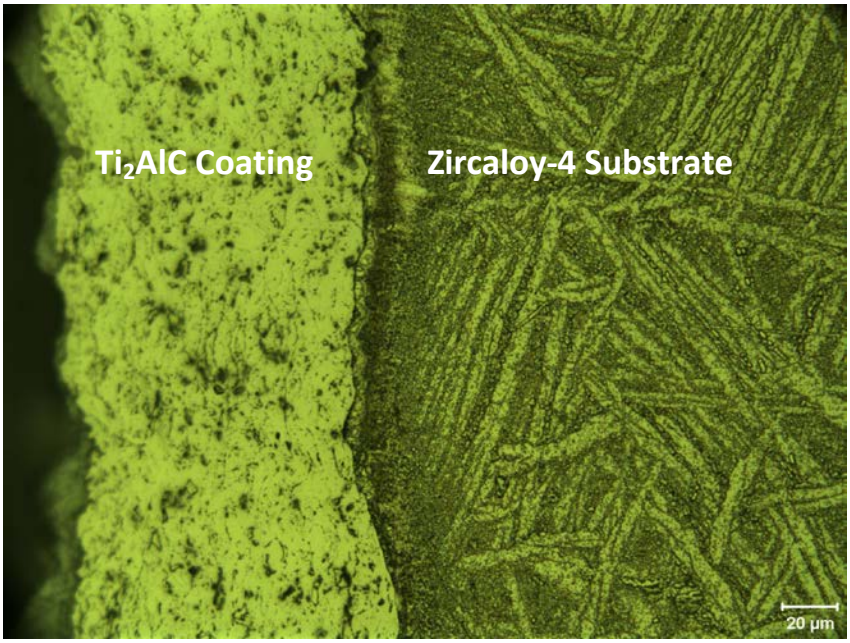

Figure 67: Low magnification micrograph of Zircaloy-4 with the cold-spray coating after testing at LOCA conditions.

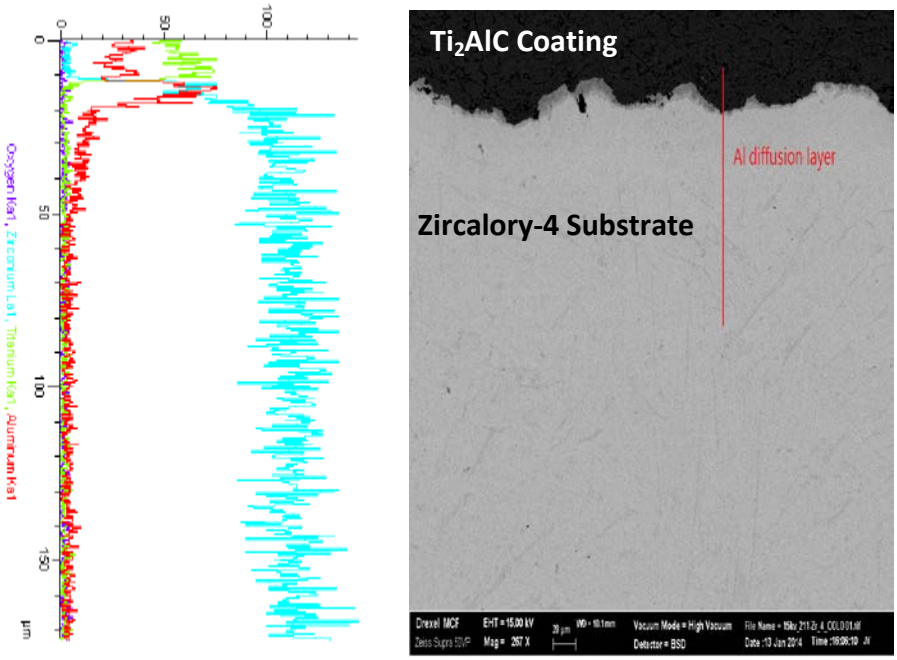

Figure 68: SEM/EDS analysis of the interface between a Ti_2AlC cold-spray coating and the Zircaloy-4 substrate.

At ~200 µm, the cold-spray coating (Figure 67), was thinner than the HVOF coating. In general, the bonding between the cold-spray coating and Zircaloy-4 was significantly better than that between the HVOF and Zircaloy-4 (Figure 67) after oxidation. The better adhesion of the CS coating was especially evident at the edges of the sample. Figure 68 also shows 5-10 µm oxide layers formed at the outside surface of the Ti_2AlC coating that was significantly thinner than the 40-50 µm oxide layers formed on the external surface of the HVOF coating. After oxidation of the sample at LOCA conditions, SEM/EDS analysis showed that some Al diffused from the coating into the substrate. The diffusion of Al is of the order of 10 -20 µm (Figure 68). The Al diffusion layer at the interface was not observed in the pre-oxidation SEM image in Figure 66 and therefore this diffusion occurred during oxidation at LOCA conditions. Oxygen was not detected at the coating/substrate interface, which confirms that cold-sprayed Ti_2AlC coating protected the substrate out to the edges of the sample.

6.1.4. CONCLUSIONS

MAX Phase cold-spray coatings of Ti_2AlC showed excellent ability to reduce the oxidation of Zircaloy-4 substrate under LOCA conditions. This was demonstrated by both a decrease in the weight gain that was proportional to the surface area of the sample that was coated and the SEM center-cut micrographs showing negligible oxidation between the coating and the Zircaloy-4 interface. The cold-spray coatings were better at preventing substrate oxidation than HVOF coatings. The HVOF coatings

showed signs of oxidation during the spraying process and this is one likely reason why they did not protect the Zircaloy-4 substrate as well as the cold-spray coatings. These results indicate that the MAX cold-spray coatings are promising for protecting zirconium alloy cladding from oxidation under LOCA conditions.

7.0 FUTURE TESTING

Several engineering challenges remain for development of MAX-Phase coated cladding in the next phase of testing. First, the tests to date have been conducted on flat samples which maximize the oxygen diffusion along the edges leading to the premature oxidation of the underlying Zircaloy-4. Therefore, the challenge remains to minimize the edge oxidation effect to allow differentiation as to whether oxidation of the interface between the coating and Zircaloy-4 is caused by oxygen diffusion through the coating or from the edges. Future testing on small diameter tubes will be an advantage due to the minimization of the edge oxidation effect enabling unbiased evaluation of the coating protection qualities. Second, a specific challenge with Ti_2AlC is that titanium has a rather large neutron absorption cross section. Other MAX compounds without titanium are being explored in addition to composite layers that will minimize oxygen diffusion through the protective coatings. Third, other deposition methods will be explored that minimize the impact on Zircaloy-4 microstructure during application. Future testing should seek to address many of these concerns by looking at altering MAX coating compositions and exploring composite layers while minimizing the edge oxidation effect, as well as, evaluating alternative application methods that minimize impact to the Zircaloy-4 microstructure and at the same time decrease coating porosity.

8.0 SUMMARY OF CONCLUSIONS

8.1. MATERIAL

MAX Phase coating materials are a good choice based on their good thermal conductivity, elevated temperature ductility, fracture toughness, weldability, high temperature mechanical stability, chemical stability, and high resistance to chemical attack.

Specifically Ti_2AlC for fuel cladding advantages include a relatively high resistance to elevated temperature oxidation, a high thermal conductivity and a coefficient of thermal expansion that is close to that of zirconium. Ti_2AlC has been shown to form a coherent, protective Al_20_3 oxide layer in high-temperature oxidizing environments.

Maxthal 211 Aluminum Titanium Carbide (Ti_2AlC Powder) is available at a specified size of d90 = 25 µm / d50 = 10 µm (i.e., 90% of the particles are below 25 µm in size and 50% of the particles are below 10 µm). The actual PSD was measured and the results indicate that over 50% volume was less than 13 µm. This underscores the need for characterization and quality inspections in manufacturing.

8.2. SPRAY METHODS

HVOF process resulted in a discoloration on the back surfaces of the samples, indicating that the Zircaloy-4 substrate had been heated to high temperatures and the composition of the deposited coating was substantially different from that of the original powder.

Microcracks were observed in HVOF coatings.

The HVOF process resulted in a more porous coating than CS.

Al_20_3 grains were observed at the interface for both spray processes. These are the grit blast used in surface preparation. Altering the surface preparation technique is required.

The HVOF sprayed MAX coating is mostly TiC with no Ti_3AlC_2 while the cold-spray coating shows mostly Ti_2AlC and Ti_3AlC_2 MAX Phase powders.

The surface roughness of the coating exceeds current fuel rod design limits which are nominally nearer to the bare sheet sample roughness.

The CS coating has a minimal effect on the microstructure of the substrate.

8.3. PERFORMANCE TESTING RESULTS

8.3.1. MECHANICAL

The high thermal diffusivity of Ti_2AlC is retained when applied as a coating.

The Ti_2AlC MAX coatings applied by both HVOF and Cold-Spray hold up beyond the SON design-base scratch load.

For the HVOF-coated Zircaloy-4, partial spalling is estimated to occur at 66 N. For the cold- spray coated Zircaloy-4, the coating appeared to spall off at a position corresponding to approximately 150N.

The CS coating provides 10 times more wear resistance than the bare Zircaloy-4.

The grinding of thicker coatings yields stronger and denser layers due to the removal of the less compressed outer layers. The increased strength and density may confer an increase in coating protectiveness.

8.3.2. INITIAL SCOPING

The initial scoping tests revealed poor corrosion results after 144 hours at 500°C and 3600 psi. This showed that more realistic conditions are needed for performance testing to separately represent Normal Operation, DBE, and BDBE.

8.4. NORMAL OPERATING CONDITIONS ASTM-G2 TESTING

After G2 testing, HVOF coatings showed cracks running through the coating thickness, and oxidized regions were clearly visible.

Normal operating conditions resulted in oxygen permeating the coating, forming aluminum and titanium oxides.

For multi-pass CS application, as the number of passes increased, the apparent surface waviness decreased.

There is oxygen diffusion/steam permeation along cracks, pores, and edges that leads to oxidation of the underlying Zircaloy-4.

For sintered samples, less oxidation of the interface was observed in cold-spray samples, but more oxidation of the uncoated Zircaloy-4 was observed, probably due to the significant microstructure changes to the Zircaloy-4 base material with the high temperature heat treatment.

The Ti_2AlC HVOF sample had a weight gain 55% less than the uncoated Zircaloy-4 sample. The Ti_2AlC cold-spray sample had a weight gain that was 57% less than the coated sample.

For HVOF coatings, significant oxidation at the sample edges and delamination shows that the

HVOF coating is not bound well to the substrate at the edges.

8.5. LOCA CONDITION TESTING

LOCA condition testing showed that the coatings did protect the substrate.

For CS coatings, the Zircaloy-4 substrate did not oxidize significantly beneath the MAX coating and remained well adhered to the surface. The there was no significant diffusion of steam beneath the edges of the coating. This result suggests that the coating adheres well to the surface and blocks lateral diffusion even if the bond at the surface is mostly a mechanical bond.

After oxidation at LOCA conditions, some AI diffused from the coating into the substrate. The diffusion of AI is of the order of 10 -20 m. Oxygen was not detected at the coating/substrate interface, which confirms that cold-sprayed Ti_2ALC coating protected the substrate out to the edges of the sample.

The cold-spray coatings were better at preventing substrate oxidation than HVOF coatings. The HVOF coatings showed signs of oxidation during the spraying process and this is one likely reason why they did not protect the Zircaloy-4 substrate as well as the cold-spray coatings.

The MAX cold-spray coatings are promising for protecting zirconium alloy cladding from oxidation under LOCA conditions.

8.6. OVERALL CONCLUSIONS

The CS method of depositing MAX Phase coatings ofTi_2AlC was proven. The HVOF method of applying coatings was eliminated.

Sintering the coatings was eliminated.

The wear resistance of the coatings was demonstrated.

It was shown that coatings are able to provide significant reduction in Zircaloy-4 oxidation for LOCA conditions.

APPENDIX H

Nano-Particles in Coolant during Accident Conditions for the Phase 1A Final Report for Enhanced Accident Tolerant Fuels

Prepared by:
AREVA Federal Services, LLC

TABLE OF CONTENTS

1.0 INTRODUCTION 1
2.0 CHARACTERISTICS OF NANO-FLUIDS 2
2.1. NANO-FLUIDS AND QUENCHING HEAT TRANSFER 2
2.2. CRITICAL HEAT FLUX OF NANO-FLUIDS BOTH IN POOL BOILING AND IN FLOW AT LOW PRESSURE CONDITIONS 3
2.3. WETTABILITY AND NANO-POROSITY OF SURFACES EXPOSED TO NANO-FLUIDS IN POOL BOILING CONDITIONS AT ATMOSPHERIC PRESSURE 4
3.0 CONCEPTUAL PRACTICAL USES OF NANO-FLUIDS 4
4.0 CONCLUSIONS 5
5.0 APPENDIX G REFERENCES 8

1.0 INTRODUCTION

Safe and secure operation of a reactor and the associated fuel under all conditions is best achieved by a defense in depth strategy. Most of the work conducted by AREVA under the Enhanced Accident Tolerant Fuel (EATF) program is focused on improvements to the performance of the fuel. Another potential path to secure the safety of the reactor in beyond design accident conditions is the introduction of nano-particles into the coolant that would adhere to the surface of the fuel cladding and protect it from oxidizing. This paper reports on the study conducted by AREVA into this potential technology enhancement.

Nano-fluids are colloidal dispersions of nano-particles (solid particles ranging in size from 1 to 100 nanometers) in water. A large number of experiments with nano-fluids using various nano-particle materials have been performed since 2000. The following have been generally observed:

- Better quenching capabilities due to a higher minimum heat flux (MHF) or Leidenfrost point (LFP) as compared to the pure water case at very low nano-particle concentrations (the MHF occurs at a higher wall superheat, up to 150°C higher than for pure water)[1],
- An enhanced (higher) observed critical heat flux (CHF)[2],
- Better wettability in pool boiling conditions at atmospheric pressure, and
- Higher thermal conductivities of nano-fluids under relatively high concentrations of nano-particles in fluids (around 100 – 1000 ppm and higher)[3].

The reason for the first three characteristics, according to the author of this study, is the deposition of nano-particles on the heated surfaces, which results in the creation of nano-porosity. The nano-porosity, in turn, leads to a radical change of the contact angle between steam bubbles and the heated surfaces which increase considerably the wettability of that surface. Nano-porosity also allows a substantial increase in the number of steam chimneys and capillaries present per unit surface, which increases the capability to evacuate heat from a nano-deposited surface.

The increased thermal conductivity of nano-fluids (i.e. the fourth characteristic cited above) results mainly from nano-particle loading, and particle aspect ratio.

For the convective heat transfer characteristics, there is not enough data to decide on the existence or not of improvements due to presence of nano-particles in liquids [4]. When compared with calculations made for the turbulent flow by the Dittus-Boelter equation, and to laminar flow by the Shah equation, it seems that the experimental data show a real improvement in the laminar flow regimen, while the enhancements shown in the turbulent regimen could be an analysis artifact.

The nano-fluids for all of these experiments were prepared in water using alumina, zirconia, silica, carbon, gold, platinum, and iridium nano-materials. Alumina, silica, and carbon (diamond) were the preferred materials of the initial nano-fluids experiments. Gold, platinum, and iridium were also studied because of their known stability, but later discarded due to their radiochemistry. Zirconia was selected and used in experiments based on engineering judgment.

All of the nano-particles used to prepare the nano-fluids were commercially available.

Based on a number of research studies sponsored by AREVA, both at Massachusetts Institute of Technology (MIT) and at the University of Florida, the following potential applications were considered useful for protecting fuel pin material integrity.

- Use of nano-fluids in injection systems associated with the Emergency Core Cooling Systems (ECCS) to increase margins during design basis events;

- Use of nano-fluids for reactor cavity flooding, supplementary to, and independent of the ECCS conditions, to increase safety margins during severe accidents.

Differently from other research organizations [5], AREVA has not considered the use of nano-fluids in the primary coolant in Pressurized Water Reactors (PWRs) to increase the power density in cores during power operation as a viable alternative. Two major concerns exist: 1) crudding of fuel surfaces during normal operation, and 2) licensing such a change in the primary system is a high economic risk. AREVA's experience in modeling CRUD indicated that additions of 100 – 1000 ppm colloids to the primary reactor water incur a serious increase in the fuel failure risk during normal operations.

In cases of accidents, the quantity of colloids (e.g. nano- particles) introduced in reactor water can be safely increased orders of magnitude larger than during normal operation, provided that sump evacuation is not degraded.

2.0 CHARACTERISTICS OF NANO-FLUIDS

2.1. NANO-FLUIDS AND QUENCHING HEAT TRANSFER

When a very hot solid object is immersed in a cooler fluid, the process is commonly known as quenching. In the following we provide the experimental evidence showing that in nano-fluids coolants, the heat transfer rates can greatly increase when successive quenching occurs.

Since quenching plays an important role during some sequences of nuclear power plant (NPP) severe accidents, when cooling of nuclear fuel rods happens, mainly through successive quenching, the use of nano-fluids may create an opportunity for significant performance improvements in such applications. The practical implementation of nano-fluids in these applications will be presented in Section 3.0 of this study. The present information, more extensively treated in [6] focuses on the mechanisms causing the acceleration of quenching by nano-fluids as studied on metallic rodlets of different diameters and also on spheres due to the effect of nano-particle deposition on destabilization of vapor film and progression of the quenching front.

The results of the testing also showed that the quenching behavior in nano-fluids is nearly identical to that in pure water for the first transition to film boiling, suggesting that the effect of the nano-fluid is negligible for the quenching performance. However, it was found that some nano-particles remain attached on the sphere or rodlet surfaces during the quenching process. In subsequent quenching tests they accelerate more and more at the end of the film boiling, bringing the MHF at a higher wall superheat than on a first time quenched metallic surface.

Quench tests with stainless steel spheres and rodlets in pure water, and in water-based alumina nano-fluid conducted at saturated and subcooled conditions under atmospheric pressure resulted in the following conclusions:

- The MHF temperature and quench front speed are significantly increased due to the nano-particle deposition on the surface, which occurs during repetitive quenching in nano-fluids. This effect is magnified at high sub-cooling and is expected with certitude at higher nano-fluid concentrations deposited.

- The significantly increased MHF temperature and quench front speed data cannot be predicted by the traditional correlations and models for MHF temperature, or the classical model for quench front speed. This suggests that the vapor film is destabilized and disrupted by a different mechanism associated with the nano-particle deposition.

- The successive nano-particle layers increase the water retention capabilities of the layers and, as such, the duration and area of the liquid–solid contacts during film boiling, which efficiently destabilizes the vapor film at higher temperatures.

- The very fast propagation of the quench front on the alumina nano-particle-fouled rodlets is also associated with the presence of numerous local liquid–solid contacts during film boiling phase, which creates fast traveling perturbation waves along the liquid-vapor interface with the ultimate effect of total disruption of the vapor film.

2.2. CRITICAL HEAT FLUX OF NANO-FLUIDS BOTH IN POOL BOILING AND IN FLOW AT LOW PRESSURE CONDITIONS

A number of experiments have shown that addition of alumina, zinc oxide, and diamond particles can enhance the CHF limit of water in flow boiling. This section presents results from experiments sponsored by AREVA and performed both at MIT [7] and at AREVA labs in Le Creusot, France [8].

The results of both sets of experiments lead to the same conclusion; improvements in CHF are real in the presence of nano-fluids and are essentially due to the deposition of nano-particles on the hot surfaces constituting the test sections. The higher the thickness of the nano-deposition in the heated area, the higher is the observed CHF. Values for CHF obtained were usually 30- 54% higher than those for the deionized (Appendix D, Reference 1) water tests. For the Le Creusot tests, the increase in CHF exceeds 54% and can be more than 100% for the test where the CHF is not reached due to a high temperature in the heater holder.

2.3. WETTABILITY AND NANO-POROSITY OF SURFACES EXPOSED TO NANO-FLUIDS IN POOL BOILING CONDITIONS AT ATMOSPHERIC PRESSURE

Film boiling phenomenon happens when a liquid droplet is placed on a surface held at a temperature much higher than the liquid's boiling point. The liquid droplet hovers on a vapor cushion without wetting the surface. This occurs at surface temperatures beyond the so-called LFP. If the surface temperature is at or above the LFP, heat transfer from the surface to the liquid takes place by conduction and radiation through the vapor layer separating the heating surface from the droplet, and thus the liquid takes a significantly longer time to evaporate than it would on a surface held at lower temperature. Therefore, higher LFP is desirable for rapid cooling of overheated components in high-power-density thermal systems, such as nuclear fuel rods during hypothetical accidents.

The film boiling heat transfer studies with nano-fluids, sponsored by AREVA, demonstrated that deposition of nano-particles on a surface significantly increases the nominal LFP up to ~500°C under atmospheric and saturated conditions, considerably accelerating the transient cooling of overheated objects [9]. However, such a high LFP could not be explained by the traditional LFP models based on hydrodynamic instability of the vapor film. A different mechanism associated with the thin nano-particle deposition layer has to disrupt and destabilize the vapor film. Characterization of the deposition layer suggested changes in roughness, wettability, and nano-scale porosity can be the causes for such a high LFP. The testing did not allow identification of the exact physical mechanism of LFP enhancement because nano-particle deposition in those experiments changed roughness height, wettability, and porosity simultaneously.

The LFP phenomena was investigated with custom-fabricated surfaces for which one could precisely separate the effects of roughness height, wettability, and nano-porosity [10] such as to be able to explain the contribution of each of these independent factors to the LFP phenomena.

The detailed study of the evaporating water droplets concluded that nano-porosity (not solely high surface wettability) is essential to enhance the LFP. The nano-porosity prevents establishment of a stable vapor film. The roughness of the surface (the micro-posts) only intensifies the effect of nano-porosity promoting intermittent liquid–surface contacts.

3.0 CONCEPTUAL PRACTICAL USES OF NANO-FLUIDS

The practical uses of nano-fluids considers both the main improvement characteristics to the use of nano-fluids (e.g. better quenching capabilities, higher critical flux, better wettability) as well as a number of other properties related to a practical day by day use of nano-fluids in a NPP. This section intends to present a study of some characteristics of nano-fluids more closely related to an immediate application of nano-fluids at a NPP.

Differently from other research organizations [5], AREVA has not considered the use of nano-fluids in the primary coolant of PWRs to increase the power density in cores during power operations as a viable alternative. AREVA's experience in crudding of fuel surfaces during normal operation and its experience in modeling CRUD indicate that additions of 100–1000 ppm colloids to the reactor coolant incur a serious increase in the fuel failure risk during normal operations.

For fuel CRUD risk assessments being currently performed, AREVA considers two types of conditions:

- Risk Conditions where the operating conditions for the fuel in the new cycle are similar to those experienced in the previous cycle, with allowance made for anticipated operating changes, and

- Margin Conditions where a number of plant transients with unfavorable operating and water chemistry conditions are considered for the new cycle.

The reason for looking at both situations during power operations is to bound the reasonably conceivable operating conditions from mild to very adverse, and then observe the fuel behavior under these conditions.

Running under very adverse conditions, one can reach deposition levels or characteristics of the deposit (composition or density of deposit) that approach the fuel manufacturer's limit. Adding nano-fluids increases the deposition of nano-particles in the deposit, resulting in additional densification of the deposit. If the deposit at a margin case has a density very close to that needed to create steam blanketing on the cladding surface under the deposit, adding the nano-fluids would add another layer of risk bringing even closer the steam blanketing condition. Plant operators do not want this added risk.

There are a number of other conditions specific to long term (on line) application of nano-fluids that have only been studied in a limited manner, such as cavitation, effect of nano-deposition on resin beds, distribution of nano-fluids in reactor vessel during accident conditions, hydraulic stability conditions during accidents, etc. Those define the differences between the two concepts of using the nano-fluids in NPP during accident conditions (MIT and AREVA).

Cavitation behavior and the effect of nano-deposition on resin beds have an effect on the long term operation of nano-fluids in NPP, but are tolerable for short term applications during accident conditions.

If it is found that the nano-particle coating discourage the formation of CRUD, then applying the CHF credit from those coatings may be further developed.

4.0 CONCLUSIONS

AREVA has pursued the application of nano-fluids during accident conditions in NPP's since 2006, sponsoring a number of studies on the subject performed at MIT and the University of Florida and in AREVA' own technical centers. The conclusions of these studies are summarized below.

1. Compared with water, the nano-fluids generally show:

    - Better quenching capabilities at very low nano-particle concentrations due to a higher MHF or LFP. The MHF occurs at a higher wall superheat, up to 150°C higher than for pure water [1].

    - An enhanced (higher) observed CHF [2],

2. The nano-fluids also show better wettability in pool boiling conditions at atmospheric pressure. The flow boiling CHF in water-based nano-fluids with alumina, zinc oxide, and diamond nano-particles performed by MIT in 2008 (sponsored by AREVA) and with zinc oxide by AREVA in 2012 had the following findings:

    - The nano-fluids exhibited a significant CHF enhancement (up to 40–50%) with respect to pure water at high mass flux (2000–2500 $kg/m^2 \cdot s$).

    - The enhancement did not occur at lower mass flux (1,500 $kg/m^2 \cdot s$).

    - The enhancement appeared to be weakly dependent on nano-particle concentration for the alumina nano-fluids, while it increased more pronouncedly with nano-particle concentration for the zinc oxide and diamond nano-fluids.

3. The wettability of heated boiling surfaces is increased by the nanoparticles deposited on the boiling surface during the experiments. There are models connecting higher wettability with increased CHF.

4. In nano-fluid coolants the heat transfer rates can greatly increase when successive quenching occurs. After four successive quenchings, the time to reduce the maximum temperature of a rod from 1,000°C to 100°C is reduced in half.

5. Nano-porosity (not solely high surface wettability) is essential to enhance the LFP. The nano-porosity prevents the stable vapor film establishment. The roughness of the surface (the micro-posts) intensifies the effect of nano-porosity by promoting intermittent liquid–surface contacts and increases the LFP temperature.

6. The presence of nano-fluids increases the cavitation erosion rate.

7. Comparison of resins after DI water or nano-fluid operation (two weeks continuous run) shows no change in kinetic performance of the typical NPP ion exchange resin due to interaction with diamond nano-particles.

8. Scanning electron microscope (SEM) imaging suggests that, once agglomerated, the diamond particles adhere to the NPP resin surface without affecting resin kinetics.

9. Short term stability of nano-fluid slurries with relatively high solids loading (~20 - 40%) under acidic conditions (pH around 4) have been proven. Long term stability studies for nano-fluids conceived for use in NPP have not been performed.

10. Dilution of concentrated nano-fluids in large masses of water is performed maintaining the nano-particle size following 24 hours of exposure. More experiments for stability of nano-fluids in the conditions of the sump chemistry during accident conditions are still needed.

11. Particle size, concentration, and pH did not change significantly when the nano-fluid was exposed to solutions of boric acid and lithium hydroxide at any concentration within the ranges tested. However, with alumina nano-fluid, significant particle flocculation and sedimentation occurred when the nano-fluid was mixed with concentrated solutions of trisodium phosphate. This may make alumina unsuitable for plants using trisodium phosphate.

12. Under radiation exposure nano-fluids show:
    - No visible agglomeration,
    - pH remains constant, and
    - Particle concentration remains unchanged.

13. Two concepts for use of nano-particles in ECCS in accident conditions were presented (MIT and AREVA). It was concluded that the AREVA concept is more flexible.

14. A simulation of the maximum power removed from containment in a Large Break Loss of Coolant Accident (LB-LOCA) indicated that working at 28 MWt removal capacity with nano-fluids provides sufficient margin from the static instability limit calculated for the system at 32 MWt.

15. A Probabilistic Risk Assessment (PRA) of the use of nano-fluids in an In Vessel Retention (IVR) accident indicates that when the operator will still have to actuate the nano-fluid injection system manually, there is a significant increase of the failure probability.

16. The PRA indicates that increase in risk due to the use of nano-fluids is insignificant compared to the overall risk, which is dominated by the probability of an accident progressing to the point where IVR is required. The increase in failure probability must be evaluated against the benefit of increased reactor safety when using nano-fluids.

17. A simulation of the LB-LOCA performed by MIT for a Westinghouse AP 1000 indicated that for PWR plants that are not Loss of Coolant Accident-limited but CHF-limited, an improvement of the CHF using nano-fluids provide provides significant additional protection for the plant during a LB-LOCA.

18. An experimental study of the post-CHF heat-transfer characteristics of nano-fluids at prototypical reactor conditions is needed before the merit of nano-fluids for the ECCS application can be fully judged.

    AREVA has concluded that an enhancement to ECCS systems which utilizes the benefits of nano-fluids is feasible.

5.0 APPENDIX G REFERENCES

1. H. Kim, B. Truong, J. Buongiorno, L. W. Hu, "On the effect of surface roughness, wettability and nano-porosity on Leidenfrost phenomena", App*lied Physics Letters*, 98, 083121, 2011.
2. S.J. KIM, B. TROUNG, J. BUONGIORNO, L.W. HU, I.C. BANG, *Study of Two-Phase Heat Transfer in Nanofluids for Nuclear Applications, Proceedings of ICAPP '06*, Reno, NV USA, June (2006).
3. Buongiorno, D. C. Venerus, N. Prabhat, T. McKrell, J. Townsend, R. Christianson, Y. V. Tolmachev, P. Keblinski, …. (and >60 other authors) "A Benchmark Study on the Thermal Conductivity of Nanofluids", *J. Applied Physics*, Vol.106, Issue 9, 2009. (Selected for the November 30, 2009 issue of Virtual Journal of Nanoscale Science & Technology).
4. N. Prabhat, J. Buongiorno, and L.-W. Hu, "Convective Heat Transfer Enhancement in Nanofluids: Real Anomaly or Analysis Artifact?", *J. Nanofluids*, 1, 55–62, 2012
5. J. Buongiorno, L. W. Hu, S. J. Kim, R. Hannink, B. Truong, E. Forrest, "Nanofluids for Enhanced Economics and Safety of Nuclear Reactors: an Evaluation of the Potential Features, Issues and Research Gaps", *Nuclear Technology*, Vol. 162, 80-91, 2008.
6. H. Kim, T. McKrell, J. Buongiorno, L. W. Hu, "Nanoparticle Deposition Effects on the Minimum Heat Flux Point and Quench Front Speed during Quenching of Rodlets and Spheres in Water-Based Alumina Nanofluids", *Int. J. Heat Mass Transfer*, 53, 1542–1553, 2010.
7. S. J. Kim, T. McKrell, J. Buongiorno, L. W. Hu, "Experimental Study of Flow Critical Heat Flux in Alumina-Water, Zinc-oxide-Water and Diamond-Water Nanofluids", *ASME J. Heat Transfer*, Vol. 131, 043204, 2009.
8. Mourgues, V. Hourtané, T. Muller, M. Caron-Charles, "Boiling behaviors and critical heat flux on a horizontal and vertical plate in saturated pool boiling with and without ZnO nanofluid," *Int. J. Heat Mass Transfer*, 57, 595–607, 2013.
9. H. Kim, T. McKrell, J. Buongiorno, L. W. Hu, "Nanoparticle Deposition Effects on the Minimum Heat Flux Point and Quench Front Speed during Quenching of Rodlets and Spheres in Water-Based Alumina Nanofluids", *Int. J. Heat Mass Transfer*, 53, 1542–1553, 2010.
10. H. Kim, B. Truong, J. Buongiorno, L. W. Hu, "Effects of micro/nano-scale surface characteristics on the Leidenfrost point temperature of water", *Journal of Thermal Science and Technology*, Vol. 7, No. 3, 453-462, 2012.

APPENDIX I

Fuel Cycle Impacts
for the
Phase 1A Final Report
for Enhanced Accident Tolerant Fuels

Prepared by:
AREVA Federal Services, LLC

TABLE OF CONTENTS

1.0 INTRODUCTION 1
2.0 FUEL CYCLE IMPACTS 1
3.0 APPENDIX I REFERENCES 2

LIST OF TABLES

Table 1: Pellet Change 1
Table 2: Table of Thermal Absorption Cross Sections 2

1.0 INTRODUCTION

This appendix investigates the impact of the pellet modifications and cladding coatings on fuel assembly energy production.

Previous work [1] investigated the costs and benefits of increasing enrichments past 5 weight percent.

It is concluded that:

1. Applying the benefits found in Reference [1] can compensate for the impacts of all pellet modifications and coating materials and thickness investigated in the project. The largest enrichment increase required will be less than 1%.

2. Further increases in enrichment beyond that required to compensate for the negative effects of the pellet modifications and coatings on fuel assembly energy production will yield an economic benefit that can offset the additional cost of enhanced accident tolerant fuel (EATF).

2.0 FUEL CYCLE IMPACTS

Effects of fuel pellet changes under consideration for the EATF project were evaluated and the overall impact of each was estimated based on the neutronics effects. These estimates are approximate in nature and are based on lattice calculations. The CASMO3 code was used to model the pellet changes although not all materials are available in the library; in that case similar materials were selected that had nuclear cross section properties that were close and/or number densities were modified. For all pellet changes, a 2D depletion was performed and compared to the base case depletion. The difference in reactivity towards EOC was calculated and converted to equivalent enrichment deficit. The deficit represents the additional fresh fuel enrichment that would be needed to overcome the cycle length decrease of the pellet changes.

While there are some approximations made for this work due to the very limited scope, the results should be representative of a more detailed analysis when that is performed. The relative ranking of these effects is still useful input to design decisions.

The following table summarized the effects of each fuel pellet change and the additional U235 enrichment needed to overcome the decrease in energy from the pellet change.

Pellet Change U235 w/o	Additional
10% (by mass) Silicon Carbide (SiC) uniformly distributed in the pellets	0.22
50 micrometer coating of TiO_2 on the pellets	0.06
50 micrometer coating of Ti_2AlC on the pellets	0.07
50 micrometer coating of YSZ on the pellets	0.01

Table 1: Pellet Change

In conclusion, the **total enrichment impact of a pellet containing 10% SiC in a Zircaloy rod with a 50 micron coating of Ti_2AlC will be about 0.3%**. This will be factored into future updates of the Business Plan.

Also of potential interest is a table of thermal absorption cross sections:

Material	Neutron Absorption Cross Section, barns
O	0.28 x 10 -3
Si	0.171
C	3.5 x 10 -3
Ti	6.1
Al	0.233
V	5.0
Y	1.28

Table 2: Table of Thermal Absorption Cross Sections

From this table, we see that the thickness of the coating is an important parameter affecting fuel assembly energy production. This data implies that the option to investigate alternatives to Ti_2AlC should be kept open. For example, replacement of the Ti in the MAX Phase coating with a metal that has a lower neutron cross section should be investigated.

3.0 APPENDIX I REFERENCES

1. AREVA, Task Order 5: Advanced Fuels for Future Light Water Reactors, RPT-3005805-001, November 18, 2011, Chapter 14.

APPENDIX J

ATR Irradiation Tests
for the
Phase 1A Final Report
for Enhanced Accident Tolerant Fuels

Prepared by:
AREVA Federal Services, LLC

TABLE OF CONTENTS

1.0 INTRODUCTION 1
2.0 RESPONSIBILITIES FOR PRODUCTION OF PELLETS 1
3.0 FUEL COLUMN/PELLET REQUIREMENTS 2
3.1. GENERAL 4
3.2. RODLET FABRICATION PROCESS 4
4.0 AS-BUILT DATA 6
4.1. MEASURED PELLET DATA 6
4.2. AS-BUILT MEASUREMENTS EVALUATION 6
5.0 RODLETS 10
6.0 POST-IRRADIATION EXAMINATIONS FOR ATR RODLETS 11
6.1. OPTICAL MICROSCOPY OF FUEL (TRANSVERSE SECTION) 11
6.2. THERMAL CONDUCTIVITY MEASUREMENTS 11
6.3. GAS PRESSURE AND VOID VOLUME MEASUREMENTS 11
6.4. SCANNING ELECTRON MICROSCOPY OF FUEL 11
6.5. VISUAL INSPECTION OF INTACT RODLET 11
6.6. SCANNING ELECTRON MICROSCOPY OR ELECTRON PROBE MICROANALYSIS OF CLADDING (FUEL SIDE) 11
6.7. PELLET DENSITY 12
6.8. GAMMA SCAN 12
6.9. OPTICAL MICROSCOPY OF FUEL (LONGITUDINAL SECTION) 12
6.10. RADIOCHEMICAL ANALYSIS 12
6.11. FISSION GAS ANALYSIS 12
7.0 CONCLUSION 12
8.0 REFERENCES 13

LIST OF TABLES

Table 1: Summary of Fuel Types to be Tested 1
Table 2: Tasks and Responsibilities 2
Table 3: Fuel Pellet Compositions 3
Table 4: Fuel Pellet Physical Properties 3
Table 5: Fuel Analysis Requirements and Limits. 3
Table 6: Cladding Tube Attributes. 4
Table 7: EATF ATR Rodlet Loading Plan 5
Table 8: ATR Irradiation Test Pellet Measurement Averages 8
Table 9: ATR Irradiation Test Pellet Tolerance Limits 8

LIST OF FIGURES

Figure 1: Lengths of Pellets for ATR Irradiation Tests 6
Figure 2: Diameters of Pellets for ATR Irradiation Tests 7
Figure 3: Volumes of Pellets for ATR Irradiation Tests 7
Figure 4: ATR Irradiation Test Pellet Length vs Number Produced for 4.95 w/o Pellets 9
Figure 5: Photographs of Rodlets ATF-A01 through ATF-A06 10

1.0 INTRODUCTION

The Enhanced Accident Tolerant Fuel (EATF) pellet includes 10% of either SiC or nano-diamond additive, which is incorporated by the use of a new process called Spark Plasma Sintering (SPS). Measurements of a number of parameters, discussed in Section 6, are required to support licensing and prove the benefits of the technology concept.

There are many tests that can be performed on fresh fuel to measure various parameters. However, irradiation testing is required to evaluate some of the most important ones, including thermal conductivity (TC), changes in fuel microstructure, and fission gas release (FGR), so pellets were produced for irradiation testing.

The testing will be performed in the Advanced Test Reactor (ATR) at Idaho National Laboratory (INL). Pellets of several types were produced for this irradiation testing. Table 1 lists the rodlets to be tested, and their contents [8].

This Appendix describes production of the pellets, characteristics of the pellets, production of rodlets, and characteristics of the rodlets. A final section describes plans for postirradiation examination.

Rodlet ID	Rodlet End Cap ID	Fuel ID	Fuel Pellet Type	Target Burnup, GWd/MTU
ATF-A01	A 01	Base-1	UO_2	10
ATF-A02	A 02	Base-2	UO_2	50
ATF-A03	A 03	SiC(f)-1	UO_2 with SiC fibers	10
ATF-A04	A 04	SiC(f)-2	UO_2 with SiC fibers	50
ATF-A05	A 05	Diamond-1	UO_2 with diamond particles	10
ATF-A06	A 06	Diamond-2	UO_2 with diamond particles	50

Table 1: Summary of Fuel Types to be Tested

2.0 RESPONSIBILITIES FOR PRODUCTION OF PELLETS

Production of pellets was a cooperative effort by AREVA, the University of Florida (UF), and INL. The major tasks in preparing and irradiating the rodlets are listed in Table 2. “Provider” indicates the organization responsible for performing the task, and “Recipient” indicates the organizations that receive the material or information produced as a result of completing the task. In broad terms, AREVA was responsible for defining the pellet design and providing special nuclear materials. AREVA was also responsible to ensure that UF personnel fabricating fuel for the ATF project had adequate training and qualifications. All training records in support of fuel fabrication were included and managed in the AREVA records management system identified in

Reference 1. UF was responsible for procuring fuel pellet additives and fabricating the pellets under the AREVA Federal Services LLC QA Program [7] and Manufacturing Procedure [4], and INL was responsible for assembling the rodlets and irradiating them.

Table 2 includes a summary of responsibilities for verification, inspection and acceptance of ATF-1 rodlet components.

Task #	Provider	Description	Recipient
1	AREVA	Provide rodlet design information	INL
2	AREVA	Provide pellet specification	INL, UF
3	AREVA	Provide conditions for irradiation (LHGR)	INL
4	INL	Determine the U_{235} enrichment needed to meet test objectives	AREVA, UF
5	AREVA	Provide enriched UO_2 powder	UF
6	AREVA	Provide certificate for UO_2 powder	INL, UF
7	UF	Procure additives (Cr_2O_3, SiC, diamond)	N/A
8	UF	Procure other supplies and tooling	N/A
9	UF	Fabricate pellets	N/A
10	AREVA	Ship pellets to INL	INL
11	AREVA	Provide certificates for additives	INL
12	AREVA	Provide pellet manufacturing certificates	INL
13	AREVA	Provide cladding	INL
14	AREVA	Provide cladding certificates	INL
15	INL	Report on pellet dimensional inspection	UF, AREVA
16	INL	Provide plenum springs and end caps	N/A
17	INL	Assemble rodlets	N/A
18	INL	Report on rodlet assembly	UF, AREVA
19	INL	Provide capsule components	N/A
20	INL	Assemble capsules	N/A
21	INL	Irradiate capsules/rodlets	N/A
22	INL	Report on irradiation conditions	AREVA, UF
23	AREVA	Provide Fuel Material Properties	INL

Table 2: Tasks and Responsibilities

3.0 FUEL COLUMN/PELLET REQUIREMENTS

This section provides information on the design of the fuel pellets. It has been noted in Table 1 that there are three types of rodlets, which are denoted as Base, SiC(f), and Diamond. However, there are four types of fuel pellets, which are denoted as Base, SiC(f), Diamond, and Blanket. The Base and Blanket pellets are UO_2, and they differ only in their U_{235} enrichments. The SiC(f) and Diamond pellets contain 10% of SiC fibers, and diamond, respectively, where the percentage is given on the basis of solids volume. The balance of the SiC(f) and Diamond pellets is UO_2, which may be doped with a small concentration of Cr_2O_3. The resulting compositions, on a mass basis, are provided in Table 3. Physical properties of the pellets are given in Table 4, along with the pellet count for each type. Each rodlet was to contain ten pellets. (Because of stack length

limits, rodlet ATF-A04 was built with only nine pellets.) The middle eight (seven for ATF-A04) form the active stack, which is composed of pellets corresponding to the rodlet type. The two end pellets are Blanket type and help to control power peaking at the ends of the rodlets. The pellet counts in Table 4 reflect the total number of pellets that were to go in the rodlets. The fuel pellets were produced at the University of Florida and shipped to INL for loading into rodlets.

Limits on impurities for Base and Blanket fuel pellets are provided in Table 5. Calculated impurity concentrations for SiC(f) and the fuel Diamond pellets were provided. Additional requirements are provided in Reference 2.

Pellet Type	Constituent Mass Fraction (wt. %)*			U-235 enr. (%)*
	UO_2	SiC	Diamond	
Base	100.00	---	---	4.95
SiC(f)	96.84	3.16	---	4.95
Diamond	96.56	---	3.44	4.95
Blanket	100.00	---	---	0.21
* All values ± 10%				

Table 3: Fuel Pellet Compositions

Pellet Type	Diameter (inch) ± .0010	Length (inch) ± .050	Typical Density (g/cm^3)**	Pellet Count
Base	0.3225	0.40	10.58	16
SiC(f)	0.3225	0.40	9.83	16
Diamond	0.3225	0.40	9.86	16
Blanket	0.3225	0.40	10.58	12
** For information only				

Table 4: Fuel Pellet Physical Properties

Element	Maximum concentration (µg/g U)
Al	250
Ca + Mg	200
Co	100
F	15
Fe	500
Th	10

Table 5: Fuel Analysis Requirements and Limits.

3.1. GENERAL

Material acquisition and fabrication were performed to Quality Level-3 per QLD MSA-000203 and the ATF Quality Implementation Plan [Reference 6] for the rodlet components (Items -1, -7 and -8) as identified in Drawing 604287

3.2. RODLET FABRICATION PROCESS

Rodlet components were fabricated using materials provided by AREVA according to the INL process. Material identification was maintained to ensure component traceability.

3.2.1. RODLET MATERIALS

AREVA provided a single section of Zircaloy-4 stock tubing with associated certifications. The tube was cut to length at INL per drawing dimensions in Reference 3. The composition was similar to that of UNS R60804 as defined in Table 2 of ASTM B811-13 [Reference 5]. Characteristics of the cladding tube are provided in Table 6.

INL provided the end caps, plenum spring, and fill gas.

Design Parameter	Nominal Value
Length	4.50 inch
Outside Diameter (OD)	0.374 inch
Inside Diameter (ID)	0.327 inch
Rodlet material composition	Zircaloy-4
Liners/coatings thickness	not applicable

Table 6: Cladding Tube Attributes.

Rodlet 1

Diamond-1	Height	Avg OD	Mass (g)
AB-4	0.391	0.3222	5.52
AD-20a	0.3822	0.3219	5.1929
AD-22	0.3822	0.3222	4.9129
AD-24	0.3825	0.3207	4.9215
AD-25	0.3849	0.3222	4.9471
AD-17	0.4036	0.3201	5.19
AD-19a	0.4052	0.3208	5.1791
AD-3	0.4075	0.3223	5.2148
AD-15a	0.4077	0.3226	5.2508
AB-10	0.392	0.3224	5.424
Stack Height	3.9388		51.7531
Margin	0.0612		

Rodlet 2

Diamond-2	Height	Avg OD	Mass (g)
AB-24c	0.3961	0.3225	5.5263
AD-1	0.39	0.3228	5.046
AD-23	0.3907	0.3217	4.9593
AD-5a	0.3964	0.322	5.1626
AD-2	0.397	0.3231	5.1218
AD-7a	0.3985	0.3218	5.1552
AD-14a	0.3992	0.3231	5.1636
AD-16	0.402	0.3227	5.1677
AD-11c	0.4022	0.3235	5.1927
AB-5	0.3843	0.3221	5.428
Stack Height	3.9564		51.9232
Margin	0.0436		

Rodlet 3

SiC-1	Height	Avg OD	Mass (g)
AB-7	0.3756	0.3232	5.2656
AW-21a	0.388	0.3214	4.8651
AW-20a	0.3949	0.321	4.9846
AW-19a	0.3956	0.3205	4.9775
AW-2	0.399	0.3207	4.7003
AW-14	0.4056	0.3222	5.1504
AW-13	0.406	0.3214	5.1242
AW-15	0.4044	0.3211	5.1182
AW-24a	0.402	0.3212	5.0488
AB-29a	0.391	0.3224	5.5079
Stack Height	3.9621		50.7426
Margin	0.0379		

Rodlet 4

SiC-2	Height	Avg OD	Mass (g)
AB-32e	0.4007	0.3211	5.5469
AW-10	0.4136	0.3215	5.1839
AW-16a	0.4147	0.321	5.1696
AW-1	0.413	0.3218	5.1869
AW-17a	0.4152	0.3207	5.1764
AW-11c	0.4086	0.3217	5.1495
AW-26a	0.4122	0.3212	5.1955
AW-12	0.4127	0.3223	5.1303
AB-27a	0.3823	0.3232	5.4929
Stack Height	3.673		47.2319
Margin	0.327		

Rodlet 5

Base-1	Height	Avg OD	Mass (g)
AB-15b	0.389	0.3226	5.4246
AE-10c	0.38615	0.3242	5.4751
AE-21	0.405	0.3244	5.6831
AE-25	0.3882	0.3228	5.5033
AE-27	0.3896	0.3234	5.5285
AE-11	0.3961	0.32315	5.545
AE-22	0.3976	0.323	5.5765
AE-30a	0.399	0.3232	5.641
AE-29e	0.3877	0.3222	5.845
AB-31a	0.3975	0.3232	5.5762
Stack Height	3.93585		55.7983
Margin	0.06415		

Rodlet 6

Base-2	Height	Avg OD	Mass (g)
AB-25a	0.3891	0.3227	5.4935
AE-8	0.391	0.3229	5.5005
AE-14	0.39	0.3226	5.4943
AE-X	0.39	0.3228	5.5298
AE-19a	0.3908	0.3228	5.5289
AE-18	0.3912	0.3235	5.537
AE-23	0.3947	0.3223	5.5493
AE-28a	0.3954	0.3229	5.5411
AE-12	0.3942	0.3219	5.5258
AB-26a	0.3962	0.3239	5.4994
Stack Height	3.9226		55.1996
Margin	0.0774		

One Blanket Pellet (AB-Orange) should be loaded at each end of the stack
Pellets in yellow should be loaded at the stack ends next to the blankets
Remaining interior pellets may be loaded in any order

Table 7: EATF ATR Rodlet Loading Plan

4.0 AS-BUILT DATA

4.1. MEASURED PELLET DATA

The measurements of pellet length, diameter, and mass are provided in Table 7.

4.2. AS-BUILT MEASUREMENTS EVALUATION

The pellets manufactured for the ATR irradiation tests were evaluated to see if any trends in dimensions and volumes could be found. It should be noted that any trends exhibited may reflect the process or the process operator actions.

The following parameters were evaluated:

1. the pellet length
2. the pellet diameter (average of the two diameter values)
3. the pellet volume (relative to the average volume of all of the pellets)

The lengths, diameters, and volumes are plotted in Figure 1, Figure 2, and Figure 3, respectively.

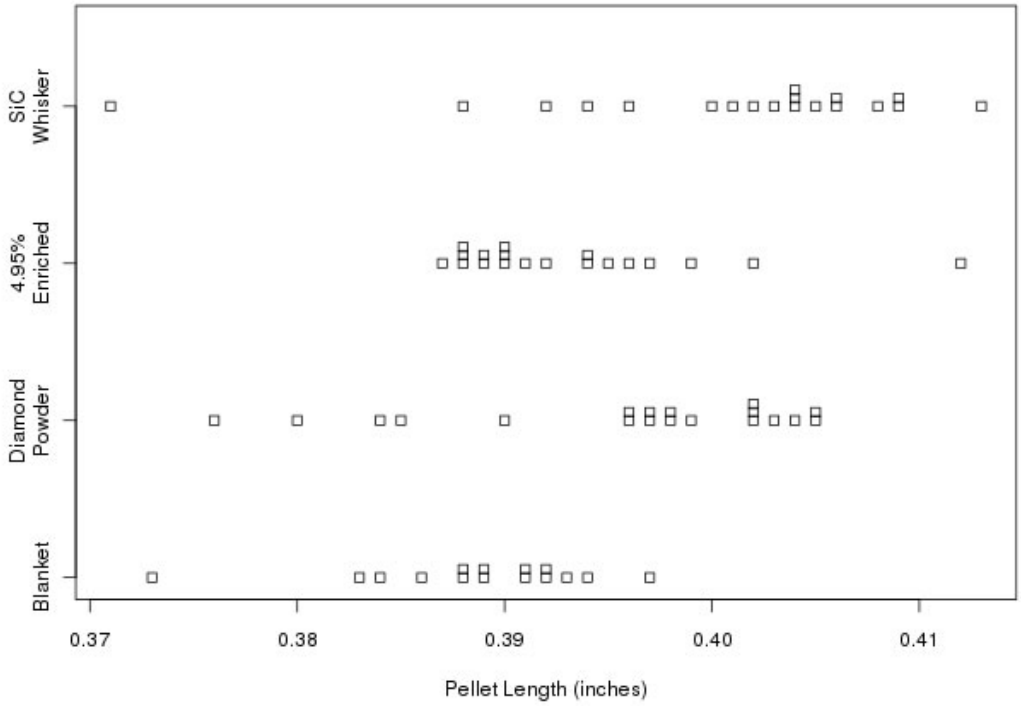

Figure 1: Lengths of Pellets for ATR Irradiation Tests

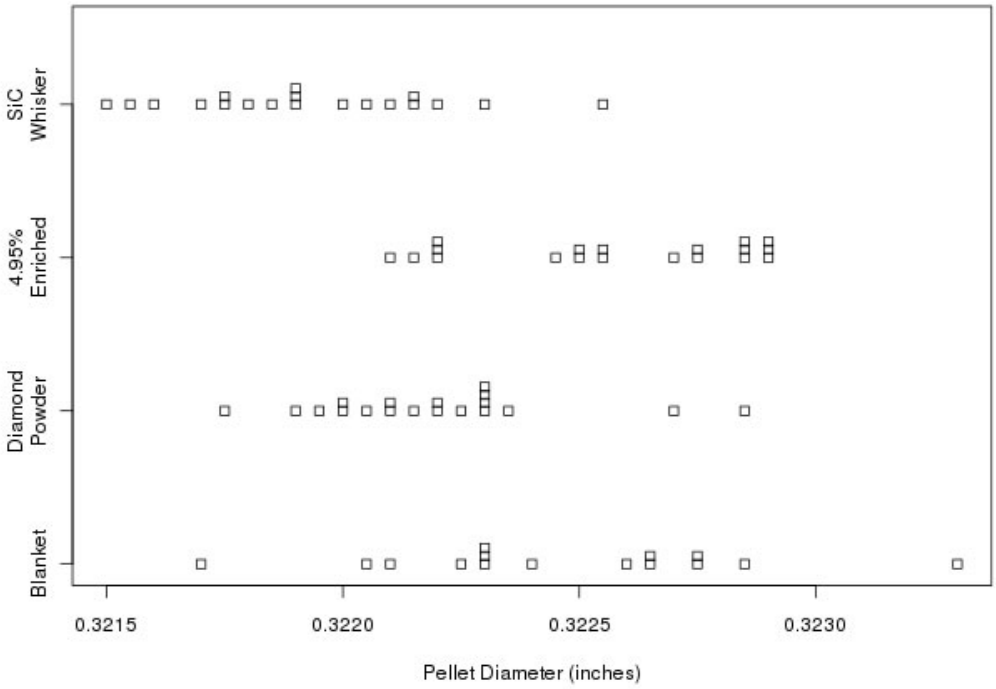

Figure 2: Diameters of Pellets for ATR Irradiation Tests

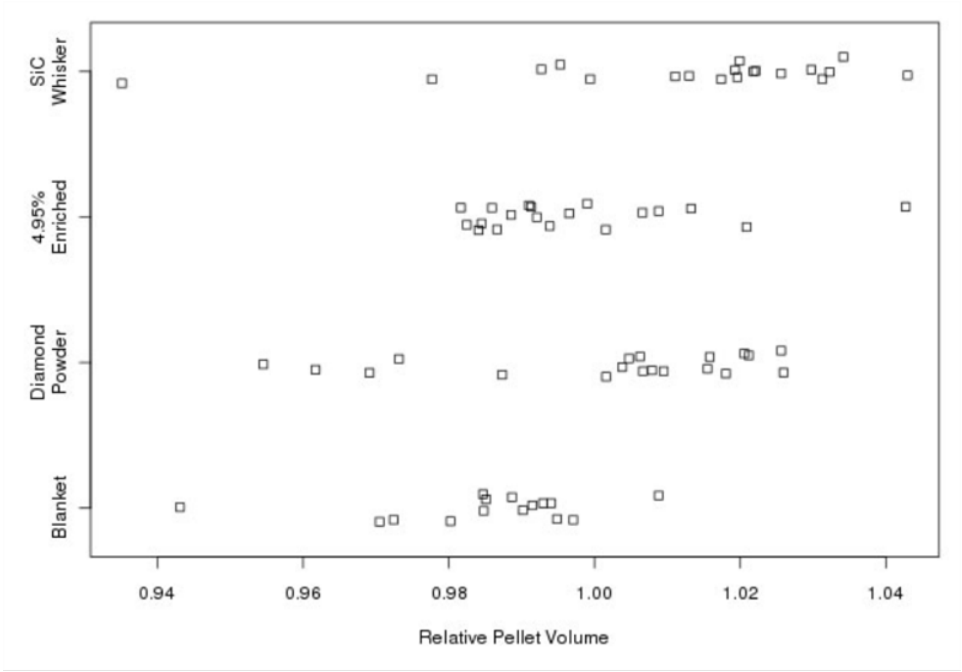

Figure 3: Volumes of Pellets for ATR Irradiation Tests

The only solid conclusion that can be made is that the SiC(f) pellets seem to be slightly longer and larger, and the diamond powder pellets seem to be slightly shorter and smaller. Notice that the resolution of the measurements is clearly visible for the lengths and diameters.

The averages of the pellet lengths, diameters, and volumes are presented in Table 9.

Pellet Type	Length (in)	Diameter (in)	Volume
SiC whisker	0.3887	0.3225	0.9853
4.95% enriched	0.3957	0.3222	1.0020
Diamond powder	0.3932	0.3226	0.9974
Blanket	0.4008	0.3219	1.0130

Table 8: ATR Irradiation Test Pellet Measurement Averages

With the exception of the Blanket pellets, the lengths of the pellets are not normally distributed, which makes calculating tolerance limits difficult and not very meaningful. The 95%/95% tolerance interval for the length of the Blanket pellets is

Blanket pellets: length = 0.3887 ± 0.0170

The 95%/95% tolerance intervals for the diameters of the pellets are given in Table 9. Again, the diameters of the Base pellets were not normally distributed, so tolerance limits were not calculated.

Pellet Type	Diameter (in)
SiC whisker	diameter = 0.3219 ± 0.0008
Diamond powder	diameter = 0.3222 ± 0.0007
Blanket	diameter = 0.3225 ± 0.0012

Table 9: ATR Irradiation Test Pellet Tolerance Limits

None of the pellet types had volumes that were normally distributed.

In looking for trends in the data, there was nothing interesting to be seen in the diameter or the shape (comparison of the two diameters) of the pellets. The pellets tended to be very nearly round.

Only the Base pellets had a statistically significant trend with respect to order of manufacture. The length of the pellet increased as more pellets were produced, as shown in Figure 4. It is noted this reflects both process and operator action trends.

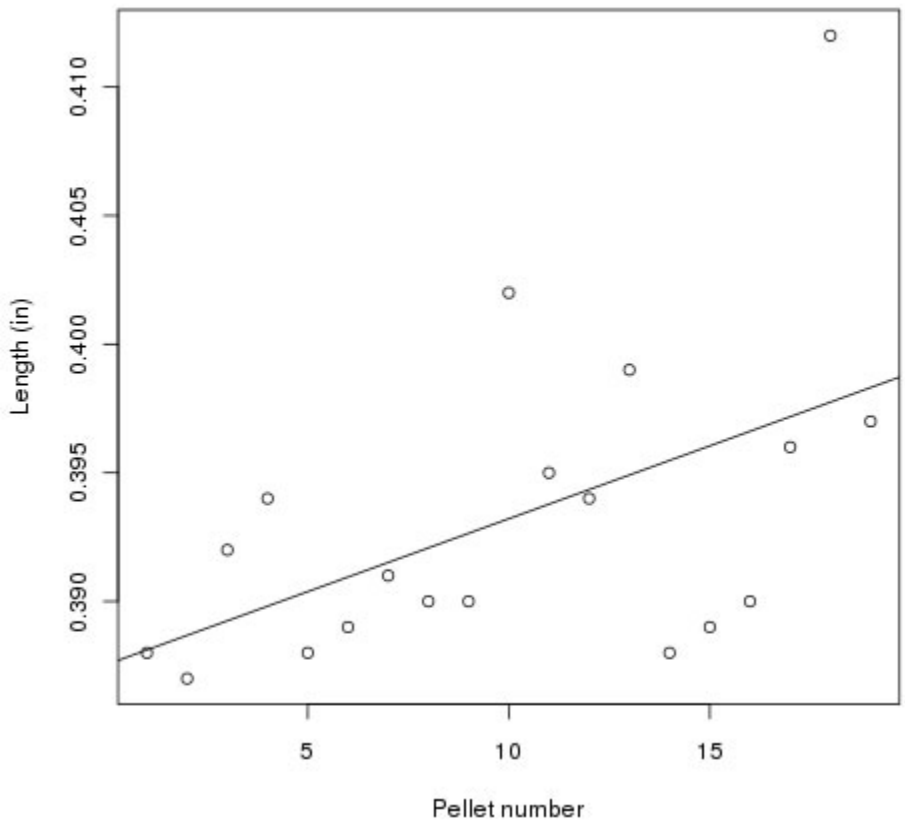

Figure 4: ATR Irradiation Test Pellet Length vs Number Produced for 4.95 w/o Pellets

Because of this increase in length, there also was a statistically significant increase in the pellet volume.

5.0 RODLETS

Pictures of the finished rodlets are provided in Figure 5.

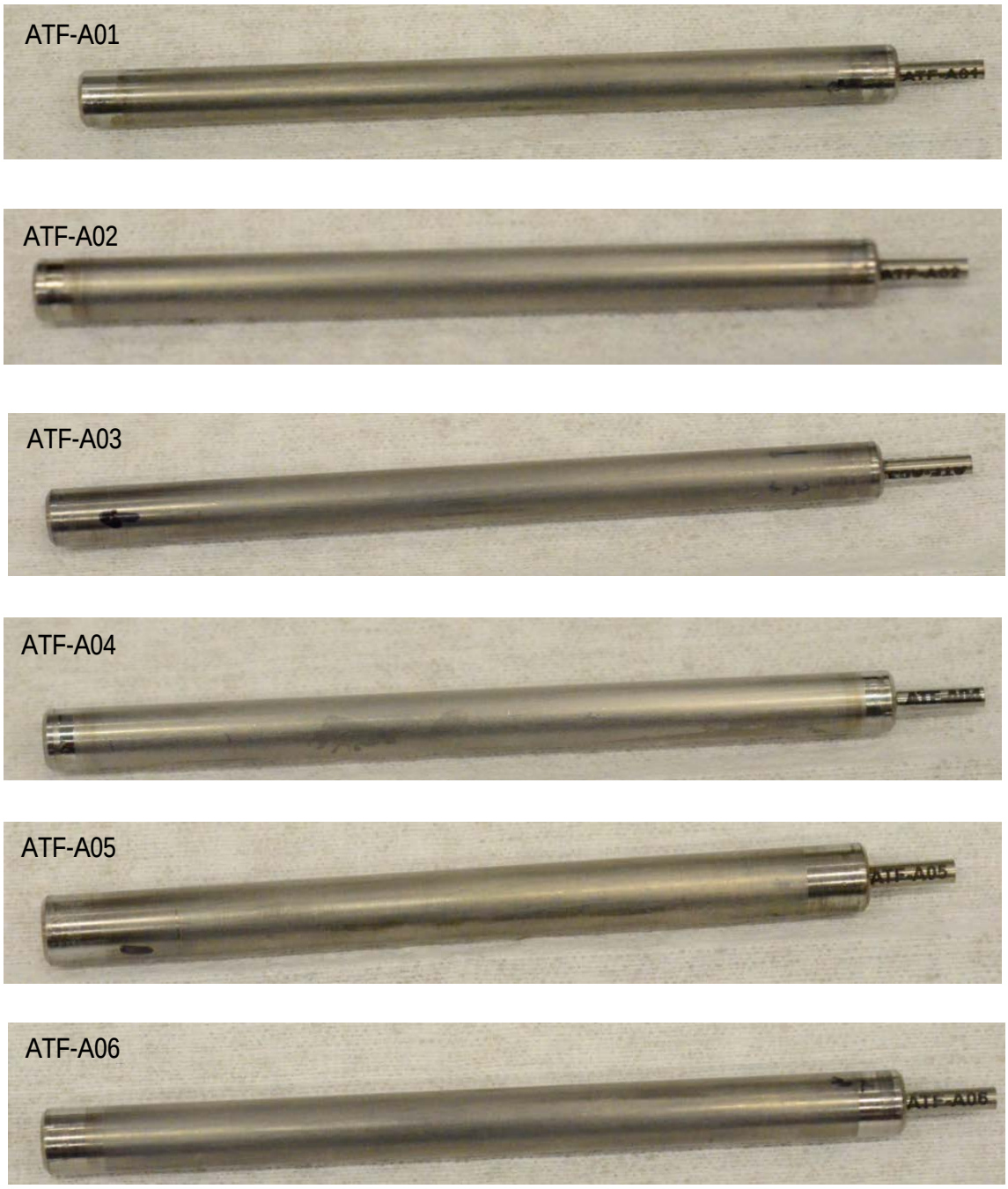

Figure 5: Photographs of Rodlets ATF-A01 through ATF-A06

6.0 POST-IRRADIATION EXAMINATIONS FOR ATR RODLETS

After irradiation, the rodlets will be examined in a hot cell. The following sections describe the proposed examinations. The examinations described in Sections 6.1 through 6.4 should have the highest priority; those in Sections 6.5 through 6.8 should have intermediate priority, and those in Sections 6.9 through 6.11 should have lower priority.

6.1. OPTICAL MICROSCOPY OF FUEL (TRANSVERSE SECTION)

Each rodlet should be cut transversely to provide at least one metallographic mount. A second mount might be useful if the first one shows interesting results. Low-magnification optical microscopy will provide information about cracking, which may or may not be different than that of standard pellets. Higher-magnification optical microscopy may provide information about the microstructure that is indicative of fuel temperatures or of degradation of the silicon carbide and diamond. Grain size measurements may be useful.

6.2. THERMAL CONDUCTIVITY MEASUREMENTS

A transverse slice should be cut from each rodlet for TC measurements. It may be necessary to treat the slice (e.g., by bonding it to a thin substrate or infiltrating it with epoxy) to prevent crumbling.

6.3. GAS PRESSURE AND VOID VOLUME MEASUREMENTS

Each rodlet should be punctured. Gas pressure and void volume measurements should be measured, probably by a double expansion method. The results will provide information about FGR, and that may be indicative of fuel temperature.

6.4. SCANNING ELECTRON MICROSCOPY OF FUEL

At least one sample from each SiC-containing rod should be examined by scanning electron microscopy. This exam will provide information about degradation of the silicon carbide and diamond. Secondary electron imaging is suggested, with comparison of the center, mid-radius, and rim, which will be exposed to different temperatures. The thickness of the fuel-side oxidation of the cladding should be measured. Optical metallographic mounts can be reused for all of the examinations listed above. Additional microscopy may be in order if indicated by the initial exams.

6.5. VISUAL INSPECTION OF INTACT RODLET

This is a basic inspection, though an encapsulated rod is unlikely to show any interesting features on its surface.

6.6. SCANNING ELECTRON MICROSCOPY OR ELECTRON PROBE MICROANALYSIS OF CLADDING (FUEL SIDE)

The silicon carbide and diamond could affect the oxygen potential in the fuel, and that could affect the deposition of fission products on the inner surface of the cladding. Preparation for the exam would require slitting a sample of fuel longitudinally and mechanically defueling the cladding. The defueled cladding could then be examined by wavelength dispersive spectroscopy.

6.7. PELLET DENSITY

The presence of silicon carbide or diamond may affect swelling, so it would be useful to measure the density of the irradiated pellets. One sample per rodlet should suffice. Fuel fragments removed to allow examination of the inner surface of the cladding could be reused for this examination.

6.8. GAMMA SCAN

One-dimensional (elevation) gamma scans are appropriate for each rod. The scans will provide the final stack length, the location of any stack gaps, and maybe the axial burnup profile. If it is concluded that burnup profiles are needed, a semiconductor detector would be preferable, and four scans should be done at azimuth angles of 0, 90, 180, and 270°.

6.9. OPTICAL MICROSCOPY OF FUEL (LONGITUDINAL SECTION)

A longitudinal mount may provide information about dish-filling.

6.10. RADIOCHEMICAL ANALYSIS

A neutronic prediction of burnup will presumably be available, but a confirmatory measurement by the Nd-148 method would be helpful. Selected rods (e.g., one for each fuel type) would be analyzed.

6.11. FISSION GAS ANALYSIS

The presence of silicon carbide or diamond is not expected to affect the composition of the released fission gas, but a gas analysis would confirm that.

7.0 CONCLUSION

Rodlets containing fuel pellets with additives to enhance accident tolerance were successfully fabricated. These pellets, fabricated with the SPS process contain 10% of either SiC whiskers or nano-diamond additive. Irradiation in the ATR and subsequent Post-Irradiation Examination in the ATR will provide data necessary for licensing EATF for use in a commercial reactor.

8.0 REFERENCES

1. "Records Management", AFS-RM-PRC-001 (current revision), AREVA Federal Services.

2. "Technical Specification for Nuclear Fuel Pellets to Be Irradiated in the Advanced Test Reactor", AREVA Federal Services, SPC-3009802-0031, February 4March 12, 2014.

3. "AREVA ATF (Accident Tolerant Fuel) Experiment Fuel Rodlet End Cap and Tube Details", DWG-604287, INL, 2013.

4. "Manufacturing Procedure for Pellet Lot Intended for Irradiation in the Advanced Test Reactor", AREVA Federal Services LLC, ATF-MFG-PRC-001, February 5March 12, 2014.

5. "Standard Specification for Wrought Zirconium Alloy Seamless Tubes for Nuclear Reactor Fuel Cladding", ASTM B811-13.

6. PLN-4608, "Quality Implementation Plan for the Irradiation Testing of Accident Tolerant Fuels"

7. "Project Quality Assurance Plan (PQAP) – Enhanced Accident Tolerant Fuel (EATF) Project", AREVA Federal Services LLC, PQAP-3008012-001, February 2. 2014.

8. PLN-4623, "Fabrication Control Plan".

9. Drawing 604287, Idaho National Laboratory.

APPENDIX K

Enhanced Accident Tolerant Fuel Test Plan for the Phase 1A Final Report for EATF

Prepared by:
AREVA Federal Services, LLC

TABLE OF CONTENTS

1.0 INTRODUCTION 1
1.1. TYPES OF TESTING 1
1.2. RANGE OF TESTING 2
2.0 GOALS AND OVERALL PLAN 2
3.0 EATF TECHNOLOGY 3
3.1. FUEL PELLETS 3
3.2. CLADDING 4
4.0 EATF PROGRAM SCHEDULE 4
5.0 ACCIDENTS IMPACTED AND ANTICIPATED BENEFITS 5
6.0 ANALYTICAL CODES AND METHODS 5
6.1. NUCLEAR 5
6.2. THERMAL 6
6.3. ACCIDENT 6
6.4. FUEL MECHANICAL PERFORMANCE 6
7.0 TESTING SUMMARY 9
8.0 REFERENCES 10

LIST OF TABLES

Table 1: Types of Testing Required by Qualification Component 10

LIST OF FIGURES

Figure 1: Enhanced Accident Tolerant Fuel Testing Plan 2
Figure 2: Scope of EATF Testing 3
Figure 3: EATF Schedule 5

1.0 INTRODUCTION

In response to the Fukushima accident, the U.S. Department of Energy is supporting a program to enhance the accident tolerance of nuclear fuels for power reactors. The ultimate goal of this program is to produce one or more lead assemblies that can be irradiated in a commercial power reactor within ten years.

This program involves development of pellets which have higher thermal conductivity; hence, lower stored energy. It also involves the development of cladding coatings and a new cladding material. Once initial manufacturing and selected performance tests are performed, successful candidates were selected for irradiation testing. These test results will then be used to qualify the fuel modification for use in a Lead Fuel Assembly (LFA). Other testing will be needed to support licensing. This document describes that testing

In the development and qualification of a new fuel product, testing is required to support licensing, and prove performance relative to customer requirements. This testing is extensive. The various types of tests are outlined in this appendix.

1.1. TYPES OF TESTING

MATERIAL PROPERTIES

This data is necessary to establish material properties and behaviors and develop models for predicting material performance for both unirradiated and irradiated fuel. Thermo-mechanical properties like thermal conductivity must be measured and microstructural evaluations must be made to evaluate material phases, grain size, etc. Elements of this testing do not require purely prototypical conditions. Material properties data must cover the needs from several engineering analysis areas including neutronics, thermal-hydraulics, thermo-mechanical, and mechanical analyses. This testing covers both pellets and cladding.

COMPONENT INTERACTIONS

This data is necessary to characterize component and environmental interface interactions and performance and also support model development for integral system predictive tools. These tests evaluate component performance within a more complex system of components. For example pellet and clad systems are tested in more prototypical conditions such as in a flow loop under irradiation. Power levels may be steady-state or transient depending on the data required. This allows for evaluation of more complex component interactions such as PCI and oxidation of materials. Later full assembly tests will build on this and are used to evaluate phenomena such as growth and clad creep down and its impact on the overall fuel assembly.

MANUFACTURING COMPATIBILITY

This data is used to demonstrate that the desired EATF pellet and clad concepts can either be achieved with the current manufacturing processes or that any newly proposed manufacturing processes can produce acceptable fuel. For example, coated clad fuel rod must be inserted into fuel assembly cages. This process must be shown not impact the coating coverage or adhesion (i.e. through scratching or gouging) with the base cladding

or it must be modified. Another critical area of manufacturing is welding. The introduction of new clad materials or coatings may introduce challenges to the welding processes which require testing to confirm an acceptable process moving forward.

1.2. RANGE OF TESTING

A wide range of testing is performed, including a range of operating regimes, component parts and physical aspects. Typically these regimes include both normal operating reactor conditions as well as postulated accident conditions. Other regimes such as manufacturing, shipping/transportation, and spent fuel storage and disposal must also be considered. Data must be generated to allow for analysis across the range of operating conditions within each regime. This entails data as a function of parameters such as burnup, temperature, pressure, and in air or water environments.

An initial test plan is presented in this appendix. It must support the Regulatory Plan for licensing, described in Appendix N. As that plan develops, the Test Plan will require minor adjustments.

2.0 GOALS AND OVERALL PLAN

Figure 1 depicts the schedule for testing of Enhanced Accident Tolerant Fuel (EATF) to support LFA irradiation. The overall goal of this testing is to support licensing and to verify both vendor and customer performance requirements. This fuel qualification process is discussed further in the appendix covering the Regulatory Plan, Appendix N. This testing will include the pellet, cladding, and coatings comprising the EATF, including the fuel rod and fuel bundle. It will cover Normal Operation, including shipping and handling, irradiation, and storage, Design Basis (DB) Events (DBE), and Beyond Design Basis Event (B-DBE) conditions. It will supply data for the development of analytical models in the areas of nuclear, thermal, fuel mechanical and chemical performance. This extensive scope is depicted in Figure 2.

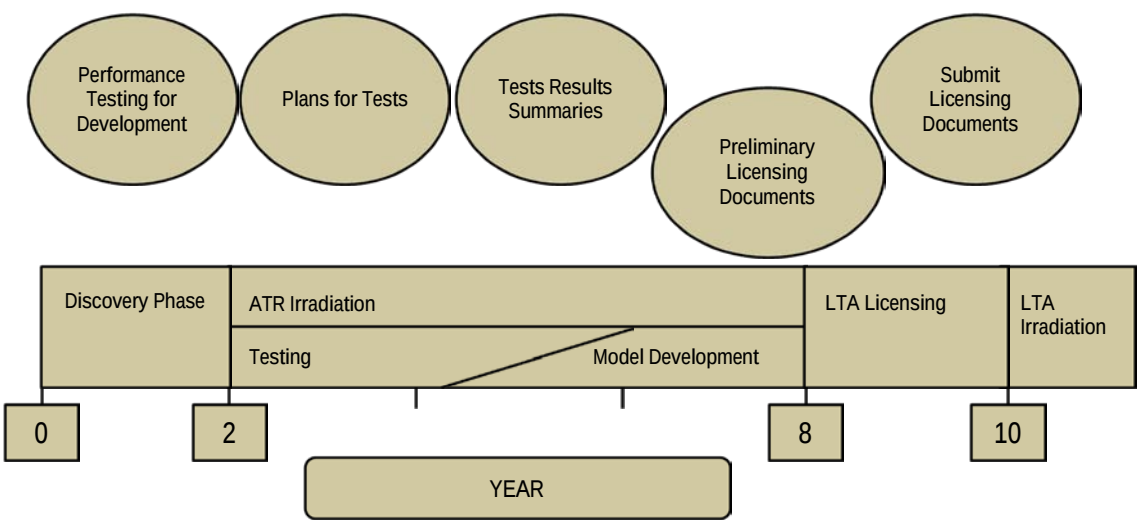

Figure 1: Enhanced Accident Tolerant Fuel Testing Plan

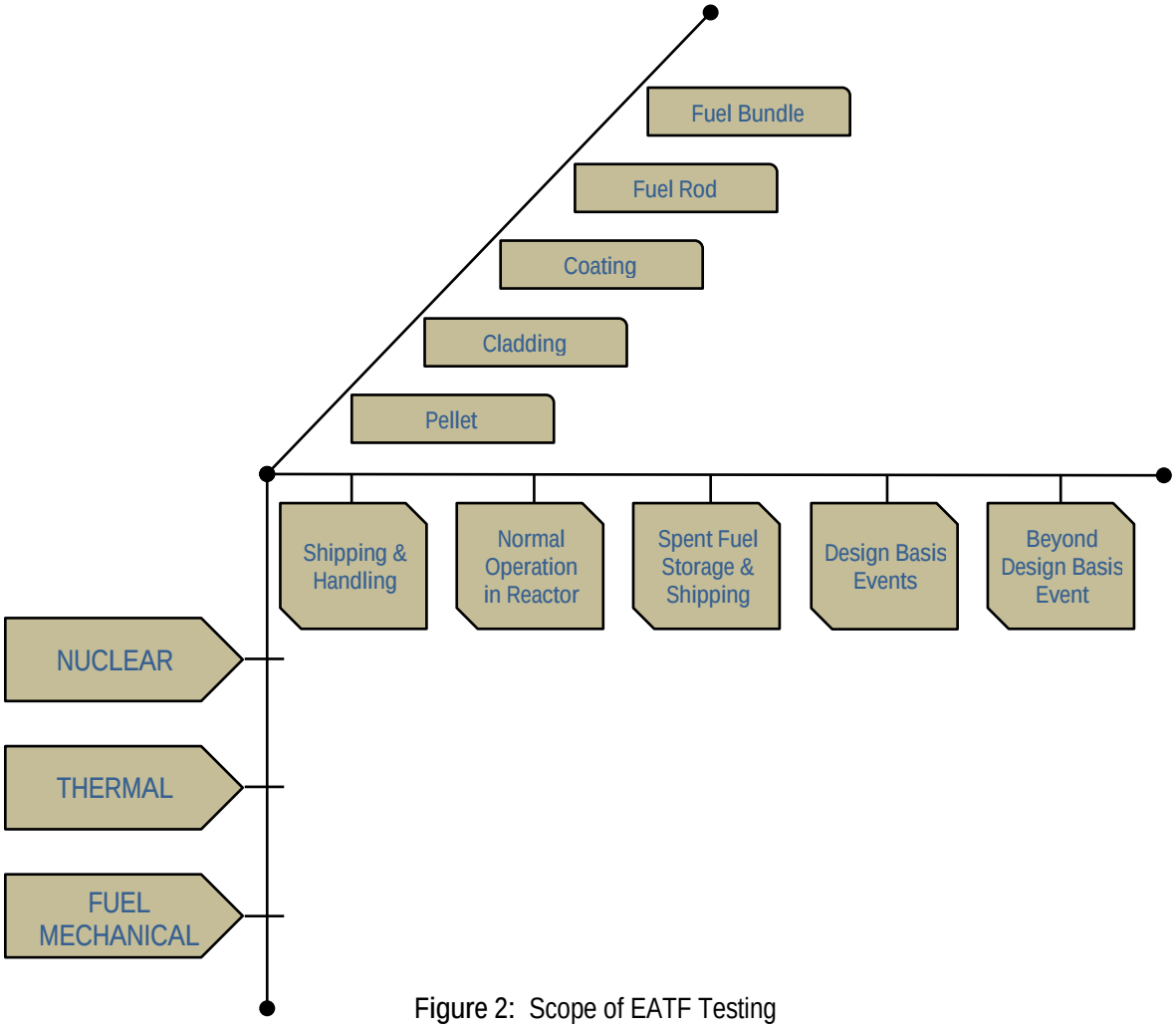

Figure 2: Scope of EATF Testing

3.0 EATF TECHNOLOGY

The EATF technology approach is a multi-prong approach to improve fuel pellets, cladding, and emergency coolant performance during Normal Operation, DBEs and BDBEs. The testing for each of the parts of the fuel-coolant system, including fuel pellets, cladding, and coolant, will be described.

3.1. FUEL PELLETS

A number of nuclear fuel forms have been designed and evaluated over the years. The two most practical ones operating and licensed, in terms of experience for today's power reactors, are uranium oxide and the plutonium-uranium mixed oxide (MOX) forms. The testing performed in the development of these fuels will be used as a starting point for testing of EATF.

The EATF fuel pellet is modified with additives to provide an increased thermal conductivity which leads to lower centerline fuel temperatures and therefore stored energy. The increase in thermal conductivity will be tested across the range of potential burnups to be achieved in the fuel. Further irradiation testing is needed to establish pellet performance under irradiation. Models for predicting pellet parameters such as swelling, or fission gas release (FGR) are needed to predict fuel system performance during normal operating and accident conditions. This requires power ramp testing. In later stages, before the new fuel forms can be licensed, Reactivity insertion accident (RIA) testing will be required to validate current energy deposition limits for certain severe accidents.

Additionally, the fuel pellet must be tested to ensure sufficient strength to handle fuel assembly fabrication and shipping without pellet damage.

3.2. CLADDING

LWRs have successfully operated in the US with zirconium alloy cladding. New clad materials and coatings face many barriers to successful implementation. As a result, testing is required, especially corrosion testing, to demonstrate that the clad-coolant and coolant-reactor structure interactions are well understood.

Certain properties can be quickly and easily established, for example the mechanical performance of the clad-coating interface. Others, such as corrosion rates, will require extensive testing in corrosion experiments. Testing with corrosion loops will take time, which must be included in the fuel qualification schedule. Unirradiated corrosion loop testing can be done at a reasonable cost and can be effective in selecting suitable candidate concepts for further testing. Ultimately though, the final cladding concepts must be tested in a corrosion loop under irradiation to allow for the interaction of the neutron fluence and chemical corrosion processes. This testing is more expensive and requires significant time to accumulate sufficient interaction to provide a basis for design licensing..

The approach relative to the fuel cladding is to find a cladding coating material that can be reliably applied; maintain integrity during normal operation and which will reduce cladding oxidation and hydrogen generation during DBEs and BDBEs. The additional option of replacing the cladding material with molybdenum will also be considered, along with additional testing.

4.0 EATF PROGRAM SCHEDULE

The EATF Program for the LFA is presented below. This includes the initial two-year discovery portion followed by the irradiation testing portion and then the design, licensing and implementation of an LFA.

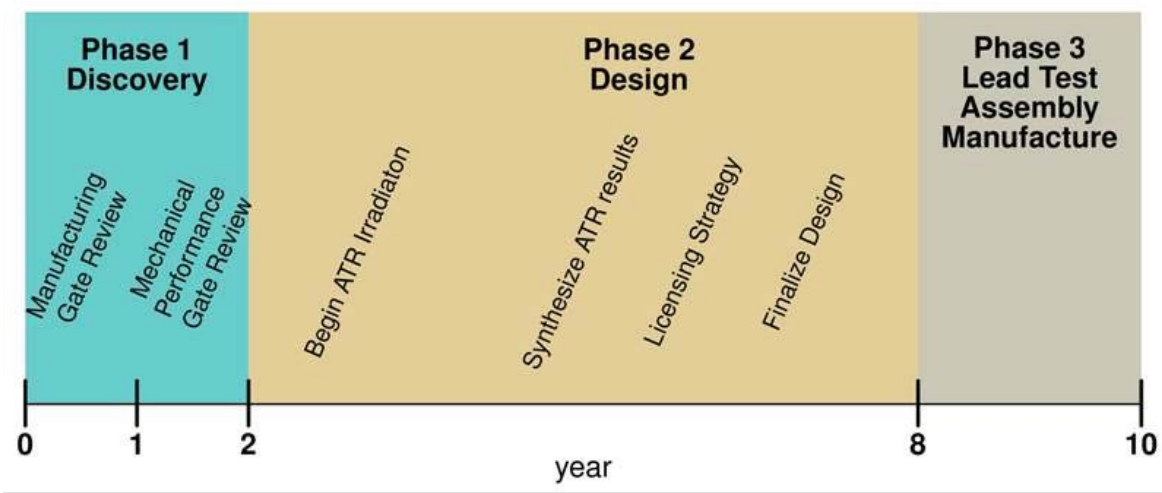

Figure 3: EATF Schedule

5.0 ACCIDENTS IMPACTED AND ANTICIPATED BENEFITS

Since the present AREVA Project does not include specific work to analytically quantify all the benefits of the EATF, work will be done at the National Laboratories, particularly INL, in the area of defining the B-DBE the benefits of EATF. As the program progresses, accident condition testing will be completed to confirm the models used in the accident assessments.

The testing during development and that anticipated to demonstrate and quantify EATF benefits during DBEs and BDBEs will be performed.

6.0 ANALYTICAL CODES AND METHODS

Part of the licensing process involves establishing the applicability of the computer codes and models to reliably predict the behavior of the reactor and the fuel under all conditions, including normal operation, anticipated transients, and DB accidents. Developing these models requires a mathematical model of the processes occurring in and around the reactor, and the evaluation of the data necessary to adjust and benchmark these models. Four main technical areas related to fuel licensing will be discussed. These include nuclear, thermal, accident and fuel mechanical performance.

6.1. NUCLEAR

Nuclear models predict the behavior of the neutron and gamma-ray population under varying conditions. These models use neutron and gamma-ray cross sections to predict their interaction with the reactor materials. There are several large sets of data available from various sources, including the ENDF/B and JEFF cross section sets and work continues to improve these sets. In most cases, the isotopic constituents in the EATF are contained in these data sets. If any gaps are found in the technical adequacy of the current cross section databases then it may require some experimental testing to generate adequate cross section data.

In addition, the NRC will require evidence that the EATF concepts can be adequately modeled with current vendor codes. This may require benchmarking of various models. For minor changes to the fuel, it may be reasonable to compare vendor code results with a higher fidelity tool such as Monte Carlo modeling. More extensive change to the fuel may require benchmarking to experimental results. This experimental testing can take the form of setting up critical experiments to model EATF or obtaining pin/pellet isotopic and burnup data at various burnups usually through hot cell examinations.

The final test of the core physics codes will be to benchmark against measured:

- Core Power Distributions (radial and axial)
- Reactivity Parameters (i.e. control rod worths, MTC, etc.)
- Incore Detector Signals

6.2. THERMAL

Thermal models predict the transfer of the heat from the fuel, through the clad, and to the coolant and ultimately establish the amount of margin to specified acceptable fuel design limits (SAFDL's) like departure from nucleate boiling ratio (DNBR) and fuel centerline melt (FCM) which define the limits for reactor operation. Qualification of these models first requires data on thermo-mechanical properties of the fuel pellet and cladding (e.g. thermal conductivity, specific heat, etc.) across the expected range of fuel burnups. Additionally, processes such as FGR as a function of burnup and power level changes must be understood sufficiently to allow characterization of the fuel rod gas pressures and isotopic constituents.

Cladding thermo-mechanical properties must also be understood including changes as a function of neutron fluence received. It is also possible that CHF testing could be required in the event that a clad coating or new clad material was used that significantly affects surface roughness or surface tension in a manner as to change the dynamics for bubble formation on the cladding surface.

6.3. ACCIDENT

Phenomena critical to accident modeling include:

- FGR
- Pellet cracking and relocation
- Deposited enthalpy at failure

This data is primarily obtained through transient ramp and RIA testing. Before that testing can be done, test specimens must be developed by irradiating fuel rods in a prototypical LWR environment to several burnups spanning the range of allowable rod burnups.

6.4. FUEL MECHANICAL PERFORMANCE

Fuel mechanical performance includes the behavior of the fuel and cladding over the lifetime in the core and over the range of operational conditions. This includes such

things as swelling, creep, fatigue, corrosion resistance, cracking, and FGR. Fuel mechanical performance models are largely based on measured data. The use of a common fuel form, such as oxides, will permit the use of presently existing measured data. The use of a fuel form with little or no experience, such as oxides with SiC additives, will require generating more data than may presently exist. Generating this data will require irradiation testing which will then become critical path items in the development schedule and which will provide the basis for licensing the LFA.

FGR could be a limiting factor. Typical engineered approaches to address FGR include accounting for pellet and rod growth, minimizing fuel rod pre-pressure, or changing the geometric structure of the fuel. This must be studied early because of the cascade of effects throughout the fuel assembly design.

6.4.1. FUEL

The program would be similar to that developed for the nuclear model development and critical experiment benchmarking for Uranium Gadolinia (DOE/ET/34212-41, BAW-1810) and MOX fuel.

In general, the first step in the qualification is to establish the material chemical composition through the development program. This includes all composition limits and impurity limits, plus all manufacturing steps. Many of these material parameters need to be evaluated during development. Once the final material is established by composition and processing, the final properties need to be documented to support licensing analyses, code benchmarking, etc. It is important to recognize the subtleties of chemical composition sensitivity and impurities on material properties. That is a critical part of the material development program.

Characteristics of the new fuel material to be qualified include, but are not limited to:

- thermal conductivity versus burnup,
- swelling,
- FGR and retention,
- stored energy properties,
- operating temperatures and heat capacity, and
- characteristics of thermal cracking
- Solubility in water (i.e. related to washout)

Also necessary is an understanding of potential phase changes in the material at accident temperatures and in the case of fuel additives, the potential for chemical reactions between the fuel and additioves must be understood.

The inclusion of burnable poison materials, such as Gd_2O_3 or Er_2O_3 would add another level of benchmarking and qualification to quantify the interaction and impact on new fuel materials.

6.4.2. CLADDING

Material characterizations and tests are likely needed for a new clad material (e.g., molybdenum). The first step in the qualification of a new clad material is to establish the material chemical composition through the development program. This includes all base alloy composition limits and impurity limits, plus all manufacturing steps, particularly heat treatment. Many of these material parameters need to be evaluated during development. Once the final material is established by composition and heat treatment, the final properties need to be documented to support licensing analyses, code benchmarking, etc. It is important to recognize the subtleties of chemical composition sensitivity on material properties. This is a critical part of the material development program.

The following material properties will require qualification and characterization:

- Crystal lattice parameters and density
- Crystallographic texture (Kearn's factors)
- Thermal properties (thermal conductivity, emissivity, specific heat, enthalpy, expansion)
- Melting point and phase transformations versus temperature
- Elastic constants (Poisson's ratio, Young's Modulus, Shear modulus)
- Strength:
  - Uniaxial and biaxial (burst) yield strength (room and versus temperature, both unirradiated and irradiated)
  - Uniaxial and biaxial (burst) (UTS) (room and versus temperature, both unirradiated and irradiated)
  - Uniaxial and biaxial (burst) elongation (room and versus temperature, both unirradiated and irradiated)
  - Hardness (room and versus temperature, both unirradiated and irradiated)
  - High strain rate circumferential fracture/ductility (ramp tests)
  - Fatigue
- Thermal creep (axial and circumferential, both irradiated and unirradiated material)
- Irradiation creep (axial and circumferential, both irradiated and unirradiated material)
- Free growth versus burnup
- Oxidation: ex-core and in-core versus burnup
- Hydrogen uptake: ex-core and in-core
- Stress corrosion cracking behavior
- High temperature swelling and rupture (Accident conditions)
- High temperature oxidation testing (Accident conditions)
- High Temperature Fatigue properties including eorrosion and irradiation effects
- Irradiation Growth

6.4.3. MECHANICAL PROPERTIES SUMMARY

The data to support the development and justification of fuel mechanical models is well defined.

The mechanical properties of unirradiated fuel to be established to support fuel qualification include the following.

- Chemical and phase compositions
- Heat capacity
- Thermal conductivity
- Thermal expansion

Unirradiated and irradiated properties such as volume and density are needed to determine such properties as:

- FGR
- Swelling with irradiation
- Heat capacity
- Thermal conductivity
- Thermal expansion coefficient
- Initiation conditions and energy release for any potential fuel and cladding or coolant interactions

The fuel element mechanical properties will also need to be quantified. This includes:

- Relationships between stress and strain
- Tensile and compressive strengths
- Creep resistance
- Fatigue properties

Data on the fuel element interaction with the coolant and fuel assembly structure is needed for:

- Cladding corrosion
- Flow resistance
- Fretting resistance

7.0 TESTING SUMMARY

A summary of the types of testing, the fuel qualification area, and the focus of the testing is provided in Table 1.

The major components of fuel qualification, beyond the initial discovery period, are depicted in Figure 2. The presently existing data on fuel performance and manufacturing are the starting point for the models and fuel design. The fuel mechanical design will take about 2 years and the non-irradiation testing another 2 to 3 years. The mechanical testing will either confirm or improve the preliminary design and also fill in the gaps where data is missing. Previous irradiation-related data will have to be used in the models until the final qualification testing is complete. At this point, the fuel is qualified to begin irradiation to a point approved by the NRC. This point will be a fraction of the total planned irradiation time, perhaps 1/5 or 1/4 of the total. The irradiation time is the long part of the qualification schedule, requiring at least the amount of time required to achieve the desired discharge burnup. In this case this would be 10 years.

Type of Testing	Fuel Qualification Area	Focus of Testing
Materials Properties	Model Development Code Qualification & Benchmarking Manufacturing	Metallurgical Laboratory Testing of Pellet/Cladding/Coating: • Mechanical Properties • Thermo-mechanical Properties In-Reactor Testing (Hot Cell exam) • Change in mechanical/thermo-mechanical properties with irradiation
Component Interactions	Model Development	Out-of-Reactor Testing • Pellet solubility • Autoclave testing of clad-coating performance In-Reactor Testing (Flow Loop) • Cladding oxidation performance • Pellet swelling • Clad Creep • etc. Transient Reactor Testing • PCI performance • FGR • RIA performance (deposited enthalpy) • etc.
Manufacturing Compatibility	Manufacturing	Process Qualification of pellet and cladding manufacturing • Bundle Assembly (grid/rod interface) • Welding qualification • Spark Plasma Sintering (SPS) qualification

Table 1: Types of Testing Required by Qualification Component

8.0 REFERENCES

1. AREVA Federal Services LLC, Requirements Traceability Matrix, RPT-3008640-000, Enhanced Accident Tolerant Fuel, Contract Number: DE-NE-000567.

2. AREVA Federal Services LLC, Technical Feasibility of Using Nano-Particles in Coolant During Accident Conditions, RPT-3008771-000, Enhanced Accident Tolerant Fuel, Contract Number: DE-NE-000567.

APPENDIX L

Publications
for the
Phase 1A Final Report
for Enhanced Accident Tolerant Fuels

Prepared by:
AREVA Federal Services, LLC

TABLE OF CONTENTS

1.0 INTRODUCTION 1
2.0 PUBLICATIONS 1
3.0 TECHNIQUES 1
4.0 PATENTS 2
5.0 WEB SITES 2

1.0 INTRODUCTION

This appendix provides a list of the work products developed under this contract, including publications, patents, and techniques.

2.0 PUBLICATIONS

The following publications were produced based on this work.

1. B. Garcia-Diaz, L. Olson, C. Verst, R. Sindelar, E. Hoffman, B. Hauch, B. Maier, and K. Sridharan, "MAX Phase Coatings for Accident Tolerant Nuclear Fuel", B. Garcia-Diaz, L. Olson, C. Verst, R. Sindelar, E. Hoffman, B. Hauch, B. Maier, and K. Sridharan, proc. Trans. American Nuclear Society Conf., Reno, NV, 2014

2. Rich Kochendarfer, Kevin McCoy, Patrick Blanpain, "Use of Gate Reviews to Select Approaches for Enhancing Accident Tolerance Fuel, LWR Fuel Performance/Top Fuel, Charlotte, NC, September 15-19, 2013.

3. Rich Kochendarfer, Kevin McCoy, Bert Dunn, "Review of Progress on Enhanced Accident Tolerant Fuel", Fontevraud 8, Avignon, France, September 14-18, 2014.

4. Jitesh Kuntawala, Hunter Browning-Smith, "Economic Feasibility of Spark Plasma Sintering High-Throughput Processing of UO_2 Fuel", ANS Winter Meeting 2013, November 11, 2013.

5. Jitesh Kuntawala, Hunter Browning-Smith, "Analysis of High Thermal Conductivity Composite UO_2 Fuels Fabricated by Spark Plasma Sintering", ANS 2013 Winter Student Poster Session, November 11, 2013.

6. Jitesh Kuntawala, Andrew Cartas, PHD, James Tulenko, "An Innovative Accident Tolerant UO_2 Composite Fuel for Use in LWRs", 2013 ANS Winter Meeting and Nuclear Technology Expo.

3.0 TECHNIQUES

The production of nuclear fuel pellets for irradiation testing in the ATR required the production of a number of procedures and specifications meeting specified quality standards..

1. "Technical Specification for Nuclear Fuel Pellets to Be Irradiated in the Advanced Test Reactor", AREVA Federal Services, SPC-3009802-0031, February 4March 12, 2014.

2. "AREVA ATF (Accident Tolerant Fuel) Experiment Fuel Rodlet End Cap and Tube Details", DWG-604287, INL, 2013.

3. "Manufacturing Procedure for Pellet Lot Intended for Irradiation in the Advanced Test Reactor", AREVA Federal Services LLC, ATF-MFG-PRC-001, February 5March 12, 2014.

4. PLN-4608, "Quality Implementation Plan for the Irradiation Testing of Accident Tolerant Fuels"

5. "Project Quality Assurance Plan (PQAP) – Enhanced Accident Tolerant Fuel (EATF) Project", AREVA Federal Services LLC, PQAP-3008012-001, February 2. 2014.

4.0 PATENTS

There were no patents generated as a result of this work.

5.0 WEB SITES

1. "SRNL and partners explore coatings for the generation of nuclear fuels", DOE Pulse – Science and Technology Highlights from the DOE National Laboratories, Number 401/November 18, 2013, http://web.ornl.gov/info/news/pulse/no401/story2.shtml.

2. "SRNL Scientists Working to Develop Accident Tolerant Nuclear Fuel", Enformable Nuclear News, http://live.enformable.com/post/67501922043/srnl-scientist-working-...

APPENDIX M

Typical LFA Acceptance Review
for the
Phase 1A Final Report
for Enhanced Accident Tolerant Fuels

Prepared by:
AREVA Federal Services, LLC

TABLE OF CONTENTS

1.0 INTRODUCTION 1
2.0 SCOPE OF DOCUMENT 1
3.0 OTHER POTENTIAL REQUIREMENTS SOURCES 2
4.0 TYPICAL PROCESS 2
4.1. ESTABLISHING A NEED FOR THE CHANGE 2
4.2. DETERMINING IF THE CHANGE IS TECHNICALLY SOUND 3
4.3. IDENTIFYING THE REGULATORY LICENSING REQUIREMENTS ASSOCIATED WITH THE CHANGE 3
4.4. OBTAINING PLANT AND REGULATORY APPROVAL FOR THE CHANGE 5
5.0 TECHNICAL DATA NEEDS 5
5.1. RELIABILITY 6
5.2. LICENSING 6
5.3. ECONOMICS 6
6.0 SUMMARY 6
7.0 REFERENCES 7

1.0 INTRODUCTION

In the fall of 2012, the Department of Energy (DOE) circulated a funding opportunity on the development of Enhanced Accident Tolerant Fuels (EATF) for commercial Light Water Reactors (LWRs). AREVA Federal Services (AFS) commissioned a team composed of several leading universities, national laboratories, and nuclear utilities to evaluate potential concepts that could improve cladding and/or pellet performance during severe accident conditions. The AREVA team was subsequently awarded funding to investigate concepts focused on coatings, UO_2 pellet additives, and coolant nano-particles, with the goal of improving Zircaloy clad oxidation performance, pellet temperature and fission gas release (FGR), and clad heat transfer.

Throughout the first 2-year phase, the EATF concepts were analyzed and/or tested to assess the manufacturability, suitability, and performance of the concepts. The information obtained was utilized to evaluate and down-select to a short list of concepts that offer the most viable and beneficial enhancements. The AREVA EATF team's Advisory Board reviewed all of information produced for the concepts during periodic Gate Reviews allowing for an efficient and objective investigation of several EATF concepts.

The initial 2-year project was described as the first phase of a multi-phase effort culminating in the introduction of an EATF concept lead fuel assembly (LFA), targeted for CY2022, into a commercial nuclear power plant (NPP). In order to ensure that appropriate information is available to obtain license approval for a LFA insertion, the AREVA team gathered a listing of utility recommendations. This report provides a summary of the recommendations of the Tennessee Valley Authority (TVA) and Duke Energy (Duke), both nuclear utilities operating LWRs where future LFAs with EATF may be demonstrated.

2.0 SCOPE OF DOCUMENT

This document reflects the typical process utilized by utilities to review and evaluate changes, tests, and experiments for plants with Nuclear Regulatory Commission (NRC) operating licenses. TVA and Duke expect to utilize a similar process to review proposed EATF concepts for operation at their plants.

This document addresses the general scope of information typically required; it does not address specific requirements for particular EATF concepts. There may be additional review and requirements for EATF, depending on how different the proposed LFA is from the currently operated fuel. It should also be noted that in a highly risk averse industry, review requirements may vary considerably between utilities based on their level of risk averseness.

The document does not present any information for the review and evaluation itself (for example, the document notes that fuel should be operated in non-limiting core locations, but does not specify where the non-limiting core locations reside).

Note that any regulatory requirements discussed within this document are paraphrased and based to some extent on past experience licensing new fuel designs; the reader should refer directly to the regulations for guidance and be aware that this regulatory guidance is subject to review and revision during the time frame of the overall EATF project.

3.0 OTHER POTENTIAL REQUIREMENTS SOURCES

This summary represents the minimal utility review requirements to consider operation of new fuel concepts in a commercial reactor; it does not address all of the needs for evaluation and licensing of the concept. Additional requirements can be found within the NRC's guidance (in particular NUREG-0800 and Regulatory Guides) and within the Code of Federal Regulations. Supplementary information can also be found within ANSI/ANS-57.5-1996, ANSI N18.2/ANS 51.1/52.1.

4.0 TYPICAL PROCESS

The typical process for a utility to integrate and operate a new or revised fuel design includes three major steps: 1) establishing a need for the change, 2) determining if the change is technically sound, and 3) identifying the regulatory licensing requirements for obtaining plant and regulatory approval for the change. Each of these major hurdles is addressed within the following sections. Those pursuing a demonstration program at the utility should engage the appropriate utility staff 3 to 5 years in advance of the expected first date of operation.

4.1. ESTABLISHING A NEED FOR THE CHANGE

Typically, a fuel design change is the result of the utility establishing a new fuel contract with a different fuel vendor or a request from the current fuel vendor to upgrade the currently operated fuel product. In the case of the former, the new fuel design often has different hydraulic or neutronic performance that can lead to temporary operating penalties and temporarily lower fuel reliability rates due to compatibility issues with the co-resident fuel, and quite often requires prior NRC approval for implementation. The latter is usually in the form of an evolutionary change, requiring very little analysis, but providing some functional improvement. An example of this is the adoption of an improved debris filter - the basic form and functionality of the fuel is preserved, and there is virtually no change to the operational performance. These types of changes usually do not require prior NRC approval and are the easiest to adopt. Neither option though offers a zero-cost implementation for the utility.

Given the fact that any change represents a cost investment and a risk for the utility, it is important to establish the purpose and benefit of the final product. Proposed fuel design changes that cannot be demonstrated as ready for batch implementation represent a relatively large risk. These changes must first be demonstrated as successful through the introduction of lead fuel rods (LFRs) and/or lead fuel assemblies (LFAs). For LFRs and LFAs, the final benefit to the utility, in terms of increased safety margin, cost reduction, improved reliability, etc., should be quantified at the reload batch level, with independent data to support the value, as possible. The utility staff (including Fuel and Reactor Engineering departments) that will eventually be tasked with evaluating and approving the LFR/LFA should be informed on the requested design change and the benefits and risks as early as possible.

The fuel designer will be required to provide a detailed design description, including engineering drawings, a topical/technical report supporting licensing of the design, a listing of relevant operating experience and/or testing, a failure modes and effects analysis (FMEA) with regard to the proposed changes, and a risk assessment that

addresses operation of the fuel with other fuel designs residing in the reactor core and risk to other components of the reactor.

4.2. DETERMINING IF THE CHANGE IS TECHNICALLY SOUND

Once the utilities Fuel Engineering team agrees that there is a need for the fuel design change or LFR/LFA, a review of the design will begin. The Core Cycle Design Engineer will review the core cycle design and the predicted performance of the design with respect to the core power distribution and margins to power peaking limits. Other utility staff will review documentation supplied by the fuel designer in support of the performance bases for the design to ensure it complies with technical specifications and regulations related to criticality safety, mechanical fit up, seismic, dead weight, fuel handling equipment, wet and dry storage, and any other operating considerations. The team will also review the documentation to determine if any of the proposed fuel design changes invalidate assumptions that were made on other systems/licensing calculations.

The utility will verify the applicability of routine fuel and core performance monitoring systems and procedures, including fuel receipt inspection, startup physics testing, core reactivity anomaly evaluation, incore flux mapping of core power distribution and margins to power peaking limits, at-power Moderator Temperature Coefficient (MTC) measurement, and fuel integrity evaluations.

For LFR/LFAs, a very important document is the risk assessment discussion, usually provided by the fuel designer. The risk assessment should include an FMEA, a review of any relevant operating experience, contingency plans for potential adverse performance, specification of monitoring and Post Irradiation Examination (PIE) to be completed, and any operator training requirements. The risk assessment should detail the impacts of any fuel failures that may result on co-resident fuel and the reactor components.

LFAs should be planned for operation in non-limiting core locations for several cycles. The LFA power should be closely monitored; thus, it is preferable to plan for operation in an instrumented core location. A target burnup should be specified.

Finally, a disposal plan (including temporary storage on site) should be provided if LFAs or LFRs will be operated.

4.3. IDENTIFYING THE REGULATORY LICENSING REQUIREMENTS ASSOCIATED WITH THE CHANGE

All operated fuel designs should utilize approved evaluation methods. The fuel vendor usually prepares or references a topical report that describes the fuel design and establishes performance limits, evaluation methodology, and failure modes. The topical report is usually reviewed and approved by the NRC. An alternative mechanism is to include parts or all of this description and analysis within the license amendment request (LAR) which will be submitted to the NRC for approval prior to insertion of the LFR/LFAs.

The regulatory process mandated for evaluation of proposed changes to safety-related nuclear components is primarily contained within References 1 and 2. Initially, the utility will screen the proposed change as a “50.59 change” per the requirements of Reference 1. If the screening review determines the change may require prior NRC

approval for implementation (that is, it has the potential to impact the licensing basis of the plant), the change is further evaluated against the criteria in10CFR50.59(c)2. When deemed necessary, a LAR is prepared per Reference 2.

4.3.1. DETERMINING IF A LICENSE AMENDMENT IS REQUIRED

Per 10CFR50.59, a licensee may make changes in the facility (as described within the latest revision of the final safety analysis report (FSAR)) or conduct tests and experiments not described within the FSAR without obtaining a license amendment if a change to the plant technical specifications is not required, and if the test/experiment does not:

- Result in more than a minimal increase in the frequency of occurrence of an accident previously evaluated within the FSAR;
- Result in more than a minimal increase in the likelihood of occurrence of a malfunction of a structure, system, or component (SSC) important to safety;
- Result in more than a minimal increase in the consequences of an accident;
- Result in more than a minimal increase in the consequences of the malfunction of an SCC important to safety;
- Create a possibility for an accident of a different type than previously evaluated within the FSAR;
- Create a possibility for a malfunction of an SCC important to safety with a different result than any previously evaluated;
- Result in a design basis (DB) limit for a fission product barrier as described in the FSAR being exceeded or altered; or
- Result in a departure from a method of evaluation described in the FSAR to establish the design bases or safety analyses.

It should be noted that the 50.59 rule is only meant to specify the conditions under which a licensee may make changes to the facility or conduct tests without having to receive prior NRC approval; it is not meant to determine if the change is safe and effective. Information pertaining to each of the preceding questions should be provided by the fuel designer, as the answers define the duration and expense of operating the proposed fuel design change.

A utilities 50.59 process typically includes the following activities (References 3 and 4):

- A review of the design function, design bases and supporting calculations for the item being changed (in this case, the fuel system);

- A review of the plant's technical specifications and operating license to determine any impacts of the proposed change;
- A review of the FSAR;
- Preparation of a 50.59 review report and change request.
- Submittal to the Plant Oversight Review Committee (PORC) for approval of the change.

It should be noted that this document provides information on the current approach for evolutionary fuel designs (that is, fuel designs that use zirconium-alloy based clad and UO_2 fuel pellets). Most proposed accident tolerant fuel is not considered to be evolutionary in nature; thus, it would be important to have a meeting with NRC to brief them on the change and the plan (50.59 or LAR) well in advance of the schedule required for an LAR. Even if the case could be made to accept the change on the basis of 10CFR50.59, there is a good chance NRC would expect a LAR for accident tolerant fuel.

If a LAR is required, the fuel designer should include at least 15 to 24 months for NRC review within the schedule although more exotic fuel design changes could potentially lead to longer review periods. Usually the LAR is approved in advance of LTA manufacturing or other core reload planning milestone to mitigate budget risks. Schedule should consider the contingency plan for the plant if LAR is not approved.

4.4. OBTAINING PLANT AND REGULATORY APPROVAL FOR THE CHANGE

Once the need for the change has been established, the technical reviews have been completed, and the path for licensing the change has been established, the utility engineer leading the change must submit the supporting information with a request for change to the PORC for approval. This is typically accomplished through a series of review meetings which fuel DB and supporting technical information are presented.

Once approved by the PORC, the work is not complete. All licensing paperwork must be submitted to the NRC for approval; the FSAR may need to be updated and submitted as well; any procedure changes necessary to support the change must be implemented. Thus, this document addresses only those steps leading to acceptance for operation.

5.0 TECHNICAL DATA NEEDS

The data necessary to justify LFR/LFA implementation into a commercial reactor generally falls into three categories:

1. Demonstrating that the fuel will perform reliably (Reliability)
2. Demonstrating that plant licensing needs can be attained (Licensing)
3. Demonstrating an economic benefit to the utility (Economics)

An LFR/LFA campaign may not require the full rigor necessary to implement batch reloads but sufficient data must be available to satisfy the utility in the three categories above.

5.1. RELIABILITY

This requires data to demonstrate to the utility with a reasonable degree of confidence that the fuel change(s) can be operated under normal conditions in the reactor without adverse consequences. These consequences generally consist of ensuring compatibility of all mechanical interfaces both within the fuel and between the fuel and other core components such as control rods. In addition, fuel designer must ensure that no adverse thermal, hydraulic, and/or neutronic conditions might evolve during the life of the fuel which includes core operation and spent fuel storage. These adverse conditions could, for example, reduce maneuvering flexibility or increase plant maintenance activities.

5.2. LICENSING

This requires data to demonstrate to the utility with a reasonable degree of confidence that the fuel change(s) can be shown to either improve or have minimal impact on licensing margins under postulated accident conditions. This includes having sufficient data to demonstrate that analysis codes can reasonably predict fuel behavior under normal irradiation and accident conditions.

5.3. ECONOMICS

This requires data to demonstrate to the utility that the economic benefits of making the fuel change outweigh the potential costs. This data may include fuel cycle economic studies quantifying the change in fuel cycle costs with implementation of the fuel design change. It may also be data estimating relative margin improvement in one or more safety criteria or in the ability to expand operating envelopes or relax safety equipment availability requirements. It can also comprise data demonstrating that the fuel can be manufactured at a lower cost.

6.0 SUMMARY

In summary, the utility process includes a rigorous review of the proposed EATF concept. The majority of EATF concepts are expected to require a LAR. In determining the need for a LAR, the utility will perform a 50.59 review, and all changes must be approved by the PORC. LARs must be submitted as much as two years in advance of operation, and reviews leading to the LAR submittal are dependent upon the tests, approved methods, and calculations completed that support the acceptable performance of the concept under all conditions of operation and considering co-resident fuel and reactor components.

7.0 REFERENCES

1. Title 10 Code of Federal Regulations, Part 50.59 (10 CFR 50.59), Changes, Tests and Experiments.

2. Title 10 Code of Federal Regulations, Part 50.90 (10 CFR 50.90), Amendment of License or Construction Permit at Request of Holder.

3. TVA NPG-SPP-09.4 (Revision 7), 10 CFR 50.59 Evaluations of Changes, Tests and Experiments.

4. NEI 96-07, Revision 1, Appendix E, User's Guide for NEI 96-07, Revision 1, "Guidelines for 10CFR 50.59 Implementation", October, 2011.

APPENDIX N

Regulatory Plan
for the
Phase 1A Final Report
for Enhanced Accident Tolerant Fuels

Prepared by:
AREVA Federal Services, LLC

TABLE OF CONTENTS

1.0 INTRODUCTION 1
2.0 FUEL QUALIFICATION PROCESS 1
2.1. DEVELOP LIST OF REQUIREMENTS AND GOALS 2
2.2. DESIGN, FABRICATE, IRRADIATE, AND EXAMINE RODLETS 3
2.3. EVALUATE PERFORMANCE OF RODLETS RELATIVE TO REQUIREMENTS AND GOALS 4
2.4. DESIGN, FABRICATE, IRRADIATE, AND EXAMINE LEAD RODS 4
2.5. EVALUATE PERFORMANCE OF LEAD RODS RELATIVE TO REQUIREMENTS AND GOALS 5
2.6. PREPARE, SUBMIT, AND PURSUE LICENSE AMENDMENT REQUEST FOR POWER PLANT 5
2.7. PREPARE, SUBMIT, AND PURSUE TOPICAL REPORTS ON METHODS 6
2.8. PREPARE, SUBMIT, AND PURSUE TOPICAL REPORT ON FUEL DESIGN 7
2.9. PREPARE, SUBMIT, AND PURSUE TOPICAL REPORT FOR SHIPPING CASK 7
2.10. PREPARE, SUBMIT, AND PURSUE LICENSE AMENDMENT REQUEST FOR FUEL MANUFACTURING FACILITY 8
2.11. DESIGN, FABRICATE, IRRADIATE, AND EXAMINE LEAD ASSEMBLIES 9
2.12. EVALUATE PERFORMANCE OF LEAD ASSEMBLIES RELATIVE TO REQUIREMENTS AND GOALS 10
3.0 CONCLUSION 10
4.0 REFERENCES 10

LIST OF TABLES

Table 1: Tasks Required for Fuel Qualification 2

1.0 INTRODUCTION

In response to the Fukushima accident, the U.S. Department of Energy (DOE) is supporting a program to enhance the accident tolerance of nuclear fuels for power reactors. The goal of this program is to produce lead assemblies and irradiate them in a commercial power reactor, in hopes that irradiating batches of Enhanced Accident Tolerant Fuel (EATF) will eventually be common practice.

The purpose of this appendix is to provide a regulatory plan for EATF. The current program is intended to culminate in irradiation of lead assemblies of EATF, so the appendix lists the tasks needed to achieve that goal. The tasks with regulatory and licensing aspects are discussed. Additional tasks, not discussed in this appendix, will be needed before batch irradiation.

Section 2.0 provides a list of the tasks needed to qualify EATF for irradiation in lead assemblies, and the tasks with regulatory and licensing aspects are discussed in the subsections of Section 2.0. Section 3.0 provides conclusions, and Section 4.0 lists references.

This program will investigate, evaluate and qualify, as appropriate, the use of new pellet materials, new cladding materials, and cladding coatings. Various tests on these materials will be needed. A description of those tests is provided in Appendix K. The use of nanoparticles in the emergency coolant is also being investigated. Because that approach to improving accident tolerance is so different than the others, licensing for it is discussed in Appendix N.

2.0 FUEL QUALIFICATION PROCESS

The fuel qualification program will demonstrate the safe and reliable operation of EATF and that its use in commercial nuclear reactors is acceptable from public safety, regulatory, and performance perspectives. Table 1 lists the major tasks for achieving fuel qualification, including tasks that have already been completed, those in progress, and those that are still in the future. The fuel qualification process starts with development of conceptual approaches for improving accident tolerance and progresses through various stages of evaluation, testing, selection, design, fabrication, irradiation, and examination. Because of the cost of irradiation tests and of examining irradiated material, the project starts with testing of unirradiated material and progresses to irradiation tests of small and then increasing quantities of material. Progress through the successive stages will increase confidence in the performance of the fuel.

Table 1 lists the task for achieving fuel qualification and identifies those with regulatory and licensing aspects, which are discussed in the following subsections. For each of those tasks, the following items are discussed: (1) the relevance to licensing is described. (2) the entities that are responsible are identified and the status of the task is given. (3) To the extent possible, the activities associated with the task are described. A final design has not been selected yet, so describing some details of fuel qualification and licensing must be left for future work. (4) The assumptions required for successful completion of the fuel qualification effort. (5) Any interactions with the Nuclear Regulatory Commission (NRC) are identified.

Some of the tasks are considered complete, but revisiting them may become necessary in the future. That might occur, for example, if regulations or regulatory guidance documents change, or if new research results change the understanding of safe fuel performance.

Related to Licensing	Tasks
	Select potential materials and designs
X	Develop list of requirements and goals
	Evaluate materials and designs relative to requirements and goals
	Test materials and designs for manufacturability
	Evaluate manufacturability of materials and designs relative to requirements and goals
	Test unirradiated materials and designs for performance
	Evaluate performance of materials and designs relative to requirements and goals
X	Design, fabricate, irradiate, and examine rodlets
X	Evaluate performance of rodlets relative to requirements and goals
	Select materials for lead rods
	Choose utility partner for irradiation of lead rods
X	Design, fabricate, irradiate, and examine lead rods
X	Evaluate performance of lead rods relative to requirements and goals
	Select design for lead assemblies
	Choose utility partner for irradiation of lead assemblies
	Design modifications to power plant
X	Prepare, submit, and pursue license amendment request for power plant
	Complete detailed design of lead assemblies
X	Prepare, submit, and pursue topical reports on methods
X	Prepare, submit, and pursue topical report on fuel design
	Design shipping cask
X	Prepare, submit, and pursue topical report for shipping cask
	Fabricate shipping cask
	Design modifications to fuel manufacturing facility
X	Prepare, submit, and pursue license amendment request for fuel manufacturing facility
	Install and qualify modifications to fuel manufacturing facility
	Reach commercial agreement on irradiation of lead assemblies
X	Design, fabricate, irradiate, and examine lead assemblies
X	Evaluate performance of lead assemblies relative to requirements and goals

Table 1: Tasks Required for Fuel Qualification

2.1. DEVELOP LIST OF REQUIREMENTS AND GOALS

Developing a list of requirements is relevant to licensing because the requirements will form the basis for a topical report on the fuel design, as is discussed in Section 2.8. The requirements are supplemented by goals, which are attributes that are desirable but not required. Criteria from regulatory guidance (such as References 1, 2, and 3) are often stated in general terms that apply to either standard fuel or EATF. In some cases, new requirements are proposed for EATF, such as requirement 73, “Coating must be stable and adherent under LWR operating conditions.” Such requirements have been chosen to ensure safe operation of the fuel.

This task is primarily the responsibility of the fuel vendor, but utility partners also provided input to the list of requirements and goals. The task is considered complete, and the results are documented in Appendix A.

The activities for developing the requirements and goals, and the sources used, are discussed in Appendix A. Many of the requirements and goals are currently qualitative. In some cases, compliance with a requirement or achievement of a goal can be determined already. For example, achievement of goal 17, "The process should not lead to formation of mixed wastes" can be determined by inspection of the process. In other cases, a better understanding of performance must wait until more detailed information is available, for example, about the fuel rod or reload design.

Although the requirements form part of the basis for design, no interactions with the NRC were included in this task. Requirements will be discussed with the NRC in the context of lead rod and lead assembly design, as is discussed in Sections 2.4 and 2.8.

2.2. DESIGN, FABRICATE, IRRADIATE, AND EXAMINE RODLETS

This task involves work that is related to rodlets for irradiation in a test reactor. The task is relevant to licensing because results from these tests may be used as supporting data for a license application. For example, fuel pellets might be tested to determine how quickly their thermal conductivity degrades under irradiation. The rodlets may be either encapsulated or unencapsulated, according to the goal of the experiment.

Responsibility for this task is divided according to the activity. The technology supplier (for example, the University of Florida (UF) for fuel pellets) is responsible for supplying the material to be tested. The testing laboratory (for example, Idaho National Laboratory (INL)) is responsible for designing, fabricating, irradiating, and examining the rodlets. The fuel vendor is responsible for selecting test conditions and appropriate post-irradiation examinations, as well as providing input to the design of the rodlets. The utility partners provide similar inputs.

One activity in this task was well under way during September 2014. Pellets for irradiation in capsule tests had been produced by UF, and the pellets have been assembled into rodlets by INL. Irradiation is expected to begin shortly. A second activity is related to rodlets that will be tested in the flow-through loop of the Advanced Test Reactor (ATR). That activity is just beginning, with discussions of possible test conditions and materials to be tested. A third activity is related to transient testing. That activity has not begun because it requires irradiated samples from one of the first two activities. The final activity is to examine the irradiated rodlets. That activity lies in the future; it cannot begin until the rodlets have been at least partially irradiated.

One or more meetings with the NRC should be included in this task. The basic principles of fuel development, such as compliance with the quality requirements of 10 CFR 50 Appendix B and testing under conditions that are prototypical of actual operation, are well understood. However, more detailed guidance, for example on the number of samples or the details of the test conditions, may be needed to ensure that the testing program is consistent with NRC's expectations. These meetings could be combined with those described in Section 2.3.

2.3. EVALUATE PERFORMANCE OF RODLETS RELATIVE TO REQUIREMENTS AND GOALS

This task includes the analysis of results from the task described in Section 2.2. The task will be relevant to licensing if experimental results from irradiation of the rodlets are used to support a license application. On the other hand, the task will not be relevant if the results are not used. That situation could occur, for example, if the test concerns a material that is later rejected, or if it is determined that the experimental conditions were actually not prototypical of operation or postulated accidents.

This task is primarily the responsibility of the fuel vendor, but the utility partners may also provide inputs. The task lies in the future; it cannot begin until the rodlets have been at least partially irradiated and some information is available on their performance.

The first activity associated with this task will be review and approval of reports from the testing laboratory on postirradiation examination of the samples. The second will be interpretation of the results and determination of whether the results support the conclusion that a fuel rod or fuel assembly design will comply with the requirements.

One or more meetings with the NRC are included in this task. The meetings will keep the fuel vendor and utility partner up-to-date on NRC's concerns and will keep the NRC informed about the actual performance of the fuel. These meetings could be combined with those described in Section 2.2.

2.4. DESIGN, FABRICATE, IRRADIATE, AND EXAMINE LEAD RODS

In contrast to the work described in Section 2.2, this task involves work that is related to lead fuel rods (LFR) for irradiation in a commercial power reactor. The task is relevant to licensing because it is expected that results from these tests will be used as supporting data for a license application. The examinations are expected to provide information on a variety of performance measures, such as crud deposition, fuel rod growth, cladding corrosion, and internal gas pressure.

Responsibility for this task is divided according to the activity. The fuel vendor is responsible for designing the lead rods and selecting appropriate postirradiation examinations. The utility partner will provide inputs on rod design and must approve irradiation in its reactor. It is preferable that fabrication be done by the fuel vendor, but it may be necessary to use another supplier, such as a laboratory, if the fuel vendor's license does not allow fabrication of the rods. In the latter case, the fuel vendor should do as much work as possible because that will help to ensure that the lead rods are prototypical. Such work might include providing components or doing the initial stages of fabrication. Irradiation will be the responsibility of the utility partner. Responsibility for examination of the irradiated fuel will probably be shared by the fuel vendor, the utility, and a laboratory. The task has not been started.

Design, fabrication, and irradiation fall into three separate activities. If the fuel is examined only at poolside, examination will be a single activity and will be the responsibility of the fuel vendor and the utility. If a hot cell examination is added, however, it would be appropriate to add other activities. The utility and fuel vendor will be responsible for harvesting the rods. A transportation contractor will be responsible for shipping the rods to a hot cell, and possibly for licensing the transportation cask for

EATF. A laboratory will be responsible for examining the rods. The design, fabrication processes, irradiation conditions, and postirradiation examinations should all be chosen to provide strong support for a topical report on the projected fuel design.

One or more meetings with the NRC should be included in this task. As is discussed in Section 2.2, the basic principles for demonstrating safe operation are well understood, but more detailed guidance is needed to ensure that the testing program is consistent with NRC's expectations. The meetings should describe the work to be done and should show that the expected results will indicate compliance with applicable regulations and regulatory guidance. If existing guidance is insufficient or not applicable to EATF, that fact should be discussed and an alternative approach should be proposed.

NRC approval will be needed prior to irradiation of a Lead Fuel Assembly (LFA) in a commercial reactor.

2.5. EVALUATE PERFORMANCE OF LEAD RODS RELATIVE TO REQUIREMENTS AND GOALS

This task includes the analysis of results from the task described in Section 2.4. The task is relevant to licensing because it is expected that an interpretation of the results will be needed for a license application.

This task is primarily the responsibility of the fuel vendor, but the utility partners may also provide inputs. The task lies in the future; it cannot begin until the lead rods have been at least partially irradiated and some information is available on their performance.

If the task described in Section 2.4 includes a hot cell examination, the first activity associated with this task will be reviewing and approving reports from the laboratory on postirradiation examination of the samples. With or without a hot cell examination, an activity will be needed to cover interpretation of the results and determination of whether the results support the conclusion that a fuel rod or fuel assembly design will comply with the requirements.

One or more meetings with the NRC should be included in this task. The meetings will keep the fuel vendor and utility partner up-to-date on concerns from the NRC and will keep the NRC informed about the actual performance of the fuel.

2.6. PREPARE, SUBMIT, AND PURSUE LICENSE AMENDMENT REQUEST FOR POWER PLANT

The technical specifications for a nuclear power plant (NPP) typically include descriptions of the fuel assemblies that are approved for irradiation. Lead assemblies with EATF will be different from assemblies used previously, so it is expected that a license amendment request (LAR) will be needed. This task is relevant to licensing because it involves work on a LAR for a NPP.

The task is primarily the responsibility of the utility partner, but the fuel vendor will provide information about the lead assembly design and may provide other support. The task lies in the future; it cannot begin until a power plant has been selected and until the lead assembly design is sufficiently developed that the impact of the lead assemblies on the remainder of the power plant is understood.

The first activity will be to prepare and submit the LAR. When the fuel assembly design is sufficiently well developed and the behavior of EATF is sufficiently well understood, the utility partner can determine the effects of the lead assemblies on plant operations and safety. It is expected that the following items will be needed to support the request:

- A markup of the plant's technical specification and associated bases with proposed changes to allow insertion of the lead assemblies
- Background information, a discussion of each proposed change, and supporting technical information to justify the changes
- An analysis showing that the changes involve no significant hazards consideration
- An assessment of environmental consequences
- If appropriate for the lead assembly design, a request for exemption from selected NRC regulations.

The second activity will encompass the remaining activities for pursuing the license amendment, such as responding to requests for additional information.

Formal written interactions with the NRC will include notification of intent to submit a license application request, the submittal itself, and responding to requests for additional information. It is expected that multiple meetings with the NRC will also be required for this task. One or more early meetings could be used to discuss the benefits of EATF and any changes to the plant or plant operations that might be needed. These early meetings could be combined with those described in Sections 2.7 and 2.8. An additional presubmittal tactical meeting and presubmittal meeting will also be helpful.

2.7. PREPARE, SUBMIT, AND PURSUE TOPICAL REPORTS ON METHODS

Analyses of both lead assemblies and reloads depend on topical reports that describe approved methods of analysis. Analysis of EATF will require modifications to at least some of these methods. For example, existing thermal-mechanical codes for design of conventional fuel rods are unlikely to be applicable to a fuel pellet with additives that improve thermal conductivity, to cladding materials other than zirconium-base alloys, or to a cladding with a coating. New or revised topical reports on methods will therefore be needed. This task is relevant to licensing because it involves work on such reports.

The division of responsibility for this task will depend on how the fuel vendor and the utility partner divide the work of reload design. Topical reports that apply to analyses of the fuel rod and fuel assembly designs will be the responsibility of the fuel vendor. Reload design and plant safety analysis could be done either by the fuel vendor or the utility partner, according to their commercial agreements, and the division of responsibility for the related topical reports will presumably follow the agreements. The task lies in the future; it cannot begin until the lead assembly design is sufficiently developed that the impacts of the design on the methods of analysis are understood.

For each topical report that needs revision, the first activity will be to prepare and submit the report. When the fuel assembly design is sufficiently well developed and the behavior of EATF is sufficiently well understood, the entity responsible for the report can determine how the methods of analysis need to be changed. Alternatively, if a new topical report is needed, the entity responsible for the report will define the methods of analysis.

The second activity will encompass the remaining activities for pursuing approval of the topical reports, such as responding to requests for additional information.

Formal written interactions with the NRC will include notification of intent to submit the topical reports, the submittals themselves, and responding to requests for additional information. It is expected that multiple meetings with the NRC will also be required for this task. One or more early meetings could be used to discuss the performance of EATF, explain how analysis of performance differs between EATF and conventional fuel, and propose methods of analysis for any aspects of EATF that are not adequately covered by existing regulations or regulatory guidance. These early meetings could be combined with those described in Sections 2.6 and 2.8. An additional presubmittal tactical meeting and presubmittal meeting for each report will also be helpful.

2.8. PREPARE, SUBMIT, AND PURSUE TOPICAL REPORT ON FUEL DESIGN

A topical report on an EATF assembly design is the culmination of the efforts described in Sections 0 through 2.5, and such a report will clearly be needed because EATF represents a significant departure from conventional fuel. This task is relevant to licensing because it involves work on such reports.

This task will be the responsibility of the fuel vendor, though the utility partner may provide some inputs. The task lies in the future; it cannot be finished until the lead assembly design is essentially complete and the applicable methods of analysis are fully defined.

The first activity for this task will be to prepare and submit the report. The report will describe the fuel assembly design in sufficient detail to show that, with the exception of cycle-specific analyses, the fuel assemblies will comply with the applicable regulations and regulatory guidance. The analyses supporting the fuel design report will presumably use some of the methods discussed in Section 2.7, so it would not be surprising if the fuel design report and at least one methods report are submitted concurrently.

The second activity will encompass the remaining activities for pursuing approval of the topical report, such as responding to requests for additional information.

Formal written interactions with the NRC will include notification of intent to submit a topical report, the submittal itself, and responding to requests for additional information. It is expected that multiple meetings with the NRC will also be required for this task. One or more early meetings could be used to discuss the performance of the fuel design and to demonstrate that the design complies with existing regulations and regulatory guidance, as well as with any proposed criteria for aspects of EATF that are not adequately covered by existing regulations or regulatory guidance. These early meetings could be combined with those described in Section 2.6 and 2.7. An additional presubmittal tactical meeting and presubmittal meeting will also be helpful.

2.9. PREPARE, SUBMIT, AND PURSUE TOPICAL REPORT FOR SHIPPING CASK

Because of the differences between EATF and conventional fuel designs, it may be necessary to design a new shipping cask for fresh EATF. Alternatively, it may be necessary to reanalyze an existing shipping cask to show that it is appropriate for EATF.

Those situations would call for either a new topical report or a revision or supplement to an existing topical report. For convenience, this section refers to the report, revision, or supplement simply as a "report".

This task will be the responsibility of the fuel vendor or possibly a separate cask vendor. The utility partner may provide some inputs. The task lies in the future; it cannot be finished until the lead assembly design has been defined to the point that it is possible to describe the conditions that must be provided to protect the assembly during shipping.

The first activity for this task will be to prepare and submit the report. The report will describe the design and operation of the cask and will demonstrate that it will adequately protect the fuel assembly during shipment. It is possible that EATF will require the application of criteria that are not provided in existing regulations and regulatory guidance. In that case, the report should propose additional criteria and demonstrate that the cask complies with them.

The second activity will encompass the remaining activities for pursuing approval of the topical report, such as responding to requests for additional information.

Formal written interactions with the NRC will include notification of intent to submit a topical report, the submittal itself, and responding to requests for additional information. It is expected that multiple meetings with the NRC will also be required for this task. If it is found that special conditions are needed to protect EATF during shipping, one or more early meetings could be used to discuss those conditions and to demonstrate that the cask adequately protects the fuel. An additional presubmittal tactical meeting and presubmittal meeting will also be helpful.

2.10. PREPARE, SUBMIT, AND PURSUE LICENSE AMENDMENT REQUEST FOR FUEL MANUFACTURING FACILITY

It is assumed that EATF will be manufactured at an existing facility. However, because of the differences between EATF and conventional fuel designs, a LAR may be needed for the fuel manufacturing facility. That situation could arise, for example, if the enrichment of EATF is higher than what is currently allowed at the facility, or if the design uses materials that are currently forbidden at the facility.

This task will be the responsibility of the fuel vendor. The task lies in the future; it cannot be finished until the lead assembly design has been defined to the point that it is possible to describe the conditions that must be provided for safe manufacturing.

The first activity for this task will be to prepare and submit the LAR. The request will describe the facility and will demonstrate that its design ensures safety during manufacturing. It is possible that manufacturing of EATF will require the application of criteria that are not provided in existing regulations and regulatory guidance. In that case, the LAR should propose additional criteria and demonstrate that the facility complies with them.

The second activity will encompass the remaining activities for pursuing approval of the license amendment, such as responding to requests for additional information.

Formal written interactions with the NRC will include notification of intent to submit a LAR, the submittal itself, and responding to requests for additional information. It is expected that multiple meetings with the NRC will also be required for this task. If it is found that new criteria are needed to ensure safety during manufacturing, one or more early meetings could be used to discuss the criteria and to demonstrate that the plant complies with them. An additional presubmittal tactical meeting and presubmittal meeting will also be helpful.

2.11. DESIGN, FABRICATE, IRRADIATE, AND EXAMINE LEAD ASSEMBLIES

This task involves work that is related to lead assemblies for irradiation in a commercial power reactor. The task is relevant to licensing because it is expected that the fuel design report described in Section 2.8 will include a commitment for fuel surveillance. Reference 1 describes expected levels of surveillance. Examinations are expected to provide confirmatory information on a variety of performance measures and some recent NRC concerns, such as crud deposition, fuel rod growth, cladding corrosion, and internal gas pressure.

Responsibility for this task is divided according to the activity. The fuel vendor is responsible for designing and fabricating the lead assemblies and selecting appropriate postirradiation examinations. The utility partner will provide inputs on fuel design and must approve irradiation in its reactor. Irradiation will be the responsibility of the utility partner. Responsibility for examination of the irradiated fuel will probably be shared by the utility, the fuel vendor, and, if a hot cell examination is needed, a laboratory. The task has not been started. Design work cannot start until the tasks described in Sections 0 through 2.5 have been completed. Fabrication requires that the task described in Section 2.10 be completed, and irradiation requires that all the work described in Sections 0 through 2.10 be completed.

Design, fabrication, and irradiation fall into three separate activities. If the fuel is examined only at poolside, examination will be a single activity and will be the responsibility of the fuel vendor and the utility. If a hot cell examination is added, however, it would be appropriate to add other activities. The utility and fuel vendor will be responsible for harvesting the rods. A transportation contractor will be responsible for shipping the rods to a hot cell. A laboratory will be responsible for examining the rods.

At the current stage of development, it is difficult to provide a more detailed description of the various activities. The design, irradiation conditions, and postirradiation examinations should all be chosen to confirm the performance of the fuel and to address any concerns from the fuel vendor, the utility partner, or the NRC.

The licensing actions needed to authorize this task are described in Sections 2.6 through 2.10. Nevertheless, one or more meetings with the NRC should be included in this task. The meetings will keep the fuel vendor and utility partner up-to-date on concerns from the NRC and will keep the NRC informed about the actual performance of the fuel. These meetings could be combined with those described in Section 2.12.

2.12. EVALUATE PERFORMANCE OF LEAD ASSEMBLIES RELATIVE TO REQUIREMENTS AND GOALS

This task includes the analysis of results from the task described in Section 2.11. The task is relevant to licensing because it is expected that an interpretation of the results will be needed to confirm that the lead assemblies performed safely, reliably and as expected. That confirmation will be needed to support later plant LARs for batch irradiation.

This task is primarily the responsibility of the fuel vendor, but the utility partner may also provide inputs. The task lies in the future; it cannot begin until the lead assemblies have been at least partially irradiated and some information is available on their performance.

If the task described in Section 2.11 includes a hot cell examination, the first activity associated with this task will be reviewing and approving reports from the laboratory on postirradiation examination of the samples. With or without a hot cell examination, an activity will be needed to cover interpretation of the results and determination of whether the results support the conclusion that the fuel rod or fuel assembly design performed safely, reliably and as expected.

One or more meetings with the NRC should be included in this task. The meetings will keep the NRC informed about any changes in understanding of fuel performance. These meetings could be combined with those described in Section 2.11.

3.0 CONCLUSION

This appendix provides a regulatory plan for EATF irradiation. It provides a list of tasks and identifies those that are related to licensing (Table 1). The tasks start with exploratory efforts to select materials and designs and to define requirements and goals. The tasks then progress through successive stages that increase confidence in the performance of the fuel and support licensing. The plan lists regulatory actions that are needed to approve EATF for irradiation. Implementation of the plan will demonstrate safe and reliable operation of EATF and that its use in commercial nuclear reactors is acceptable from public safety, regulatory, and performance perspectives.

4.0 REFERENCES

1. U.S. Nuclear Regulatory Commission. Standard Review Plan for the Review of Safety Analysis Reports for Nuclear Power Plants: LWR Edition. NUREG-0800, Section 4.2, "Fuel System Design", Rev. 3, March 2007.

2. U.S. Nuclear Regulatory Commission. General Design Criteria for Nuclear Power Plants. 10 CFR Part 50, Appendix A, February 19, 2013.

3. U.S. Nuclear Regulatory Commission, Office of Nuclear Regulatory Research. Assumptions Used For Evaluating The Potential Radiological Consequences Of A Fuel Handling Accident In The Fuel Handling And Storage Facility For Boiling And Pressurized Water Reactors (PWR). Regulatory Guide 1.25, Revision 0, March 1972.

APPENDIX O

Materials Effects of EATF Pellet Additives and Coatings for the Phase 1A Final Report for Enhanced Accident Tolerant Fuels

Prepared by:
AREVA Federal Services, LLC

TABLE OF CONTENTS

1.0 PELLET ADDITIVES AND COATING MATERIALS 1
1.1. PELLET ADDITIVES: 1
1.2. CLADDING COATING MATERIAL: 1
2.0 MATERIALS EFFECTS OF EATF PELLET ADDITIVES AND COATINGS 1
3.0 COLD SPRAYED TI_2ALC COATING 1

1.0 PELLET ADDITIVES AND COATING MATERIALS

1.1. PELLET ADDITIVES:

As a result of the work performed on this project three (3) pellet additives currently remain under consideration for further development of EATF fuel pellets.

- SiC(p) – Silicon Carbide (particle form)
- SiC(w) – Silicon Carbide (whiskers)
- DP - Diamond Powder (nanoparticles, 12 microns average size)

The UO_2-SiC pellet composite is comprised of 10% SiC by volume for both SiC particle and whisker additive forms. The UO_2-Diamond pellet composite is also comprised of 10% DP.

1.2. CLADDING COATING MATERIAL:

As a result of the work performed on this project a single cladding coating material, Maxthal 211 - Aluminum Titanium Carbide (Ti_2AlC) currently remains under consideration for further development as an EATF clad coating. The Ti_2AlC material, procured in powder form, is deposited using the Cold Spray (CS) process. The final desired thickness of the Ti_2AlC coating is targeted at 50 µm or less.

2.0 MATERIALS EFFECTS OF EATF PELLET ADDITIVES AND COATINGS

The proposed coating and pellet additives have numerous potential effects on fuel performance. Some of these can currently be evaluated, and others cannot. This section provides a list of effects and, for each effect, either a tentative evaluation or a suggestion on what is needed to support an evaluation.

3.0 COLD SPRAYED TI_2ALC COATING

Volume occupied in core: Any coating will occupy some volume in the core and will therefore displace fuel, cladding, or water. Determining the effect on fuel performance will require neutronic, thermal-hydraulic, and mechanical analyses. The coating clearly cannot perform the energy production function of the fuel or the coolant and moderator functions of the water, so the best possible outcome might be if some structural credit can be claimed for the coating. Mechanical tests on coated cladding, preferably irradiated, might help to determine that.

Reaction with base metal: Autoclave and steam oxidation tests suggest that there are no significant reactions between the coating and the base metal of the cladding.

Reaction with high-temperature steam: Steam oxidation tests suggest that coating oxidation in steam is slow.

Additional tests will be needed to quantify the reaction rate.

Thermal conductivity: The thermal conductivity of Ti_2AlC is similar to that of zirconium alloys, so a coating will not significantly increase the temperature of the fuel pellets. Tests should be performed on irradiated material.

Surface finish: The surface finish of a coating will be different from that of current cladding tubes, so there is the potential that drag, critical heat flux (CHF), and crud deposition will be affected. Tests of heated rods in a flow loop may provide some information about these effects. Tests of grid wear during rod insertion are also needed.

Porosity: Sprayed coatings typically have some porosity, so there is a possibility that coolant will penetrate through at least part of the coating and boil in the pores. Tests of heated rods in a flow loop may provide some information about the effects of porosity.

Neutron absorption: The thermal neutron capture cross section of natural titanium (about 6.1 barns) is substantially larger than that of zirconium (0.184 barns), so the neutronic penalty from a Ti_2AlC coating will set a limit on the acceptable thickness. The neutronic penalty could be reduced by using titanium that is depleted in Ti-48, but that is expected to be costly. Neutronic analyses are needed to determine the acceptable thickness.

Fatigue: Fuel rods are designed to withstand a certain number of transients without failure by fatigue. The fatigue properties of a coated rod are currently unknown, so tests are needed to determine them.

Creep and irradiation growth: Zirconium-alloy cladding creeps down onto the fuel pellets because of the pressure of the coolant, and later the diameter increases as the pellets swell. Cladding also increases in length as a result of irradiation growth and pellet swelling. Creep and irradiation growth rates for the coating probably differ from those of the cladding, so fuel rod performance will be affected. Irradiation tests on rodlets, preferably in a flow loop, will be needed to determine the creep and growth rates of coated cladding.

Fretting: Ti_2AlC appears to be significantly harder than typical unirradiated zirconium alloys, so fretting should be less of a concern for a coated rod than for an uncoated one.

Effect on heat treatment: Despite its name, cold spraying produces locally high temperatures as particles impact the substrate, and there is some concern that the heat treatment of the base metal will be affected. Transmission electron microscopy of an as-coated sample will provide information about possible changes in the second-phase particles in the base metal.

PELLET ADDITIVES (SILICON CARBIDE WHISKERS, SILICON CARBIDE PARTICLES, AND DIAMOND PARTICLES)

Volume consumed: It has typically been proposed that silicon carbide or diamond additives should occupy about 10% of the volume of the fuel pellets, so they would displace 10% of the uranium. That appears to be a severe penalty, though it might be mitigated by neutronic effects of lower pellet temperature or by a slight increase in pellet density. Thermal-mechanical and neutronic calculations are needed, as are pellet density measurements.

Degradation by irradiation effects: The effect of irradiation on thermal conductivity is unknown but clearly important. Four processes are at work: (1) When a uranium atom fissions, the two fission fragments travel perhaps 8 µm through the UO_2 and displace many atoms in the process. In a UO_2-SiC or UO_2-diamond fuel pellet, the SiC or diamond phase is so finely divided that the

fission fragments can easily penetrate the material and displace atoms of C (and Si if applicable) almost as if they were in the UO_2 matrix. (2) As the fission products travel through the fuel pellet, they cause repeated local melting in the fission tracks. Maximum temperatures of 6000 K have been calculated for fission tracks in UO_2, and for typical heat generation rates in a power reactor, each part of a fuel pellet is expected to melt (and quickly solidify again) several times per day. It is at least conceivable that similar melting will occur in the SiC or diamond particles. For diamond, the crystal structure may change to a more stable form, such as graphite. (3) At end of life, roughly 5% of the uranium atoms in a UO_2 pellet will have fissioned, so there will be a significant concentration of fission product impurities in the fuel, and those impurities will presumably be in the SiC or diamond particles as well as in the matrix. (4) High steady-state temperatures in the fuel pellet are expected to anneal the radiation damage. The thermal conductivity of the fuel pellets will depend on the balance among these processes. Irradiation tests on rodlets are needed, followed by microscopy and measurements of thermal conductivity.

Chemical reaction with UO_2: The oxygen potential in an LWR fuel pellet without SiC or diamond typically increases during irradiation, reaching levels (in the vicinity of −400 kJ/mol O2) that are expected to oxidize SiC and possibly even diamond. However, the quantity of SiC or diamond additive may be large enough that reaction of a fraction of it will hold down the oxygen potential. An evaluation of the pellet chemistry would be helpful, though microscopy of an irradiated fuel pellet (preferably at high burnup) may also be needed.

Chemical reaction with cladding: No significant reactions between the SiC or diamond additives and the cladding are expected.

Neutron absorption: Carbon has an especially small thermal neutron capture cross section, so neutron absorption by diamond should be acceptable. Silicon has a somewhat larger cross section, so a neutronic calculation on the effects of SiC is in order. It is noted that the SiC whiskers used by the University of Florida (UF) have a significant concentration of boron, which should be taken into account unless a source of low-boron whiskers is found.

Thermal expansion: The coefficients of thermal expansion of SiC and diamond are smaller than that of UO_2, so these additives will not cause excessive thermal expansion of the fuel pellets.

Melting point: Carbon remains solid at the melting point of UO_2, so diamond will not reduce the melting point of the pellets. SiC appears to decompose at a temperature slightly below the melting point of UO_2. However, the intended effect of adding SiC or diamond to a fuel pellet is reducing fuel temperatures, so there may be no loss of margin to centerline melting. Thermal-mechanical calculations are needed and should reflect the thermal conductivity of irradiated pellets.

Fission gas release (FGR): Additions of SiC or diamond are intended to reduce fuel temperature for a given linear heat generation rate (LHGR), so if they serve that purpose, there should be a significant reduction in FGR, with relaxation of associated limits on fuel rod operation. Cesium and iodine are normally not considered to be fission gases, but lower fuel temperatures will presumably slow their transport to the pellet-cladding annulus. Irradiation tests and subsequent hot cell exams can be used to quantify the benefit.

Pellet-cladding mechanical interaction: Adding SiC or diamond to fuel pellets can be expected to have some effect on pellet-cladding mechanical interaction simply because the properties of these additives differ from those of UO_2. However, the effect should be small because the additives will compose only about 10% of the volume and will presumably be a dispersed phase. Ramp tests will be needed to evaluate the effect.

APPENDIX P

Performance Test Plan
for the
Phase 1A Final Report
for Enhanced Accident Tolerant Fuels

Prepared by:
AREVA Federal Services, LLC

TABLE OF CONTENTS

1.0 INTRODUCTION 1
2.0 NORMAL OPERATION 1
3.0 DESIGN BASIS EVENTS 1
4.0 BEYOND DESIGN BASIS EVENTS 1
5.0 SUMMARY OF PERFORMANCE TESTING CONDITIONS 2
6.0 REFERENCES 2

LIST OF TABLES

Table 1: Summary of Estimate 2

1.0 INTRODUCTION

New fuels are being developed with enhanced accident tolerance. Metrics are needed to measure the success of the various options. Idaho National Laboratory (INL) has provided a document [2] outlining these metrics. To support the present discovery phase of EATF development the AREVA Team has summarized these in three main categories. These are Normal Operation, Design Basis Events (DBE), and Beyond Design Basis Events (BDBE). The impacts on these areas are provided in sections 2, 3, and 4 respectively. A summary table of performance test conditions for the discovery phase is provided in Section 5.

2.0 NORMAL OPERATION

Normal Operation testing of fuel is generically performed using conditions specified in ASTM G2. This test provides an indication of the effect of the coolant on the cladding during normal operation for long periods of time. Although operation extends over many years, the 72 hours of the test is deemed sufficient to indicate the potential effect of the coolant on the cladding. In this test, the temperature is held at 400 degrees C at 1500 psi for 72 hours. The effectiveness of EATF options are assessed by comparing the effects of this test to the effects of the same test on un-coated Zircaloy cladding presently in use.

3.0 DESIGN BASIS EVENTS

DBE for LWRs include both Large Break (LB) and Small Break (SB) Loss of Coolant Accidents (LOCA). The LB-LOCA is terminated by the reflood of the core at about 4 minutes into the event. The peak cladding temperature (PCT) is expected to reach 1100 degrees C. Because of the depressurization due to the assumed double-ended pipe break, a pressure of 1 atmosphere is used for the performance testing. The SB-LOCA is expected to maintain a higher pressure; therefore a pressure of 2200 psi is used. Since the center of the core stays covered with coolant, a peak temperature of 300 degrees C is used for 90 seconds.

These conditions are summarized in Table 1. These values will vary from one plant design to another. Used generically they are approximate but still adequately represent these kinds of events for the testing of EATF performance relative to the present technology.

4.0 BEYOND DESIGN BASIS EVENTS

BDBE take the fuel trough a wider range of environments than the DBE. INL is presently preparing models to predict the behavior of EATF in these events. These models are necessary to evaluate the performance of EATF in these events due to the complex interactions during them. Therefore, no simple set of parameter values has been established that will adequately compare EATF concepts performance with present fuel.

5.0 SUMMARY OF PERFORMANCE TESTING CONDITIONS

The performance testing conditions used for the discovery phase of EATF development are summarized in Table 1. In conclusion, the testing conditions used by the AREVA Team, to evaluate EATF concept performance, closely correspond with those developed by INL for the Normal Operating and Design Basis Event conditions. The conditions that represent the BDBE will have to be more completely defined, along with any supporting analysis models that will be required to evaluate EATF performance.

	Normal Operation	Design Basis Events	Beyond Design Basis Events
Present AREVA[1]	ASTM G2 400°C / 1500 psi / 72 hrs	LB-LOCA 100°C / 1 atm / 4 min SB-LOCA 300°C / 2200 psi / 90 sec	1500°C / 1 atm / 4 hr
New INL[2]	ASTM G2	<17% oxidation at 1200°C / 1000 sec	Not Summarized

Table 1: Summary of Performance Testing Conditions

6.0 REFERENCES

1. AREVA specified conditions representing conditions that are expected in each operating regime.

2. LWR ATF Performance Metrics, INL/EXT-13-29957, February 2014.

APPENDIX Q

ATF Fuel Design Impacts
for
Phase 1A Final Report
for Enhanced Accident Tolerant Fuels

Prepared by:
AREVA Federal Services, LLC

TABLE OF CONTENTS

1.0 INTRODUCTION 1
2.0 DEVELOPMENT HISTORY 1
2.1. COLD SPRAY COATINGS 2
2.2. EPD COATINGS 3
2.3. PELLET FUEL ADDITIVES 4
2.4. OTHER INCLUDED TECHNOLOGY 6
3.0 ENGINEERING ASSESSMENT OF EATF IMPACTS 6
3.1. LOCA EFFECTS OF EATF PELLET ADDITIVES AND COATINGS 7
3.2. MECHANICAL EFFECTS OF EATF PELLET ADDITIVES AND COATINGS 8
3.3. NEUTRONIC EFFECTS OF EATF PELLET ADDITIVES AND COATINGS 9
3.4. NON-LOCA EFFECTS OF EATF PELLET ADDITIVES AND COATINGS 9
3.5. ESTIMATE OF THE IMPACT OF THE SIC FUEL ADDITIVE ON LARGE-BREAK LOCA SAFETY ANALYSIS 12
3.6. MATERIALS EFFECTS OF EATF PELLET ADDITIVES AND COATINGS 13
4.0 CONCLUSION 13

LIST OF TABLES

Table 1: Result of the Estimate and Expected Time 12

1.0 INTRODUCTION

In response to the Department of Energy (DOE) funded initiative to develop and deploy lead test assemblies (LTAs) of Enhanced Accident Tolerant Fuel (EATF) into a US reactor within 10 years, AREVA put together a team to develop promising technologies for improved fuel performance. The team consists of the University of Florida (UF), the University of Wisconsin (UW), Savannah River National Laboratory (SRNL), Duke Energy and Tennessee Valley Authority (TVA).

EATF technology concepts that our team considered were:

1. Additives to the fuel pellets.

   a. Reduce cost of pellet manufacture improving fuel economics.

   b. Chromia doping to:
      - reduce fission gas generation.
      - improve load following characteristics.
      - increase uranium density.
      - improve wash out characteristics in rod failure.
      - lock cesium into fuel matrix.

   c. Silicon carbide whiskers, silicon carbide particles, or diamond particles to:
      - improve thermal heat transfer in normal conditions improving fuel efficiency.
      - improve margin in an accident condition.
      - lock iodine into fuel matrix.

2. Nine coatings on the existing zirconium cladding.
   - Potential to reduce hydrogen pickup and mitigate hydride reorientation in the cladding.
   - Increased coping time during accident condition.

2.0 DEVELOPMENT HISTORY

AREVA adopted a formal “Gate Review Process” that was used to review results and focus resources onto promising technologies to reduce costs and identify the technologies that will be carried forward to LTAs.

During the first Gate Review, each of the team members presented their initial findings to a board evaluating the manufacturability of each concept. The results of this initial board identified that:

1. Two (2) of the four coatings under development by SRNL should continue to the next phase of testing.

2. Two (2) of the five coatings under development by UW should continue, but be reviewed early in the next year.

3. SiC whiskers, nano-diamond and chromia doping should continue, but the work should be focused on demonstrating the repeatability of the pellet data obtained so far, and testing of the pellets in the Advanced Test Reactor (ATR).

During the second Gate Review the Electrophoretic Deposition (EPD) process was eliminated, leaving only the Cold Spray (CS) Process.

2.1. COLD SPRAY COATINGS

The Gate Review for Manufacturability recommended that Ti_2AlC and Ti_3AlC_2 CS coatings under development by SRNL should continue to the next phase of testing, but be reviewed early in the next year.

The board had some concerns regarding the work:

1. The coatings are typically thick, about 200 μm. The desired range is a few micrometers. The thickness means that the coating takes up a substantial volume in the core of a reactor and will affect the thermal hydraulic performance of the fuel assembly. The Zircaloy surface is also roughened by the application of the coating material. Therefore, the coating must fill in these peaks and troughs and this sets the minimum coating thickness.

2. Roughening of the substrate provides a mechanical bond with the coating, but a metallurgical bond is needed to prevent steam oxidation of the substrate. It is also possible that water or steam penetrates through the coating and causes delamination.

3. Coupons of coated Zircaloy sheet showed discoloration on their uncoated faces. The discoloration suggests that the substrate reached a relatively high temperature, and its heat treatment may have been affected.

4. The board concluded that the research is possibly viable but had the following recommendations for Year 2:

    a. Work should focus on CS application only.

    b. The effect of the coating process on the microstructure of the substrate should be investigated. Annealing or phase change in the substrate is not desirable.

    c. It is important to understand whether oxidation of the substrate is caused by penetration of steam or water through the coating or by transport under the coating from the edges. This question can be answered by metallography of a lightly oxidized sample.

    d. The coating thickness must be dramatically reduced from what is currently seen.

    e. Testing of flat coupons progressing to rods should proceed.

MAX phase coatings have demonstrated promise to provide increased utility reaction time under accident conditions while having fewer validation requirements than a stand-alone cladding. The MAX Phases are layered, hexagonal carbides and nitrides, and have the general formula: Mn+1AXn, (MAX) where n = 1 to 3, M is an early transition metal, A is an A-group (mostly IIIA and IVA, or groups 13 and 14) element and X is either carbon and/or nitrogen. Generally stiff, lightweight, and plastic at high temperatures, some, like Ti_3SiC_2 and Ti_2AlC, are also creep and fatigue resistant, and maintain their strengths to high temperatures.

The two spray methods selected were the high velocity oxy-fuel (HVOF) process and the CS process. HVOF was tested and found to present some difficulties: the powder caused an energetic excursion, and the composition of the deposited coating was substantially different from that of the original powder. In addition, microcracks were observed in HVOF coatings, even though the samples were handled gently. HVOF deposition was dropped.

Initial corrosion/oxidation testing of Ti_2AlC MAX-coated Zircaloy-4 was conducted at the UW in a pressurized autoclave system, but the supercritical conditions chosen (144 hours, 500°C, 3600 psia) were not representative of nuclear reactor accident environments. SRNL and UW are working with AREVA to define temperature, pressure, and time of exposure test parameters for design basis (DB) (Large- break and Small-break Loss of Coolant Accidents (LOCA)) and beyond design basis events (BDBE). The next phase of testing used more realistic conditions for hypothetical DB and beyond design basis (BDB) reactor events and enhancement of tolerance to the Design Basis Events (DBE) was demonstrated.

2.2. EPD COATINGS

The first Gate Review for Manufacturability recommended that yttria-stabilized zirconia (YSZ) and TiO_2 coatings under development by UW should continue, but be reviewed early in the next year.

Without sintering, the EPD coatings were soft. A concern with laser sintering was a Zircaloy phase change.

If the EPD coating process precedes the thermal treatment used to produce the desired cladding microstructure, detrimental thermal exposure for the cladding could be mitigated.

Cracks are detrimental to oxidation performance, but may increase heat transfer.

The board had some concerns regarding the work:

1. Consolidation of the coatings is a key problem in manufacturing that has not been successfully addressed yet. Tests with laser treatment have resulted in either too little or too much energy absorption, with the coatings being either inadequately consolidated or ablated. The alternative is low-temperature furnace sintering. The fineness of the deposited particles may make this approach feasible, though the temperatures that cause changes to the microstructure of cladding are low in comparison to those typically used for sintering. It is not

clear that long, low-temperature heat treatments will provide a solution, because longer heat treatment times may also promote changes to the cladding.

2. There is the possibility that the increase in critical heat flux (CHF) will be lost during irradiation. Even in PWRs, parts of the fuel undergo nucleate boiling, and that raises questions about the possibility that crud will be deposited over the coating and degrades its performance.

3. An increase in CHF is welcome, but it does not provide a large benefit during the long accidents that are of interest with EATF.

The board concluded that the research is possibly viable but had the following recommendations for year 2:

1. Work should focus on producing well-consolidated coatings. The presenter suggested YSZ and TiO_2 as promising coating materials, and the board accepts that suggestion. Work on all other coatings should stop immediately. Reducing the number of coating materials is recommended so that more effort can be put into making high-quality coatings of the two chosen materials.

2. If well-consolidated, adherent coatings can be produced, the effects of the consolidation treatment on the microstructure of the substrate should be investigated.

3. An additional gate review was recommended for March 2014 to determine whether progress is being made in coating consolidation or the work should be terminated.

4. Related work (such as quench testing, CHF testing, and laser engraving) was NOT recommended unless the next gate review is passed

During the second Gate Review, the EPD process was dropped due to difficulty with sintering the applied coatings.

2.3. PELLET FUEL ADDITIVES

The Gate Review for Manufacturability recommended that work on SiC particles, SiC whiskers, and diamond, all with chromia doping, should continue, but the work should be focused on demonstrating the repeatability of the pellet data obtained so far, and on testing of the pellets in the ATR.

SiC powder and whiskers are potential additives for increasing the thermal conductivity of fuel pellets. The primary advantages of an increased thermal conductivity are anticipated to be (1) decreased cracking of the fuel pellets, (2) reduced fuel swelling, (3) decreased stored heat in the pellets at the time of LOCA initialization, and (4) greatly reduced fission gas release (GFR).

The board had some concerns regarding the work:

1. Decreased cracking may contribute to retention of fission gas, but the size of the benefit is not clear. Cracking results from thermal stresses, which are reduced by

an increase in thermal conductivity, but thermal stresses can also be reduced by reducing the linear power density, and studies of conventional pellets have not shown a strong effect of power density on cracking.

2. Reduced fuel swelling maintains a gap between the pellet and cladding for a longer period, which is beneficial in controlling pellet-cladding interaction. The thermal benefits are less clear. A larger pellet-cladding gap means a larger temperature drop across the gap, but if the GFR is reduced, the thermal conductivity of the gas will be higher because the effects of released xenon and krypton will be smaller.

3. It is reasonable to expect that the claimed increases in thermal conductivity, if realized, will produce a large reduction in GFR. A key question is whether the increase in thermal conductivity will be sustained until end of life. Direct implantation of fission products, implantation of knock-on atoms, and neutron irradiation effects all have the potential to degrade the silicon carbide.

4. The silicon carbide or diamond takes up a substantial volume of the pellet and thus displaces fuel. As a result, the uranium loading and energy extraction per fuel assembly will be reduced.

The board concluded that the research is viable but recommended a close investigation of how thermal conductivity degrades with irradiation and the impact of thermal conductivity improvement on potential for cracking is in order. This will be addressed by the ATR irradiation experiments. Since cracking could be a threshold effect, a study to look at an equivalent linear power decrement for introduction of SiC or diamond compared to conventional pellets could add some insight.

2.3.1. R&D NEEDED TO MATURE THE CONCEPT

Spark Plasma Sintering (SPS) allows the sintering of all forms of conventional powdered metals plus most forms of exotic, ultra-pure nanophase ceramics, composites, polymer-metallic composites, and high porosity materials. UF has developed and demonstrated a novel fuel manufacturing concept that can sinter UO_2 pellets within 30 seconds and UO_2-SiC pellets within 5 minutes. The total SPS fabrication time for each pellet is less than 90 minutes, a significant improvement over the typical runtime in the conventional sintering process, which can be several hours.

A major challenge for future R&D will be adapting SPS for the mass production of fuel pellets. Both DOE and UF facilities should be developed to fully meet this challenge.

The UF has shown that the SPS process is needed to produce a composite UO_2-SiC pellet having better properties than the standard UO_2 fuel. SPS is the only means presently available to properly fabricate a high quality composite fuel with the needed density, interfacial contact, and enhanced thermo-mechanical properties. Good interfacial contact between UO_2 and SiC is only observed in SPS-fabricated pellets.

2.4. OTHER INCLUDED TECHNOLOGY

In consideration of EPRI joining the AREVA EATF team in the next phase of the program the board reviewed the progress of EPRI to date in their self-funded development program. The performance of zirconium alloys in severe accidents is limited by their loss of strength at high temperature and by hydrogen generation in high-temperature, oxidizing environments. Molybdenum alloys are being investigated for fuel cladding because they provide superior strength at high temperatures. A common concern about molybdenum is that it will oxidize to volatile MoO3 at high temperatures, but tests showed surprising resistance to that. In any case, oxidation could be addressed by applying an outer coating of zirconium or a FeCrAl alloy. The outer layer could be applied by coating techniques (physical vapor deposition, vacuum plasma spray, etc.) or by coextrusion. Molybdenum has a thermal neutron capture cross section comparable to that of FeCrAl, so there will be a neutronic penalty unless the molybdenum is depleted in Mo-95.

Also included in the Interim Report is a discussion of the introduction of various nanoparticles into the emergency coolant to increase the heat transfer, CHF, and quenching capabilities needed to prevent overheating and damage to fuel assemblies during a DBE. Results demonstrate that the injection of nanoparticles into the reactor coolant effectively creates a colloidal dispersion known as a “nanofluid”. The deposition of nanoparticles from the nanofluid to the fuel cladding surface can considerably increase the CHF, which is the heat flux corresponding to a departure from nucleate boiling (DNB) in the reactor core. AREVA studies have shown that a corresponding benefit from these CHF improvements is on the order of 150 °C in cladding temperature margin.

AREVA is now testing pre-operation oxide film on improved zirconium alloy cladding. The cladding is processed during manufacturing to produce a thin zirconium oxide film on the cladding. The oxide film acts like that on anodized aluminum, forms a protective oxide layer that prevents further oxidation by providing a barrier, and prevents the formation of hydrides in the cladding.

3.0 ENGINEERING ASSESSMENT OF EATF IMPACTS

In review of these various aspects of the EATF program, AREVA solicited the opinions from the various engineering disciplines concerning the potential or perceived advantages and/or disadvantages of the various pellet additives and clad coatings. This input is presented briefly in the ensuing sections. One should note that from an engineering standpoint some of these concepts may appear promising or detrimental to the overall fuel design and operation; however, these areas will require testing and validation in the “normal” operating environment then extension to the accident regime before acceptance by the industry.

The concerns identified in these sections are provided so that they may be addressed in future work. Their enumeration here does not imply that they have been identified as eliminating any of the EATF concepts proposed by the AREVA Team. Concepts are eliminated by the Gate Review process described in Appendices C and D.

3.1. LOCA EFFECTS OF EATF PELLET ADDITIVES AND COATINGS

3.1.1. COLD SPRAY CLADDING COATING PROS & CONS

During normal operation the advantages seem minimal, e.g. corrosion resistance. The disadvantages of cladding coatings also seem obvious. Spallation of the coating would cause increased debris in the coolant stream, increased cladding roughness causing additional pressure loss through the bundle, and a potential for increased thermal conductivity causing higher fuel temperature.

During DBE the benefits seem equally obvious. If the coating can reduce the rate of oxidation or hydrogen uptake, there is a safety advantage, although it should be noted that when M5 cladding is used cladding oxidation is rarely limiting from a LOCA standpoint. The impact on CHF may be advantageous, due to enhanced turbulence; however, this would be countered by the increased pressure loss along the length of the bundle. The impact on cladding deformation characteristics has yet to be determined, although the coating may provide more durability at high temperatures.

Additional information needed to license a lead test rod (LTR) includes Oxidation Kinetics, impact on CHF, and deformation characteristics.

3.1.2. EPD CLADDING COATING PROS & CONS

From a safety analysis standpoint, the technology used to deposit the coating would seem to make little difference, so the same advantages and disadvantages will apply. There are, obviously, concerns about the inability of the EPD coating to be fused to the substrate and the potential for spalling. There is perhaps less concern about the roughness of the coating since it would seem to be more evenly applied.

3.1.3. SIC FUEL ADDITIVE PROS & CONS

This technology is the most interesting, and probably the most challenging for safety analysis. Although the benefit of reduced stored energy in the pellet is tempting there is a significant amount of additional information that is needed to understand its impact. Assuming that increasing pellet enrichment can exceed 5%, as is suggested in Appendix H of the Interim Report, little is known about the pellet structure at high burnup with this type of additive. The rim effect and the fine pellet fragmentation that has been observed in some high burnup fuel may be significantly reduced. This would have a significant impact on pellet relocation during cladding swell and rupture.

It has been conjectured that the reduction in radial temperature gradient will cause retention of fission gases in the pellet at mid- and end-of-life conditions, causing additional pellet swelling with a consequent increase in Pellet-Clad Mechanical Interaction (PCMI) and will certainly impact fuel fragmentation. The consequent pellet pulverization could impact fuel relocation and fuel dispersal after and during cladding rupture. Chromia doping has been shown to increase induced micro-cracking on the surface of the pellet, which tends to evenly distribute stress and reduce the consequence of PCMI. Therefore these phenomena may be in opposition.

Additional information is required to confirm that GFR during LOCA is not enhanced over UO_2 and/or not greater than current design. The GFR rate at Limit of Core Operation (LCO) conditions with a fuel additive needs to be confirmed.

The benefit of cladding coating will be to improve hydrogen uptake. However, advanced alloys without coatings have already addressed this safety concern, and would be of no additional benefit in this area when used on these advanced alloys.

3.2. MECHANICAL EFFECTS OF EATF PELLET ADDITIVES AND COATINGS

From a mechanical viewpoint, the following potential benefits and concerns are envisioned based on review of the proposed EATF concepts. As with all significant changes to the fuel design, quantifying the commercial benefit to the customers is considered the most significant challenge. This assessment/guidance relates primarily to properties directly impacting fuel manufacturability and structural design properties. Impacts resulting from changes to cladding wall thickness and coating thickness are discussed:

3.2.1. CLADDING WALL THICKNESS

A reduction in the fuel cladding wall thickness to accommodate an added coating layer would have several adverse effects. The primary concern relates to the fuel rod resistance to creep collapse. Changes to the cladding wall thickness greater than a few percent will cause significant design challenges. The typical PWR cladding is Zircaloy-4 or M5®, with wall thicknesses are around 0.025”.

The lateral strength and stiffness properties would also be impacted by changing the cladding wall thickness, introducing additional concern relative to fuel rod bow. Potential benefits/concerns would need to be evaluated and tested based on the proposed change to wall thickness.

Any changes to the wall thickness are assumed to preserve the existing diametrical clearance between the pellet and cladding inner diameter, as gap conductance limitations are a significant Thermal/Hydraulics limiting parameter. Any changes relating to the cladding wall thickness should consider the resulting effects in these areas.

Concerns identified include cladding creep collapse margin, impact to gap conductance, and material strength.

3.2.2. COATING THICKNESS

The application of a coating to fuel rods presents a number of concerns/ challenges from a fuel manufacturing perspective. Current fabrication practices allow fuel rod insertion forces to approach 500 lbf during insertion into the fuel bundle. During the fuel rod insertion process, it is common for the grids to cause scars on the fuel rods (<0.002” depth). The addition of a coating to the fuel rods would need to be sufficiently hard to resist scarring during bundle fabrication to remain effective. Changes to the cladding outer surface can ultimately impact grid slip loads. Slip loads are key input parameters to mechanical performance

predictive models. The surface hardness and uniformity limits of any applied coating ultimately would need to be tested and evaluated.

Another concern is coating susceptibility to detachment in-core, as this could potentially lead to crud deposition issues. If operating/accident conditions could cause detachment of the coating, there is potential for debris generation – a significant concern for long-term fuel cooling.

Coatings should be able to demonstrate sufficient adherence to the substrate when considering typical operation accidents.

- Benefits: increased hardness resulting in improved fuel rod insertion during fabrication
- Concerns: cladding scarring, coating detachment

3.2.3. PELLET DOPING

Chromia-doping has recently been evaluated by the AREVA Fuel Organization. From a manufacturability and design perspective, there are no significant concerns with the utilization of such pellets. Based on experience, chromia-doped pellets should exhibit slightly larger outside diameters, reducing the available pellet/clad gap. Changes to pellet composition should be evaluated and modelled by the thermal-mechanical group to assess impact to PCI (pellet clad interaction) margin and swelling/creep.

- Benefits: introduction of a larger pellet, allowing for increased fuel material volume
- Concerns: thermal-mechanical margins.

3.3. NEUTRONIC EFFECTS OF EATF PELLET ADDITIVES AND COATINGS

The effects of the EATF changes on fuel burnup are presented in Appendix I.

3.4. NON-LOCA EFFECTS OF EATF PELLET ADDITIVES AND COATINGS

The two areas for examination for enhanced fuel design include coatings applied to the fuel cladding and additives to the fuel pellets to address common design issues in the industry. The issues and perspective for non-LOCA are provided for each below.

3.4.1. COATINGS

Coatings are suggested to enhance the hydrogen pickup rate, mitigation of hydride reorientation, and increase coping time during severe accident conditions. The effects of the coating would include higher thermal resistance, changes to CRUD pickup/loss, and potential changes to flow losses.

FLOW EFFECTS

It is expected that to support current fuel assembly designs, the overall pin diameters will not be changed significantly, thereby alleviating any concerns relative to increased pressure drops and flow rate changes in the core region.

THERMAL RESISTANCE

Any coating is expected to increase thermal resistance of the cladding, leading to changes in the fuel temperatures and CHF predictions. These are expected to be negative effects leading to more restrictive operating limits.

If the effect on fuel temperature were large, the limiting analyses would need to be re-performed to ensure the plant response was understood. It is not expected that even if the conditions were modeled that the limiting events and conclusions would change.

CRUD PICKUP/LOSS

Current non-LOCA methods do not model crud deposition or removal. Thus the methods assume that the effects of crud would be accommodated in any peaking and fuel analysis uncertainty factors. This would not change with the addition of coatings unless the coating significantly affects fuel performance. The same approach and methods used today would be expected to be maintained into the future.

COPING TIMES FOR SEVERE ACCIDENT CONDITIONS

The current analyses for coping times during severe accidents are highly variable due to the number of factors related to the plant behavior such as: initial secondary inventories, actual valve and pump sizing, primary and secondary system heat losses, and passive system performance characteristics. As such, the time of coping is a stronger function of the secondary and primary inventories than specific fuel behavior once it has been uncovered. Although positive relative to severe accident mitigation, the benefit, if any, would not be expected to significantly affect the operator guidance or equipment management issues.

SUMMARY

Although there may be small changes to the fuel performance due to coatings, the net effect will be at best neutral, but is deemed more likely to be slightly negative for non-LOCA considerations.

3.4.2. FUEL PELLET ADDITIVES

Various additives have been postulated to be added to fuel pellets to address performance characteristics such as fission gas generation, locking up of cesium and iodine in the fuel matrix, and potential improvements in thermal conductivity. Each of these items will have some effect on fuel temperature, fission product release and uranium loading as the additives will displace normal fuel compounds in the pellet.

CHROMIA

This additive is intended to reduce GFR into the gap, lock some byproducts in the fuel matrix, as well as uranium densities in the fuel. The ability to maintain some byproducts in the fuel will assist in radiation release, assuming that the failure of fuel cladding (first barrier to the gas release) does not lead to other release mechanisms for the gases. Additionally, some documents indicate that the introduction of chromia will lead to lower uranium density, thereby requiring higher enrichments to offset the small decrease. The overall effect would seem to be slightly positive (potential dose benefit) to neutral for this additive.

SILICON CARBIDE

The use of silicon carbide (SiC) in the fuel has some structural and thermal benefits. Additionally, SiC has the potential to also lock iodine in the fuel matrix.

The displacement of uranium (up to 10%) will require greater enrichments to achieve the same cycle lengths. This effect is larger than chromia.

The increased thermal conductivity is a benefit for transients that result in additional energy deposited into the fuel. The result will be reduced fuel temperatures, as compare with standard fuel pellets, and less reactivity feedback for a given power change. The effect will potentially be to place a higher heat flux at the surface of the cladding and slightly higher peak powers since Doppler feedback will be less. This will be a transient specific effect that will tend to shift the worst case DNBR point and peak power points (break size, rod worth, etc), but should not alter the overall conclusions for acceptability of the fuel performance.

The ability of the SiC to lock iodine in the fuel matrix should lead to reduce dose for events since the inventory of iodine available for release to the environment will be less.

DIAMOND

Diamond has superlative thermal conductivity and contains only low neutron cross section carbon. This material is hydrophobic, eliminating problems with absorption of water from the atmosphere during manufacture. It also has a high chemical stability. About 1,000 metric tonnes of synthetic diamonds are produced each year, making their use practical.

SUMMARY

Based upon the review, if an increase in enrichment is possible, the overall effects of SiC are positive relative to non-LOCA issues and would seem to be a better solution than chromia. However, manufacturing issues, and impact on the actual dose benefits of each dopants would need more detailed testing.

3.5. ESTIMATE OF THE IMPACT OF THE SIC FUEL ADDITIVE ON LARGE-BREAK LOCA SAFETY ANALYSIS

This section evaluates the effects of incorporating of SiC whiskers into an LWR fuel pellet. This concept would:

- improve thermal heat transfer in normal conditions improving fuel efficiency.
- improve margin in an accident condition.
- lock iodine into fuel matrix.

During the evaluation of this concept, it was assumed that the addition of SiC to the fuel pellet would result in a decrease of 230 °F in the average fuel temperature. As a part of this task, the impact of such a decrease on the LOCA Safety Analysis was quantitatively estimated, assuming currently approved methodology. The actual average fuel temperature decrease will vary with fuel burnup. Therefore, the estimates of improvements in LOCA limits shown here are maximum values and will have to be reduced as appropriate for a given burnup.

The early stages of a LOCA transient are driven primarily by the initial stored energy, while during the latter stages decay heat becomes increasingly important. The safety analyses for Westinghouse-3 loop (W-3), 4 loop (W-4), and CE plants were all evaluated in a similar manner. (Note that B&W plants will be discussed later.) It was assumed, based on previous experience, that if the limiting PCT for the analysis occurs prior to 60 seconds, then the PCT would be decreased by 50% of the decrease in average fuel temperature, and if the PCT occurs after 60 seconds, then the PCT would be decreased by 25% of the decrease in average fuel temperature. This is a reasonable assumption for our purposes, although it becomes less applicable at the boundaries or if PCT is delayed significantly beyond 60 seconds. The second step of this estimate was to estimate the impact on Linear Heat Generation Rate (LHGR). This estimate was performed by developing the ratio of the deviation from saturation of the original analysis with the deviation from saturation of the SiC modified PCT, i.e. (PCTorig-Tsat)/(PCTSiC-Tsat). Multiplying this ratio by the initial LHGR allowed us estimate the benefit of the decrease in stored energy to LHGR for each plant type examined.

The following table summarizes the results of this estimate, and shows the AOR PCT and time, the expected change in PCT due to SiC, the AOR LHGR, and the expected change to the LHGR.

Type	AOR PCT, °F	PCT time, s	ΔPCT, °F	AOR LHGR, kW/ft	ΔLHGR, kW/ft
W-3	1852	260	57	13.1	0.5
W-4	1941	266	57	14.9	0.5
CE	1620	8.5	115	16.1	1.6

Table 1: Result of the Estimate and Expected Time

An LHGR increase of 0.5 kW/ft for the Westinghouse plants seems reasonable; however, the estimate of 1.6 kW/ft for CE may be overly optimistic. This is because this estimate challenges the assumptions, and therefore, it was decreased to 1 kW/ft.

For the B&W plants, it was estimated that the expected decrease in average fuel temperature would decrease the PCT, but this reduction could not be used to increase the LHGR limit since the peak LHGR for B&W plants is already at the maximum allowed by NRC SER for reflood heat transfer in most plants. The maximum B&W LHGR is approximately 17.8 kW/ft based on a 1 kW/ft limitation on the reflood phase benchmark data. Therefore, without additional higher power data (which does not exist at this time), the peaking obtained by the currently operating B&W 177 FA plants is already maximized. Nonetheless, the LBLOCA PCT would decrease by roughly 100 to 300 °F, depending on the plant using this new fuel design. The B&W 205 FA plant could take advantage of the PCT, and the LHGR limit could be increased by an estimated 0.5 to 1.0 kW/ft.

Benefits to the addition of SiC are less obvious in SBLOCA analysis. This type of transient is typically driven by decay heat and thermal hydraulic events/conditions, and therefore is not likely to experience benefit from enhanced fuel thermal conductivity.

3.6. MATERIALS EFFECTS OF EATF PELLET ADDITIVES AND COATINGS

The changes to material properties due to EATF pellet additives and coatings are presented in Appendix O.

4.0 CONCLUSION

Although potential impacts of the EATF changes to the fuel system have been identified, none of them are deemed to be impossible to address. Further work to address these impacts has been identified. The benefits of EATF to the DBE have been estimated to be between 0.5 and 1.0 KW/ft improvement to the LOCA limit, which is a significant amount of improvement.